

UNIVERSITÀ DEGLI STUDI DI NAPOLI FEDERICO II

DEPARTMENT OF EARTH, ENVIRONMENT AND RESOURCES SCIENCES



**PH.D. IN
EARTH SCIENCE, ENVIRONMENT AND RESOURCES
XXX CYCLE**

PH.D THESIS

**PETROGENESIS OF ALKALINE AND STRONGLY ALKALINE
VOLCANISM: EXAMPLES FROM AFRICAN RIFT.**

TUTOR

PROF. LEONE MELLUSO

COTUTOR

PROF. VINCENZO MORRA

PhD COORDINATOR

PROF. MAURIZIO FEDI

Ph.D CANDIDATE

MINISSALE SILVIA

2014-2017

Alla persona che crede in me, grazie papà.

e a Fabio che manca e mancherà

TABLE OF CONTENTS

Abstract	1
Introduction and aim	2
Chapter 1. Geological and petrochemical settings of studied areas	4
1.1 The East African Rift system geological setting	4
1.2 The Western branch in the Tanzanian Craton	7
1.2.1 Virunga volcanic province.....	13
1.2.2 Nyiragongo volcano	15
1.2.3 Nyamuragira volcano	17
Chapter 2. Analytical techniques	18
2.1 Sample powders preparation and thin sections preparation	18
2.2 X-RAY Fluorescence (XRF)	19
2.3 Inductively Coupled Plasma – Mass Spectrometry (ICP-MS).....	20
2.4 Thermal ionization Mass Spectrometry (TIMS)	20
2.5 Scanning electron microscopy (SEM) and Microanalyses (EDS)	21
2.6 Laser Ablation-Inductively Coupled Plasma-Mass Spectrometry (La-ICPMS).....	22
2.7 U-Th disequilibrium	23
Chapter 3. Data presentatio: rock classification and petrography	24
3.1 Rocks classification	24
3.2 Sample petrography	32
3.2.1 Nyiragongo	32
4.2.2 Nyamuragira	35
Chapter 4. Mineral chemistry	37
4.1 Mineral chemistry.....	37
4.2.1 Olivine	37
4.2.2 Pyroxene	38
4.2.3 Melilite	40
4.2.4 Feldspar	40
4.2.5 Nepheline and leucite	41
4.2.6 Other minerals	41
4.2 Glass and minerals trace elements concentration	43
Chapter 5. Petrochemistry	51
5.1 Major element composition	51
5.2 Trace element composition.....	57
5.3 Trace element distribution	63

Chapter 6 Discussion	65
6.1 Mantle source	66
6.2 Considerations on the role of CO ₂ and the model below Tanzanian Craton.....	73
6.4 Isotopes	76
6.4 U-Th disequilibria.....	82
Conclusions	83
Data tables	86
References	132

Abstract

The Virunga Volcanic Province (VVP) lies in the western segment, the Albert Rift, of the East African Rift System (EARS). The volcanism there started about 11 Ma yrs ago and continues to the present. The two active volcanoes of VVP, Nyamuragira and Nyiragongo lie along the seismically active sector of the western rift. Nyiragongo is a stratovolcano characterized by rock types such as melilitite, melilite nephelinite, pyroxene nephelinite, leucite nephelinite, leucitite and leucite tephrite. Nyamuragira located 15 km to the north of Nyiragongo, together with it, is one of the most effusive global volcanoes erupting several times in the past few decades, with rocks ranging from basanite to tephrite and basalt. Concerning to this thesis work the samples include parasitic cones and lava fields of the volcanic complexes from 1938 eruption until the last one in 2016, which products were sampled from the proximal vent area to the distal outcrops.

The mafic rocks of Nyamuragira are porphyritic with phenocrysts of olivine and clinopyroxene. Some of the basanites studied have MgO (12.05-13.60 wt.%), Cr (790-926 ppm) and Ni (245-309 ppm) contents within the ranges expected for mantle-derived liquids. The transitional basalts have higher MgO (> 15 wt.%), Cr (> 969 ppm) and Ni (> 750 ppm) contents than basanites. Such enrichment in these elements is probably due to excess of olivine phenocrysts. Nyamuragira basanites have Zr/Nb (3.9-4.0), Ba/Nb (11-12) and La/Nb (0.86-0.9) ratios typical of mantle or OIB values. The primitive mantle-normalized incompatible element patterns of Nyamuragira show positive peaks at Ba and Nb and smoothly decreasing normalized-abundances from Nb_n to Lu_n and a high La_n/Yb_n ratio (18).

The Nyiragongo melilite nephelinites and olivine melilitites have a porphyritic fabric as well as Nyamuragira products. Olivine ranges from forsterite-fayalite to kirschsteinite, clinopyroxene is diopside and melilite has akermanite composition. All samples are feldspar-free. The composition of the glass is often rich in Ba content (up to 5 wt.% BaO). These rocks have higher CaO (~16.3 wt.%) and lower SiO₂ (~ 40 wt.%), MgO (8.7-9.1 wt.%) and compatible elements concentrations (Cr = 380-395 ppm; Ni = 155-169 ppm) than Nyamuragira basanites. Their incompatible element patterns are also more enriched than those of Nyamuragira basanites with high Light Rare Earth Elements/Heavy Rare Earth Elements LREE/HREE (La_n/Yb_n = 42); in general they present a low heavy REE contents. The low Zr/Nb (2.1) value of the olivine melilitites indicates that the Nyiragongo olivine melilitites are melt products from an incompatible element-enriched source.

Based on the major and trace elemental compositions of these volcanic rocks, a bimodal character emerges between the nephelinitic Nyiragongo lavas and the Nyamuragira basanites which suggests that the nephelinitic lavas have different origin. The difference between these types of rocks depends on the degree of partial melting of a garnet-carbonate lherzolite source and it depends on the pressure and depth formation of these lithotypes: deeper source for the melilitites and shallower source for the basanites.

Introduction and aim

The East African Rift System (EARS) provides an opportunity to study the temporal evolution of magmas within an ongoing continental rifting: it consists of eastern and western branches that have contrasting alkaline chemistry characterized by sodic magmas in the eastern branch, and more potassic ones restricted to the western branch (Rosenthal et al., 2009 and reference therein). Carbonatites are also observed in the branches; they are well known from the famous Oldoinyo Lengai and Napak localities in the eastern rift, but also occur in the northernmost western rift in the Toro-Ankole field (Barker and Nixon, 1989; Holmes and Harwood, 1932) together with strongly alkaline magmas such as nephelinites and melilitites, which are very rare lithotypes occurring in the Virunga Volcanic Province (VVP).

The VVP, localized in Kivu region, consists of different volcanic edifices. Five volcanoes (Nyamulagira, Karisimbi, Sabinyo, Gahinga and Muhavura) are characterised by plagioclase-bearing lavas belonging to a K-basanite, tephrite, phonotephrite series or to a K-basanite, K-hawaiite, K-mugearite, K-benmoreite, K-trachyte series (see also Rogers et al., 1992, 1998). The other two volcanoes within the VVP, Mikeno and Visoke have emitted sometimes undersaturated lavas (foidites), with feldspathoid phenocrysts instead of feldspars. Visoke lavas evolved from plagioclase bearing rocks in the old edifice to feldspathoid-bearing rocks (leucitites) in the most recent part of the volcano (Condomines et al., 2015 and reference therein).

The Nyiragongo lavas are quite distinct from those of the other Virunga volcanoes, including Nyamuragira. Almost all Nyiragongo lavas are strongly undersaturated feldspar-free nepheline-melilitites and nephelinites; among the feldspathoids, leucite is generally far less abundant than nepheline. Plagioclase-bearing lavas from the other volcanoes of the VVP are melilite-free basanites usually with leucite as the unique feldspathoid mineral. The Nyiragongo rocks are intermediate between the main Virunga rock series and the ugandites, mafurites and katungites from the Toro-Ankole region (Bell and Powell, 1969). Although the petrogenesis of alkaline undersaturated magmas is not yet fully understood, high-pressure experimental studies have shown that these magmas can be generated by small degrees of partial melting of H₂O and CO₂ – rich mantle peridotite (*e.g.*, Bultitude and Green, 1967; Brey and Green, 1975, 1977; Wyllie, 1979).

The aim of this study is the full petrological characterization of these vulcanite outcrops at Nyamuragira and Nyiragongo to fully understand their genesis or correlation and their mantle signature.

Indeed, a major problem currently facing petrologists concerns the characterisation of the mantle source region of continental, intra-plate, alkaline magmas remains a subject of considerable debate. Whether these magmas arise in the lithosphere or in the underlying convecting asthenosphere or geochemically distinct mantle plumes or some combination of these source regions (Wilson 1995). Nyiragongo in fact results controversial from petrological point of view Platz (2004) and Chakrabarti (2009).

According to Andersen (2012) and the most recent petrogenetic models (Demant et al., 1994; Platz et al., 2004), the parent magma of the Nyiragongo nephelinites was an olivine melilititic magma formed by small-fraction partial melting at the base of the lithosphere.

The mineralogical, petrographic, geochemical and isotopic characterization of these lithotypes has been analyzed and interpreted by including within a more general geodynamic context such as the magmatism of Western branch of African Rift. The features that make the Nyiragongo and Nyamuragira areas worthy of interest are mainly related to the presence of magmatic rocks that exhibit an unusual and original mineralogical and chemical composition such as the melilitites erupted from Nyiragongo associated with more common igneous rocks such as basanites at Nyamuragira a volcano.

Chapter 1

Geological and petrochemical settings of studied area

1.1 *The East African Rift geological setting*

The East African Rift System (EARS) in East Africa (fig.1.1) is part of the broader context of the 'Afro-Arabian Rift, which extends for about 6,500 miles from Turkey to Mozambique, including the Red Sea and the Gulf of Aden, and the continental ones of East Africa. The complex tectonic movement of the plates in this area of the Earth has been under study for several authors (McKenzie, 1970, Chu and Gordon, 1998, 1999), which proposed that the African plaques and Somalia, are separating by rotating around a pole located in the Indian Ocean. Since the continental openings of the Red Sea and the Gulf of Aden have given rise to new ocean basins, (Ebinger and Casey, 2001) have suggested that east Africa, represents an initial stage of this rifting process.

A fundamental importance is given to the African rift system because of its unique place in the world where it is possible to study volcanism and continental opening phenomena before the formation of a new ocean basin, in fact the East African Rift System (EARS) represents a classical example of a young intra-continental ridge system, comprising an axial rift, where continental breakup has not been completed.

Rift system extends over 2000 km from the Red Sea in the north to Mozambique in the south and crosses the Ethiopian dome to the north and the Kenyan dome to the south, which are separated by the Turkana depression characterized by Quaternary volcanism, and the Anza graben representing a ~150 km wide zone of NW–SE trending extension.

The East African rift system shows up at the surface as a series of several thousand kilometers long line up with successions of adjacent individual tectonic basins (rift valleys), generally bordered by uplifted shoulders. Each basin is controlled by faults and forms a subsiding graben filled with sediments and/or volcanic rocks.

The rift valleys form two main lines, the Eastern and Western branches of the EARS. A third, southeastern branch is in the Mozambique Channel. The Eastern branch runs over a distance of 2200 km, from the Afar triangle in the north, through the main Ethiopian rift, the Omo-Turkana lows, the Kenyan (Gregory) rifts, and ends in the basins of the North-Tanzanian divergence in the south. The Western branch runs over a distance of 2100 km from Lake Albert in the north, to Lake Malawi in the south. It comprises several segments: the northern segment includes Lake Albert, Lake Edward and Lake Kivu basins, turning progressively in trend from NNE to N–S; the central segment trends NW–SE and includes the basins of lakes Tanganyika and Rukwa; the southern segment mainly corresponds to Lake Malawi and small basins more to the south. Most of the great lakes of Eastern Africa are located in the rift valleys, except notably Lake Victoria whose waters are maintained in a relative low area between the high mountains belonging to the Eastern and Western branches (Chorowicz J. 2005).

The morpho-tectonics of the EARS involved in divergent movements, inducing localized extensional strain in the continental lithosphere. The brittle crust has responded faulting

and subsidence, forming elongate, narrow rifts, while the lithospheric mantle is subjected to sharply defines ductile thinning, inducing ascension of asthenospheric mantle. The most characteristic features in the rift system are narrow, elongated zones of thinned lithosphere related to deep intrusions of asthenosphere in the upper mantle. On the surface, the main tectonic features are normal faults, but there are strike-slip, oblique-slip and sometimes reverse faults. Most of the fractures are syn-depositional, and when volcanism occurs, it is closely related to the tectonics (Chorowicz J. 2005).

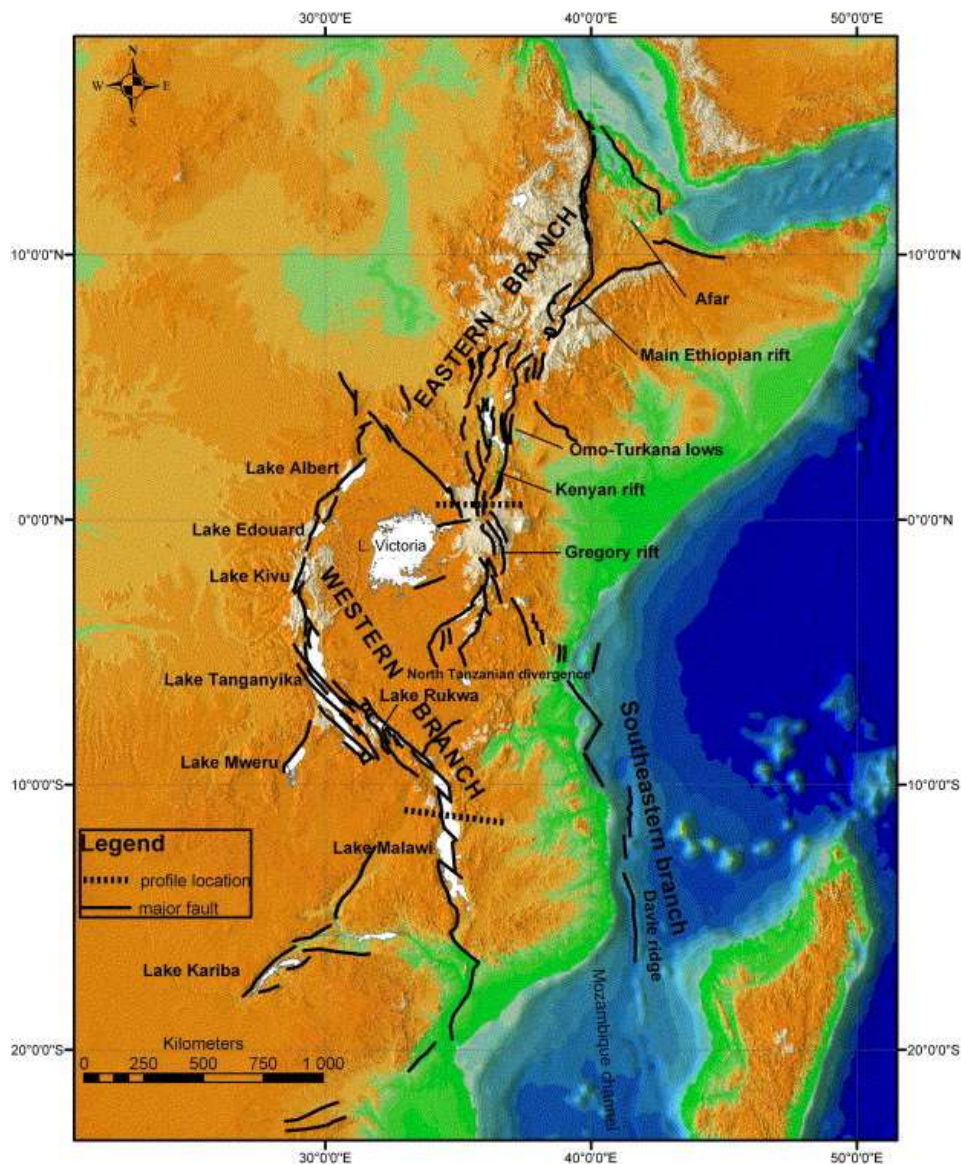


Figure 1.1: Hypsographic DEM of the East African rift system. Black lines: main faults; white surfaces: lakes; grey levels from dark (low elevations) to light (high elevations). The East African rift system is a series of several thousand kilometers long aligned successions of adjacent individual tectonic basins (rift valleys), separated from each other by relative shoals and generally bordered by uplifted shoulders. It can be regarded as an intra-continental ridge system comprising an axial rift. (from Chorowicz., 2005)

Volcanism in EARS started between 40-45 Ma in the northern Turkana depression (Ebinger et al., 2003) which has remained volcanically active since that time. In spite of this observation, the modern East African Rift magmatic area is generally described with respect to the onset of flood basalt activity in modern Ethiopia, Eritrea and Yemen that occurred in the late Oligocene and is credited to the impact of a mantle plume head at the

base of the lithosphere. This Oligocene flood basalt event is associated with the breakup of the Afro-Arabian shield, forming the Red Sea 28 Ma (Wolfenden et al., 2005) and the Gulf of Aden 35 Ma (Watchorn et al., 1998). The African Rift represents the third arm of this triple junction, although recent regional plate kinematic models indicate that the three rift zones were not joined until about 11 Ma (Acton et al., 2000; Eagles et al., 2002; Wolfenden et al., 2004).

The earliest extension documented in the East African Rift System occurred in the Turkana area 25 Ma (Morley et al., 1992; Hendrie et al., 1994). Volcanism and faulting propagated from this region to both the north and south, forming the structures of the modern rift branches.

The Holocene volcanism is scattered along the length of the EARS, but is sparse in places, such as the south western part of the Western Rift between the Virunga and Rungwe Volcanic Provinces (VVP and RVP). In north Afar, volcanic edifices are elongate shields with axial fissures (e.g., Alu-Dalafilla, Erta Ale, Alayta). Further south, central grabens within faulted and fissured terrains and central vent area with a subsided edifice are typical (e.g., Dubbahu-MandaHararo, Ardoukoba, Kammourta) (Barnie et al., 2015). The Tendao-Goba'ad Discontinuity (TGD) marks the triple junction between the Nubian, Somalian and Arabian plates (Acton et al., 1991). In the MER, there is an increasingly well-developed rift valley morphology, large normal fault boundaries and central fissure swarms and cones (e.g., Fantale, Kone, Tullu Moje) and large central volcanoes, including calderas (e.g., Corbetti, O'a). Further south, the rift branches around the Tanzanian Craton, present greater seismicity in the western branch than the eastern one. The southernmost volcanoes of the EARS are located in the Rungwe Province in northern Malawi (Fontijn et al., 2012), south of which, the rifting appears to be amagmatic (e.g., Biggs et al., 2010).

Ages of igneous rocks give some information about the evolution of the Cenozoic rifts in the EARS. The Eastern Rift developed from north to south, productive magmatism began 45–40 Ma ago in South Ethiopia, at 30–35 Ma in northern Kenya, 15 Ma ago in central Kenya and at 8 Ma in northern Tanzania penetrating into the Tanzania Craton and ending there (Chorowicz J. 2005)

Kampunzu et al. (1998) suggest an along axis southward propagation of the Western Branch (WB), based on a first cycle of volcanism at 11 Ma in the Virunga region (North Kivu), at 10 Ma in Bukavu (South Kivu) and at 9 Ma in Rungwe (near the triple junction, southern end of WR). The northernmost fourth volcanic province in the WB, Toro–Ankole southeast of Rwenzori Mountains, is Quaternary to recent and does not fit to N–S age decrease of the volcanic activity. Chorowicz (2005) suggests the Kivu dome as the origin of rift propagation with rift floors of the northern segment of the WB stepping up to Kivu and stepping down of the central segment from north to south. New age data of first volcanism at Rungwe region of 19–17 Ma (Razzkazov et al., 2003) support a propagation of the WB from south to north. Nyblade and Brazier (2002) assumed the synchronous origin of the WB initiation at 10–12 Ma in a transmission of extensive stresses through the stiff lithosphere when the N–S propagating Eastern Rift laterally encountered Tanzania Craton contemporaneously (Wallner H. and Schmelting H., 2010). The equatorial section of the East African Rift provides an opportunity to study the temporal evolution of magmas within a continental rift: it consists of eastern

and western branches that have contrasting alkaline chemistry characterized by sodic magmas in the eastern branch, and more potassic ones restricted to the western branch. Carbonatites occur in both branches; they are well known from the famous Oldoinyo Lengai and Napak localities in the eastern rift, but also occur as lavas and tuffs in the northernmost western rift in the Toro-Ankole field (Barker and Nixon, 1989). Together carbonatites and kamafugites provide the opportunity to study magma genesis at an early rift stage before the production of more voluminous magma types.

As mentioned above, the oldest known volcanism (~45 Ma) occurred in southwestern part of Ethiopia, and spread southwards with the spreading rift (Ebinger et al., 2000). Strongly alkaline-composed magmas such as melilitites and nephelinites occurred favorably at the propagating tip during its development, and on the flanks of the rift (Williams, 1982): the alkaline rocks positions in the rift axis were later overwhelmed by large, less alkaline magmas, however alkaline volcanic centers remained isolated on the flanks of both sides of the rift axis (Ebinger et al., 1999; Fig. 1.1).

1.2 The Western Branch in the Tanzanian craton

The Western Branch extends over 2500 km and is developed predominantly in mobile belts between the Archean cratons of Tanzania and Bangweulu. Volcanic provinces have developed mainly in intra-basinal positions at the intersections of at least two fault systems (Platz et al., 2004). The Western Rift, as well as the rest of the EARS, is divided into segments along its axis approximately 100 km long asymmetric basins due to an interplay of at least three factors, namely: (i) a response of old, and cold continental lithosphere to the rifting process, (ii) changing stress orientations during discrete rifting episodes, and (iii) the effect of along axis propagation of rifting; coupled with re-activation of pre-existing crustal shear zones (McConnell, 1972; Shudofsky, 1985; Ebinger, 1989; Ebinger et al., 1993). Moreover, Ebinger (1989) noted that western rift transfer faults accommodate large differences in elevation between adjoining basins and their uplifted flanks, as well as regional variations in relief related to the 1300 km-wide East African Plateau; hence half-grabens are commonly separated along the length of the rift valley by horsts or sills.

Volcanism, uplift and rifting started at about the same time, 12 Ma in Virunga (Ebinger, 1989; Zeyen et al., 1997), 8–9 Ma in the Kivu and Rungwe volcanic fields, at ~6 Ma in the Mwenga–Kamituga Province, but at less than 50000 years in the Toro-Ankole province (Ebinger, 1989; Zeyen et al., 1997; Nyblade and Brazier, 2002).

The compositional range of volcanic eruptive in the western rift branch is broad, ranging from carbonatitic and ultrapotassic, silica undersaturated lavas in the Toro-Ankole field (e.g. Combe and Holmes, 1945; Barker and Nixon, 1989; Stoppa et al., 2000; Tappe et al., 2003) to alkali basalts and tholeiitic in South Kivu (e.g. Bell and Powell, 1969; Furman and Graham, 1999). There is a systematic decrease in SiO_2 and increase in K_2O and CO_2 from south to north (Pouclet et al., 1981). Fascinatingly, the geochemistry of Rungwe volcanics (Furman, 1995) does not keep to this trend. Volcanism in the Virunga province range from silica undersaturated to slightly silica-oversaturated with numerous intermediate compositions in terms of SiO_2 (e.g. Holmes and Harwood, 1937; Rogers et al., 1992, 1998; Platz et al., 2004; Chakrabarti et al., 2009), while the Rungwe field features trachyphonolites, alkali basalts, basanites, nephelinites, and picrites (Furman, 1995). During the Late Quaternary, volcanism with a broad spectrum of compositions was active simultaneously in Toro-Ankole, Virunga, South Kivu, and Rungwe (Furman, 1995; Boven et al., 1998). The volume of volcanics in the western rift is estimated at ~100 000 km^3 (Kampunzu and Mohr, 1991), considerably less than in the eastern rift branch (e.g. Williams, 1972; Morley, 1999; Rosenthal, 2009 and reference therein). Melilitites and nephelinites occur preferentially at the propagating tip and on the flanks of the rifts (Rosenthal et al., 2009).

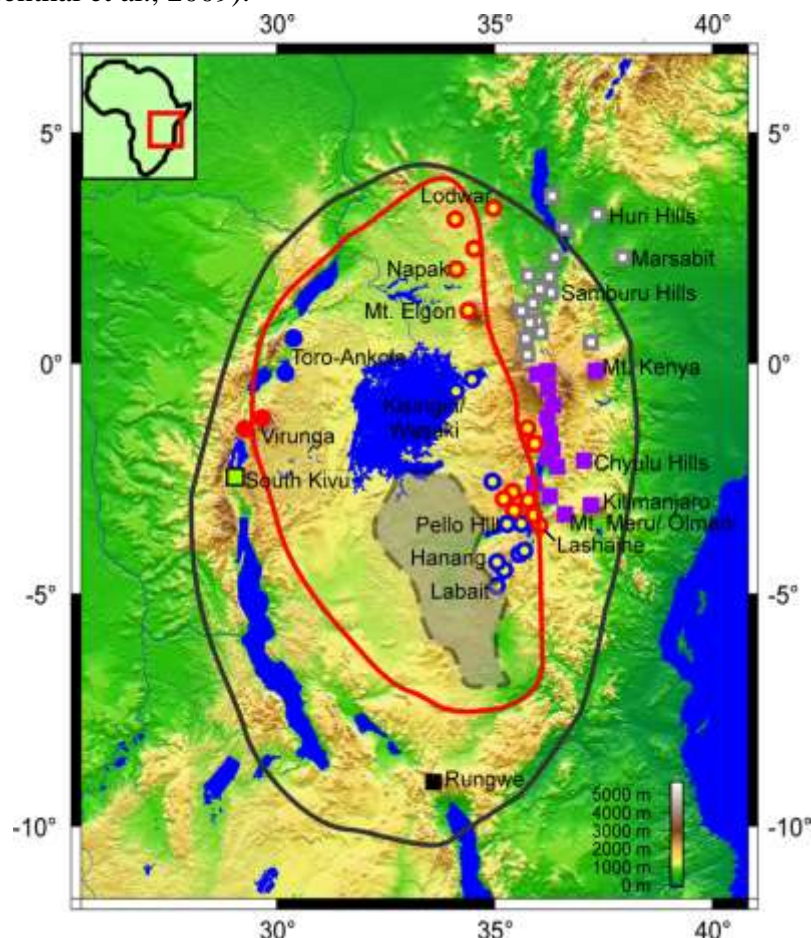


Fig 1.3: Solid red line indicate boundary of the craton, black line is the boundary of uplift (the “Kenya Dome”),

Symbols correspond to those in later geochemical figures, indicating volcanic fields in the western rift and proximity to the craton in the eastern rift (blue/yellow circles are on-craton; red/yellow circles are craton-edge; purple squares = off-craton southern Kenya rift; grey squares off-craton northern Kenya rift. Individual locations named are referred to in the text (Rosenthal et al., 2009)

The Tanzanian craton in equatorial east Africa is an area of special interest in terms of both craton development and igneous petrogenesis. In this area, the world's largest continental rift impinges on a craton that appears to be at an intermediate stage of destabilization.

Geochemical and geophysical interpretations of the thickness and state of the Tanzanian cratonic lithosphere appear to contradict each other, and the elevation of the craton surface lies above 1100 m, in contrast to many cratons that are close to sea level, reflecting buoyancy supported by a subcratonic plume whose effects are seen in the volcanics of both western and eastern rift branches (Foley et al., 2012 and references therein).

The cratons themselves are usually interpreted as virtually indestructible lithospheric blocks whose formation and stability is due to exceptionally high degrees of melting in the distant past and thus to buoyancy owing to the high degree of geochemical depletion of the peridotite (Lee, 2006). Diamond-bearing kimberlites are generally restricted to the central parts of cratons, whereas diamond-free kimberlites and lamproites occur around their margins (Janse and Sheahan, 1995).

Magmatism on the craton and at its edge has high K/Na and primitive melts show fractionation dominated by olivine. Slightly further from the craton pyroxene fractionation dominates and K/Na ratios in the magmas are lower. Off-craton melts are nephelinites, basanites and alkali basalts with low K/Na. Potassium enrichment in the melts correlates with the occurrence of phlogopite in mantle-derived xenoliths, and also with carbonate in the magmas.

In fig it is shown the spatial relationship of volcanic centres both in western and eastern branches and in the following diagrams the rocks are divided in five categories: (1) kimberlitic rocks, (2) high-MgO or picritic rocks regardless of their K/Na ratios, (3) Low MgO nephelinitic or melilititic rocks, (4) carbonatites, and (5) basanitic, alkali basaltic and basaltic rocks. This is a descriptive categorization aimed to present in a pragmatic way the composition and the differences of Tanzanian craton rocks (Foley et al., 2012) .

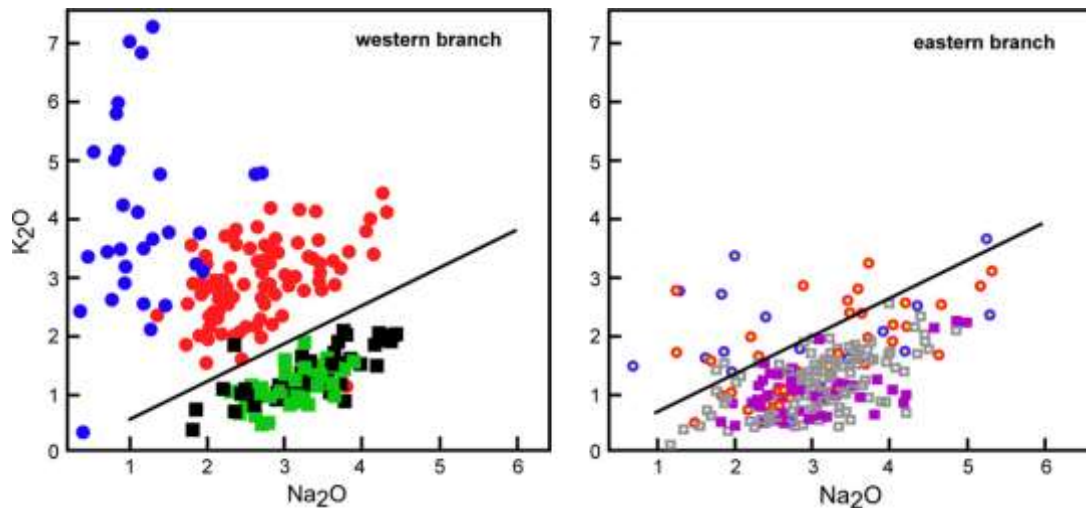


Figure 1.4: Geochemistry of K_2O and Na_2O in igneous rocks from western and eastern rift branches close to the Tanzanian craton. Western rift (left panel) symbols show volcanic fields (from north to south: blue circles = Toro Ankole; red circles = Virunga; green squares = South Kivu; black squares = Rungwe). Eastern rift symbols refer to proximity to the craton and not to volcanic fields (blue circles = on-craton; red circles = craton edge; purple squares = off-craton south; grey squares = off-craton north). Both western and eastern rift rocks show highest K_2O and lowest Na_2O in on-craton positions. The reference line is in the same position in both panels and shows the excellent distinction between northern and southern volcanic fields in the western rift corresponds broadly to on-/off-craton positions in the eastern branch, but with more overlap (Rosenthal et al., 2012).

Many studies of rocks in the western branch show that the more alkaline members are typically potassic variants of basanites, nephelinites and melilitites (Pouclet et al., 1981; Rogers et al., 1998; Tappe et al., 2003), which are globally much rarer than types with high Na/K ratios. The most extreme of these occur in the Toro Ankole field of western Uganda and contain kalsilite in addition to nepheline. In contrast, in the eastern rift branch, rocks are mostly of the globally commoner sodic varieties, with rare occurrences of potassium-enriched rocks at the eastern edge of the craton (Dawson et al., 1997).

Carbonatites occur in both branches, mostly as composite centres with nephelinite or melilitite (King and Sutherland, 1966; Woolley et al., 1995; Keller et al., 2006; Eby et al., 2009), but occasionally as single occurrences for which a relationship with silicate melts is not proven, as at Fort Portal (Barker and Nixon, 1989). Carbonatitic tuffs that include silicate material are common in the Toro Ankole and Ndale fields in the northern sections of the western rift branch (Stoppa et al., 2000; Eby et al., 2009).

The volcanics show a strong compositional gradient in terms of increasing K_2O/Na_2O from south to north Fig. (Pouclet et al., 1981; Pouclet et al., 1984). The distinction between high and low K_2O/Na_2O between the Virunga and South Kivu fields is almost free of overlap, whereas the South Kivu and Rungwe fields show complete overlap (Fig.). In the eastern rift volcanics, the abundance ranges for K_2O and Na_2O are different: K_2O/Na_2O ratios are generally similar to those in the South Kivu and Rungwe fields of the western branch, but Na_2O extends to higher abundances (>5 wt.%; Fig). The only rocks in the eastern branch that plot with high K_2O/Na_2O ratios within the range of Virunga rocks are from either on-craton or craton-edge localities in Tanzania. These include rocks referred to as katungites at Pello Hill, and potassic nephelinites at Sora Hill (Dawson et al., 1988). The line in Fig. appears to demarcate the influence of cratonic mantle sources.

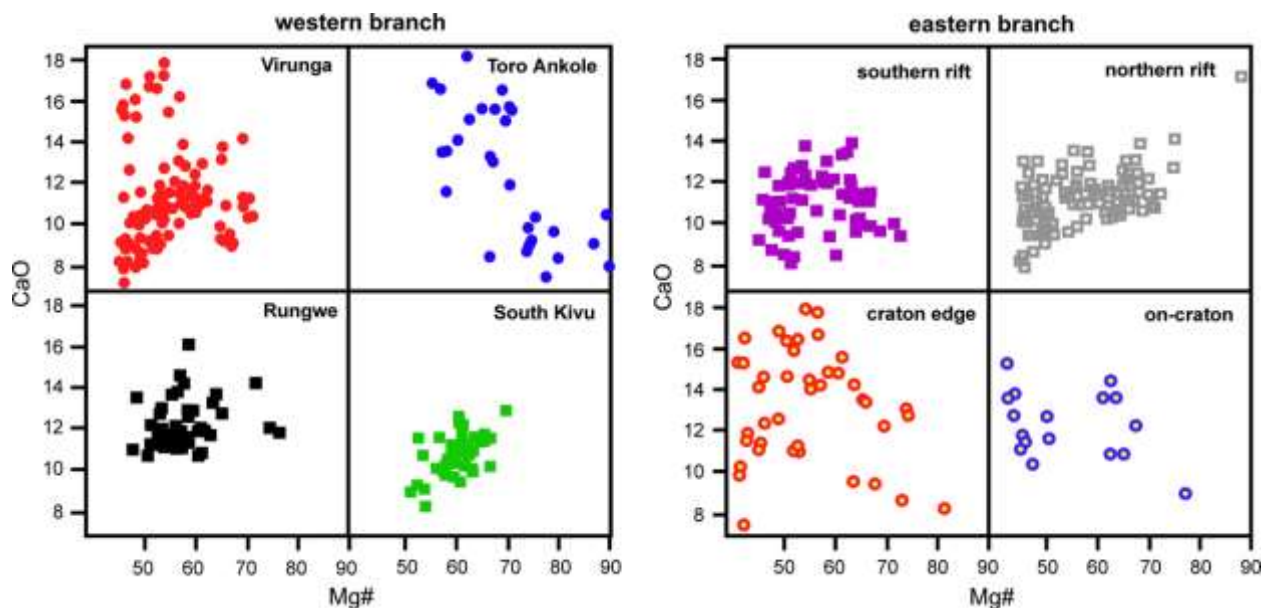


Figure 1.5: Mg# vs. CaO plots indicate olivine control by negative slopes and clinopyroxene \pm plagioclase fractionation by positive slopes. Predominantly olivine control is seen for Toro Ankole, for the eastern rift on-craton rocks, and to a minor extent for Virunga and the craton-edge eastern rift rocks (Rosenthal et al., 2012).

Fractionation of mafic phenocrysts in continental volcanic series is often illustrated on plots of Mg# or MgO versus CaO, in which olivine control lines from picritic parental melts cause increasing CaO until olivine is replaced as the dominant fractionating phase by clinopyroxene, which depletes later melts in both CaO and Mg#. These trends have been used to demonstrate this order of fractionation for flood basalts and other continental occurrences (Cox, 1980; Kerr et al., 1997). In Fig. , the subdivisions according to volcanic fields (western branch) and proximity to craton (eastern branch) are plotted separately so that trends in individual groupings are clearer. The Virunga field has several rocks with high Mg# and low CaO that may indicate both trends, whereas both Toro Ankole and Virunga fields have an appreciable number of rocks with very high CaO and low MgO, well beyond the usual turning point towards lower CaO contents which characteristically occurs at 10–13 wt.% CaO depending on pressure of fractionation. The eastern rift plots (Fig.) show similar features: high Mg#, low CaO typical of primitive picritic rocks in which olivine is the only fractionating phase are seen at the on-craton localities, whereas they are missing in the rift rocks away from the cratons (Fig. , top two panels). The craton-edge rocks (lower left panel) show features similar to Virunga, with olivine control lines and also high-CaO, low Mg# rocks. In his summary of eastern branch nephelinite volcanism, (Le Bas M.J. 1981, 1987) distinguished olivine-poor and olivine-rich nephelinites, noting that olivine-richer types are concentrated further away from the Kenya dome to the northeast, whereas the olivine-poor variety occurs to the west of the rift valley axis.

1.3 The Virunga Volcanic Province

The Virunga Volcanic Province (VVP) is located in the western branch of the East African Rift System (EARS; Ebinger and Furman, 2003), at the intersection between the Democratic Republic of Congo, Rwanda and Uganda and it is widely regarded as one of the classic intra-plate potassic provinces (Rogers et al., 1992). It comprises eight main volcanoes, including two active ones, and numerous pyroclastic cones (fig.). Among the

eight main edifices of the VVP, Nyiragongo and Nyamulagira volcanoes are currently the most active volcanoes of Africa (Wright et al., 2015). Since 1882, Nyamulagira volcano experienced at least 42 eruptions and in November 2014 a lava lake appeared (Smets et al., 2014, 2015). The eruptive activity of Nyiragongo volcano over the last 150 years is characterized by intra-crater activity, corresponding to the presence of a persistent lava lake (1928-1977, 2002-present; Sahama and Meyer, 1958; Durieux, 2003) or lava fountaining activity from 1982, 1994 and 1995 eruptions creating an ephemeral lava lake (Krafft and Krafft, 1983; Tazieff, 1984; Durieux, 2003; Komorowski et al., 2003). This intra-crater activity was interrupted by two flank eruptions, in 1977 and 2002 (Tazieff, 1977; Komorowski et al., 2003). Mikeno, Visoke and Karisimbi volcanoes are located in the central part of the VVP. Sabinyo, Gahinga and Muhavura volcanoes are located in the eastern part of the VVP. The cone field of Bufumbira represents the easternmost extension of the volcanic province. With the exception of the 1957 eruption, the Mugogo cone (Verhaeghe, 1958; Condomines et al., 2015), not documented historically eruption is known to have occurred in the central and eastern part of the VVP.

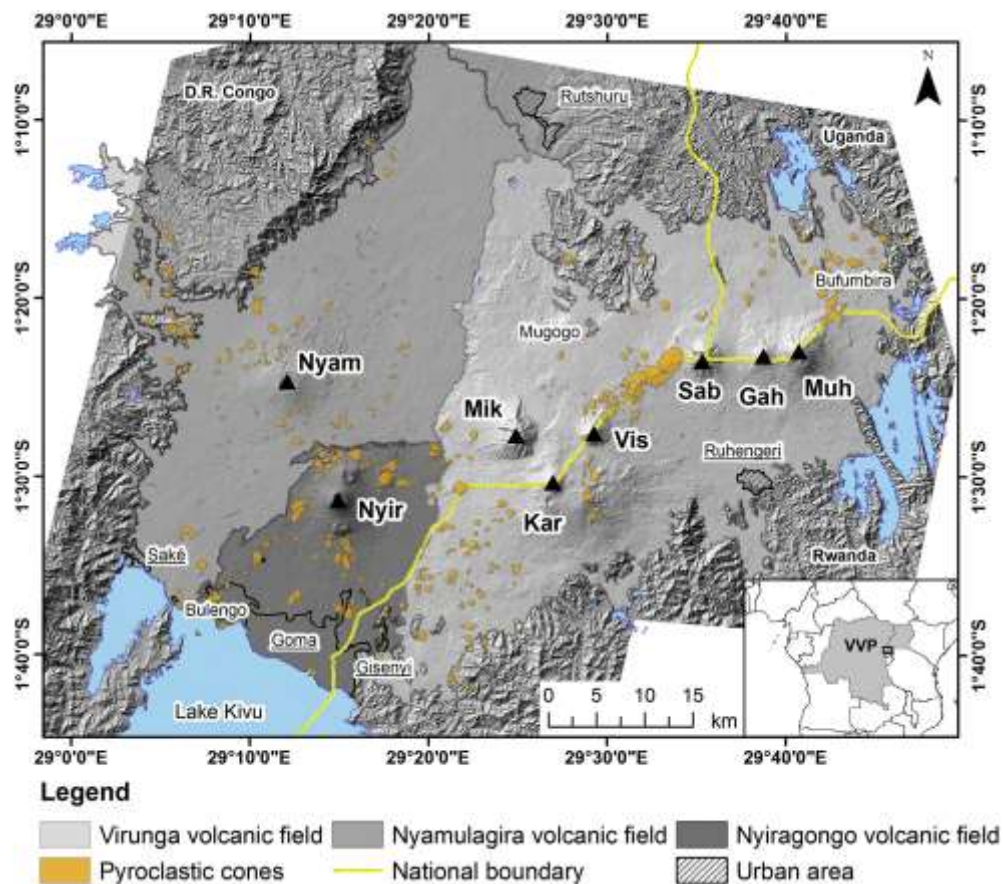


Figure 1.6: Map of the Virunga Volcanic Province showing the main volcanic edifices (black triangles) and the >500 pyroclastic cones (yellow polygons). Nyam: Nyamulagira; Nyir: Nyiragongo; Mik: Mikeno; Kar: Karisimbi; Vis: Visoke; Sab: Sabinyo; Gah: Gahinga; Muh: Muhavura. Background (Albino et al., 2015).

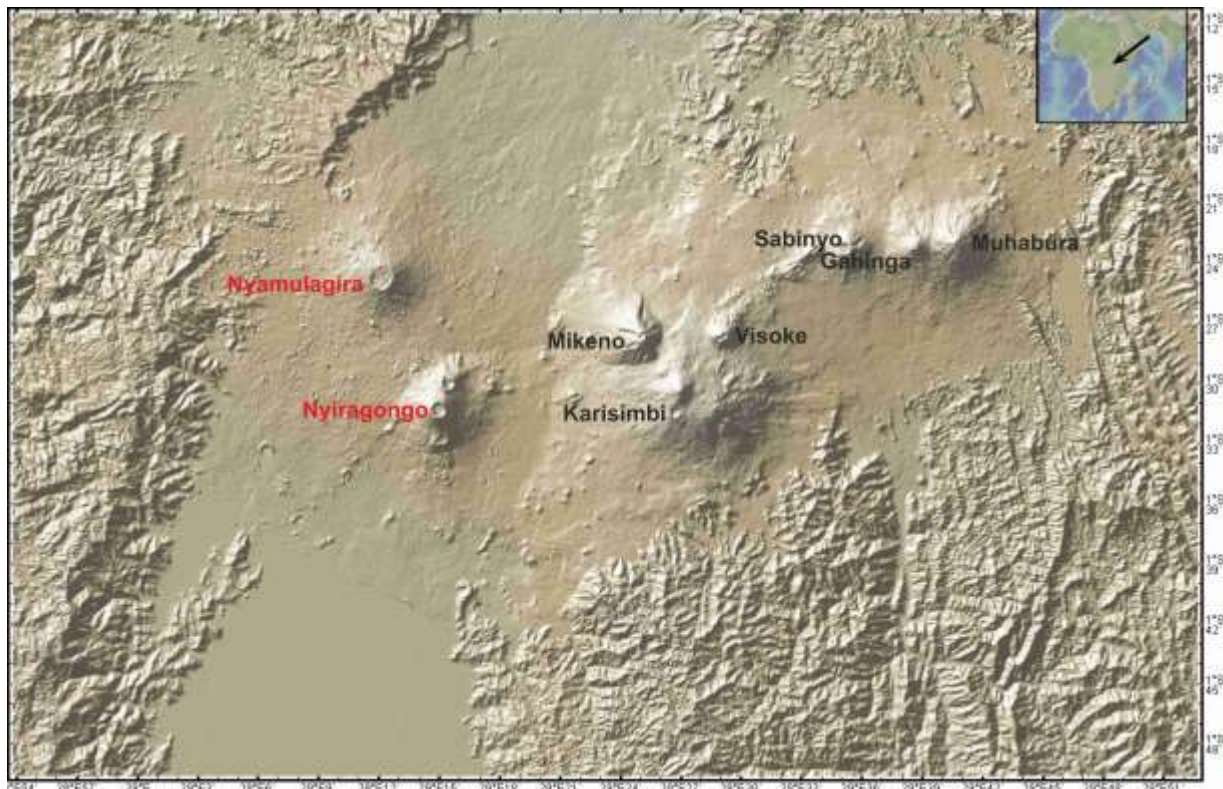


Figure 1.7: Main volcanic centres in the Virunga Volcanic province. Modified from DEM image.

The Virunga volcanic area is located at a WSW-ENE dextral shift of the rift, and sets in a classical accommodation zone (Ebinger et al., 1999). It consists from SW to NE of eight large strato-shield volcanoes like mentioned above: Nyamuragira (3058 m), Nyiragongo (3470 m), Mikeno (4437 m), Karisimbi (4507 m), Visoke (3711 m), Sabinyo (3634 m), Gahinga (3500 m), and Muhavura (4127 m). Mikeno and Sabinyo are the oldest volcanoes and are dated, respectively, to late Pliocene and to Early Pleistocene. Nyiragongo and Nyamuragira are presently active. The other volcanoes were active from middle Pleistocene to recent time.

Geochronological studies date the last eruptions of the large volcanoes of the central and eastern part of the VVP to the Late Pleistocene. A lava flow of Mikeno volcano was dated at 0.2 ± 0.1 Ma (Guibert et al., 1975), ages from 65 ± 25 k.a to 176 ± 30 k.a have been reported for Sabinyo eruptive products (Bagdasaryan et al., 1973; Rogers et al., 1998), and a Karisimbi lava flow was dated to 0.010 ± 0.007 Ma (De Mulder and Pasteels, 1986). Ages of 33 ± 9 ka and 52 ± 19 ka were obtained for two leucites of Muhavura volcano (Rogers et al., 1998). The central and eastern part of the VVP remains poorly studied, with a limited number of geochronological and geochemical studies available (e.g., Guibert, 1978; De Mulder, 1985; De Mulder and Pasteels, 1986; Marcelot and Rançon, 1988; Kampunzu et al., 1998; Rogers et al., 1998).

Two diverse magmatic suites are shown: leucite-bearing basanites and evolved lavas at Nyamuragira, Karisimbi, Visoke, Sabinyo, Gahinga and Muhavura, and leucite-melilite nephelinites and nepheline-leucitites at Nyiragongo, Mikeno and Visoke (pro parte) (Pouclet et al., 1981, 1983, 1984). Furthermore, remnants of basaltic lava flows, dated to Miocene, are conserved at the upper western edge of the rift. They preceded the major

fault motion of the rift shoulder and the building of the great volcanoes of the main Virunga area (Poucllet, 1975, 1977).

1.3.1 Nyiragongo

Nyiragongo volcano is one of the most active on Earth (Wright et al., 2015), it is located in the eastern part of the Democratic Republic of Congo, close to the border with Rwanda. Nyiragongo is considered one of the most dangerous African volcanoes (e.g., Favalli et al., 2009) due to the dense population in the surrounding area. Its eruptive activity is primarily characterized by the presence of a molten lava lake in the main crater, from which a SO₂- rich gas plume escapes continuously (e.g., Tedesco et al., 2007).

In both, 1977 and 2002, flank eruptions occurred, draining the lava lake and producing fast-moving lava flows that proved to be deadly and destructive (e.g., Tazieff, 1977; Komorowski et al., 2004). Months to years after these flank eruptions, the lava lake reappeared in the main crater.

The extent, form and the height of the Nyiragongo lava lake grew through time, modifying the morphology of the main crater. Today's crater topography is characterized by remnants of solidified levels of the lava lake, forming platforms attached to the inner flanks.

The Nyiragongo volcanic complex consists of three overlapping large stratovolcanoes aligned roughly in N-S direction and exhibiting summit craters, the older Baruta volcano (3,148 m) to the north, the Nyiragongo (3,470) located 1.5 km south and the Shaheru volcano (2,600 m) located 2 km to the south of Nyiragongo. At least 100 small volcanic lava and cinder cones have developed above parasitic flank vents on Nyiragongo along predominant NE-SW and NS trending fractures zones, often radially oriented. Many of the cones located within 150 m elevation above the present Lake Kivu level and within 1.5 km lateral distance, such as Mount Goma located in the town of Goma, show some evidence that they were formed as the result of partial interaction of magma with the lake waters during violent explosive phreatomagmatic eruptions (Tuttle and Newhall., 1988). Recent flank fissure lava flows from Nyiragongo surround and partly cover lava flows from Baruta and Shaheru and have reached lake Kivu at least twice in recent times, about 700-740 years ago (e.g. Casadevall and Lockwood. 1995; Newhall et al., 2004) and during the 2002 eruption.

Fresh lavas from Nyiragongo are typically nephelinites that contains some melilite or leucite porphyritic with a vesicular, glassy or fine-grained crystalline groundmass (Sahama, 1953, 1957, 1978). They are ranging in composition from alkali olivine basalt to nephelinite, leucite nephelinite, melilite nephelinite, and melilitite (e.g. Demant et al., 1994; Platz et al., 2004; Sahama, 1978; Toscani et al., 1990). Samples of melt from the surface of the 1950s lava lake indicate that the liquid was nephelinitic in composition, and saturated in nepheline, melilite, magnetite and apatite (Sahama, 1978). Holocrystalline melilite nephelinite occurs in the upper part of the volcanic cone which was exposed in the inner crater walls above the 1950s upper terrace (Sahama, 1978; Sahama and Meyer, 1958).

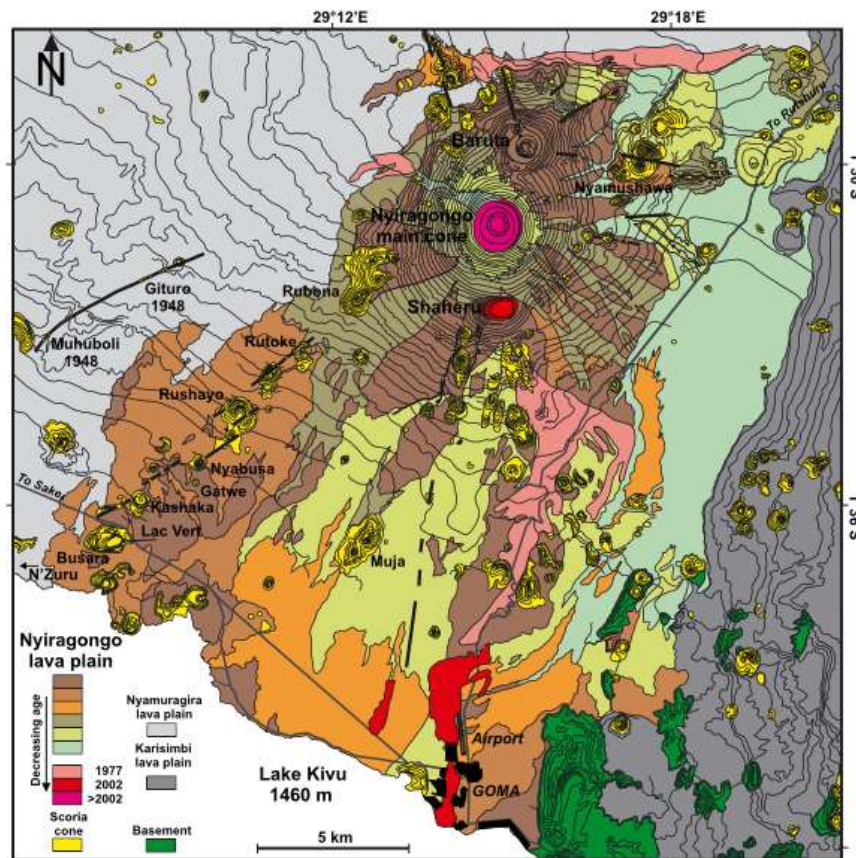


Figure 1.8: Geological sketch map of Nyiragongo (modified after Platz et al., 2004).

1.3.2 Nyamuragira

Smets (2015) states that Nyamuragira is one of the two active volcanoes with, one eruption every 2–4 years, in the VVP. It is a high shield volcano, covers over 1100 km² and is crowned by a 2.3 × 2 km shallow caldera which contains two smaller pits and it is located south of the Virunga National Park (SE part of N-Kivu, D.R. of Congo). Lavas consist of highly potassic suite of olivine basanite-tephritic phonolites (Kampunzu et al., 1982; Aoki and Yoshida, 1983; Aoki et al., 1985). Such composition results in low viscosity lavas able to flow for tens of kilometers.

Since 1938, a total of 27 flank had erupted (Smets et al., 2010) on this alkali basaltic to basanitic shield volcano. The lava lake was abruptly drained from the summit pitcrater, especially after 1938, when the volcano starts behaving as a closed degassing system that erupts when a verge of volume or pressure is reached. However, in late June 2014, a small lava lake was first observed within the eastern pit-crater (e.g. Champion R. 2014; Smets et al., 2014).

Aoki et al., (1985) suggested that Nyamuragira erupts low-silica, alkalic lavas, including alkali basalts, hawaiites, basanites and tephrites (SiO₂= 43–56 wt%, K₂O + Na₂O up to 7 wt%).



Figure 1.9: Geological sketch map of Nyamuragira volcano (modified from Smetz et al., 2010)

Chapter 2

Analytical techniques

Laboratories

Sample preparation for the geochemical and petrographic analysis were carried out in different laboratories. At laboratory of university of Napoli Federico II, the samples were cut, powdered and the thin-sections were obtained there. The major whole rock and trace elements were analysed both at University of Napoli (XRF spectrometry) and at ActLabs laboratories (LOI and ICP-MS). The major element concentrations of mineral and glass phases were determined also at University of Napoli (SEM-EDS). Trace element concentrations for mineral and glass phases were determined at the University of Pavia and Institute of Geosciences and Georesources (CNR). The Sr-Nd-Pb-isotopic analyses were measured at the University of Firenze (TIMS) and finally U-Th-Ra series disequilibria data were determined at the University of Montpellier (gamma ray spectrometry and alfa ray spec).

2.1 The Sample powders preparation and thin sections preparation

First of all the rock samples were cut with a diamond blade circular saw into smaller blocks (~2-3 cm blocks).

One block was used for standard 0.3 μm -thick thin sections, analyzed for petrographic investigations at the polarizing microscope.

The remaining blocks were shattered through the use of a chipmunk jaw crusher to ~1.5 cm rock fragments, washed in deionized water, dried out at 90°C and then pulverized. The pulverized samples were placed into a steel ball mill with agate jar and run for about thirty minutes. Next, the samples were gently sieved through a 60-micron sieve. The powders were hand-picked to >60 grams each in order to assure both sample quality and to provide enough samples for next analytical processes (like XRF and IC-PMS).

Thin sections preparation

The rock block already cut was treated to make it flat and polished. This operation was carried out using a grinding wheel with grinding disks (of silicon carbide). All the treatment consisted of subjecting the rock section to several polishing cycles, executed with progressively smaller knit disks (80, 180, 300 and 600 Mesh). Subsequently, they went hand-grinding on a glass plate on one of the slide faces to improve visibility at the microscope. The polished face then, cleaned and heated for a few minutes on a plate, was glued to the sanded face of the slide using a bi-component (binder+ hardening) resin. The slide-rock pair was subsequently reduced by thickness using a trimmer, about 100 μm from the glued surface. To reach the thickness of 30 μm (standard for thin sections of rocks), the progressive finishing abrasion gradually increased, first on the grinding wheel (300 and 600 mesh) and then onto a hand-held glass plate (600 and 800 Mesh). Finally, the sections were polished with a solution of alumina. The polishing process consists of abrasive finishing (1200, 2400, 4000 Mesh, 1 μm and $\frac{1}{4}$ μm) mounted on a lapping machine, until the section is perfectly glossy. All thin

sections were observed with an optical polarizing microscope to perform an accurate petrographic analysis of fabric and mineral paragenesis.

2.2 X-RAY Fluorescence (XRF)

The X-ray fluorescence spectroscopy (XRF) allows determining the elemental composition of a sample through the study of the X fluorescence radiation. This radiation is emitted by the atoms of the sample as a consequence of an excitation which is obtained typically by irradiating the sample with X-rays and Gamma-rays at high-energy. Similar effects were obtained using ion beams.

When an atom of the sample is exposed to incident radiation of suitable energy there is a certain probability that an electron, initially in a state of energy E_1 , is torn from it, producing a gap in the electronic structure of the atom. This phenomenon is known as the photoelectric effect (Franzini et al., 1975). To restore the equilibrium conditions, an electron with higher energy $E_2 > E_1$ replaces the empty gap by releasing a photon with energy equal to $E = E_2 - E_1$. Only the transitions that respect the rules of quantum mechanics are permitted. The term fluorescence refers to the fact that as a consequence of the irradiation a re-emission of radiation with a longer wavelength is obtained.

The fluorescence radiation emitted by a specific chemical element has a characteristic spectrum with lines at known energies, depending from the specific electronic structure of the element atoms (Leoni and Saitta, 1976). A qualitative analysis of a sample is possible by the identification of characteristics emission lines of each chemical element. According to the traditional notation, the energy levels are indicated by two letters. The first (K, L, M, ...) indicates the shell affected by the transition. The second ranking the energy of transition (α , β , γ , ...).

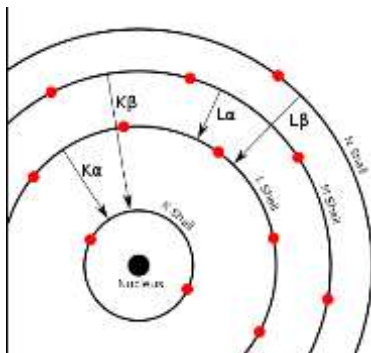


Figure 2.1: Representation of atomic energy levels.

A quantitative analysis requires a suitable processing, mainly consisting in a comparison of the intensity of X-ray lines with those of a standard samples containing known amounts of the element to be estimated.

Major elements and some of trace elements were carried out by X-ray fluorescence spectrometry using a Panalytical Axios instrument on pellets, from sample powders already obtained. Major elements concentrations are expressed as percentages by weight of oxides

and the determined elements are SiO₂, TiO₂, Al₂O₃, Fe₂O₃(t), MnO, MgO, CaO, Na₂O, K₂O, P₂O₅. Trace elements concentrations are expressed as ppm (parts per million) and the determined elements are Sc, V, Cr, Ni, Cu, Zn, Rb, Sr, Y, Zr, Nb, Ba, La, Ce. Analytical uncertainties are in the order of 1-2% for major elements and 5-10% for trace elements. The weight loss on ignition (L.O.I.) was determined with standard gravimetric techniques, after igniting one gram of powder at 1000°C for 4 h.

Disk pellets preparation

About five grams of the undersized rock powders were stucked with MOWIOL (Polyvinyl alcohol) and dried at 90°C, the prepared mixture was poured into special aluminum containers above of a layer of boric acid, with a filler function.

The dust container was, subsequently placed in a 3 cm circular saw, which was inserted into a hydraulic press Herzog and pressed at 20 Tonn/cm² for 20 seconds, thus obtaining the pressed disks.

2.3 Inductively Coupled Plasma – Mass Spectrometry (ICP-MS)

The Laser Ablation Inductively Coupled Plasma Mass Spectrometry (LA-ICP-MS) is a technique used for the *in situ* analysis of trace elements in rock samples. It can determine many elements in the periodic table to high degrees of accuracy and precision. The technique complements electron microprobe analysis, typically measuring trace elements at a lower concentration range (1 ppb - 100 ppm).

Solid particles are physically ablated due to the interaction of a high power laser beam (> 1 x 10¹⁰ Wcm⁻²) with the surface of the sample. The particles are carried in a stream of inert gas (helium or argon) into an argon plasma where they are ionised prior to measurement in a mass spectrometer. Isotopes are measured to determine elemental concentrations.

Lanthanides (REE) and other trace elements were determined some selected samples with inductively coupled plasma mass spectrometry (ICP-MS) at Activation Laboratories (Ancaster, Ontario; see www.actlabs.com for a full description of the analytical techniques).

Accuracy is generally in the range of 1-2% calculated using JB-2 and JGb-1 standards of the Geological Survey of Japan.

2.4 Thermal ionization Mass Spectrometry (TIMS))

The TIMS is an instrument that measures isotopic ratios that are used in geochemistry, geochronology, and cosmo-chemistry. TIMS is a magnetic sector mass spectrometer that is capable of making very precise measurements of isotope ratios of elements that can be ionized thermally, usually by passing a current through a thin metal ribbon or ribbons under vacuum. The ions created on the ribbons are accelerated across an electrical potential gradient (up to 10 KV) and focused into a beam via a series of slits and electrostatically charged plates. This ion beam then passes through a magnetic field and the original ion beam is dispersed into separate beams on the basis of their mass to charge ratio. These mass-resolved beams are then

directed into collectors where the ion beam is converted into voltage. Comparison of voltages corresponding to individual ion beams yield precise isotope ratios.

The whole rock sample powders (0,1 g) were leached with hydrofluoric acid and subsequently dissolved in acidic solutions such as hydrofluoric acid, nitric acid and hydrochloric acid. The acids and water used to treat the samples are extremely pure. To separate Sr and Nd from samples in solution column chromatography techniques were carried out that consist in isolating the quantities of Sr and 14 rare earths (REEs) by using cationic exchange columns and subsequently isolating Nd from REE with reverse phase chromatographic columns. To separate Sr and REE were used as 2.5N hydrochloric acid (for Sr) and acid hydrochloric 6N (for REEs). After use, columns and resins were washed with appropriate amounts of 6N hydrochloric acid and Milli-Q® water and reconditioned with hydrochloric acid 2.5N. The columns to separate the Nd from REE are different from the previous ones: the cationic exchanger is an organic acid (2-ethylhexyl phosphoric acid HDEHP). To separate Nd from REE, 0.25N hydrochloric acid was used as the eluent. After use the columns were washed with appropriate amounts of 6N and 6N hydrochloric acid reconditioned with 0.25N hydrochloric acid.

For the Pb the same methods were performed with a different procedure consisting of separate the solutions in two fractions. In a fraction a known amount of Pb 206 isotope was added to determine lead concentrations (spike solution); the other fraction was used to determine lead isotopic ratios (solution no spike). To separate Pb , we used an eluent 350 µl of a solution of nitric acid and acid hydrogen bromide.

All other information and references follow Avanzinelli et al. (2005).



Figure 2.2 Nd columns and samples manual loading

2.5 Scanning electron microscopy (SEM) and Microanalyses (EDS)

The scanning electron microscope (SEM) is an electronic instrument used for inspecting topographies of sample materials allowing a high-resolved and high-zoomed observation up to enlargements of 1-10 µm. This technique is based on the interaction between an incident electron beam and sample surface. The electron beam is focused and accelerated at high potential, by means of magnetic lenses, on the specimen, and its interaction generates several electromagnetic radiations such as backscattered electrons, secondary electrons, Auger electrons, characteristic X-rays, and visible light (Middendorf et al., 2005).

High-resolution imaging of surface morphology is generated by secondary electrons. The efficiency of production of backscattered electrons is strongly related to the material's atomic number. The higher the atomic number the brighter the material image.

If the SEM is equipped with an X-ray detector (EDS) a qualitative/quantitative determination of the chemical elements within the components of the sample is possible. The samples which are analyzed with SEM should be small and need to be covered with a conductive layer of carbon or gold, that facilitates the removal of electrical charges from the sample, which otherwise interferes with image formation (Middendorf et al., 2005). With EDS, the chemical composition of the phases can be determined (Callebaut et al., 2001).

Scanning electron microscopy (SEM) observations and chemical composition of mineralogical phases on polished thin sections were determined with an Energy Dispersive Spectrometer using a JEOL JSM-5310 electron microscope and an Oxford Instruments Microanalysis Unit, equipped with an INCA X-act detector and operating at 15 kV primary beam voltage, 50-100 mA filament current, variable spot size, from 30,000 to 200,000x magnification, 20 mm WD and 50 s net acquisition real time. Measurements were made with an INCA X-stream pulse processor and with INCA Energy software. Energy uses the XPP matrix correction scheme, developed by Pouchou and Pichoir (1988), and the Pulse Pile up correction. The quant optimization is carried out using cobalt (FWHM - full width at half maximum peak height- of the strobed zero = 60-65 eV). The following standards, coming from Smithsonian Institute, were used for calibration: diopside (Ca), San Carlos olivine (Mg), anorthoclase (Al, Si), albite (Na), rutile (Ti), fayalite (Fe), Cr₂O₃ (Cr), rhodonite (Mn), orthoclase (K), apatite (P), fluorite (F), barite (Ba), strontianite (Sr), zircon (Zr, Hf), synthetic Smithsonian orthophosphates (REE, Y, Sc), pure vanadium, niobium and tantalum (V, Nb, Ta), Corning glass (Th and U), sphalerite (S, Zn), sodium chloride (Cl), and pollucite (Cs). The K α , L α , L β , or M α lines were used for calibration, according to the element (Melluso et al., 2012; Guarino et al., 2016). Backscattered electron (BSE) images were obtained with the same instrument. Precision is 2% (relative).

2.6 Laser Ablation-Inductively Coupled Plasma–Mass Spectrometry (LA-ICP-MS)

The composition of the glass beneath the thin section has been documented before the sample analysis to promptly recognize the piercing of the rock and to eliminate any glass contribution. The gas background was measured for 60 s, as in any other routine analysis, whereas signals during ablation were acquired for approximately 20-50 s. Analyses were performed with 10 Hz repetition rate of laser and ~1-2.5 mJ/s laser power. Full details as in Miller et al. (2007).

Precautions have been taken to avoid any bias on the analytical results. Memory effects have been taken into account leaving more than 1 min between two consecutive analyses and analysing glasses after the minerals. Spurious signals related to memory effects usually affect more blanks (because less time is passed after the previous analysis), thus determining a worsening of the detection limits and hindering the quantification of elements at ultra-trace concentration level. Surface contamination during sample polishing and/or handling before the micro-analytical measurement and occurrence of micro-inclusions of glass/fluid have been monitored by detailed inspection of the signal profiles acquired during ablation. Only

intervals with parallel signals have been integrated. Anomalous signal contributions at the beginning of the ablation (due to surface contamination) and/or randomly occurring during ablation (possibly related to inclusions and/or memory effect) has been accurately documented and excluded by integration.

The trace element analysis of different mineral phases and glasses were performed on thin section samples and the elements concentrations are expressed in ppm. The spectrometer used, a Perkin Elmer DRCE, has a dual focus analyzer (Finnigan Mat, Element I) coupled with a Q-switched Nd-YAG laser source (Quantel Brilliant). The original ray emitted by the laser source (1064nm, region of near infrared) is converted to 213nm by three harmonic generators. The measuring point diameter varies between 30 and 60nm, with a variable energy of 25-30mJ. Analytical determinations were obtained using the GLITTER software. Accuracy is in the order of 10% for all the elements analyzed, and are calculated using the NIST SRM 610 and BCR-2g standards.

3.7 U-Th Disequilibrium analysis

The U-series nuclides were measured by mass and nuclear spectrometry methods. U and Th contents were determined by isotope dilution mass spectrometry (ID-TIMS) using ^{235}U - and ^{230}Th -enriched tracers and standard chemical separations. ($^{230}\text{Th}/^{232}\text{Th}$) ratios were determined by alpha spectrometry, following the procedure described by Condomines et al. (1982). The ^{226}Ra and ^{210}Pb activities were measured through gamma spectrometry, using a CANBERRA™ Ge-well high-purity detector. Around 11 g of rock powder was sealed into a gas-tight PETP (polyethylene terephthalate) cylindrical container and introduced into the Ge-well detector. The general procedure used to determine the activities of the different nuclides, by comparison of gamma-ray peaks with those of an in-house volcanic rock standard, is detailed in Condomines et al. (1995). Self attenuation corrections are systematically applied using a modified version of a Monte Carlo program implemented by J. Fain (Pilleyre et al., 2006), ^{232}Th can also be easily measured by gamma spectrometry through the activities of its daughter nuclides ^{228}Ac , ^{212}Bi and ^{208}Tl , when the ^{232}Th decay series is in secular equilibrium, reached after about 30 y. The agreement between Th contents analysed through three different techniques (multi-element ICP-MS, IDTIMS and gamma spectrometry) is excellent (better than 1 %), whereas U contents measured by multi-element ICPMS are about 5 % lower than those determined by both IDTIMS and gamma spectrometry (Condomines et al., 1982).

In sample “Nyira 2016” Bulk Cl-, bulk F and bulk S (total) concentrations were determined respectively by INAA, ISE and combustion IR techniques at ActLaboratories from 1 g of powder. Analytical error is given at +/- 0.01 wt%.

Chapter 3

Data presentation: rock classification and petrography

3.1 Rock classification

In this thesis were used rock samples from several sampling expeditions in Virunga area (Congo): they are lava samples, the majority, and scoria and ashes samples at few cases. All the volcanic products were sampled by Dario Tedesco (Università della Campania) and Charles M. Balagizi (Observatoire Volcanologique de Goma), with which there is an existing collaboration. In particular, for the Nyiragongo edifice this study focus on the 1977 eruptive event with 5 samples, on the 2002 eruptive event with 22 samples, on the 2016 eruption with one sample and six samples from older scoria cones such as Lac Vert and Mt. Goma. For the Nyamuragira volcano this study focus on the 1938 eruption with two samples, on 1948 event with two samples, two sample for 2010 event, four samples for the 2011/2012 event and six other lava samples from older lava flows (fig. 3.1).

The total amount of sampling for this thesis project consists of 47 samples (tab and fig. 3.1) Samples do not represent a complete sequence of crystallization but scattered samples from different and selected eruption events.

Number	Sample name	Volcano	Number	Sample name	Volcano
1	NYAM B 2011-2012	Nyamuragira			
2	NYAM 2011-2012 RUM	Nyamuragira	24	2nd Pause	Nyiragongo
3	NYAM 2010 Summit	Nyamuragira	25	Nyira 2002	Nyiragongo
4	Nyira SUMMIT B	Nyamuragira	26	Nyira-2	Nyiragongo
5	NYAM C	Nyamuragira	27	1977-1	Nyiragongo
6	NM 1938-2	Nyamuragira	28	1977-2	Nyiragongo
7	NM 1938-1	Nyamuragira	29	1977-3	Nyiragongo
8	NM 1948-2	Nyamuragira	30	1977-4	Nyiragongo
9	NM 1948	Nyamuragira	31	1977-5	Nyiragongo
10	NYAM A	Nyamuragira	32	M2002-1	Nyiragongo
11	NYAM B	Nyamuragira	33	M2002-2	Nyiragongo
12	MUJA	Nyamuragira	34	M2002-3	Nyiragongo
	NYAM SALT 2010	Nyamuragira	35	M2002-4	Nyiragongo
13	LV 1	Nyiragongo (Lac Vert cone)	36	M2002-5	Nyiragongo
14	LV 2	Nyiragongo (Lac Vert cone)	37	M2002-6	Nyiragongo
15	LV 3	Nyiragongo (Lac Vert cone)	38	M2002-7	Nyiragongo
16	LV 4	Nyiragongo (Lac Vert cone)	39	M2002-8	Nyiragongo
17	MG002	Nyiragongo	40	M2002-9	Nyiragongo
18	MONT Goma sand	Nyiragongo	41	M2002-10	Nyiragongo
19	Nyira 2016	Nyiragongo	42	M2002-11	Nyiragongo
20	NYIRA Summit	Nyiragongo	43	M2002-12	Nyiragongo
21	KITOKO (helicopter)	Nyiragongo		M2002-GL	Nyiragongo
22	SHAHERU Down	Nyiragongo		M2002- ST	Nyiragongo
23	SHAHERU Up	Nyiragongo		Nyira 2 b	Nyiragongo

Table 3.1

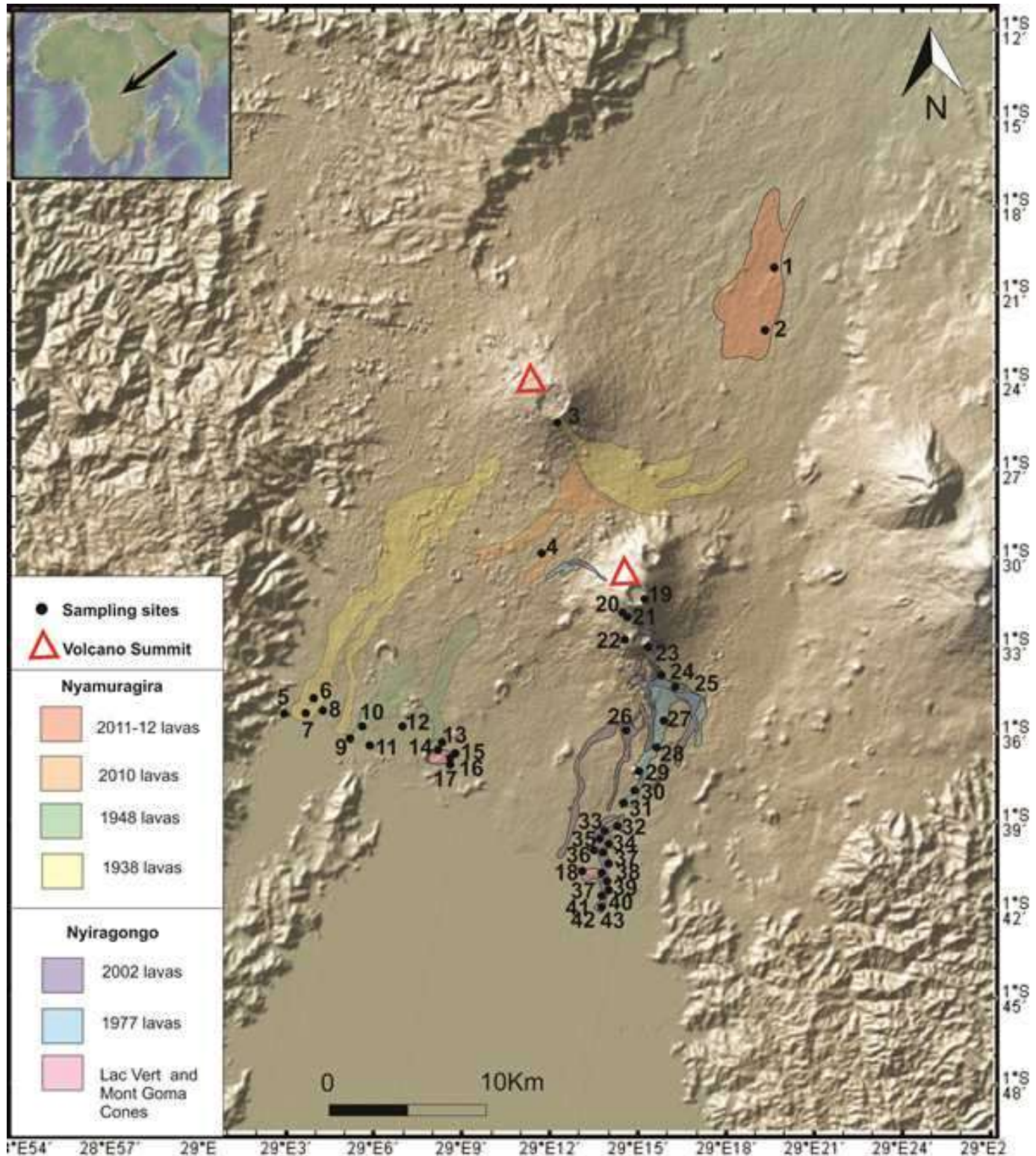


Figure 3.1 Location Map of some of the sampled rocks.

An evaluation was made first through major element composition that let us classify the sampled rocks through different diagrams. In the Total Alkali Silica diagram (TAS; Le Bas et al., 1986; fig. 3.3) all the Nyiragongo analyzed rocks all fall into the field of foid, on the contrary the Nyamuragira ones fall within the tephrite/basanite field and in the basalt field. In the diagram there are also some glass analysis.

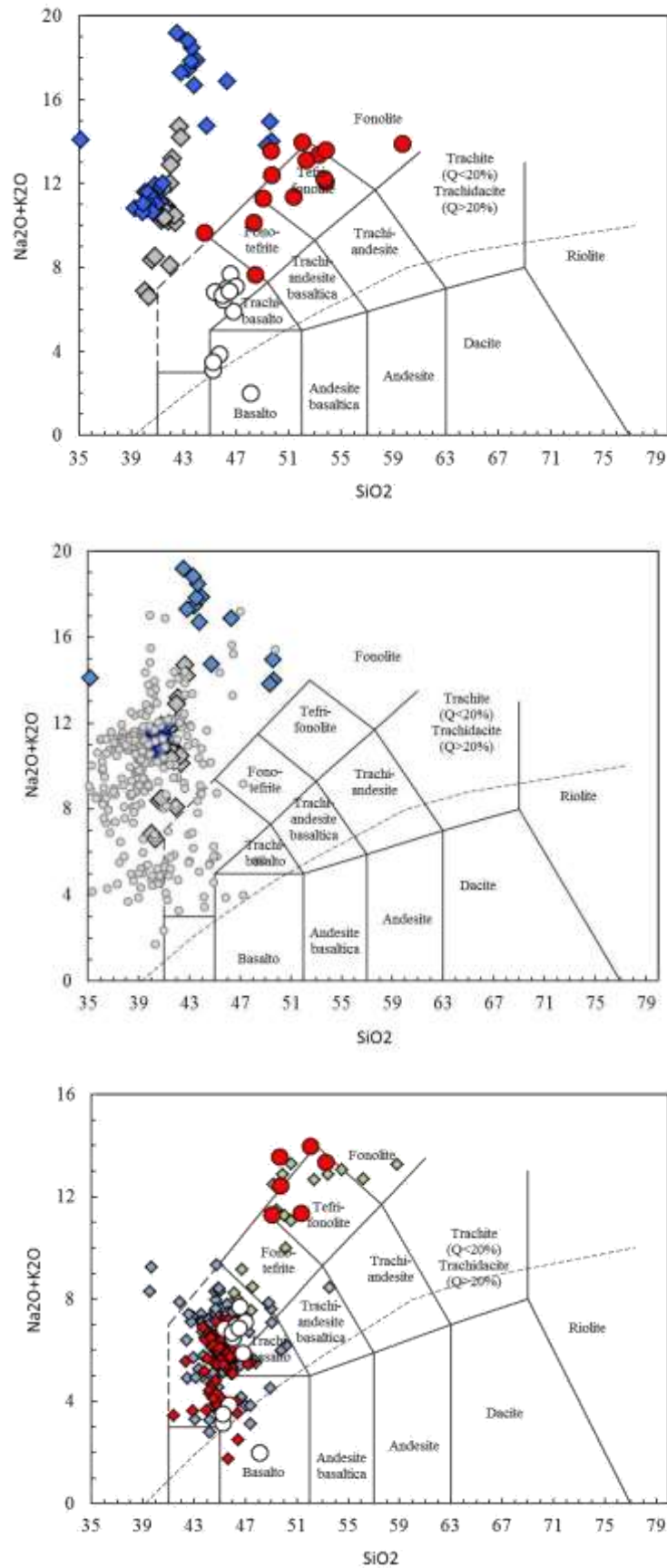


Figure 3.2 (a) Total alkali silica diagram for the studied rocks: Nyamuragira whole rocks (white circles), Nyamuragira representative glasses (red circles); Nyiragongo whole rocks (grey diamonds), Nyiragongo representative glasses (b) Nyiragongo rock samples with literature data (c) and Nyamuragira rock samples with selected literature data from Barette et al., (2016) geochemical database.

Since the rocks of the two volcanic districts are heavily undersaturated in silica, as it emerges from the TAS diagram, they are not properly distinguishable by the use of this classification chart as, as evidenced by many authors (Le Bas, 1989; fig.3.8; Woolley et al., 1996, fig.3.9), in the fields of the foidites and the basanites place a large number of different lithologies, but chemically equivalent. It was then proposed to classify these rocks by using the diagram R1 - R2 (De la Roche et al., 1980; fig 3.7) and the one especially modified for igneous lithotypes (Le Bas, 1989, fig 3.6).

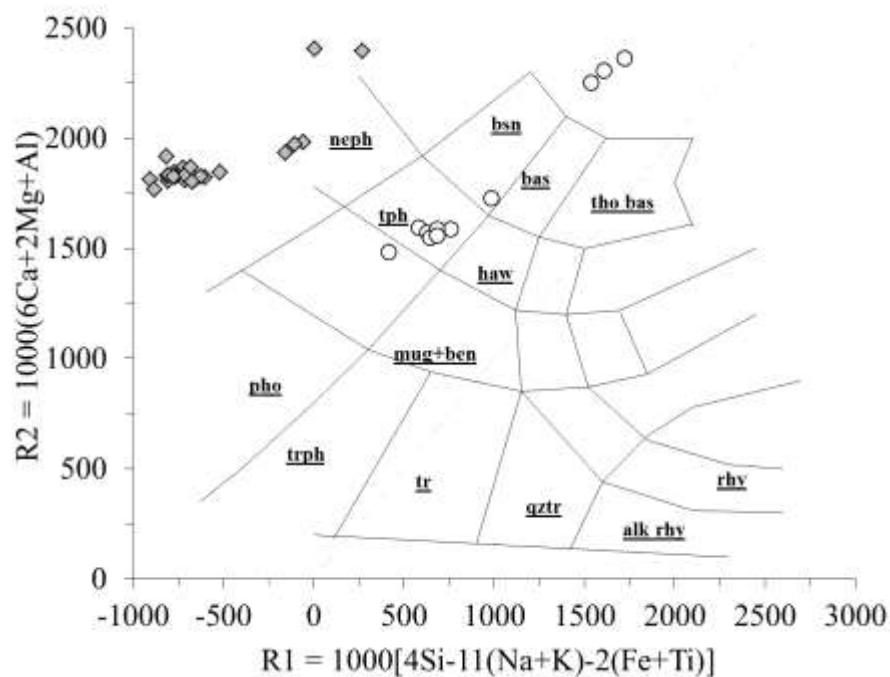
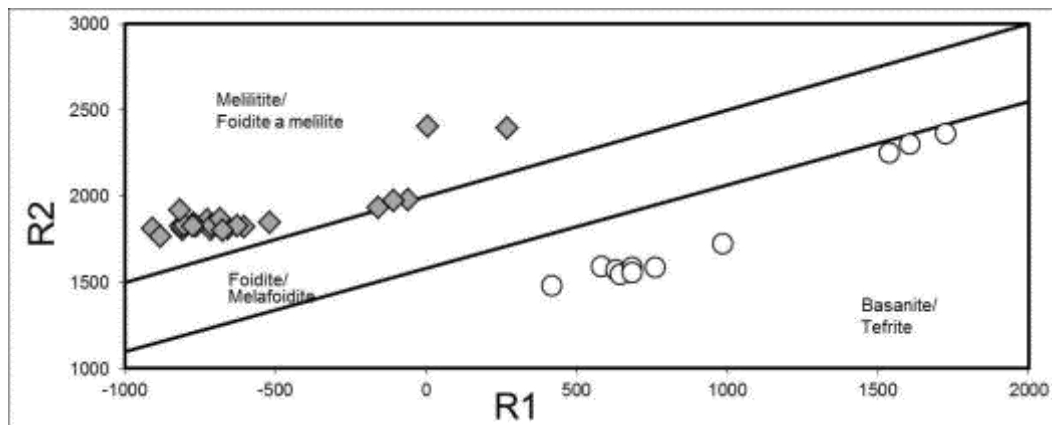


Figure 3.6-3.7 R1-R2 modified diagram and R1-R2 diagram for all the Nyiragongo (grey diamonds) and Nyamuragira (white circles) whole rocks analysis.

In the R1-R2 diagram all Nyiragongo samples fall within the field of nephelinites, and Nyamiuragira samples in the field of foidites and basanites.

Although both diagrams are more suitable for classification of undersaturated rocks, also the R1-R2 diagram and the modified one, do not discriminate between melilitites and foids.

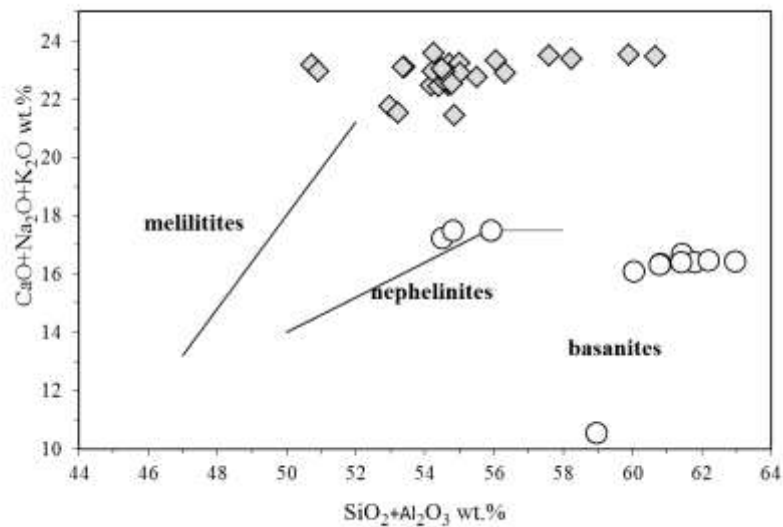


Figure 3.8 Classification of samples according to Le Bas (1989): Nyiragongo (grey diamonds) and Nyamuragira (white circles)

For this task a further classification was suggested based on CIPW norm (Cross, Iddings, Pirsson e Washington, 1903). A diagrams was advanced built Nepheline vs Larnite (Woolley et al., 1996, fig 3.9) for the Nyiragongo lithotypes excluding the scoria cone's ones that show moderately different features.

Generally speaking, the Nyiragongo melilite bearing rocks are characterized by more than 10% of CIPW-normative larnite and thus were classified as melilitites or olivine melilitites following Le Maitre (2002).

The Nyamuragira lithotypes instead are generally basanites and they are not include in this diagram.

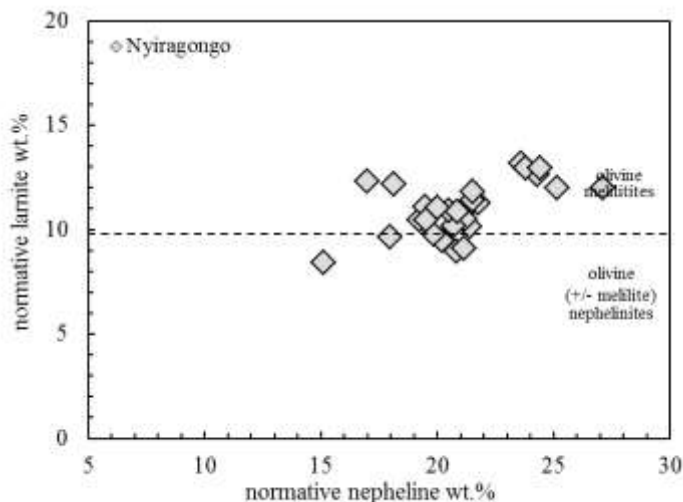


Figure 3.9 Classification of samples according to Wooley et al. (1996):Nyiragongo (grey diamonds)

From the point of view of geochemical affinity on average, Na_2O contents, ranging 3.38-7.07wt. % for Nyiragongo rocks and 1.64-4.12 wt.% for Nyamuragira rocks, are the same as K_2O contents, ranging 1.31-7.63 wt.% for the first ones and ranging 1.49-3.57 wt%. The ratio

is ~ 1 (fig 3.10) thus it means that the lava geochemical affinity is basically potassic but in general is alkaline-strongly alkaline.

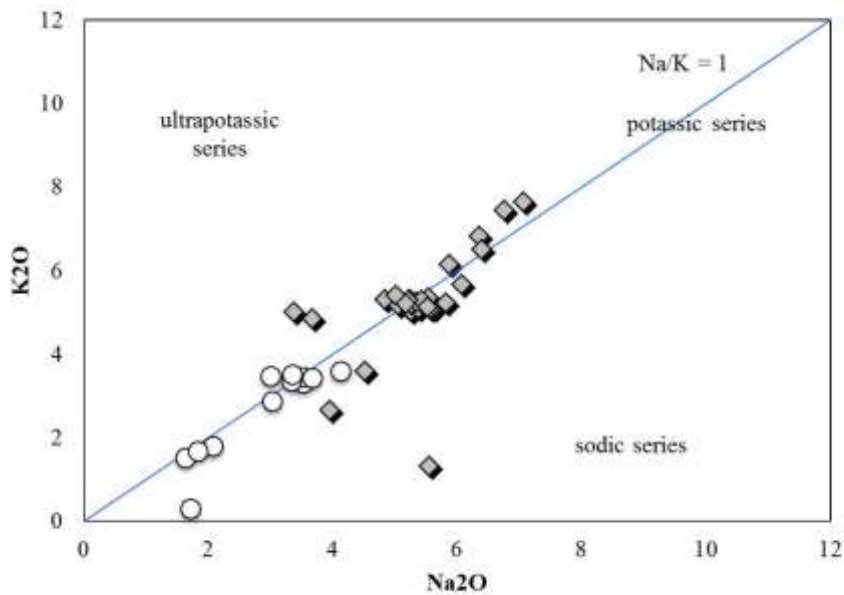


Figure 3.10 Geochemical affinity diagram: Nyiragongo (grey diamonds) and Nyamuragira (white circles)

Moreover, through the following diagrams, it is possible also to see different features: the Nyiragongo 1977 nephelinites are practically coincident with the 2002 ones, on the contrary they differ with the 2016 event. The older scoria cones also present heterogeneous patterns with a vertical trend for the Lac Vert samples.

Although the Nyamuragira lithotypes have similar trends, it is possible to note two clusters: one with the basalt and the Mg rich samples and the other with all the others (fig. 3.11-3.13).

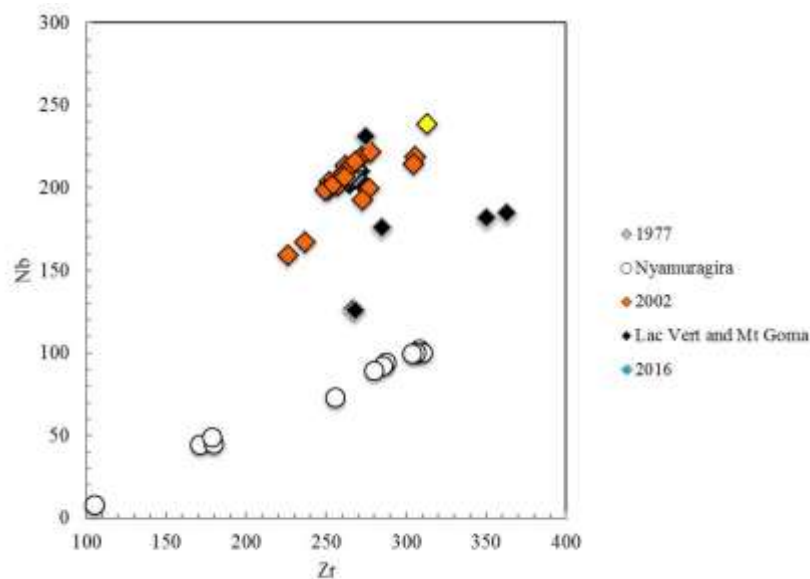


Figure 3.11 Zr/Nb diagram: Nyiragongo 2002 samples (orange diamonds), Nyiragongo 1977 samples (grey diamonds), Nyiragongo 2016 sample (yellow diamond), Nyiragongo scoria cones samples (black diamonds) and all Nyamuragira samples (white circles)

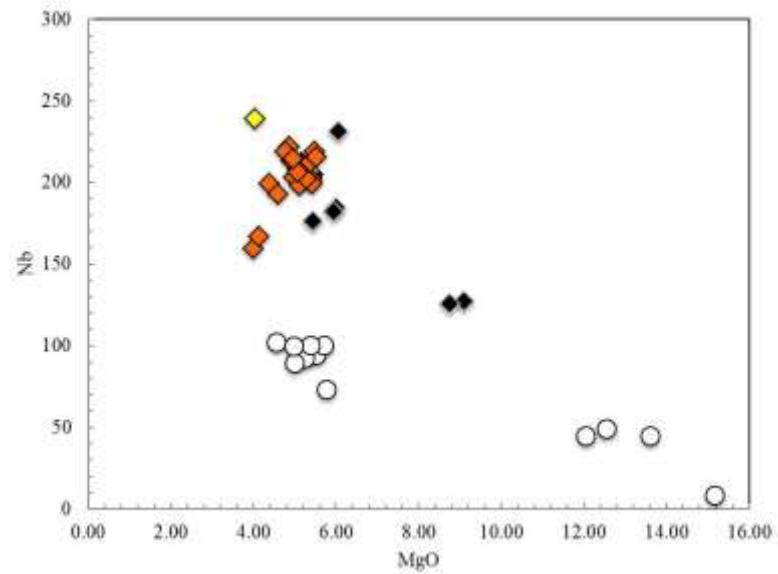


Figure 3.12 MgO/Nb diagram: Nyiragongo 2002 samples (orange diamonds), Nyiragongo 1977 samples (grey diamonds), Nyiragongo 2016 sample (yellow diamond), Nyiragongo scoria cones samples (black diamonds) and all Nyamuragira samples (white circles)

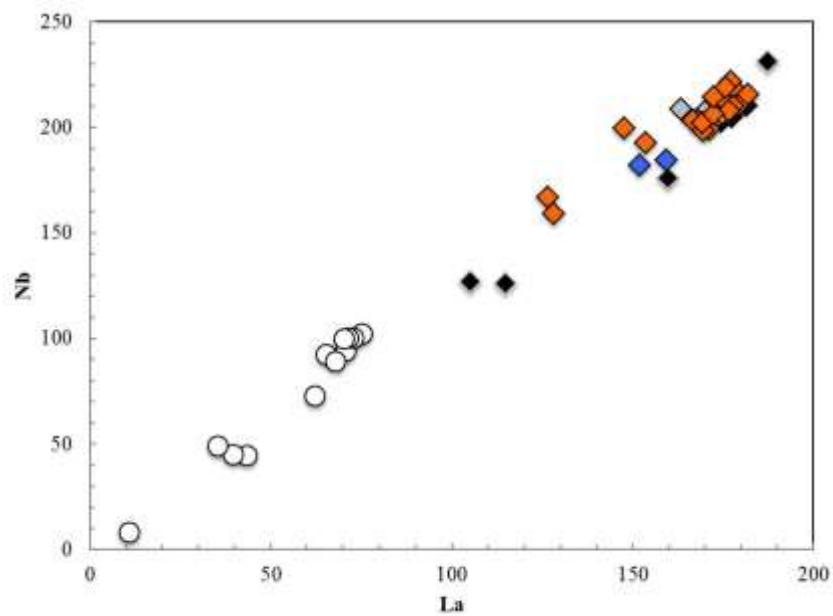


Figure 3.13 La/Nb diagram: Nyiragongo 2002 samples (orange diamonds), Nyiragongo 1977 samples (grey diamonds), Nyiragongo 2016 sample (yellow diamond), Nyiragongo scoria cones samples (black diamonds) and all Nyamuragira samples (white circles)

T and P

Magma temperatures were estimated by a geothermometer Olivine-liquid. The olivine / liquid geothermometer is based on the coexistence of the olivine balance with magmatic liquid (Putirka, 2008), in accordance with Roeder's Balance Test and Emslie (1970) proposing a Fe-Mg partition coefficient between olivine and liquid of 0.27 ± 0.03 . The determinations made with the olivine / liquid geothermometer were carried out under 0.1 kbar conditions.

The temperature values range from 1022 ° C and 1234° C for Nyiragongo and from 1023° C and 1145° C for Nyamuragira.

Magma pressures were estimated by a geobarometer Clinopyroxene-liquid in accordance with Masotta et al., (2012). The pressure values are 0,7-1,1 kbar for Nyiragongo and 0,9-1,2 kbar for Nyamuragira.

3.2 Petrography

All the thin sections produced were observed at the optical microscope and for each sample a systematic description of the fabric was made, as well as the mineral phases and the possible inclusions present, distinguishing, where possible, between phenocrysts and the mass.

This study also avail itself of the use of the scanning electron microscope (fig 3.14) to detect any minerals in the groundmass not easily distinguishable from the optical microscope alone. Petrographic analysis is described in groups with similar features.

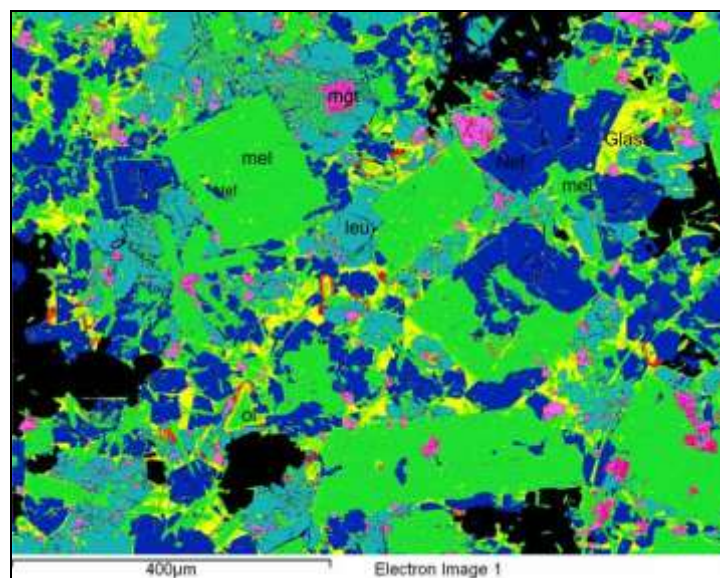


Figure 3.14 Sem image of a melilitite

3.2.1 Nyiragongo samples

Eruptive event of 1977

The 1977 lava samples resulting from an event of triggering drainage of magma stored in the crater lava lake, display a moderately porphyritic texture consisting mainly of small

phenocrysts of olivine, clinopyroxene, melilite, nepheline and occasionally apatite (Fig. 3.15-3.16) plus diffuse magnetite, set into a hypocrySTALLINE groundmass of the same phases plus leucite. All 1977 samples are characterized by fine grain size and not alteration of the mineral phases is visible but rather in some crystals glass inclusions occur.



Figure 3.15-3.16 Plane and cross polarized light images of the texture of 1977 representative sample.

Eruptive event of 2002

Also the 2002 lava samples come from a huge triggering drainage of magma from the lava lake which create few lava flows: proximal ones within Shaheru cone (Shaheru rock group) and distal ones up to the lake Kivu along the Muningi/Monigi fracture (Muningi rock group). Both rock groups are characterized by similar petrographic features: despite the different grain size distribution of crystals in all the thin sections, the texture is porphyritic and the predominant phase is euhedral melilite (fig 3.17-3.18). The groundmass varies from holocrystalline (fig 3.19) to hypohyaline (fig 3.17; 3.21), the phenocrysts consist mainly in melilite, (as previously mentioned), nepheline, olivine, leucite, clinopyroxene in decreasing order of abundance, plus diffuse magnetite microliths and accessory apatite.

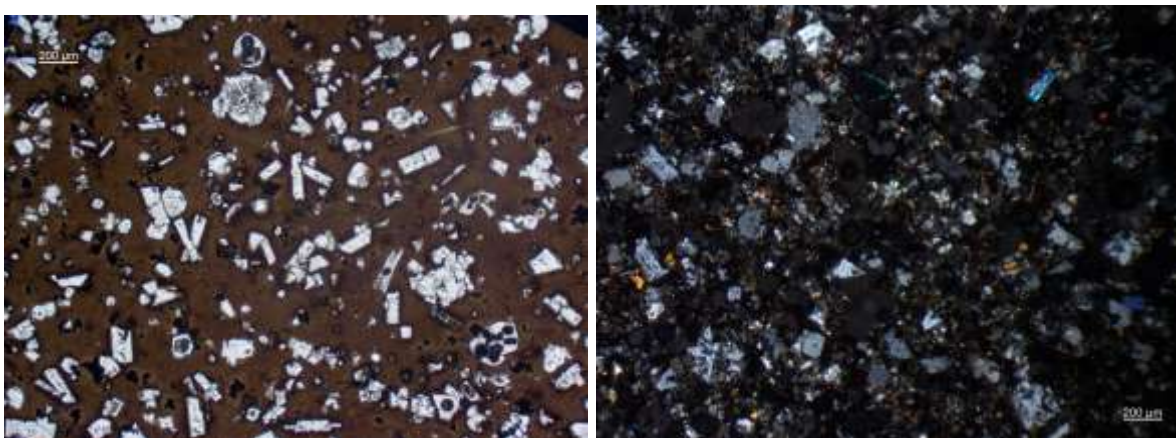


Figure 3.17-3.18 Plane and cross polarized light images of the texture of 2002 representative sample

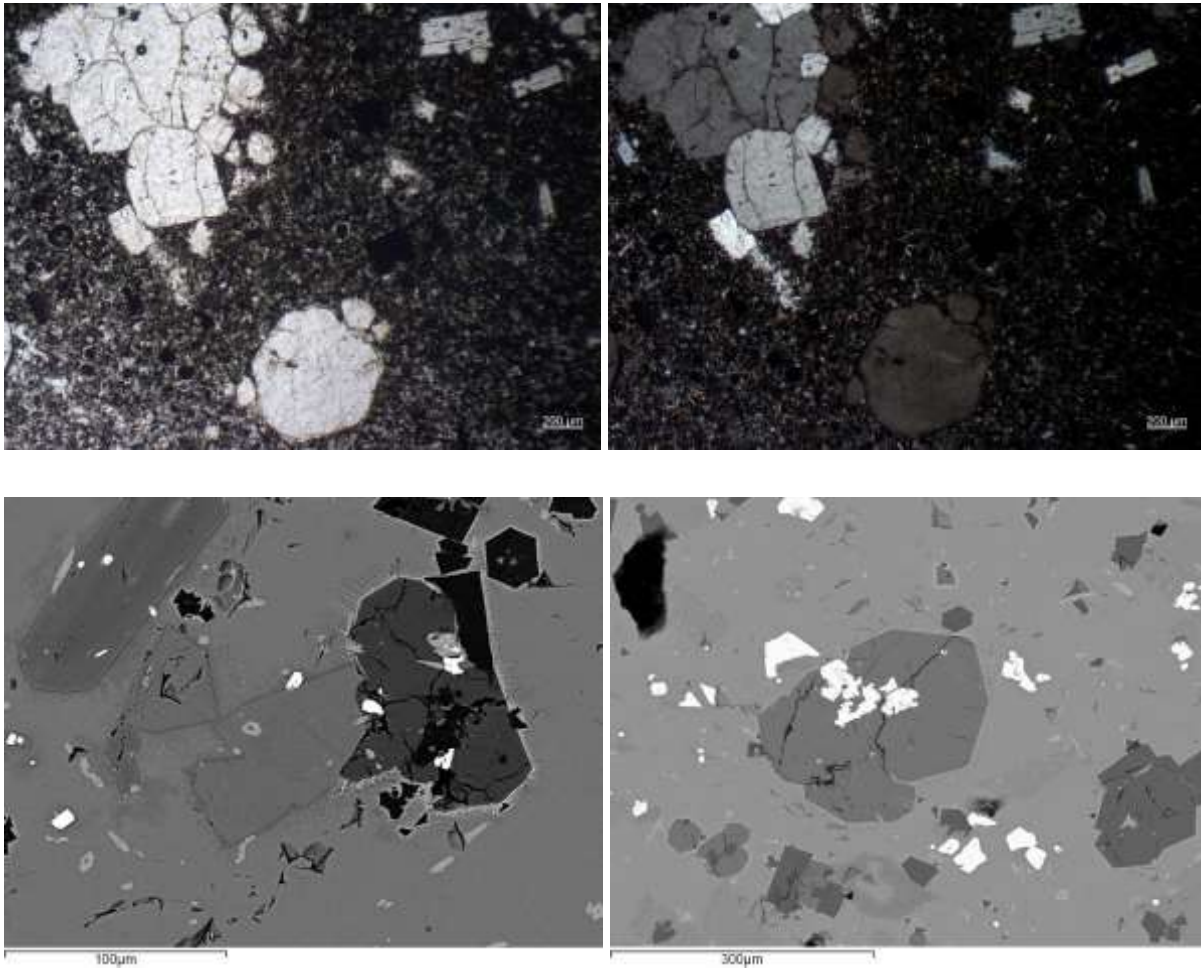


Figure 3.19-3.22 Plane and cross polarized light images and Sem images of the texture of 2002 representative sample
Eruptive event of 2016

Sample NY16 is characterized by a moderately porphyritic (porphyritic index P.I. about 3%) texture dominated by small euhedral melilite phenocrysts, euhedral to subhedral olivine, nepheline (occasionally forming monomineralic aggregates), leucite and clinopyroxene phenocrysts, generally smaller with respect to those observed in samples from 2002 eruption. The groundmass consists of a highly vesicular brown glass with sparse magnetite (locally occurring also as phenocrysts) and apatite microliths (Fig 3.23-3.24).

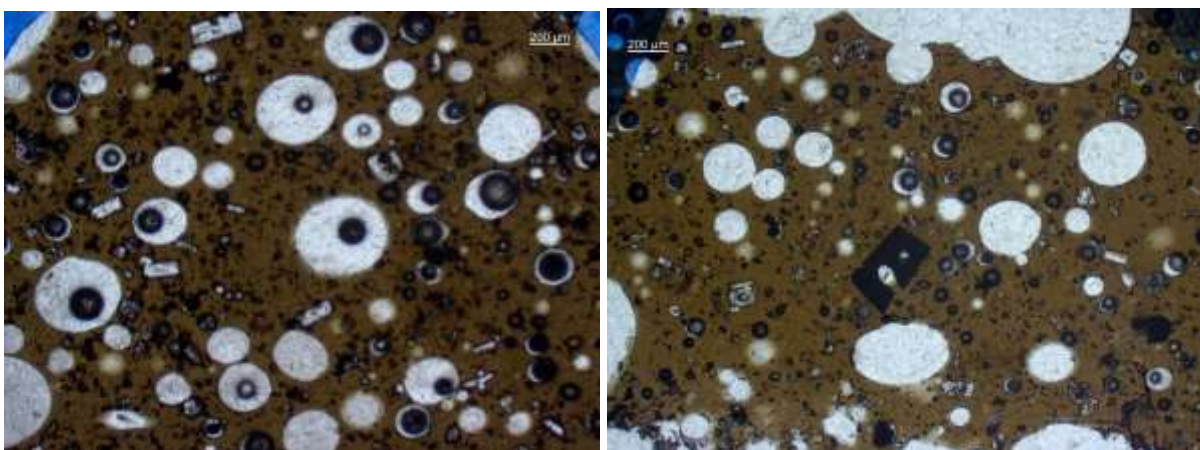


Figure 3.23-3.24: Plane polarized light images of the texture of 2016 representative sample

Scoria cones of Lac Vert and Mont Goma

Samples from Lac Vert cone present a highly porphyritic glomero-porphyritic texture consisting mainly of big phenocrysts of olivine, melilite and some clinopyroxene, set into a hypocrySTALLINE groundmass with magnetite and sparse apatite microliths plus the other principal mineal phases mentioned above.

Mont Goma samples on the contrary are ash/cineritic lithotypes and they present a vitrophiric texture with sparse phenocrysts of clinopyroxene and magnetite (fig 3.25-3.28).

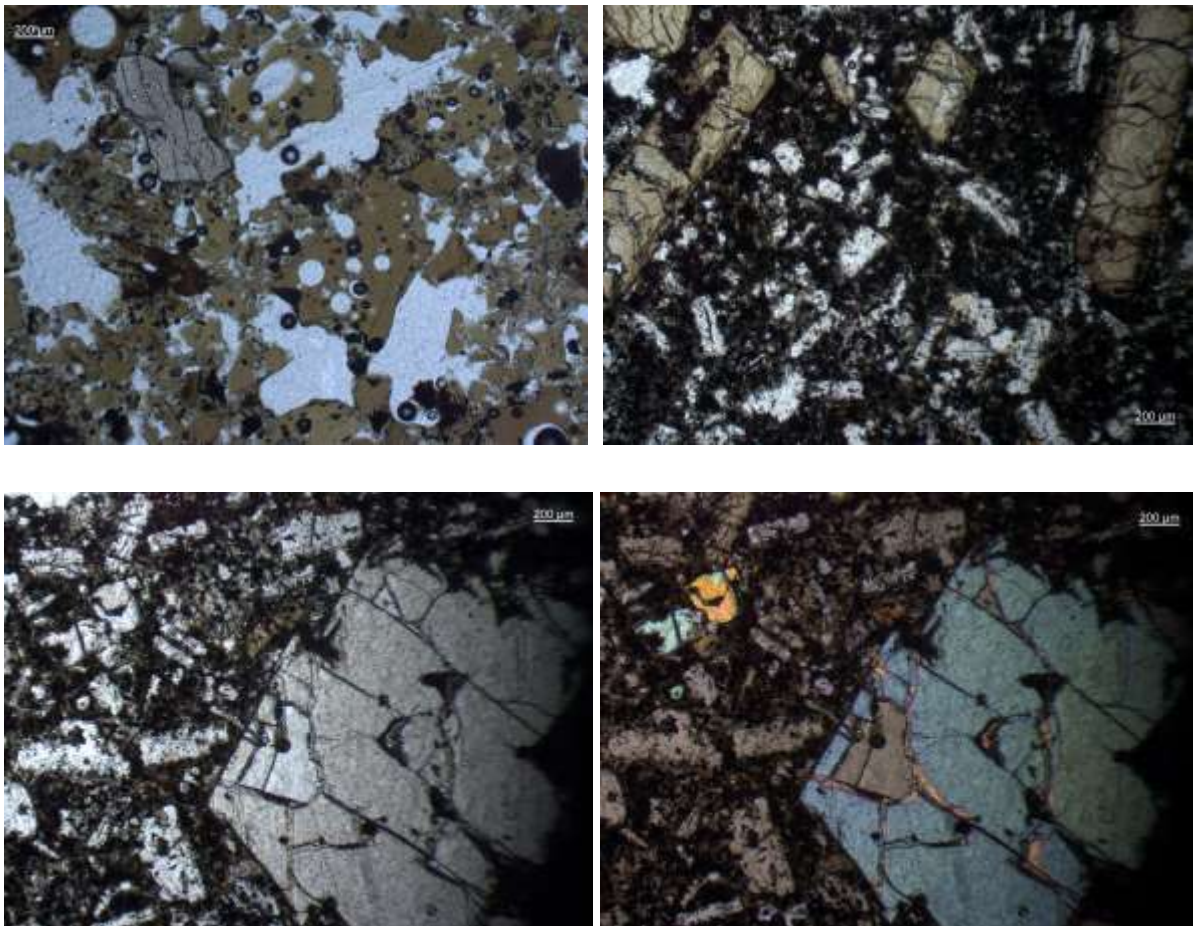


Figure 3.25-3.28 Plane and cross polarized light images of the texture of scoria cones representative sample

3.2.1 Nyamuragira samples

Eruptive events of 1938 and eruptive event of 1948

Both lava samples, 1938 ones and 1948 ones, show similar features: they display a porphyritic glomero-porphyritic texture consisting mainly of euhedral phenocrysts of olivine, clinopyroxene, plagioclase, which often occurs in small aggregates, plus diffuse magnetite as microliths as well as inclusions odd pecilitic and accessory apatite set into a hypocrySTALLINE groundmass (fig 3.29-3.30)

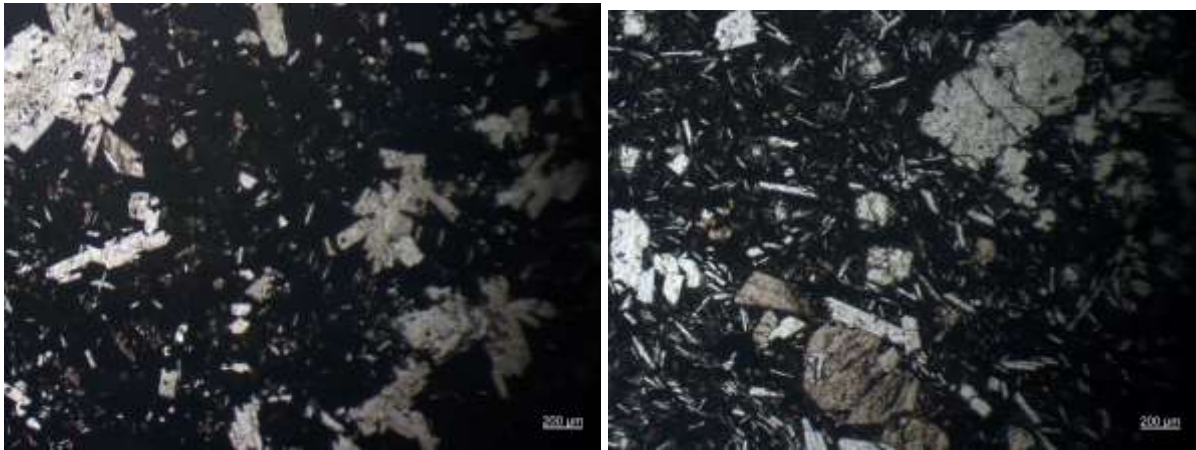


Figure 3.29-3.30 Plane and cross polarized light images of the texture of 1938 and 1948 representative sample

Eruptive event of 2010-2011

The 2010 samples are characterized by porphyritic texture too where the main phenocrysts are olivine and clinopyroxene which display high grain size and plagioclase low grain size and often in aggregates, the groundmass is holocrystalline at some cases and vitrophiric in others with microliths of magnetite, nepheline and leucite (fig 3.31-3.32)

The 2011 samples display a fluidale texture and the olivine is glomero (fig. 3.33)

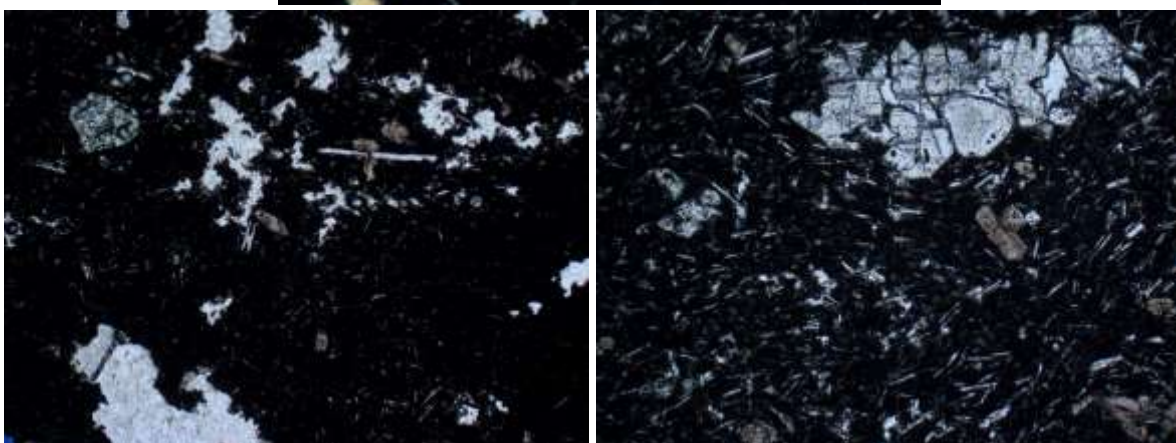
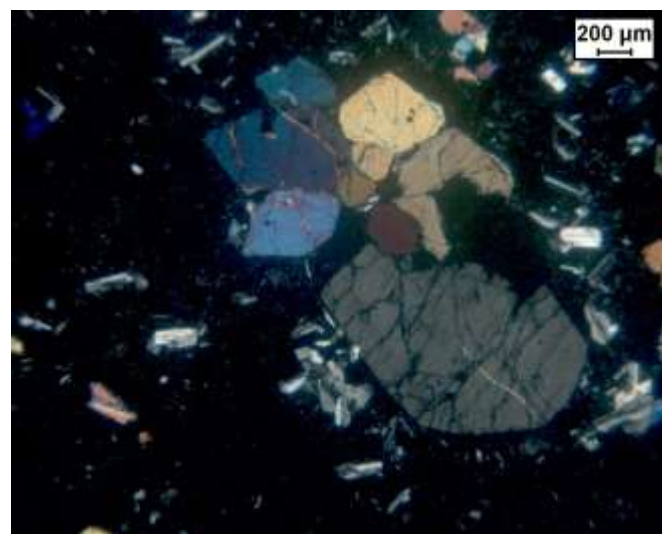


Figure 3.31-3.33 Plane and cross polarized light images of the texture of 2010/2011 representative sample

Older lavas

These lava were all sampled close to the Lake Kivu, they present a porphyritic texture and a medium grain size distribution of the mineral phases such as olivine, clinopyroxene and rare feldspar plus accessory magnetite. The groundmass is hypocrySTALLINE with the same mineral phases as megacrysts. Often the crystals display a fractured a pecilitic fabric (fig 3.34-3.36).



Figure 3.34-3.36 Plane and cross polarized light images of the texture of representative samples of older lavas of Nyamuragira.

Chapter 4

Mineral chemistry

All the data presented in this section are representative analysis of some of the samples.

4.2 Mineral chemistry

4.2.1 Olivine

Olivine is a principal mineral, present in almost all the samples of both Nyamuragira and Nyiragongo and it occurs like phenocryst as well as microlith of the groundmass. Olivine crystals in melilitites are characterized by heterogenous composition: the majority of the samples show values with forsterite content ranging from 40 to 84 wt % within all the 1977, 2002 and 2016 samples. The Ca and Mn contents increase with increasing Fe (fig 4.1). Mg# is 62-80. The kirschsteinite, the iron rich variant of monticellite, though evidently rarer, is known from silica-poor magmatic rocks such as melilite-nephelinites, is an accessory phase of some of the melilititic rocks, in particular within Shaehru samples, Nyiragongo in fact represent the first locality discover of this mineral (Sahama T.G. 1957), afterwards it was noticed also in other volcanic district like Colli Albani as taken an Italian example (Melluso et al., 2010).

Here the composition of kirschsteinite is not constant ranging from $\text{Ca}_{46}\text{Mg}_{10}\text{Fe}_{44}$, and $\text{Ca}_{22}\text{Mg}_{18}\text{Fe}_{60}$ with Mg# $[\text{Mg} * 100 / (\text{Mg} + \text{Fe})]$ clustering around 24 and 11.

Olivine in the basanites presents a similar composition with a Fo content ranging from 40 to 88 wt %, considering both phenocryst and microliths of the groundmass. Tholeiitic basalt sample shows the highest Mg# that is 88 (Fig).

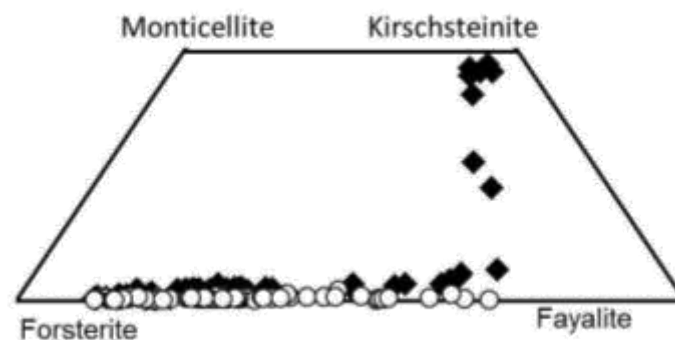
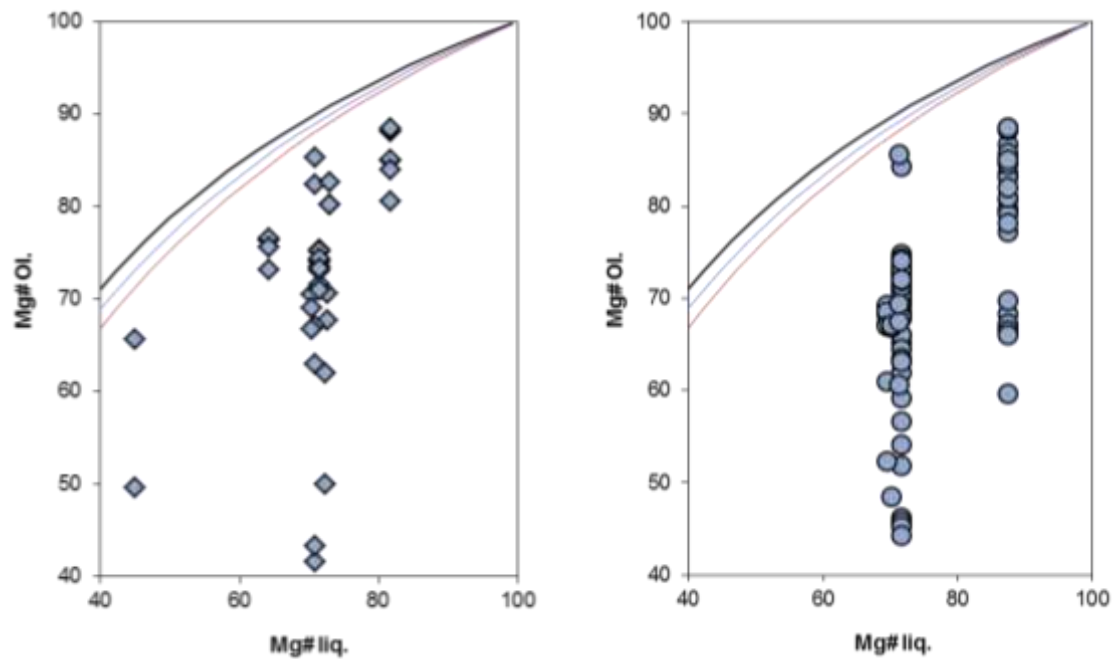


Figure 4.1 Olivine composition diagram



4.2.2 Pyroxene

Pyroxenes are both present in Nyiragongo rocks and Nyamuragira ones, but less abundant than olivines. Their presence is much abundant in the basanites where they occur often as phenocrysts and less abundant in the nephelinites where they occur rarely as phenocryst and diffuse in the groundmass.

The pyroxenes in the nephelinites of Nyiragongo are monoclinic and their composition is exclusively diopsidic $W_{O46-54}En_{24-33}Fs_{13-30}$ with Mg# 45-82 (fig 4.2).

The pyroxenes in the basanites of Nyamuragira are also all monoclinic with the exception of the tholeiitic basalt which display orthopyroxenes together with the clinopyroxenes. Thus the composition range between the diopside field ($W_{O46-50}En_{35-39}Fs_{13-14}$) the augite field ($W_{O27-37}En_{38-58}Fs_{15-28}$) and the pigeonite field ($W_{O10-16}En_{57-71}Fs_{17-27}$). The Mg# varies from 57 to 82. Finally all the clinopyroxenes are in equilibrium with low pressure (fig 4.3) as highlighted by the barometer estimation.

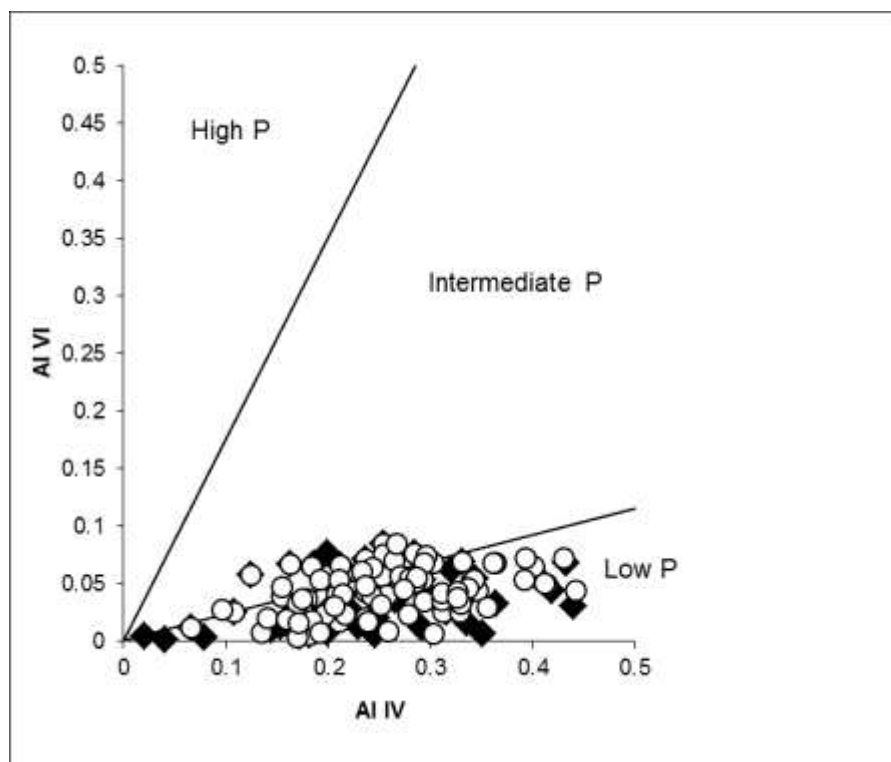
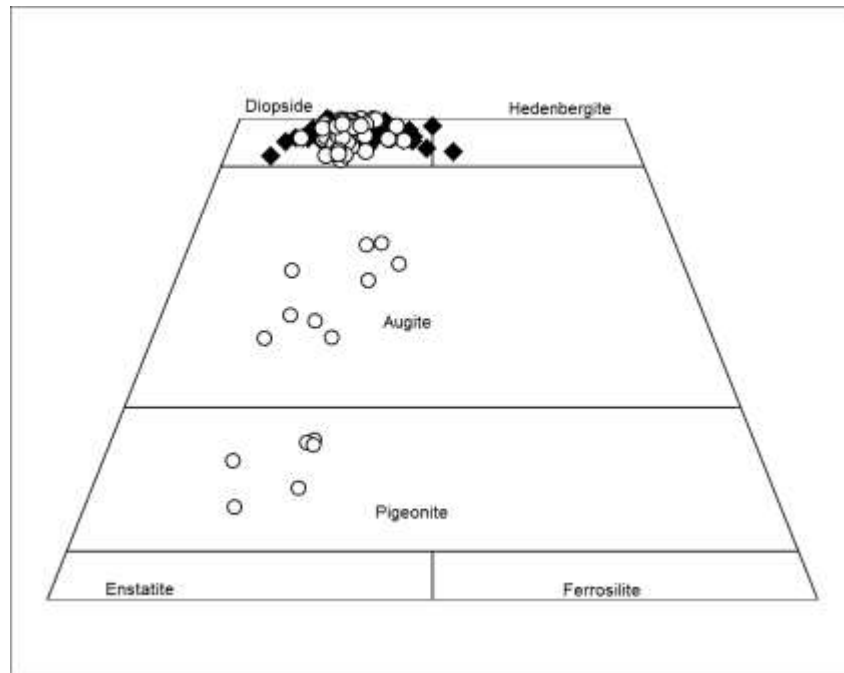
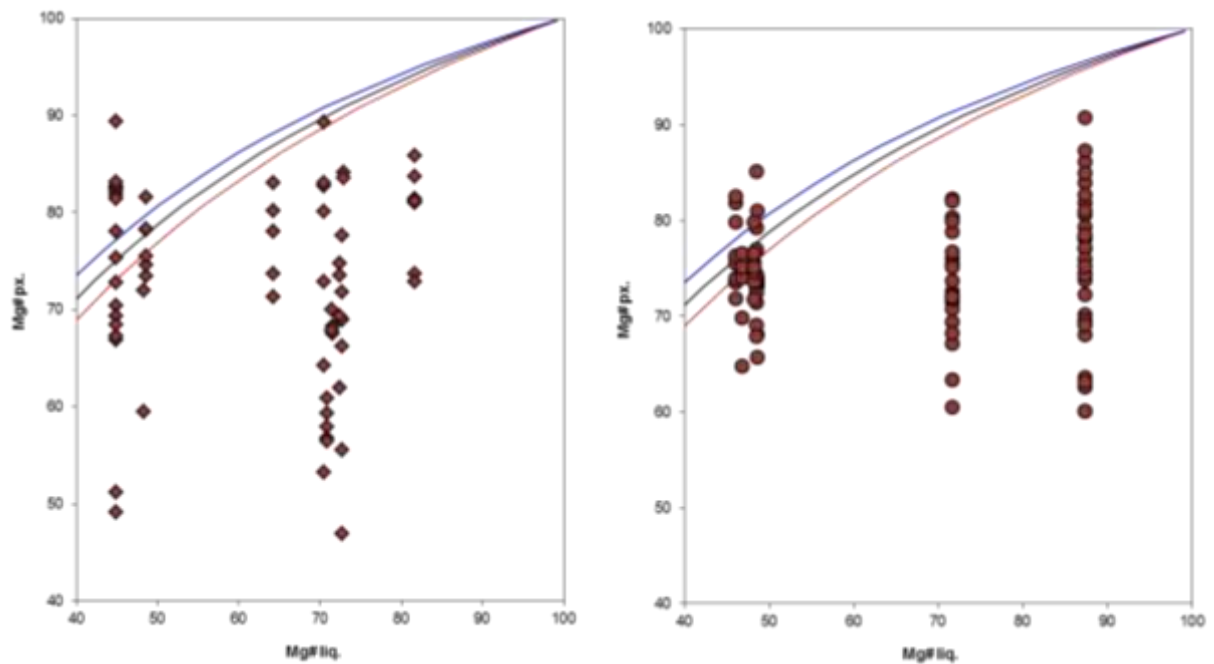


Figure 4.2-4.3 Pyroxene composition diagrams



4.2.2 Melilite

Melilite is a fundamental mineral of the nephelinites and olivine-melilitites of Nyiragongo, on the contrary it is completely absent in the basanites of Nyamuragira.

In all the samples melilite occurs as euhedral phenocrysts or microliths although the grain size distribution is variable in the samples. The composition is relatively constant, that is akermanite (40-66 mol %, fig 4.4) and the Mg# is 65-83.

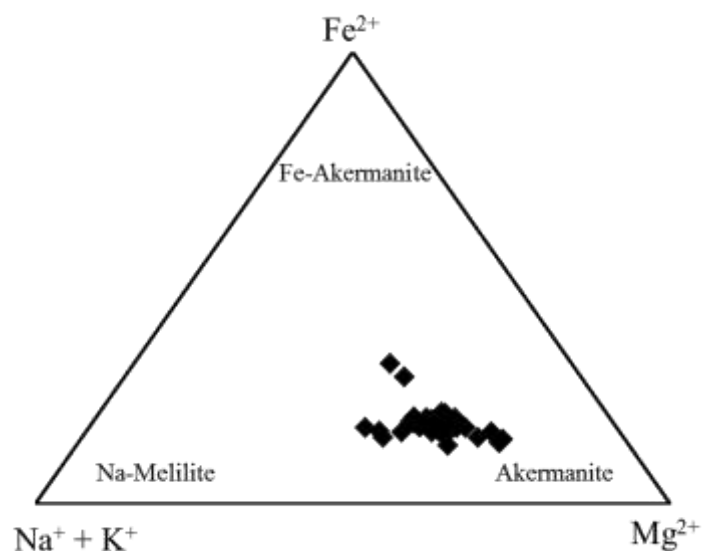


Figure 4.4 Melilite composition diagram

4.2.4 Feldspar

Feldspar is a fundamental and secondary mineral of the basanites of Nyamuragira; on the contrary it is completely absent in the nephelinites of Nyiragongo that are feldspar-free as

already mentioned. The composition plotted (fig 4.5) is related to all the mineral phases of all the samples analysed without any distinction between phenocrysts and groundmass.

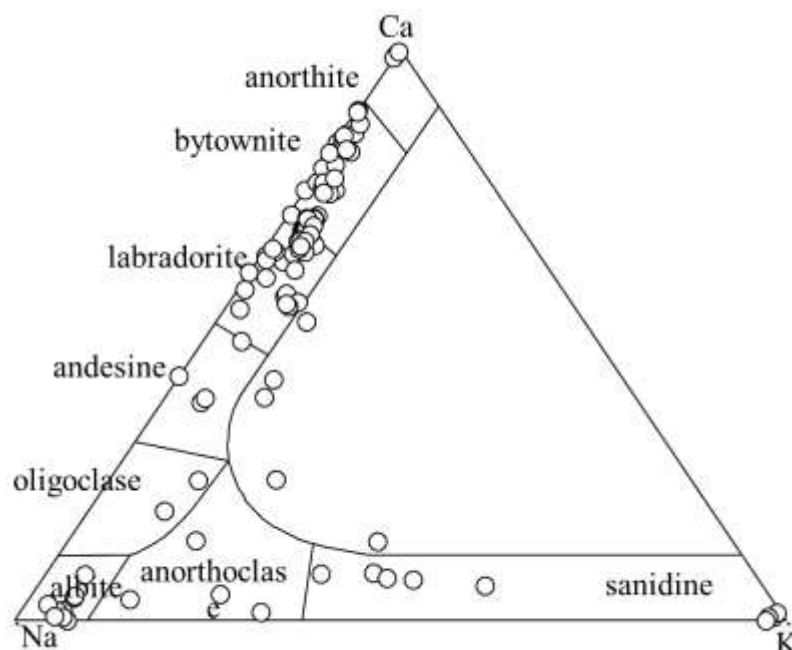


Figure 4.5 Feldspar composition diagram

4.2.5 Nepheline and leucite

Nepheline and leucite are almost ubiquitous, and often the only felsic minerals in the Nyiragongo and Nyamuragira rocks, both present in phenocrysts role as well as in the groundmass. The nephelinites contain potassic nepheline ($\text{Ne}_{54-78}\text{Kal}_{21-45}$) having K_2O from 7.2 to 13.1 wt.%, the basanites display a more K-enriched composition: ($\text{Ne}_{53-94}\text{Kal}_{3-46}$) with K-content up to 14.9 wt.% (fig 4.6). Leucite shows K-contents up to 1.99 (mol %) Fig.

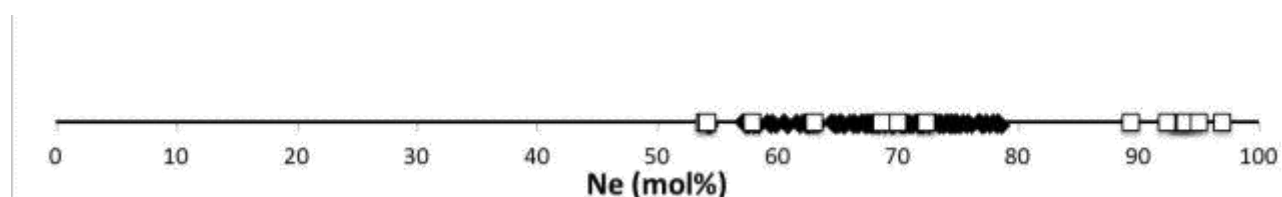


Figure 4.6 Nepheline composition diagram.

4.2.5 Other minerals

Magnetite is the main oxide of the Nyiragongo and Nyamuragira lavas, the mineral has limited compositional variations in terms of Fe (55-70 wt. %) and is relatively rich in Mn (0.6-1.9 wt. %). Chromiferous spinel is a rare phase hosted in olivine (fig. 4.7). Apatite present as an accessory phase, is moderately rich in F with content up to 2.2 wt.%, fluoroapatite.

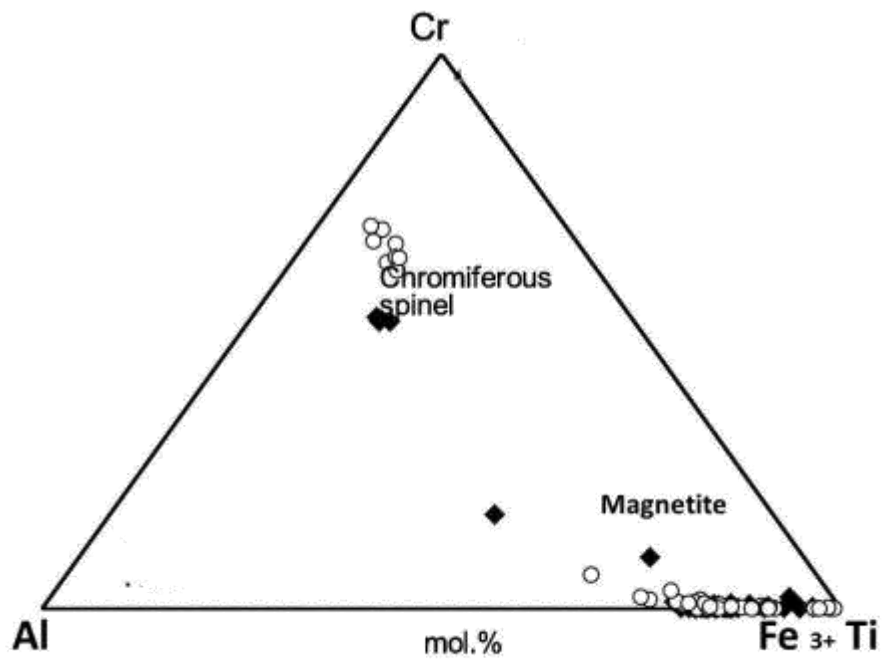


Figure 4.7 Oxide composition diagram.

4.2 Glass and mineral trace elements concentrations

The partitioning of trace elements between crystals and melts provides an important petrogenetic tool for understanding magmatic processes. Although trace-element partition coefficients are a powerful and widely used tool in modeling the evolution of magmatic systems, reliable data sets that describe the trace-element partitioning behavior in strongly silica-undersaturated, highly alkaline liquids are still scarce or lacking (Onuma N. 1981).

Here are presented a new set of partition coefficients measured for olivine, clinopyroxene, melilite, nepheline, leucite, magnetite and apatite phenocrysts in equilibrium with nephelinitic glasses at Nyiragongo volcano.

Our data refer to two fresh of lava samples from 2002 and 2016 eruption events (fig. 4.9-4.10).

Owing to their glassy nature and their moderately porphyritic character, lavas of strongly silica-undersaturated, mafic melilite-bearing volcanics from Nyiragongo represent a unique opportunity to obtain high quality data on mineral/melt trace element partitioning that can be used with confidence to model the evolution of silica-poor and alkali-rich magmas.

A new set of mineral/liquid partition coefficients for different mineral phases is here provided, obtained by LA-ICP-MS investigations of two selected samples characterized by all the crystals showing textural features consistent with a direct segregation from the host lavas and by completely glassy and fresh groundmass.

Sample NY02 displays a moderately porphyritic (porphyritic index P.I. about 6%) glomeroporphyritic texture consisting mainly of small phenocrysts of melilite, leucite, nepheline and olivine (in decreasing order of abundance), plus diffuse magnetite microliths and accessory apatite, set into a moderately vesicular brown, glassy groundmass. Sporadic aggregates of nepheline are also observed.

Sample NY16 is characterized by a moderately porphyritic (porphyritic index P.I. about 3%) texture dominated by small euhedral melilite phenocrysts, euhedral to subhedral olivine, nepheline (occasionally forming monomineralic aggregates), leucite and clinopyroxene phenocrysts, generally smaller with respect to those observed in sample NY02. The groundmass consists of a highly vesicular brown glass with sparse magnetite (locally occurring also as phenocrysts) and apatite microliths. They were both classified as melilitites following Le Maitre (2002).

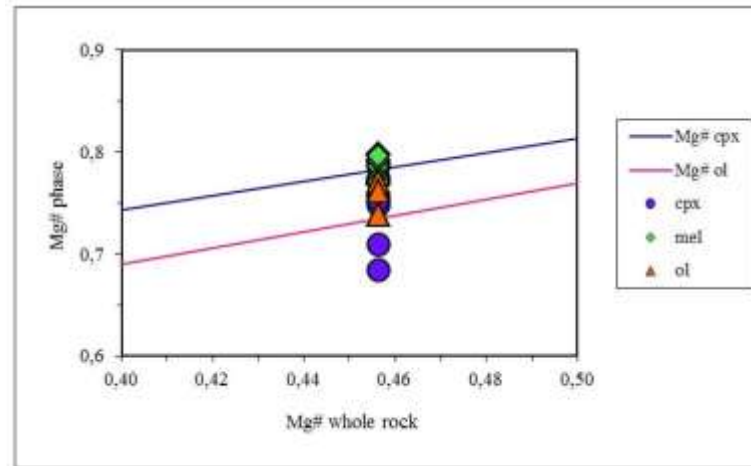


Figure 4.8 Mg# whole rock vs Mg# mineral phases for melilititic rocks, curves from Roeder & Emslie (1970) for olivines and from Grove & Bryan (1983).

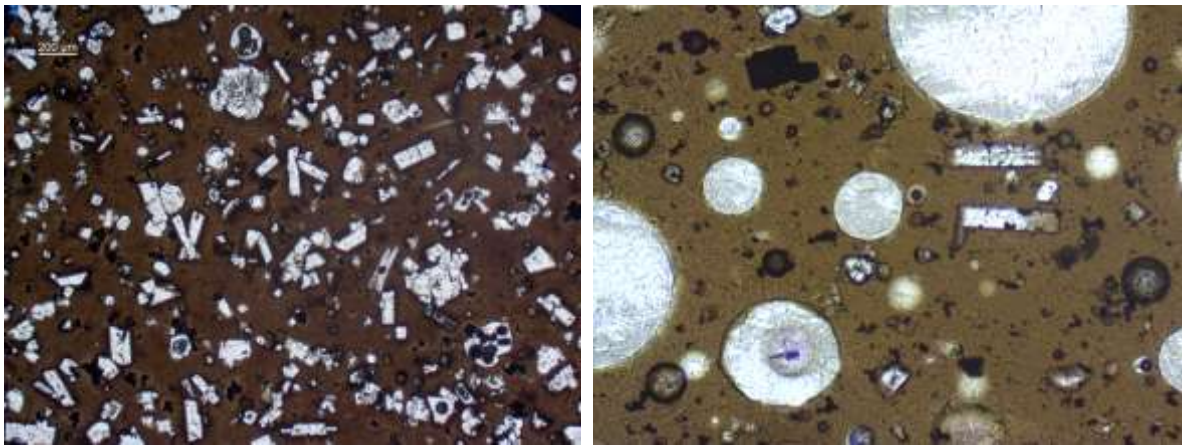
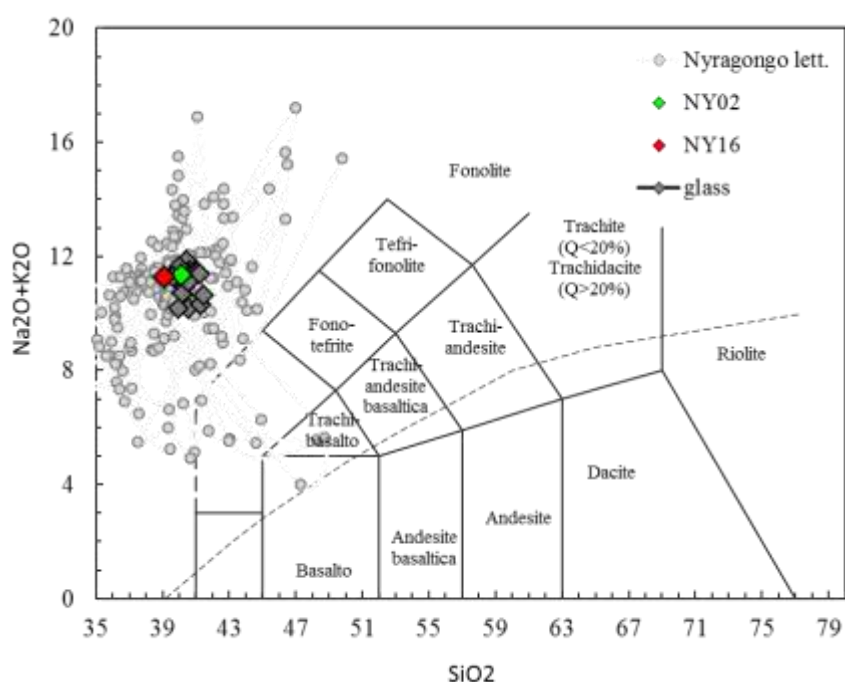


Figure 4.9-4.10 Representative textures of 2002 and 2016 samples.

Looking at the major element compositions of the two rocks, it can be said that the melilitite NY02 and the melilitite NY16 have quite similar compositions (see Table and or Fig. 4.11) with MgO ranging around 4.02 and 4.19 wt.%, SiO₂ (39.12-40.17 wt.%), the sum of alkalis is around 11.26-11.36 wt.%, CaO ranges around 12.01-12.21 wt.% and TiO₂ is 2.74 in NY02 and 2.81 in NY16. Instead Ni varies: <20ppm in NY02 and 50 ppm in NY16; Zr varies from 273 ppm and 313 ppm respectively; finally Sr and Ba are not homogeneous in the two samples with Sr ranging from 2693 ppm to 3474 ppm and Ba from 2278 ppm to 2389 ppm. The Mg# value [molar Mg*100/(Mg+Fe²⁺)] is 41 in NY02 sample and 40 in NY16 sample.

	NY02	NY16
SiO ₂	40.17	39.12
TiO ₂	2.742	2.812
Al ₂ O ₃	14.72	14.87
Fe ₂ O ₃	13.22	13.41
MnO	0.286	0.293
MgO	4.19	4.02
CaO	12.21	12.01
Na ₂ O	5.8	5.62
K ₂ O	5.55	5.64
P ₂ O ₅	1.47	1.59
LOI	-1.63	0.39
Total	98.74	99.77
Sc	5	4
V	285	287
Ni	< 20	50
Rb	140	138
Sr	3474	2693
Y	37	34
Zr	273	313
Nb	227	239
Ba	2389	2278
La	197	201
Ce	365	373

Tab 4.11 Major and trace elements of the samples.



Glass

The glassy groundmass within sample NY02 displays a relatively homogeneous nephelinitic composition, nevertheless it is characterized by some elements which show compositional ranges considerably large: low SiO₂ (39.8-40.6 wt.%), Al₂O₃ (13.4-14.6 wt.%), high Na₂O

(5.52-7.93 wt.%) and K_2O (3.67-5.79 wt.%), low MgO (2.12-3.94 wt.%), FeO (12.0-13.0 wt.%), TiO_2 (2.23-3.22 wt.%) and CaO (10.8-12.6 wt. %). The $Mg\#$ value is in the range of 23-35.

The analysed glass from sample NY16 also has a quite homogeneous nephelinitic composition but, with low SiO_2 (39.7-41.0 wt.%), Al_2O_3 (14.2-15.3 wt.%), Na_2O (4.51-5.60 wt.%) and K_2O (5.22-6.16 wt.%), high MgO (3.86-4.45 wt.%), FeO (11.4-12.4 wt.%), TiO_2 (2.09-3.29 wt.%) and high CaO (11.1-12.5 wt.%). The $Mg\#$ is generally higher with respect to sample NY02, ranging from 37 to 40.

Glasses from both melilitites have a homogeneous trace element composition that closely matches the whole rock one, with same abundances observed: Cl-normalized trace element diagram is L-REE enriched and nearly depleted in the HREE region (fig 4.13), the glass compositions plotted is an average value.

Olivine

The composition of olivine from melilitite NY02 is remarkably homogeneous, ranging from $Ca_2Mg_{71}Fe_{27}$ to $Ca_2Mg_{75}Fe_{23}$ (Table X). the $Mg\#$ values range from 72 to 75.

In the melilitite NY16 sample the olivine composition is quite similar to the previous sample with $Ca_2Mg_{75}Fe_{23}$ and $Mg\#$ up to 76.

Olivines show a REE pattern with an enrichment in LREE (La/Sm ~10) and then smoothly decreasing normalized-abundances from Gd to Lu (fig. 4.13).

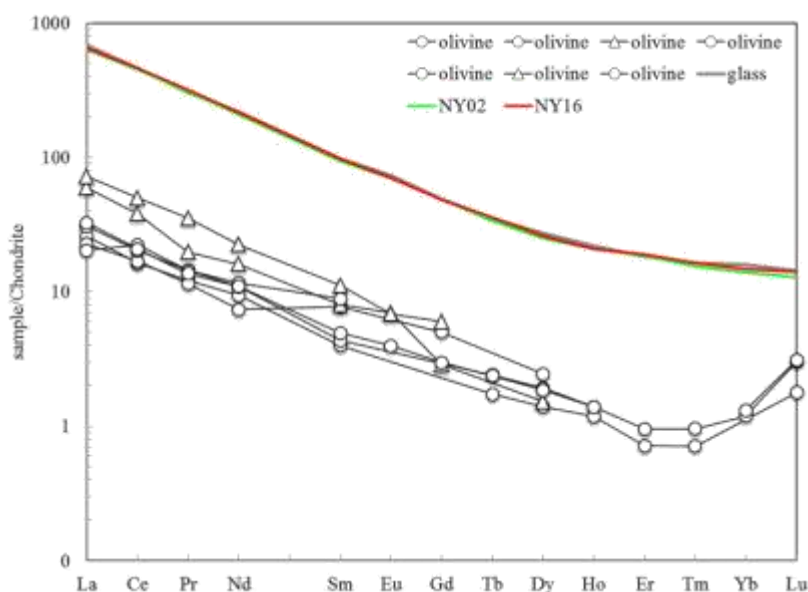


Figure 4.13 REE patterns for olivines with whole rocks (Ny02 green line; Ny16 red line) values and glass (black line) in average value. Ny02 olivines (triangles), Ny16 olivines (circles)

Clinopyroxene

Clinopyroxene was found only in melilitite sample NY16, plotting mostly above the diopside field (Fig. X) in the Ca-Mg-Fe diagram and showing $Mg\#$ values ranging from 68 to 78. The

Al-content varies considerably (Al_2O_3 1.20–8.80 wt.%) as well as TiO_2 (1.10–5.40 wt.%) like other Nyiragongo melilitites which have up to 5% TiO_2 and 8% Al_2O_3 (Platz et al., 2004). On the contrary the Fe-content is relatively constant (6.50–8.40 wt.%) and as usual in the clinopyroxene of Virunga mafic rocks, the Na contents are low (< 0.34 wt.% Na_2O). REE element patterns are more enriched than the olivines with higher LREE/HREE (La/Yb ~30) with a peak in Eu (fig 4.14).

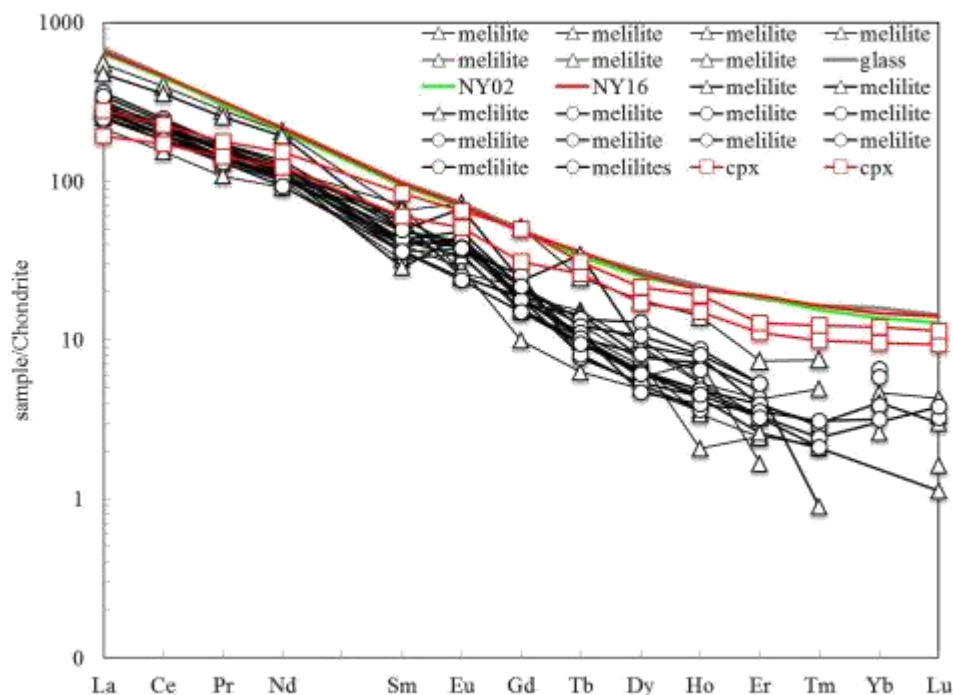


Figure 4.14 REE patterns for clinopyroxenes (red) and melilitites (black) with whole rocks (Ny02 green line; Ny16 red line) values and glass (black line) in average value. Ny02 melilitites (triangles), Ny16 melilitites (circles), Ny16 clinopyroxene (squares).

Melilite

Melilite of Nyiragongo 2002 lava is typically a solid solution of akermanite (43–55 mol.%), Fe-akermanite (14–18 mol.%), soda melilite (27–35 mol.%) and gehlenite (2–6 mol.%). The Mg# varies from 75 to 80 and less variation in Al_2O_3 (= 6–9 wt%).

Melilite of Nyiragongo 2016 lava has relatively different compositions with respect to the 2002 ones: akermanite (53–66 mol.%), Fe-akermanite (14–22 mol.%), soda melilite (23–26 mol.%) and gehlenite (2–6 mol.%). The Mg# varies from 77 to 79. The Sr content is relatively low (0.4–0.7 wt.%) like melilite of Nyiragongo rocks (Platz et al., 2004).

LREE/HREE for melilitites is also high (La/Yb ~79–160) and La/Sm is 6–16 (fig 4.14).

Nepheline and leucite

Nepheline in sample NY02 ranges in composition ($\text{Ne}_{66-78}\text{Ks}_{22-34}$, components in wt.%), whereas in sample NY16 the values are lower ($\text{Ne}_{58-66}\text{Ks}_{32-42}$). There is little excess silica in nepheline, as expected for nepheline crystallized from highly silica-undersaturated magmas (e.g., Melluso et al., 2010 and references therein). Leucite composition is stoichiometric and quite homogeneous for both samples; it is relatively poor in Ba (0–1 wt.% BaO).

The La/Yb ratio (4) for leucite and (0.8-3) for nepheline show their low REE content (fig. 4.15).

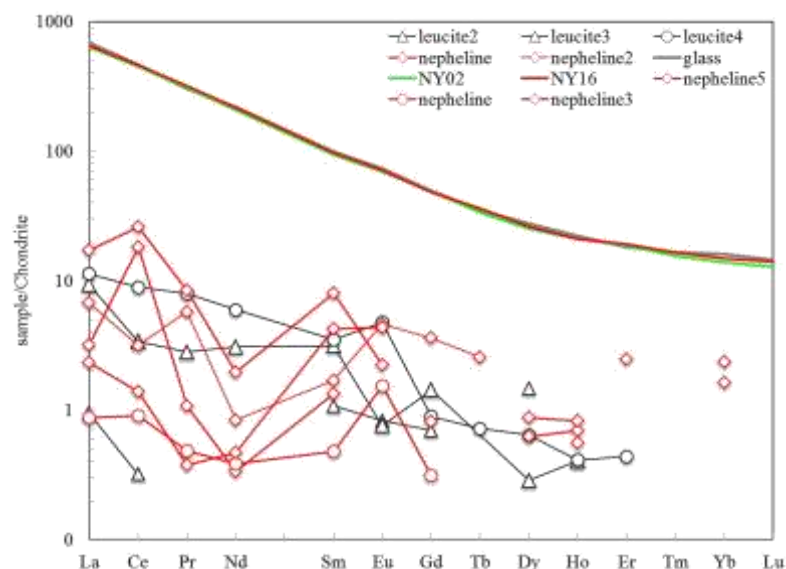


Figure 4.15 REE patterns for nephelines and leucites with whole rocks (Ny02 green line; Ny16 red line) values and glass (black line) in average value. Ny02 feldspatoids (triangles), Ny16 feldspatoids (circles)

Magnetite and apatite

The spinel mineral in the melilitites is a magnetite-ulvospinel solid solution which is quite homogenous: $\text{Mag}_{84-86}\text{Usp}_{13-15}$ in melilitite NY02 and $\text{Mag}_{80-84}\text{Usp}_{15-20}$ in melilitite NY16. Low REE content, La/Sm (0.4-4.8), fig. 4.16.

Chemical analyses for major elements (tab) in 2002 sample show that apatites are relatively homogeneous in composition (P_2O_5 ranges from 37 to 39 wt.%, and CaO from 51 to 53 wt.%). All the analysed crystals are classified as fluor-apatite, with F 1.10-1.15 wt.%, except one which is a hydroxylapatite.

The 2016 apatite crystals show slightly higher P and Ca concentrations (P_2O_5 ranging from 39 to 43 wt.%, and CaO from 54 to 56 wt.%). The crystals are both hydroxylapatite and fluoroapatite: F ranges from 0.5 to 2. Apatites are extremely enriched in REE with La/Sm (9) and La/Yb (188-205). Sr content is 4963ppm in the 2002 sample and 5967 ppm in the 2016 one.

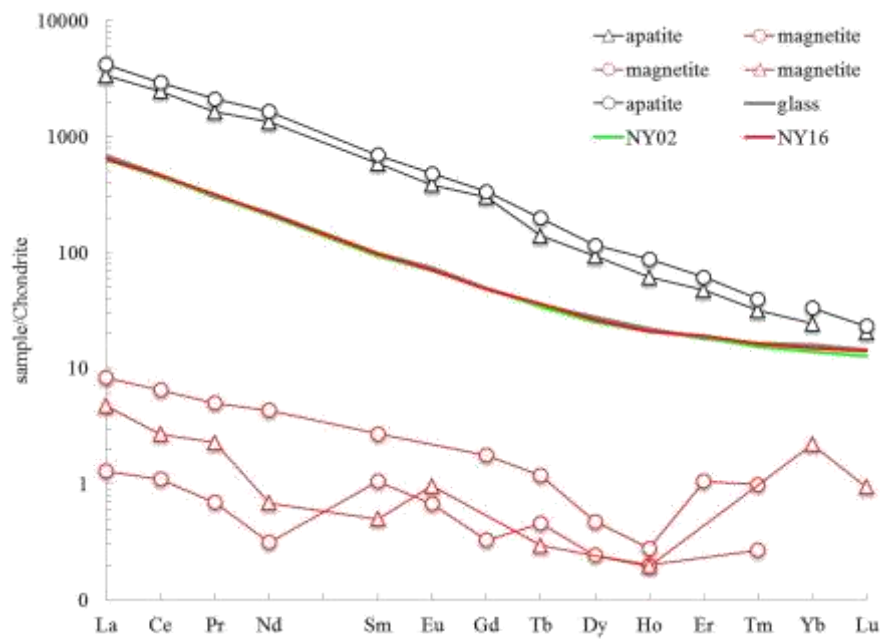


Figure 4.16 REE patterns for magnetite (red) and apatite (black) with whole rocks (Ny02 green line; Ny16 red line) values and glass (black line) in average value. Ny02 magnetites and apatites (triangles), Ny16 magnetites and apatites (circles)

Therefore, the present mineral and glass data can be used in order to calculate mineral/liquid partition coefficients

Calculation of $D^{\text{mineral/liquid}}$ values

The putative mineral/liquid trace element partition coefficients for the investigated melilitite systems have been calculated using the average composition for both mineral phases and groundmass glasses (see table below).

	Ol/glass	Cpx/glass	Mel/glass	Ap/glass	Ne/glass	Lc/glass	Mt/glass
	Average	Average	Average	Average	Average	Average	Average
Li	0.64	0.03	0.14		0.11	0.05	0.12
B	1.50	0.40	0.93	0.67	1.09	1.16	0.47
Sc	1.40	8.11	0.62		0.79	0.50	2.85
V	0.42	5.03	0.75	4.20	0.04	0.21	69.93
Cr	5.83	1.04	0.93	0.78	1.18	0.93	42.97
Co	5.17	0.93	1.05	0.06	0.02	0.03	7.94
Ni	23.50	2.26	0.83	0.29	0.07	0.12	37.97
Zn	0.78	0.15	1.07	0.07	0.04	0.04	2.22
Rb	0.23	0.13	0.65	0.04	44.69	211.52	0.05
Sr	0.01	0.23	1.11	1.22	0.14	0.01	0.00
Y	0.20	2.65	0.95	14.58	0.02	0.03	0.03
Zr	0.37	30.49	0.72	1.15	0.10	0.14	7.45
Nb	0.33	0.81	0.66	0.09	0.04	0.05	5.83
Cs	1.10		0.26		7.16	48.13	0.12
Ba	0.13	0.14	0.97	0.75	4.48	19.54	0.20
La	0.13	0.80	1.05	12.87	0.02	0.02	0.01
Ce	0.12	0.94	1.07	12.77	0.03	0.02	0.01
Pr	0.11	1.02	1.01	11.90	0.02	0.03	0.01
Nd	0.11	1.21	1.06	13.11	0.01	0.04	0.01
Sm	0.14	1.48	0.93	13.16	0.07	0.05	0.02
Eu	0.11	1.12	0.76	8.33	0.06	0.04	0.01
Gd	0.18	1.70	0.86	13.36	0.07	0.04	
Tb	0.06	0.81	0.37	4.78	0.07		0.01
Dy	0.17	1.80	0.74	9.66	0.07	0.07	0.03
Ho	0.07	0.85	0.29	3.68	0.03	0.02	0.01
Er	0.10	1.42	0.45	6.41	0.29	0.05	
Tm	0.03	0.38	0.10	1.23	0.09	0.08	
Yb	0.16	1.41	0.57	3.74	0.26	0.26	0.29
Lu	0.11	0.43	0.12	0.89	0.00	0.00	0.04
Hf	0.18	6.25	0.21	0.26	0.23	0.15	1.30
Ta	0.22	0.90	0.29	0.08	0.08	0.21	3.09
Pb	0.12	0.47	0.52	0.45	0.11	0.23	0.30
Th	0.36	0.68	0.61	13.11	0.06	0.05	0.05
U	0.11	0.35	0.32	4.94	0.07	0.13	0.05

Chapter 5

Petrochemistry

In order to identify the compositional differences between the Virunga analysed rocks, variation diagrams of the major and trace elements were built. For the construction of such diagrams requires the choice of a suitable parameter (index of differentiation) that can clearly discriminate the rocks analyzed and also to highlight the chemical variations of the studied elements studied. In this study was used the magnesium oxide.

5.1 Major Elements compositions

Variation diagrams for major elements are shown in fig.5.1-5.9 and were have been plotted both whole rocks values and values of some analysed glasses for Nyamuragira district and Nyiragongo volcanic district.

The MgO contents in Nyiragongo whole rocks range between 4.0 and 9.0 wt.%, the highest contents occur in Lac Vert group samples. Glasses have homogeneous composition.

Nyamuragira basanites have MgO (5.0-13.60 wt.%), contents within the ranges expected for mantle-derived liquids. The transitional basalts have higher MgO (> 15 wt.%), the glasses plotted show a negative correlation with MgO, increasing SiO₂.

Contents of SiO₂, like already visible in the TAS diagram, are ranging from 39 to 42 wt% in Nyiragongo samples and from 40 to 47 wt.% in Nyamuragira samples.

The TiO₂ contents vs MgO contents show clusters of the analysed data with a positive correlation for the Nyamuragira ones which also show the highest values. Fe contents (8-14 wt.%) display similar behavior and correlation as Ti.

CaO ranges from 8 to 16 wt.% in the nephelinites with the highest values linked to Lac Vert samples as well as MgO contents. The basanites show values ranging 8-14 wt.%, almost all the values display a positive correlation with MgO.

Alkali (Na₂O and K₂O) display same negative correlation and clusters with MgO, Nyiragongo rocks Na 3-7 and K 1-7; Nyamuragira rocks Na 1-4 and K 0.29-3.57, the lowest values is the basalt.

Al₂O₃ present different rock groups, quite the same groups showed in the other diagrams: it ranges 10-18 wt.% (Nyiragongo) and 9-16 (Nyamuragira).

MnO contenta are 0.17-0.29 wt.% and P₂O₅ is about 0.70-1.60wt.% in nephelinites and 0.1-0.5 wt.% in basanites.

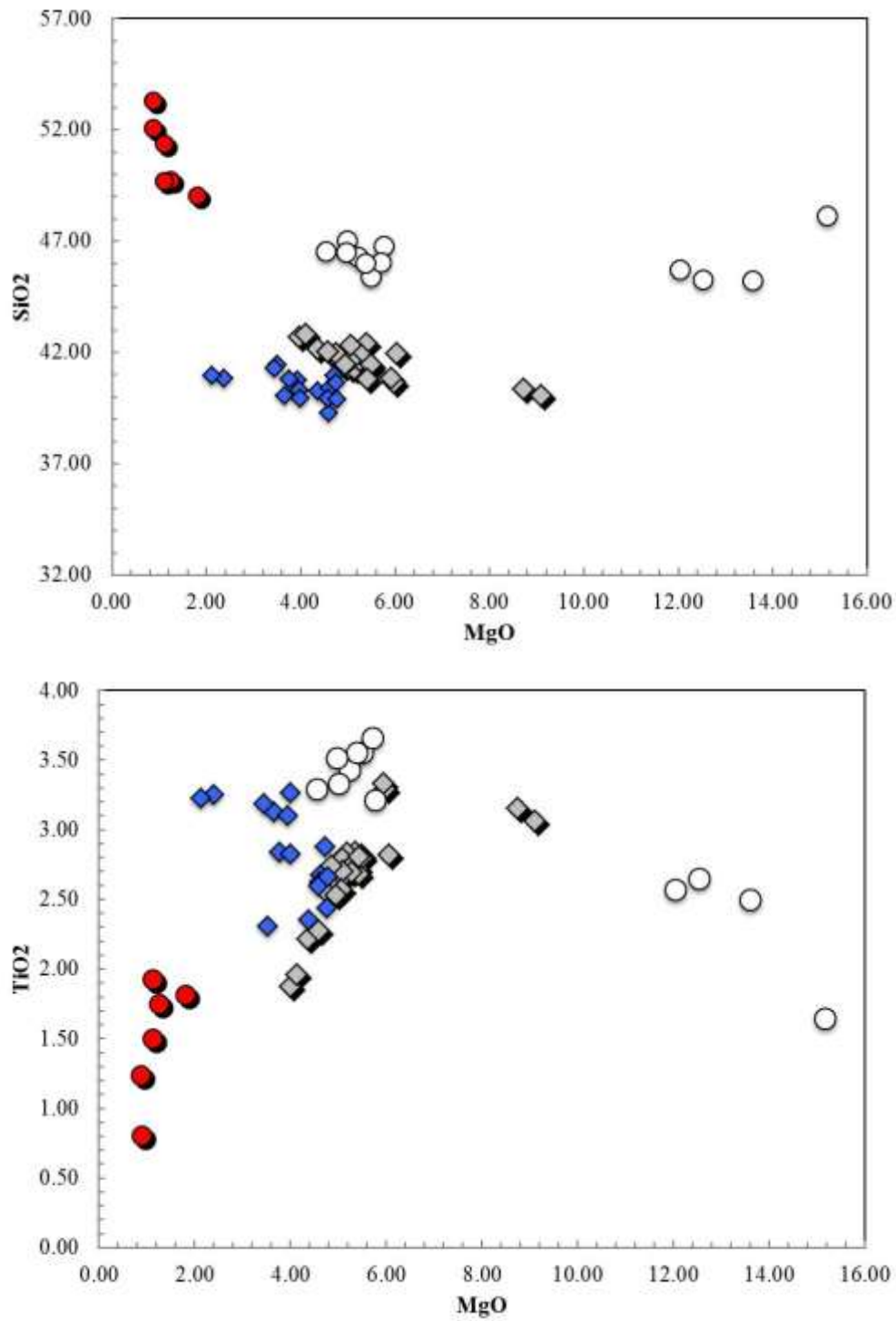


Figure 5.1-5.2 Variation diagrams: Nyiragongo whole rocks (grey diamonds), Nyiragongo glasses (blue diamonds); Nyamuragira whole rocks (white circles) and Nyamuragira glasses (red circles).

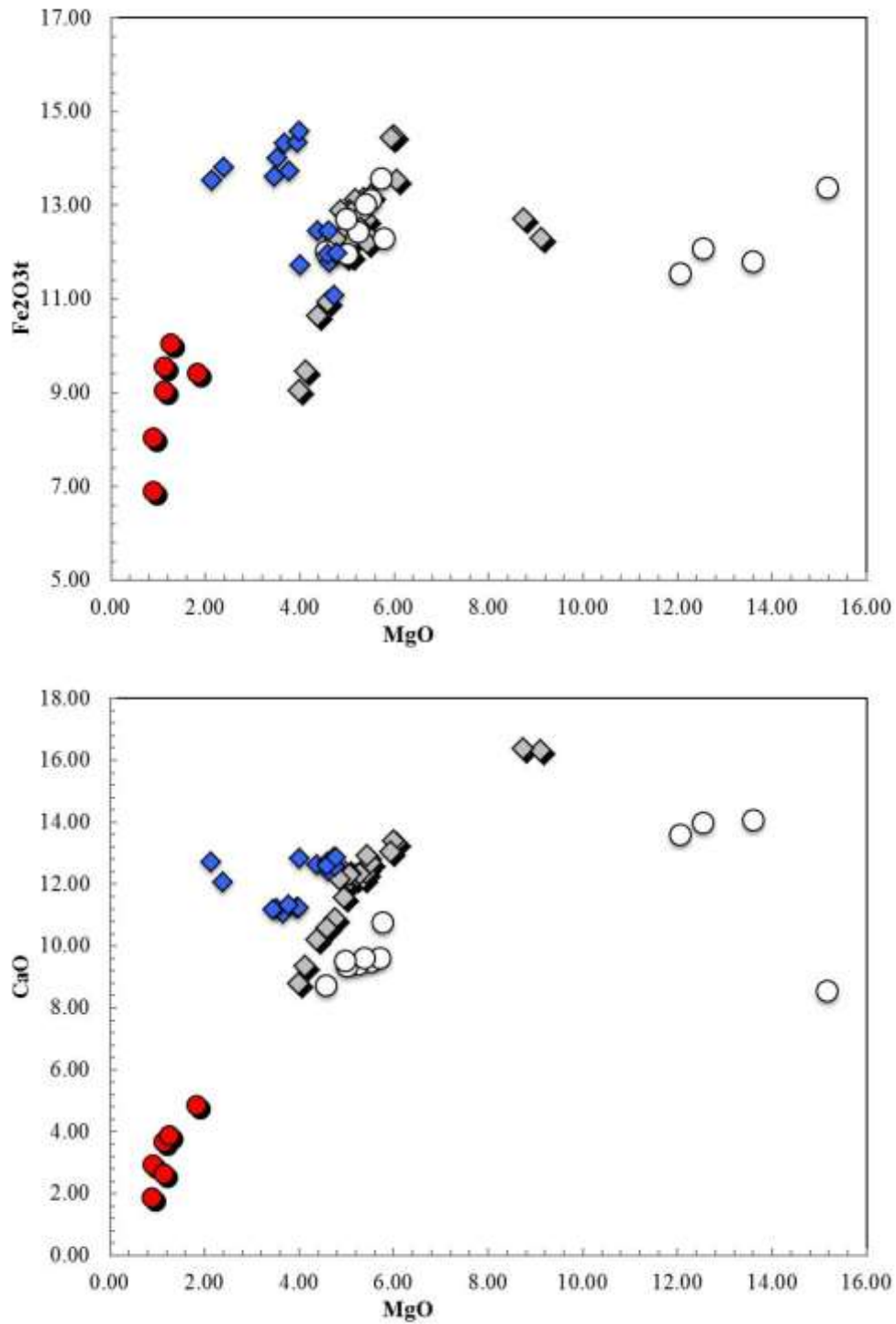


Figure 5.3-5.4 Variation diagrams: Nyiragongo whole rocks (grey diamonds), Nyiragongo glasses (blue diamonds); Nyamuragira whole rocks (white circles) and Nyamuragira glasses (red circles).

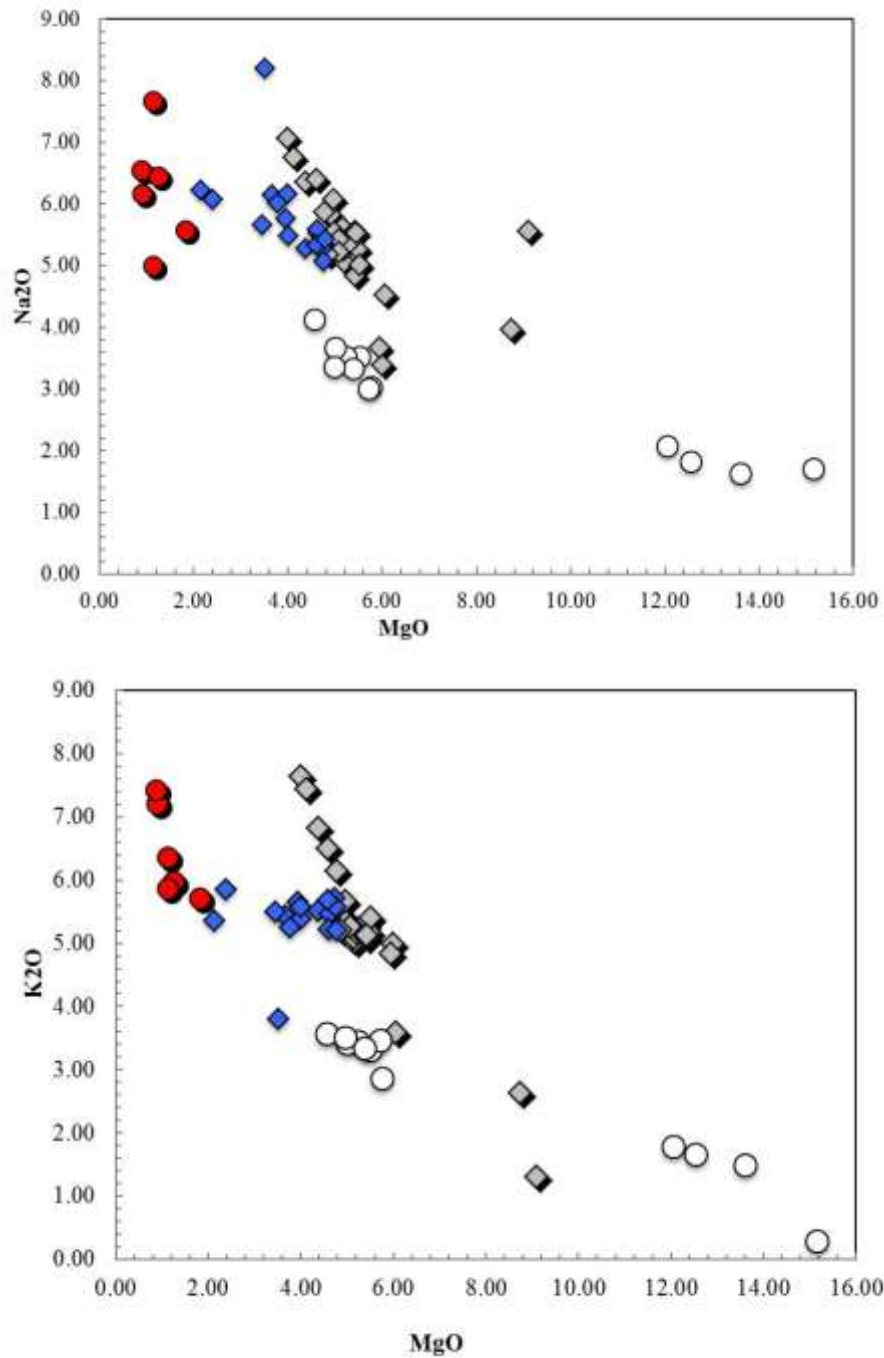


Figure 5.5-5.6 Variation diagrams: Nyiragongo whole rocks (grey diamonds), Nyiragongo glasses (blue diamonds); Nyamuragira whole rocks (white circles) and Nyamuragira glasses (red circles).

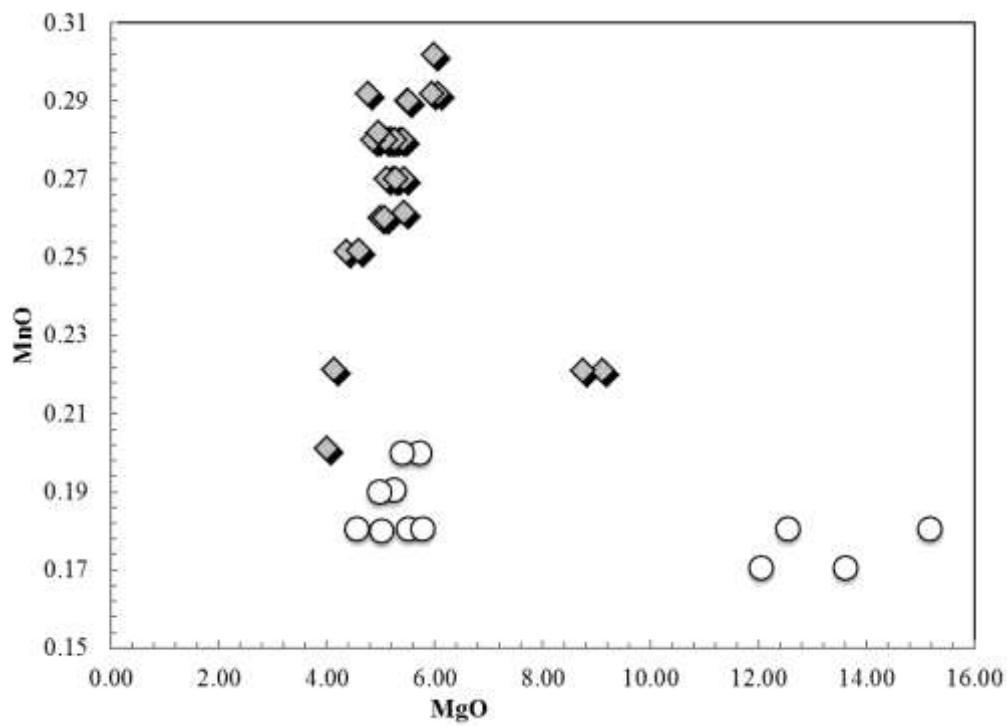
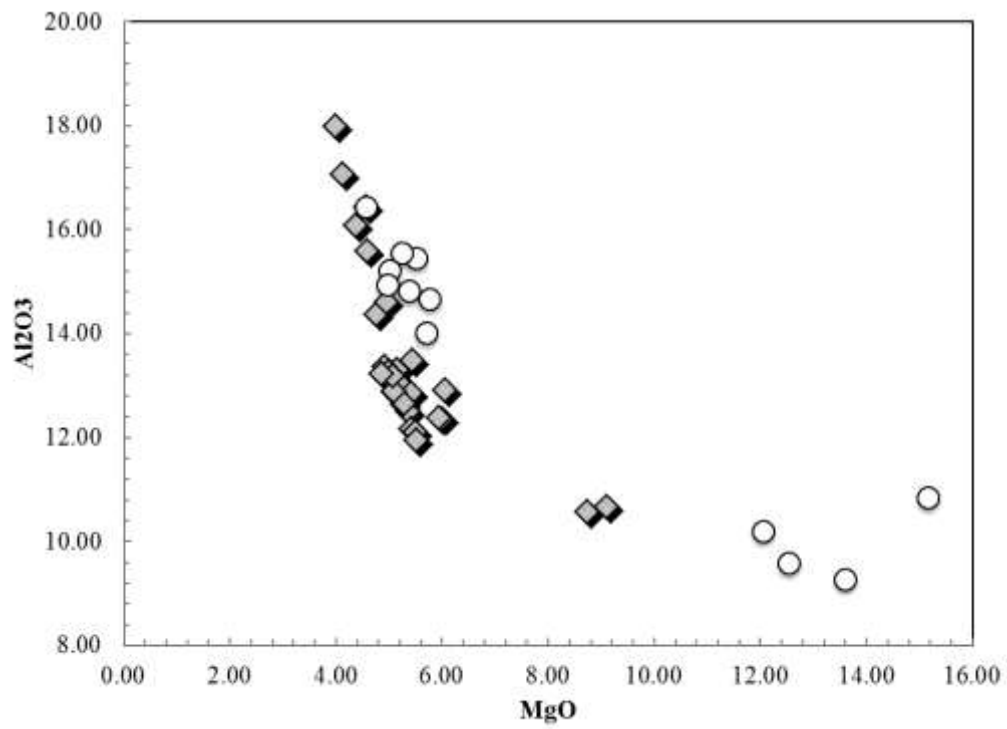


Figure 5.7-5.8 Variation diagrams: Nyiragongo whole rocks (grey diamonds), Nyamuragira whole rocks (white circles).

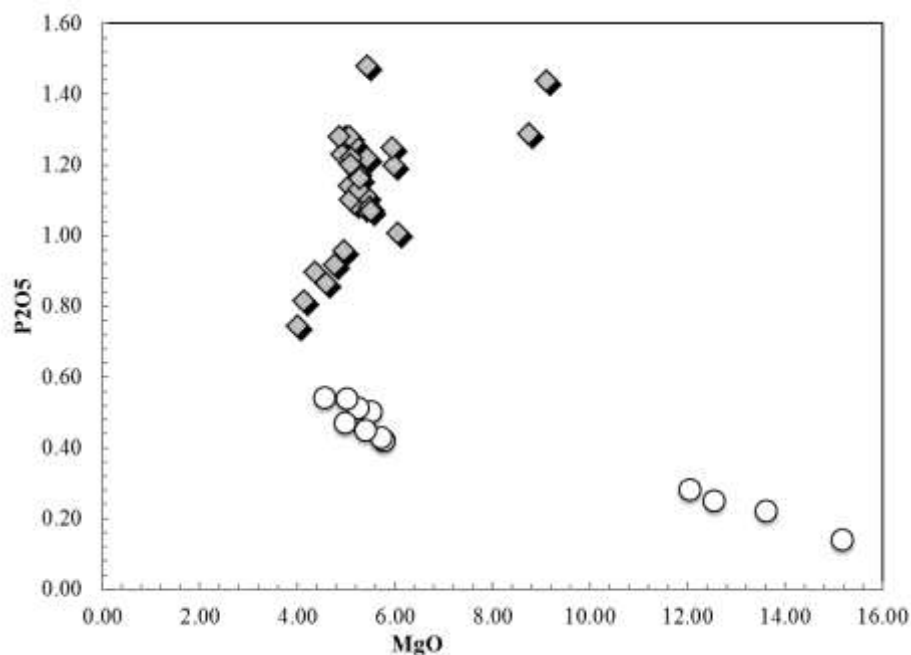


Figure 5.98 Variation diagram: Nyiragongo whole rocks (grey diamonds), Nyamuragira whole rocks (white circles).

5.2 Trace Elements compositions

Variation diagrams for trace elements (wt.% <0.1) are shown in fig. 5.10-5.21 for Nyamuragira volcanic district and Nyiragongo volcanic district.

LILE: The Nyamuragira rocks show low correlation of Rb (1-107 ppm), no correlation Sr (216-1019 ppm) and a poor one of Ba (78-1170 ppm) with MgO, on the contrary to what observed for the other Nyiragongo volcanic rocks that display higher values of Rb (20-173 ppm), Sr (1544-2950 ppm) and in particular Ba contents are high (814-2444) not only in the whole rock but also in some glasses, within the Shaehru group rock. (Ba = 1.76 - 5.74 ppm; fig). All the low values are related to the basalt. The high Ba content is probably due to the fractionation of mineral phases such as clinopyroxene, olivine, melilite, feldspatoids and magnetite, that do not contain Ba, subsequently it will concentrate in the glass matrix.

Transition Elements: Nyamuragira basanites have V (310-432ppm), Cr (26-53 ppm) and Ni (27-45 ppm) contents within the ranges expected for mantle-derived liquids. The transitional basalts have higher V (233-367 ppm), Cr (790-969 ppm) and Ni (245-750 ppm) than basanites. Such enrichment in these elements is due to excess of olivine phenocrysts.

Nyiragongo melilitites have high V (198-470ppm), low Cr (0-50 ppm) and Ni (26-55 ppm) contents compared with Nyamuragira ones. But few samples have very high contents of Cr (>380, Lac Vert) and Ni (>155, Lac Vert).

HFSE: Sc and Y show opposite trends with different values for the studied rocks but rather same clusters: Nyamuragira Sc contents (15-51 ppm) are higher than Nyiragongo (Sc 6-14 ppm) and Nyamuragira Y contents (19-32 ppm) are lower than Nyiragongo (Y 37-41 ppm).

Both in Nyamuragira Nb (8-102 ppm) and Zr (106-309 ppm) display same correlation with MgO as well as in Nyiragongo analysis (Nb 167-239 ppm; Zr 237-306 ppm). In the end, same situation for La and Ce with similar trends: Nyamuragira values (La 11-75 ppm; Ce 20-162 ppm) and Nyiragongo (La 105-201 ppm; Ce 210-373 ppm).

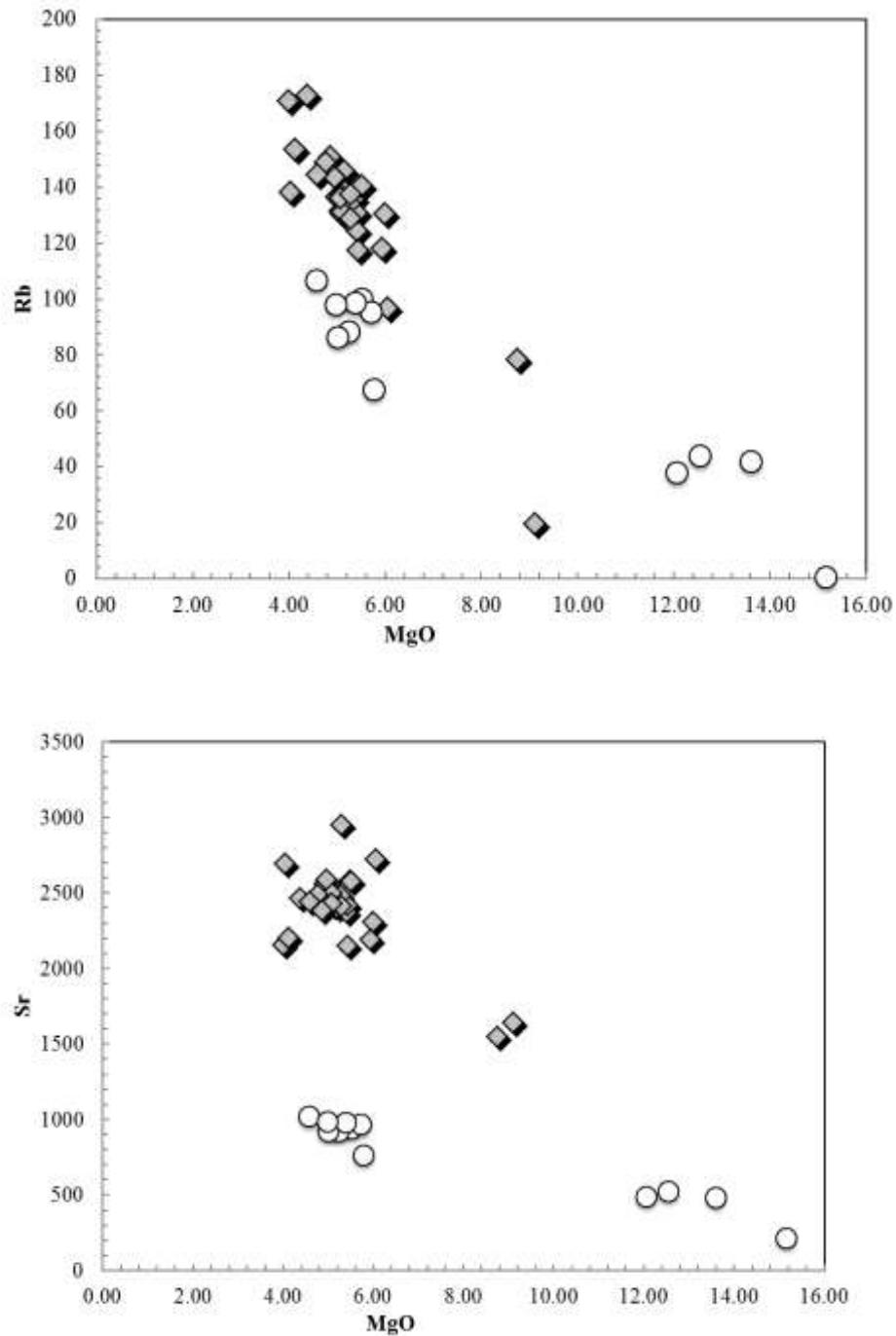


Figure 5.10-5.11 Variation diagrams: Nyiragongo whole rocks (grey diamonds), Nyamuragira whole rocks (white circles).

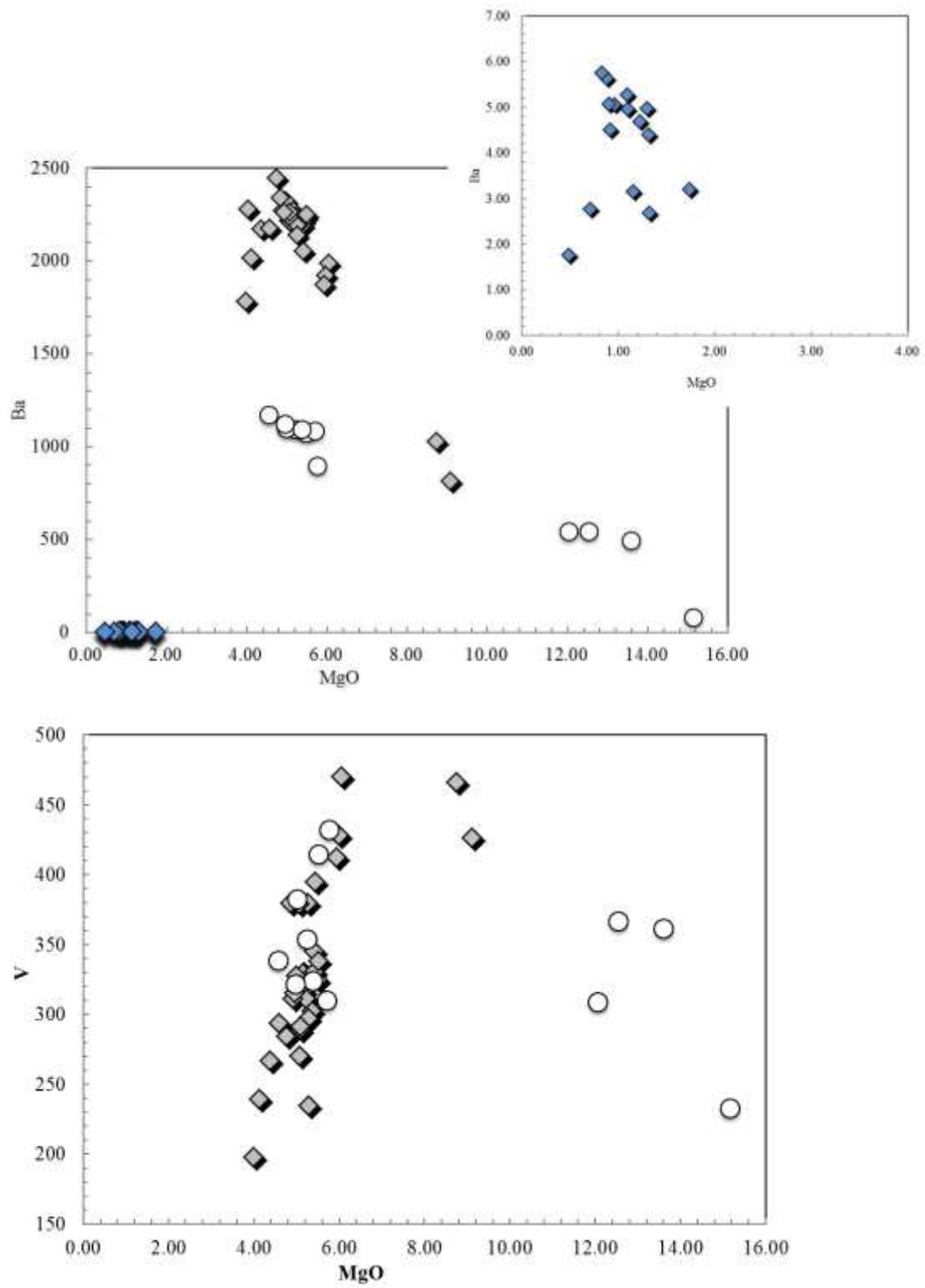


Figure 5.12-5.13 Variation diagrams: Nyiragongo whole rocks (grey diamonds), Nyamuragira whole rocks (white circles).

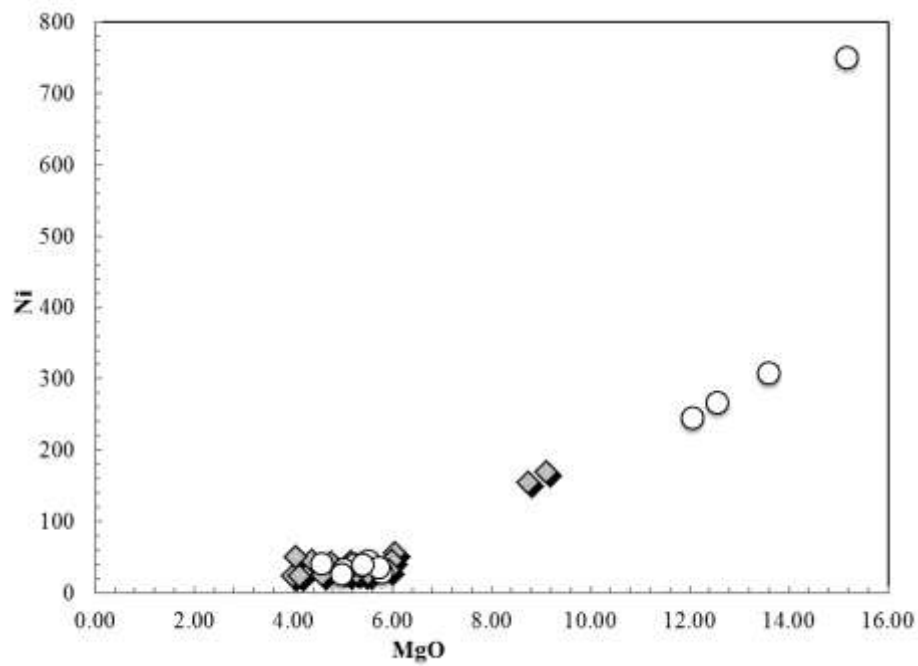
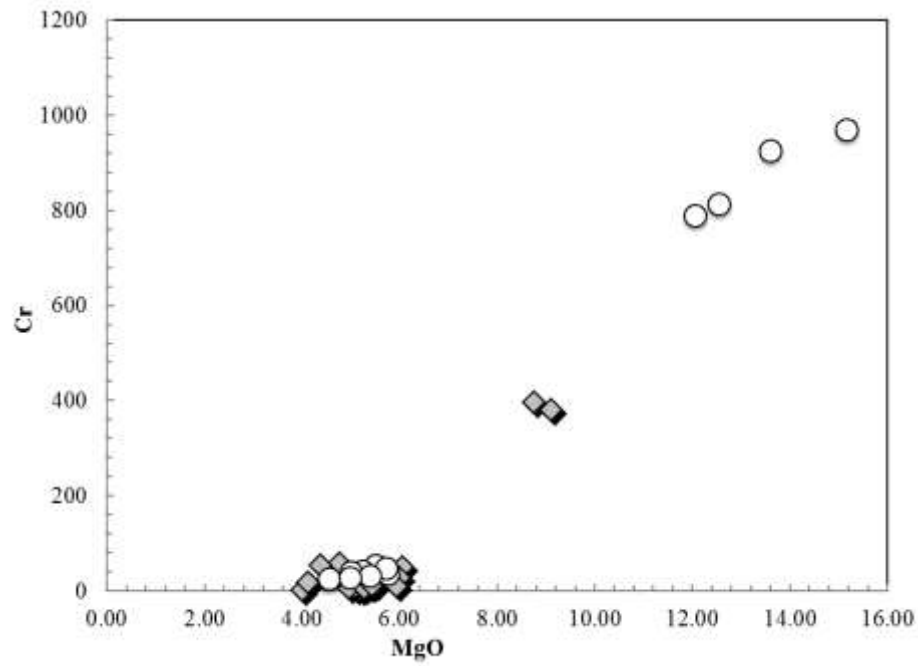


Figure 5.14-5.15 Variation diagrams: Nyiragongo whole rocks (grey diamonds), Nyamuragira whole rocks (white circles).

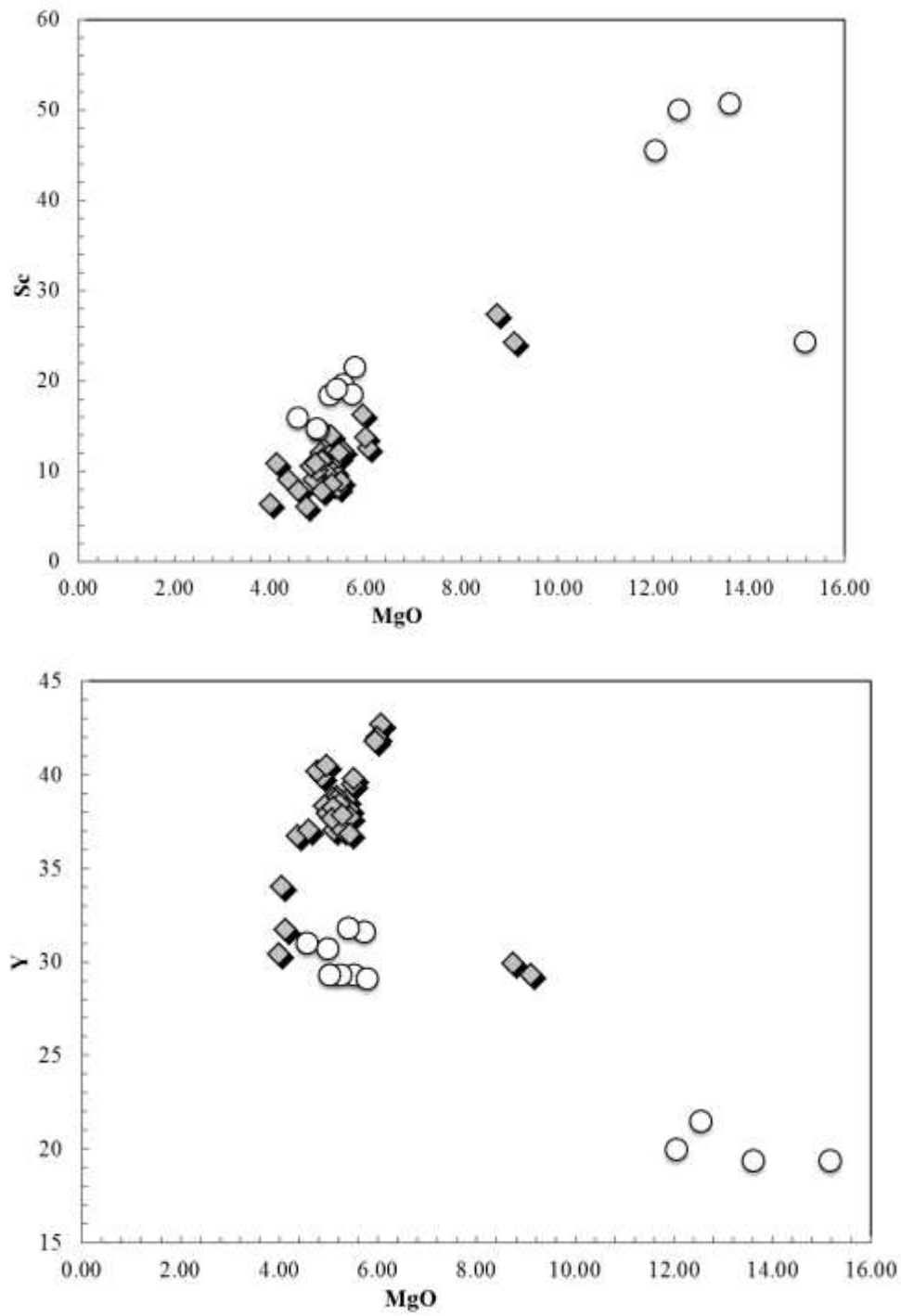


Figure 5.16-5.17 Variation diagrams: Nyiragongo whole rocks (grey diamonds), Nyamuragira whole rocks (white circles).

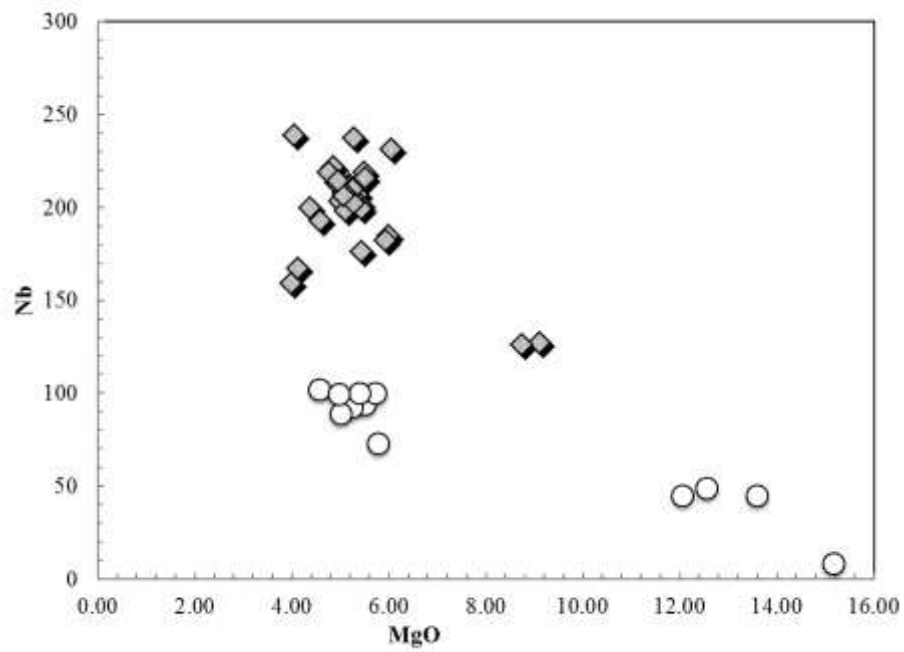
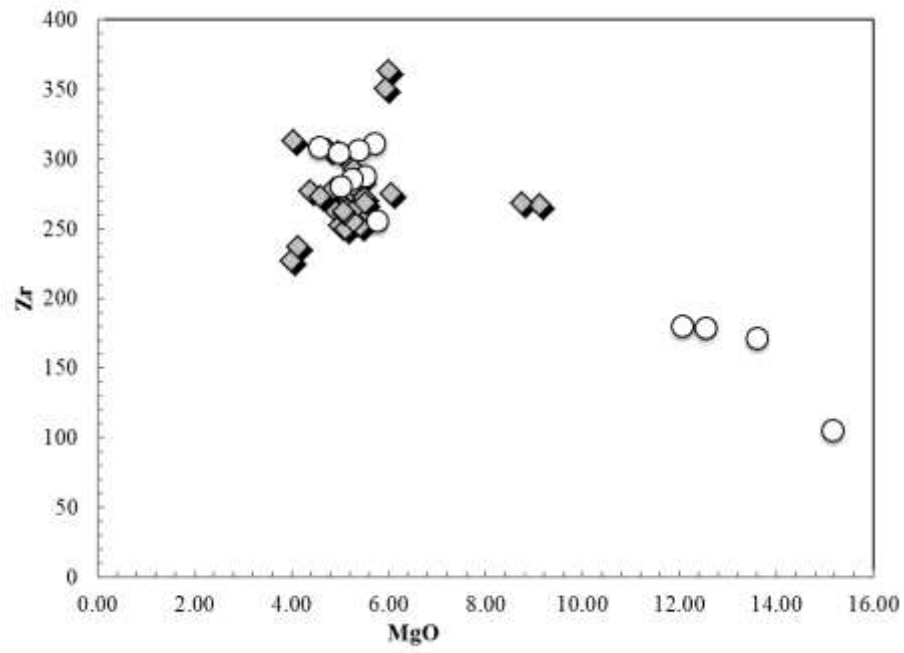


Figure 5.18-5.19 Variation diagrams: Niyiragongo whole rocks (grey diamonds), Nyamuragira whole rocks (white circles).

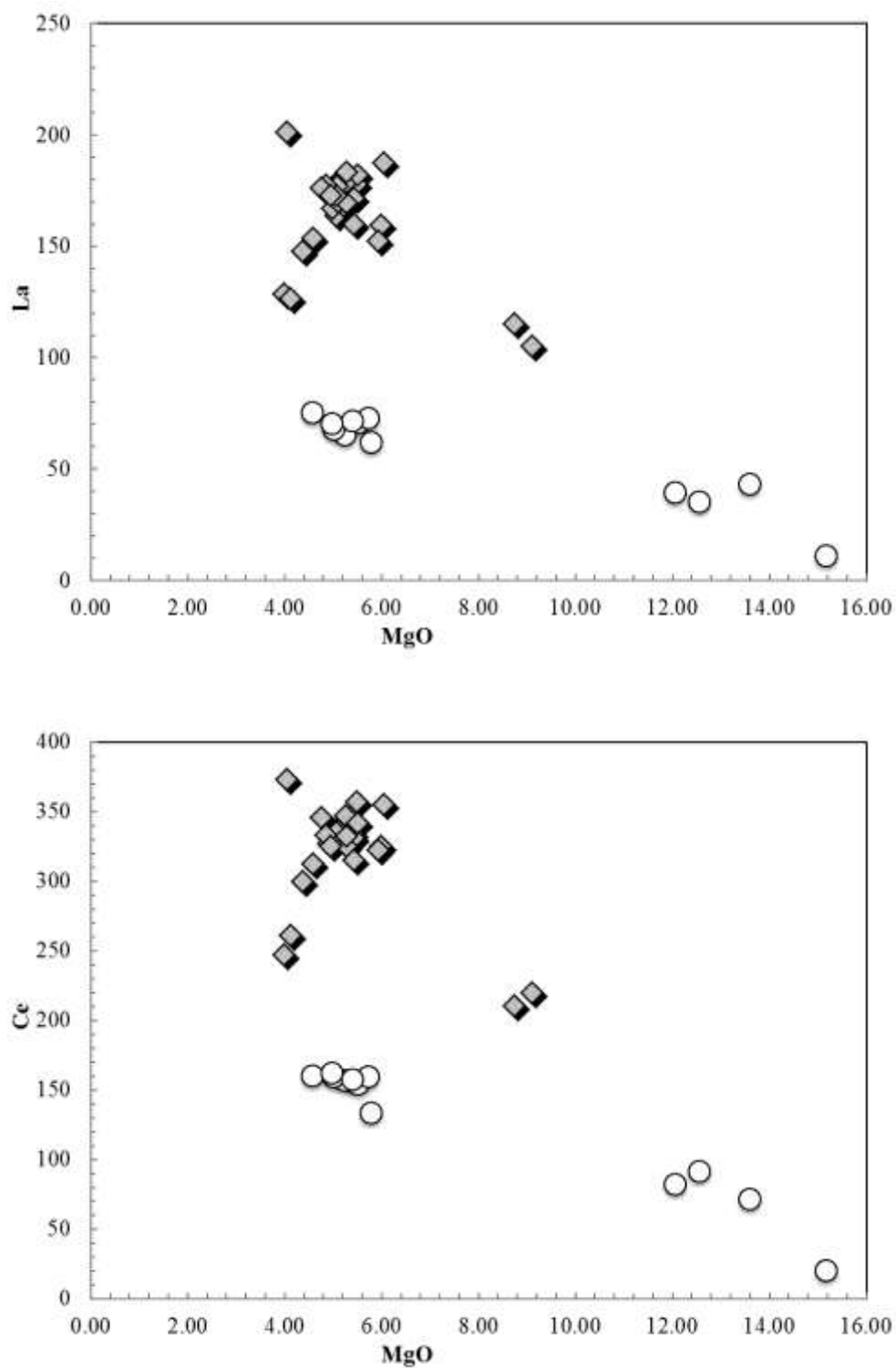


Figure 5.20-5.21 Variation diagrams: Nyiragongo whole rocks (grey diamonds), Nyamuragira whole rocks (white circles).

5.2 .3 Trace Elements distribution patterns

To study the trace elements distribution within the rocks, it is required the construction of diagrams that relate simultaneously concentrations of many chemical elements. The multi-

element diagrams used here are: the rare earth normalized to chondritic values (Boyton, 1984) fig 5.22, and the incompatible elements normalized to the mantle primordial for all the lithologies studied (fig. 5.23). The normalization values used are those proposed by Lyubetskaya and Korenaga, (2007).

All the basanites display a steep pattern of REE with an enrichment for the LREE (La/Sm 5.5-7.7) and a decreasing for the HREE, except the tholeiitic basalt which shows a flat pattern (La/Sm 1.95)

Nyamuragira basanites have Zr/Nb (3.9-4.0), Ba/Nb (11-12) and La/Nb (0.8-0.9) ratios typical of mantle or OIB values. The primitive mantle-normalized incompatible element patterns of Nyamuragira show peaks at Ba and Nb and smoothly decreasing normalized-abundances from Nb to Lu. The high La_n/Yb_n ratio (18) indicates that the Nyamuragira basanites are low degree partial melts of a slightly incompatible element-enriched mantle source in the garnet stability. On the contrary the basalt has a peak at Pb and a totally different pattern, usual for tholeiitic rocks.

The incompatible element patterns of Nyiragongo rocks are also more enriched than those of Nyamuragira basanites with higher LREE/HREE (La/Yb = 42) with negative troughs at K and Ti for Nyiragongo sample and at Pb for both volcanoes samples.

The low Zr/Nb (2.1) of the olivine melilitites indicate that the Nyiragongo olivine melilitites are melt products of an incompatible element-enriched source. In addition, their low heavy REE contents suggest that they were generated within the garnet-peridotite stability field within the lithospheric mantle.

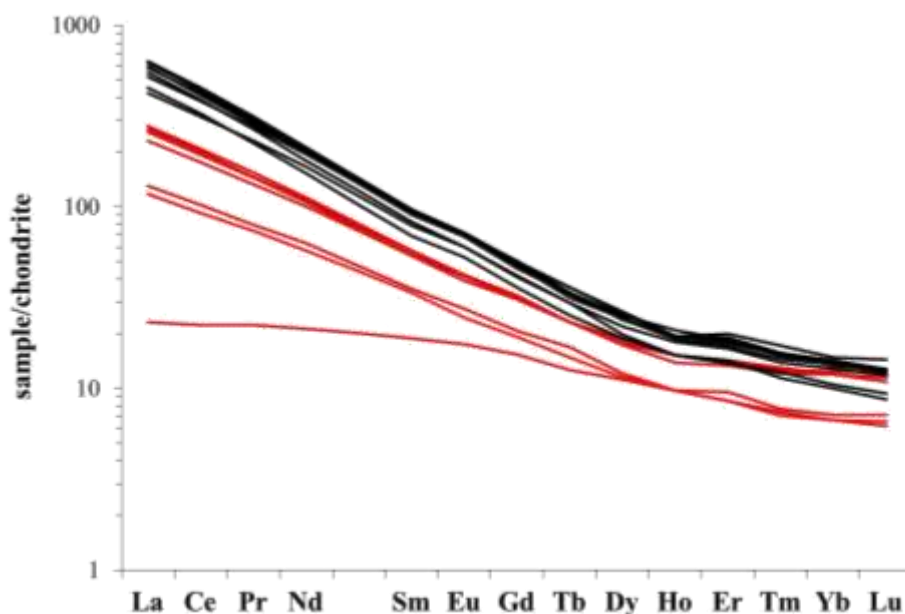


Figure 5.22 Distribution REE diagram: Nyiragongo (black lines) Nyamuragira (red lines).

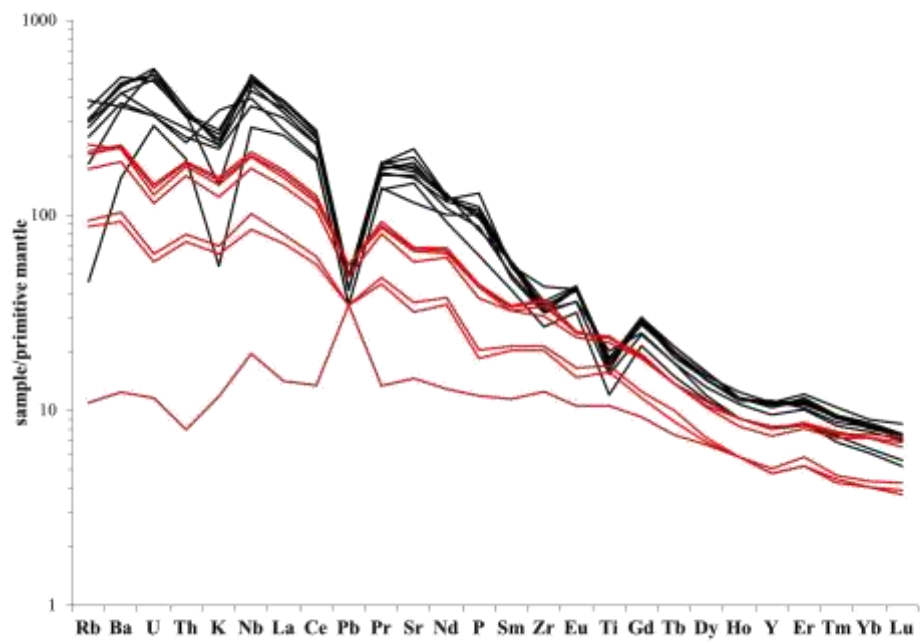


Figure 5.23 Distribution Incompatible elements diagram: Nyragongo (black lines) Nyamuragira (red lines).

Chapter 6

Discussion

Melilitites generally have very high concentrations of Sr, Ba and Rb and steep REE patterns (chondrite normalised Ce/Yb~ 20-30) compared to associated alkali basalts and basanites. (Wilson et al., 1995).

Trace element patterns of all East African Rift volcanics are enriched relative to MORB and OIB, with eastern rift tholeiites, ferrobasalts, alkali basalts and basanites being less enriched and showing smoother patterns than western rift volcanics (Furman and Graham, 1999). Furman and Graham (1999) also noted that the relative enrichment of LREE relative to HREE intensifies with the extent of silica-undersaturation of the East African volcanics, and that (LREE/MREE)_n ratios such as (La/Sm)_n are lower in the eastern compared to the western rift.

Rare data for carbonatites from Fort Portal (Nixon, 1973) show that they are slightly more enriched in incompatible elements than Ugandan kamafugites, but both are most enriched among the western branch volcanics. Carbonatites show the highest depletion in potassium in the western rift. However, extreme and similar LILE, HFSE and LREE enrichments and marked K, Pb and P depletions of all western rift volcanics are striking (Rosenthal et al., 2009).

The negative Pb anomaly is an indication of the lack of significant crustal assimilation (Rosenthal et al., 2009), whereas K anomaly is considered as a feature of the primordial mantle source like for Madagascar similar lithotypes (Melluso et al., 2007, 2016).

To constraint on the mineralogy of the possible source making up the enriched component, we must look to the major and trace element chemistry of the rocks. The high K₂O, CaO, P₂O₅, TiO₂ and CO₂, but low SiO₂ contents are not due to fractionation or crustal assimilation, and must be characteristic of the source.

bulk concentrations	
Nyira 2016	wt.%
Cl	0.13
F	0.17
Total S	0.20

6.1 Mantle source

According to previous results it is possible to state that almost all of the analyzed rocks show low evolved magma features, both nephelinites of Nyiragongo and basanites of Nyamuragira, glasses included. Indeed, in order to characterize the source of the studied lithotypes it was taken into account just the olivine melilitites that show on the contrary primitive magma features such as high MgO content (up to 9 wt%) and CaO (up to 16 wt.%) Mg# values of 62 and Mg# of olivine up to 88, also high content of Ni (170 ppm) Cr (390 ppm) and V (408 ppm). Therefore in this chapter it was considered the sample LV1 and LV2 from the Lac Vert scoria cone the possible primitive rocks and from whom all of the other rocks fractionated.

The REE patterns show high enrichments in LREE and high decreasing in HREE and no negative anomaly in Eu (Fig 6.1), thus this is consistent with the presence of garnet in the source, moreover the difference is evident between Virunga patterns than a typical NMORB pattern, generated from a spinel source (Fig 6.1).

Garnet is a stable mineral for pressures higher than 20-30 kbar, thus the depth of the source can be set between 80 and 100 Km, probably in areas of subcontinental lithospheric mantle.

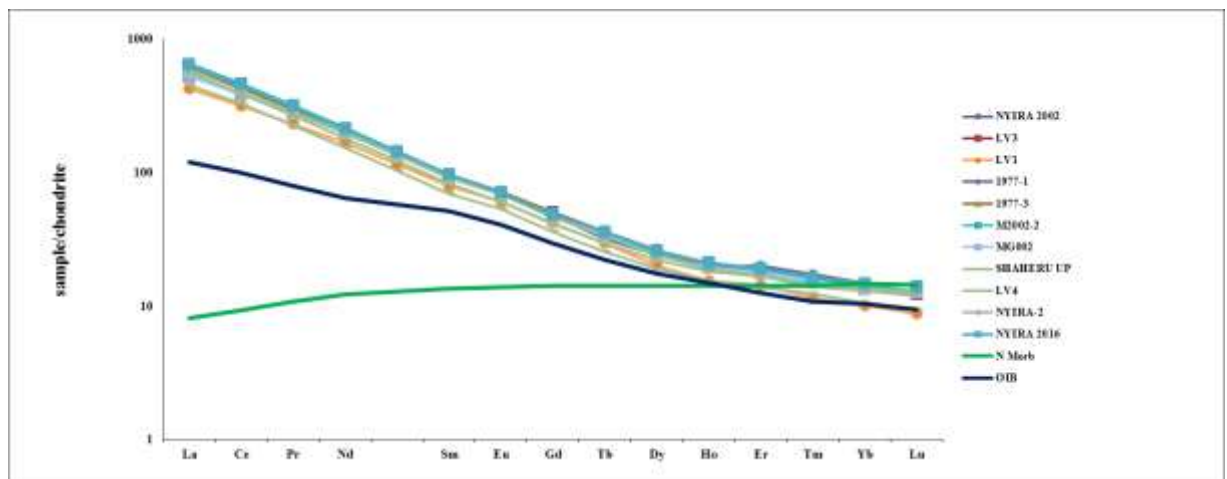


Fig 6.1

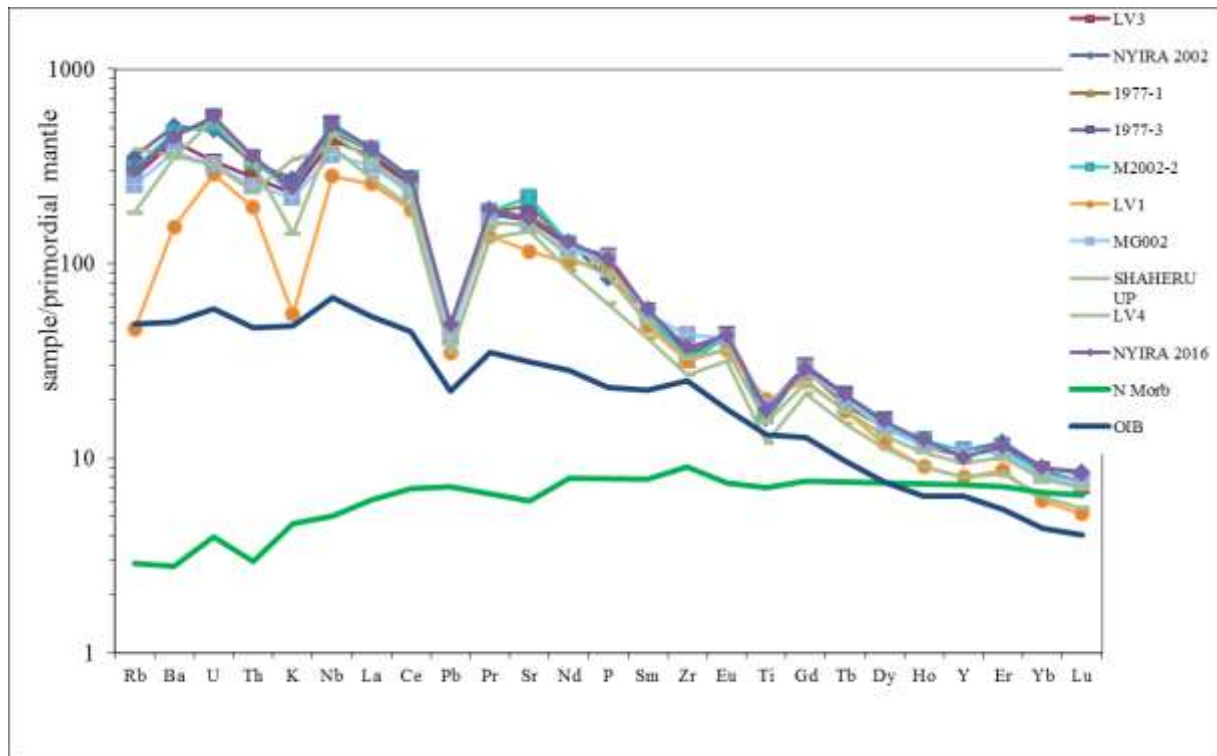


Fig 6.2

Incompatible elements patterns in the Wood diagram (Fig 6.2) show also high enrichments in LILE and HFSE, typical anorogenic patterns. Those enrichments are higher than NMORB ones. Only Y, Yb, Er and Lu show low concentrations: this difference is probably due to the degree of partial melting. In fact for melilite-bearing rocks the degree is generally low (1-2%), this fact implies a strong enrichment in the melt of the most incompatible elements than the less incompatible ones, moreover in our case, the presence of the garnet in the residual source (restite) reduces the concentration of Y, Yb, Er and Lu in the melt.

Instead for MORB, the degree of partial melting is much higher: about 20% and it shows a clear decreasing pattern.

On the contrary the OIB pattern seems to be much more similar and can be considered as an affinity.

To better constrain the possible mantle source of the lavas it was used the chemical composition and model with the classical equation of Shaw (1970) (batch melting non modal) but the reverse formula:

$$C_0 = C_1 [D + F(1 - P)]$$

Where

C_0 = composition of the elements in the source

C_1 = composition of the same elements in the liquid

D = Bulk distribution coefficient in the source (ΣKD)

F = degree of partial melting

P = Bulk distribution coefficient in the phases entering the melt (ΣKD)

The olivine melilite LV1 (Fig 6.3) was used with three different degrees of partial melting (5%; 10%; 20%) and considering a garnet lherzolite. The modal composition and the eutectic

are in the table below . The Kd used for the calculations of D and P are from website GERM <http://earthref.org/GERM/> (Tab).

For Nyamuragira samples we use the basanite NYAM A, the most primitive (fig 6.4).

Niu et al. 1996 JGR, 101, 27711-27733

	Ol	Opx	Cpx	Gt
source	0.601	0.189	0.137	0.073
eutectic	0.013	0.087	0.36	0.54

	Ol	Opx	Cpx	Gt	Dgt	Pgt
Rb	0.000035	0.000070	0.000470	0.000100	0.000106	0.000230
Ba	0.000035	0.000070	0.000470	0.000100	0.000106	0.000230
U	0.000100	0.000100	0.000360	0.000100	0.000136	0.000194
Th	0.000100	0.000100	0.000260	0.000100	0.000122	0.000158
K	0.001000	0.003900	0.005300	0.000500	0.002101	0.002530
Nb	0.002000	0.002500	0.005000	0.000500	0.002396	0.002314
La	0.000100	0.005300	0.100000	0.000500	0.014798	0.036732
Ce	0.000100	0.009000	0.162500	0.008000	0.024608	0.063604
Pb	0.000100	0.001300	0.010000	0.000500	0.001712	0.003984
Pr	0.000200	0.012700	0.225000	0.032500	0.035718	0.099658
Sr	0.016000	0.016000	0.260000	0.200000	0.062860	0.203200
Nd	0.000300	0.016300	0.287500	0.057000	0.046810	0.135702
P	0.000200	0.014500	0.256300	0.005000	0.038339	0.096232
Sm	0.000600	0.020000	0.350000	0.217000	0.067932	0.244928
Zr	0.010000	0.050000	0.100000	0.500000	0.065660	0.310480
Eu	0.004800	0.027500	0.380000	0.450000	0.092992	0.382255
Ti	0.016000	0.100000	0.300000	0.600000	0.113416	0.440908
Gd	0.009000	0.035000	0.410000	0.966700	0.138763	0.672780
Tb	0.013200	0.048000	0.440000	1.483300	0.185566	0.963730
Dy	0.017400	0.061000	0.470000	2.000000	0.232376	1.254733
Ho	0.021600	0.074000	0.500000	2.750000	0.296218	1.671719
Y	0.010000	0.080000	0.485000	2.750000	0.288325	1.666690
Er	0.025800	0.087000	0.483300	3.500000	0.353661	2.071892
Yb	0.030000	0.100000	0.466700	7.000000	0.611868	3.957102
Lu	0.034200	0.113000	0.450000	10.000000	0.833561	5.572276

It is apparent that the calculated source follow the pattern of the lavas.

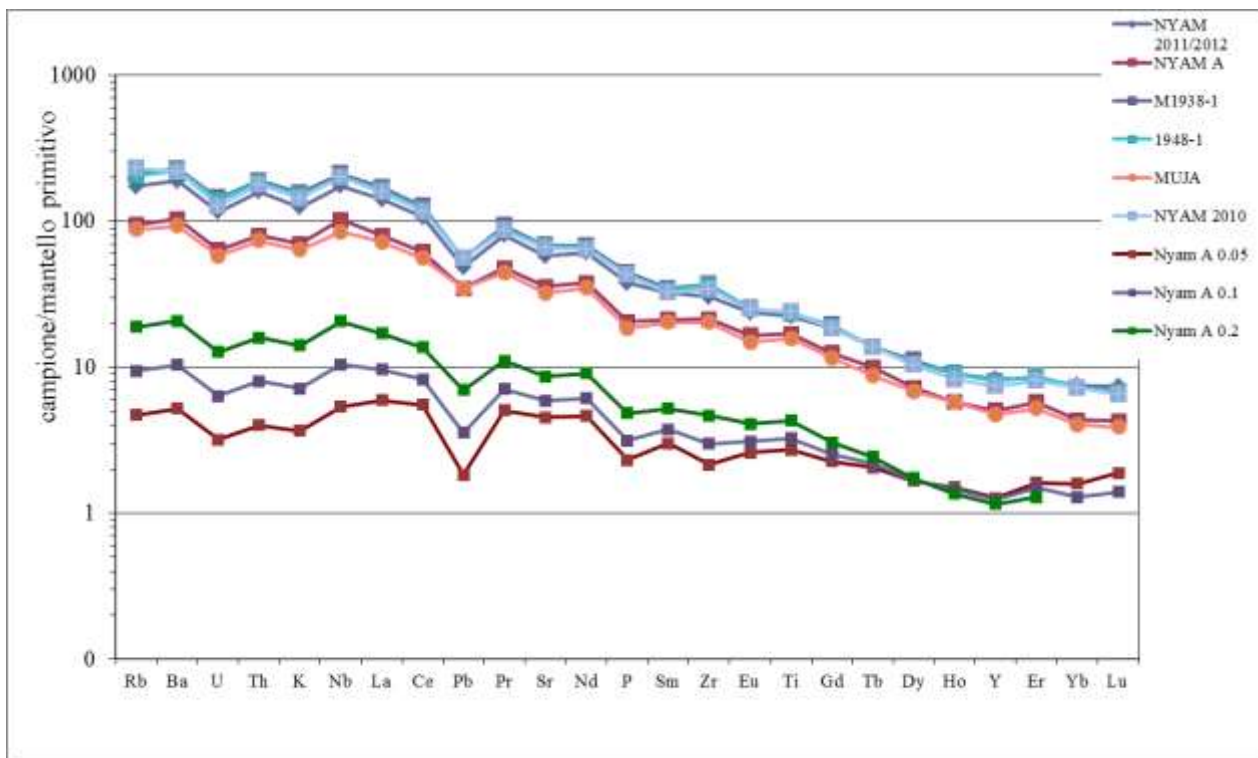
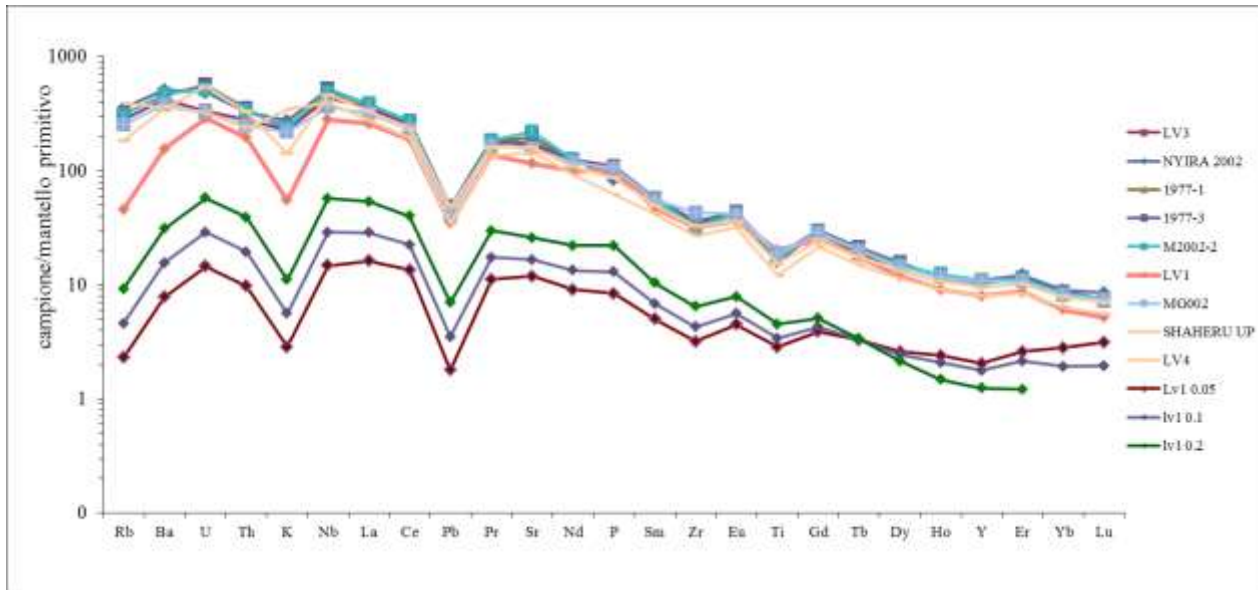


Fig 6.3 and 6.4

Melt infiltration, according to Wilson et al., (1995), could be the most likely cause of heterogeneity within the lithosphere (TBL in specific). These heterogeneities may subsequently give rise to melilitite magmas. To explain that it is proposed the diagram in Fig. where the effects of CO_2 and H_2O are experimentally visible: the presence of C-O-H volatile components in the mantle clearly has a dramatic effect on the shape and the position of the solidus curve for mantle peridotite (Wilson 1993). In the diagram is also indicated the field of amphibole stability above the solidus, in which amphibole lherzolite coexists with a carbonatite partial melt (15-30 kbar). At temperatures above 1025 C and pressures in the garnet stability field, the partial melt coexisting with carbonate peridotite changes from

carbonatite to silicate melt, similar in composition to olivine melilitite. To generate an olivine melilitite partial melt in the presence of residual garnet and phlogopite under fluid-saturated conditions would require pressures in excess of 20 kbars and temperatures in the range 1000-1200 C (Fig.6.5) and there is a xenolith to comparison from old literature. It suggests that partial melting of a carbonated phlogopite-garnet lherzolite mantle source could indeed generate continental melilitites, if this xenolith is representative of the source region of the melilitite magma. A fundamental question, however, is whether zones of carbonated phlogopite lherzolite actually exist within the mantle. No unequivocal examples of carbonate-phlogopite-bearing peridotite xenoliths have been documented in the area, for this reason it was considered the kimberlites as examples.

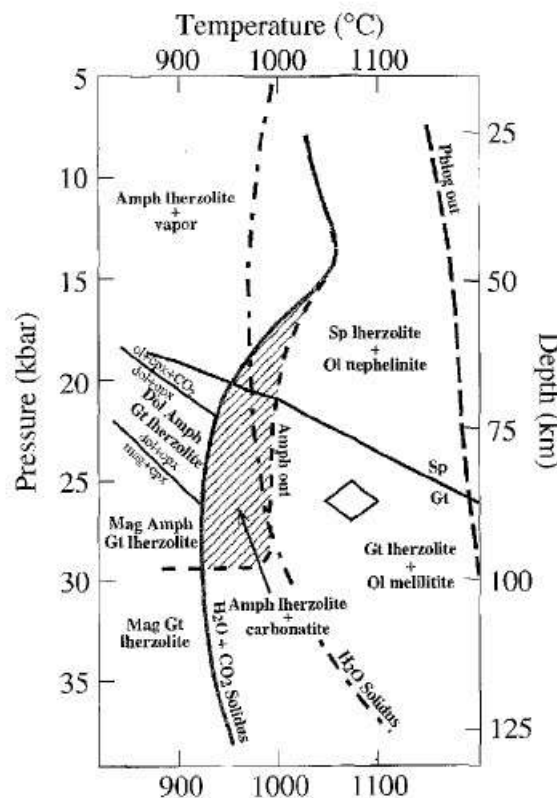


Fig 6.5 P-T diagram showing the position of the H₂O- and H₂O-CO₂-saturated solidi for a fertile mantle peridotite (after Falloon and Green, 1990). Phlogopite-out curve from Mengel and Green (1989). The equilibration conditions for a garnet-phlogopite lherzolite xenolith from the Sahara melilitites of Dautria et al. (1992) is indicated by the large diamond. (Mineral abbreviations used are: amph amphibole, cpx clinopyroxene, dol dolomite, gt garnet, mag magnesite, ol olivine, opx orthopyroxene, phlog phlogopite, sp spinel. (Wilson et al 1995)

According to Foley (2012) many volcanic localities around the Tanzanian craton bring direct evidence of mantle lithologies to the surface in the form of mantle-derived xenoliths. A first-order generalization about the distribution of rock types is that most xenoliths from the eastern rift branch or on the craton are peridotites that are modified by melt infiltration to varying degrees, whereas xenoliths in the western rift branch are mostly mica-bearing pyroxenites and not peridotites (Holmes and Harwood, 1937; Lloyd and Bailey, 1975; Lloyd et al., 1987). However, xenoliths in the western branch are known only from Toro Ankole and the easternmost section of Virunga, and not from South Kivu or the bulk of the Virunga province. Rare olivine-bearing nodules (Holmes and Harwood, 1932) may be subvolcanic

cumulates and not of mantle derivation. In the western rift, phlogopite-bearing pyroxenites dominate in the north (Lloyd et al., 1987), whereas the southern volcanic fields lack abundant xenoliths of any kind. The xenoliths of the Toro Ankole field are dominated by clinopyroxene and phlogopite and also include various amounts of titanite, titanomagnetite, apatite, perovskite, amphibole and calcite (Lloyd and Bailey, 1975): the complete absence of olivine makes their origin by pervasive replacement of peridotites by a fluid phase (Lloyd et al., 1987) less likely than crystallization from melts (Link et al., 2008).

Finally Rock (1991) emphasized the similarities between olivine melilitites, lamprophyres and kimberlites. Then, for all the reasons above, it was taken into account the kimberlite from Gregorie et al. (2003) and the calculated kimberlite from the model of Le Roex et al. (2003) as possible mantle sources because they have very similar patterns with same negative anomalies (at K, Pb and Ti) but clearly not the same enrichments, especially for the less incompatible elements (Fig. 6.6).

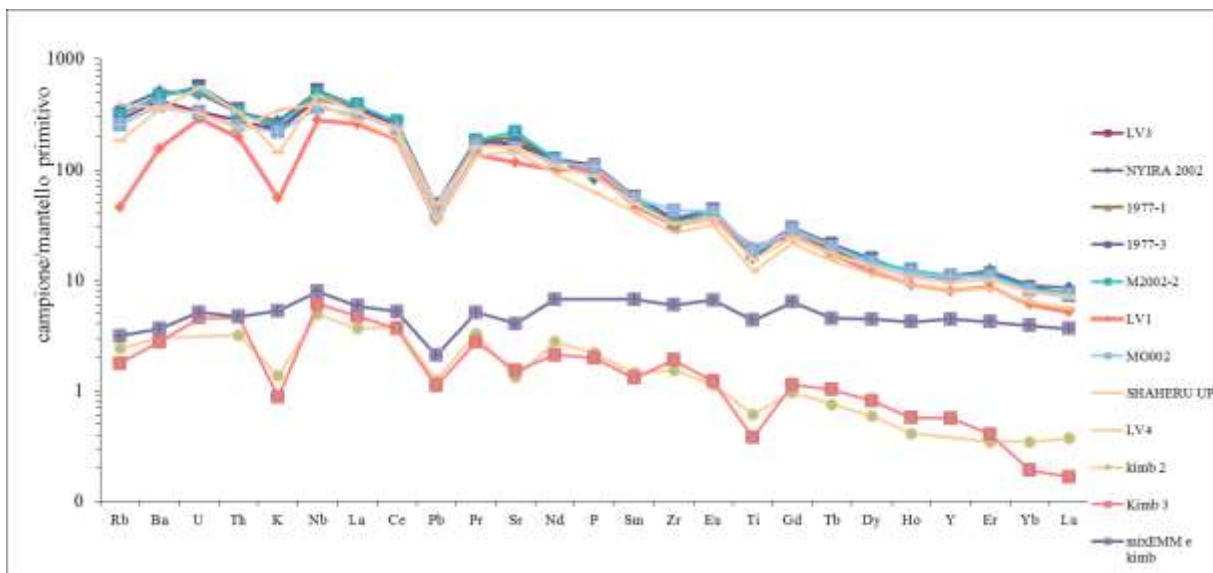


Fig 6.6 “Kimb 3” from Gregorie et al 2003; “kimb 2” from Le Roex et al., (2003); “mixEMMeKimb” calculated from 95% Enriched Mantle and 5%kimberlite.

6.2 Considerations on the role of CO₂ and model below Tanzanian craton

According to Foley (2017) partial melting of peridotite in CO₂-rich conditions can cause the production of low silica magma series (Eggler, 1976, Brey, 1978, Wyllie and Huang, 1976; Rosenthal et al., 2009). Moreover, high-pressure experiments show that the generation of the more abundant alkaline low-SiO₂ silicate melts is only possible with abundant CO₂ during melting, whereby the melt compositions richest in carbonate are produced at the lowest degrees of melting (Gudfinnsson et al., 2005, Foley et al., 2009).

carbonation reactions

(olivine + CO₂ → magnesite + enstatite; olivine + diopside + CO₂ → dolomite + enstatite)

(Green D.H. 2015)

Melilitite and nephelinite volcanoes are characteristically concentrated at the propagating tips of rifts and along rift flanks (Foley et al., 2012; Williams et al., 1978), and are joined by contemporaneous, more voluminous basaltic magmatism in the rift centres as the rift matures (Fig. 6.7). Tips and flanks represent the early stages of rifting where the lithosphere is still thick. Ultramafic, potassium- and carbonate-rich melts are associated with thick lithosphere in the East African Rift around the Tanzanian craton, and on other continents where cratons have been rifted (Foley et al., 2012, Rogers et al., 1998, Tappe et al., 2006) implying a deep source for these melts.

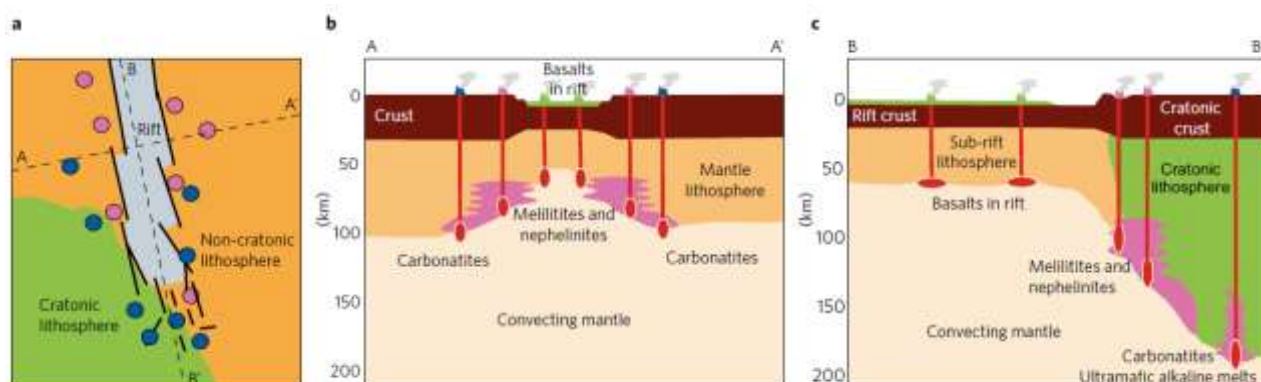


Fig 6.7 Foley (2017)

Schematic relationship of carbon-rich magmatism with rift tips and flanks. a, Archetypal map view based on the East African Rift showing carbonatites (blue) and low-SiO₂ alkaline magmas (purple; nephelinite/melilitite) at tips and flanks of the propagating rift, whereas later voluminous basalts (grey).

The extreme CO₂ release at Nyiragongo (Burton et al., 2013, Tedesco et al., 2007, Sawyer et al., 2008) further demonstrates that alkaline, silica-undersaturated melts preferentially tap CO₂-rich sources.

The storage of carbon in the lithospheric mantle results from three stages of input: (1) the original C content incorporated during its formation; (2) gradual enrichment by infiltration from below; and (3) enrichment by melts associated with the periodic passage of plumes. The carbon accumulated by these processes is then remobilized and released during rifting. At later stages, as the lithosphere thins, decompression of the upwelling asthenosphere causes more widespread melting, which results in the transition to carbonate-poorer silicate melts such as melilitites and nephelinites. Hence it is possible to argue that the strong association of

continental rifts with CO₂ release is a consequence of long-term accumulation and remobilization, which telescopes carbon into magmatic zones beneath rifts. Carbonate-rich metasomes are present beneath cratons but CO₂ accesses the surface predominantly in rifts running through post-cratonic lithosphere

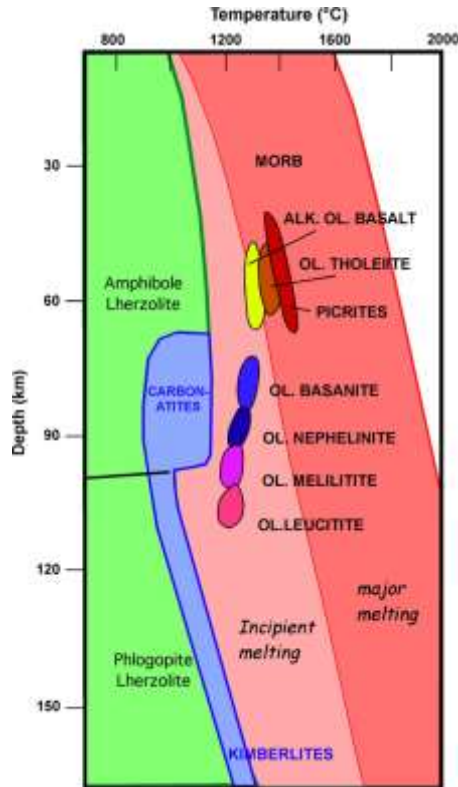


Fig 6.8 The pyrolite model for production of igneous melt types by melting of peridotite mantle (modified after Green and Falloon, 1998 and Foley et al., 2009). In the incipient melting region, the degree of melting is always low and does not increase significantly until the demarcation into the major melting region is crossed. Rock types shown by coloured balloons assume production of these melt types from peridotite \pm H₂O and CO₂. Melt in the blue area are carbonate-rich, and range from carbonatites at low pressures to a rapid transition from carbonatites to kimberlites at higher pressures. From Foley et al., (2012).

Fig 6.8 illustrates the current understanding of melting of peridotite based on melting of pyrolite summarized by Green and Falloon (1998), and modified to include more recent results on the melting of peridotite with both H₂O and CO₂ at pressures of 4–6 GPa (Foley et al., 2009). The occurrence of thin, rifted lithosphere in close proximity to thick cratonic lithosphere in the Tanzanian craton area means that melting at all depths from 250 km to <50 km may be relevant. Fig. 6.8 defines distinct pressure– temperature areas for incipient melting and major melting.

In the incipient melting region, the degree of melting is generally low (<5%), but nevertheless this area is extensive due to the strong effect of the volatile components H₂O and CO₂ in reducing the melting temperature. Almost all the rock types noted above as possible primary melts in the Tanzanian craton area are assigned to this incipient melting region on the assumption that they originate by melting of mantle peridotite. Volatile components are considered essential: nephelinites require H₂O (Bultitude and Green, 1971), whereas melilitites and kimberlites could only be derived from peridotites in the presence of both H₂O and CO₂ (Brey and Green, 1977).

Also Rosenthal (2009) supports the role of CO_2 and suggest the model in fig 6.9.

The sparsity of diamonds in both kamafugites and ultramafic lamprophyres, may be an indication of oxidizing melting conditions rather than a depth of origin above the stability limit for diamonds (Foley, 2008). The more recent carbonate rich metasomatic event can be explained by partial melting of carbonate- and H_2O -bearing peridotite at pressures of 40–60 kbar where melts are rich in K_2O and carbonate, and have MgO contents. The existence of a continuous thick cratonic lithosphere extending between the Congo and Tanzania cratons in Uganda, rather than separate cratons, explains the apparent northward plunging base of the lithosphere and of the sources of western rift magmatism (Foley, 2007; Fig. 7).

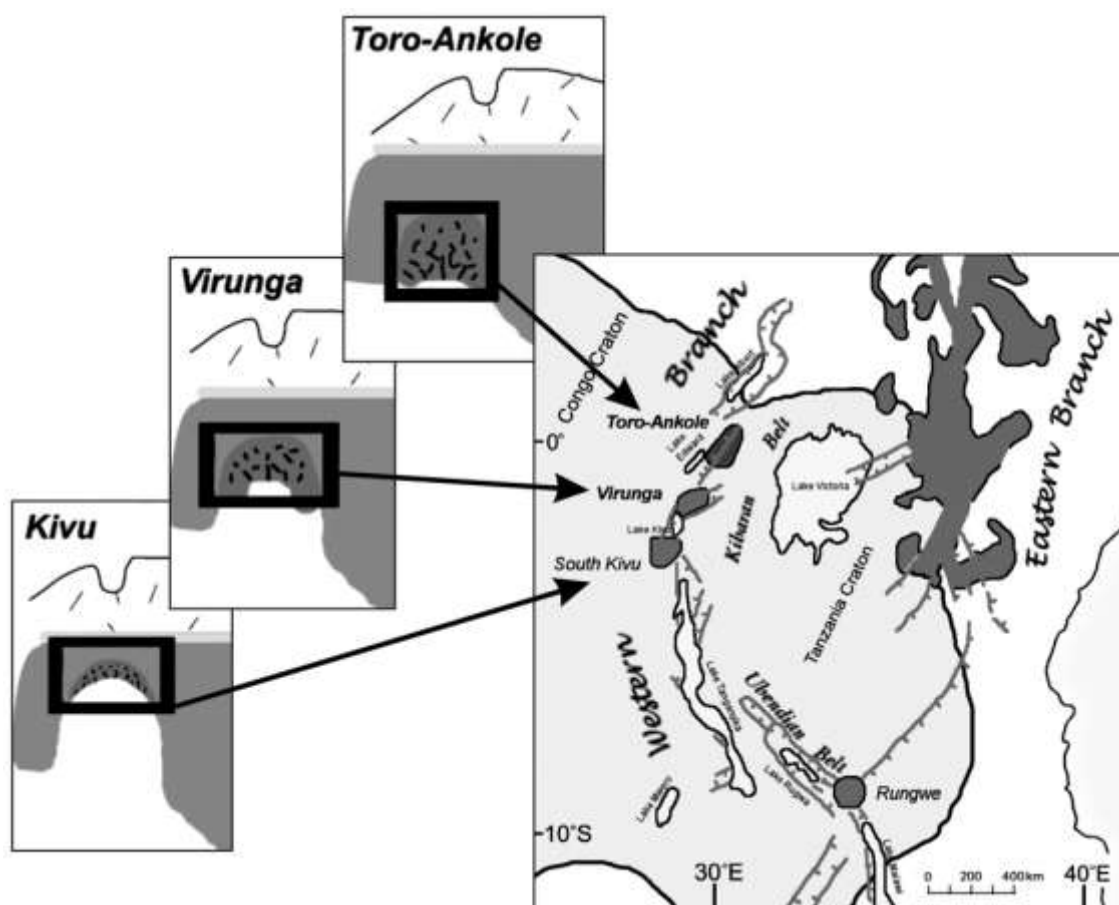


Fig. 6.9 Cartoon showing the variation in the depth of melting along the western branch of the East African rift. From Rosenthal et al. 2009

An additional Ca-rich phase that contributed to the melt compositions of olivine melilitites of Lac Vert cone and the other nephelinites (this thesis work) is visible in the diagram MgO/CaO vs. $\text{SiO}_2/\text{Al}_2\text{O}_3$ of Gudfinnson and Presnall (2005; Fig.6.10) where they plot in the carbonatitic field. The diagram indicates that the primitive magmas of melilititic composition may have been generated at pressures < 3 GPa (hence well within the stability field of mantle garnet) and show moderate CO_2 concentrations (hence with a not-negligible contribution of carbonates) on the contrary the basanitic rocks plot in a region of the diagram indicating pressures that may be as high as 3 GPa.

Further, the diagrams $\text{CaO}-\text{SiO}_2$ and $\text{MgO}-\text{SiO}_2$ (Fig. 6.10) of Herzberg and Asimow (2008) also suggest that nephelinites and melilitites formed in carbonate-bearing mantle regions, whereas basanites and basalts did not (or any contribution of carbonate was heavily diluted

during partial melting). Recent work of Mallik and Dasgupta (2013, 2014) confirms the significant role played by carbonates (likely dolomite) in shaping the chemical composition of olivine melilitites and olivine nephelinites, by releasing CO₂ and thus slightly enriching small-degree partial melts in CaO.

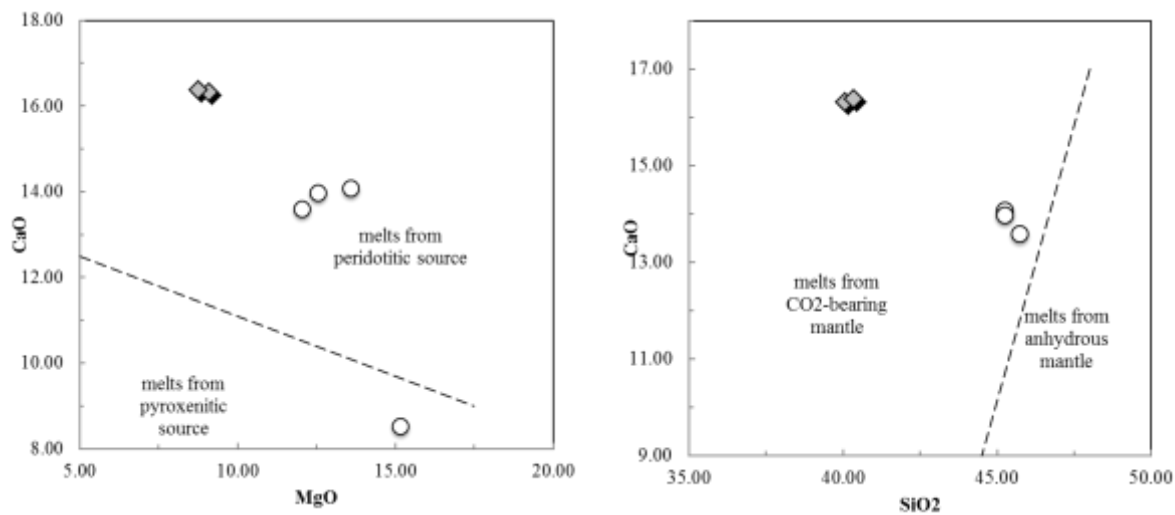
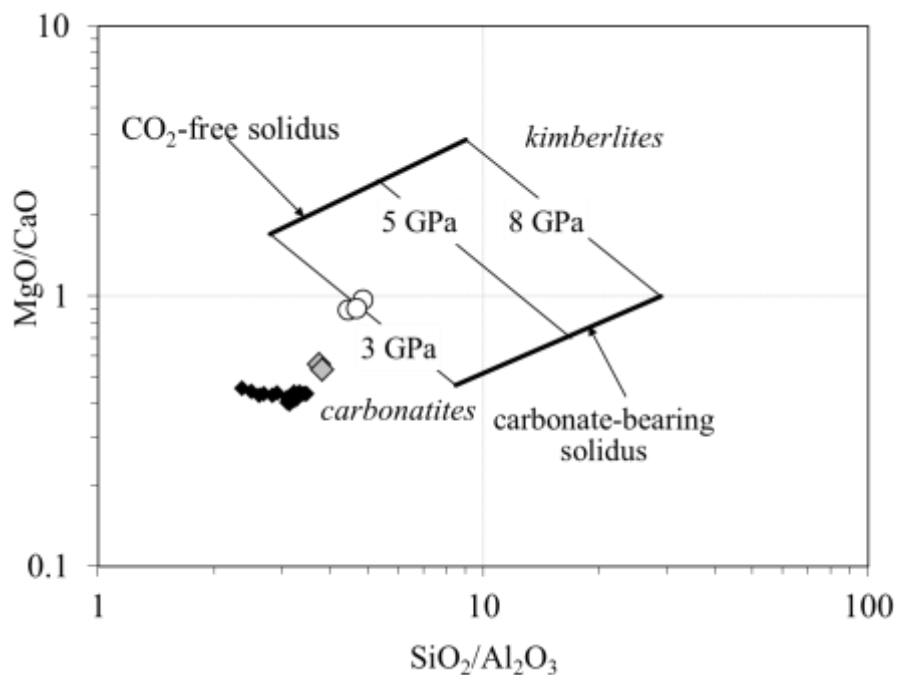


Fig 6.10

6.4 Isotopes

Initial $^{87}\text{Sr}/^{86}\text{Sr}$ and $^{143}\text{Nd}/^{144}\text{Nd}$ ratios of Nyiragongo rocks describes a narrow range of 0.70447-0.70469 and 0.51268 – 0.51272 respectively. Initial Pb-isotope ratios are slightly variable in Nyiragongo products. Initial $^{206}\text{Pb}/^{204}\text{Pb}$ is in the range 19.413 – 19.751, $^{207}\text{Pb}/^{204}\text{Pb}$ is in the range 15.663 – 15.749, $^{208}\text{Pb}/^{204}\text{Pb}$ is in the range 39.629 – 39.814. The isotopic composition measured for Nyamuragira ultramafic rocks are very different from those of Nyiragongo. The nephelinitic rocks show a great variation in Sr and Nd isotopic ratios (fig. 6.11) but not in Pb-isotopic ratios (fig 6.12-6.13), quite similar for these samples. Sr-ratios are more radiogenic and variable in comparison with the Nyiragongo nephelinitic rocks (0.70521 – 0.70590) while Nd-ratios are less radiogenic (0.51254-0.51262). Measured $^{206}\text{Pb}/^{204}\text{Pb}$ in Nyamuragira nephelinitic rocks is less radiogenic (19.192-19.305) than that measured in Nyiragongo. $^{207}\text{Pb}/^{204}\text{Pb}$ and $^{208}\text{Pb}/^{204}\text{Pb}$ measurements are quite similar (15.722 - 15.763 and 39.837 - 40.085 respectively). Totally different compositions are observed for the Nyamuragira tholeiitic basalt sample. It shows low $^{87}\text{Sr}/^{86}\text{Sr}$ (0.70386), $^{206}\text{Pb}/^{204}\text{Pb}$ (18.240), $^{207}\text{Pb}/^{204}\text{Pb}$ (15.527), $^{208}\text{Pb}/^{204}\text{Pb}$ (38.061) and high $^{143}\text{Nd}/^{144}\text{Nd}$ (0.51291).

From a preliminary point of view it is possible to see that isotopic sources of Nyiragongo and Nyamuragira samples are different and they are located between enriched mantle sources, thus presumably the source is an enriched lithospheric intraplate source.

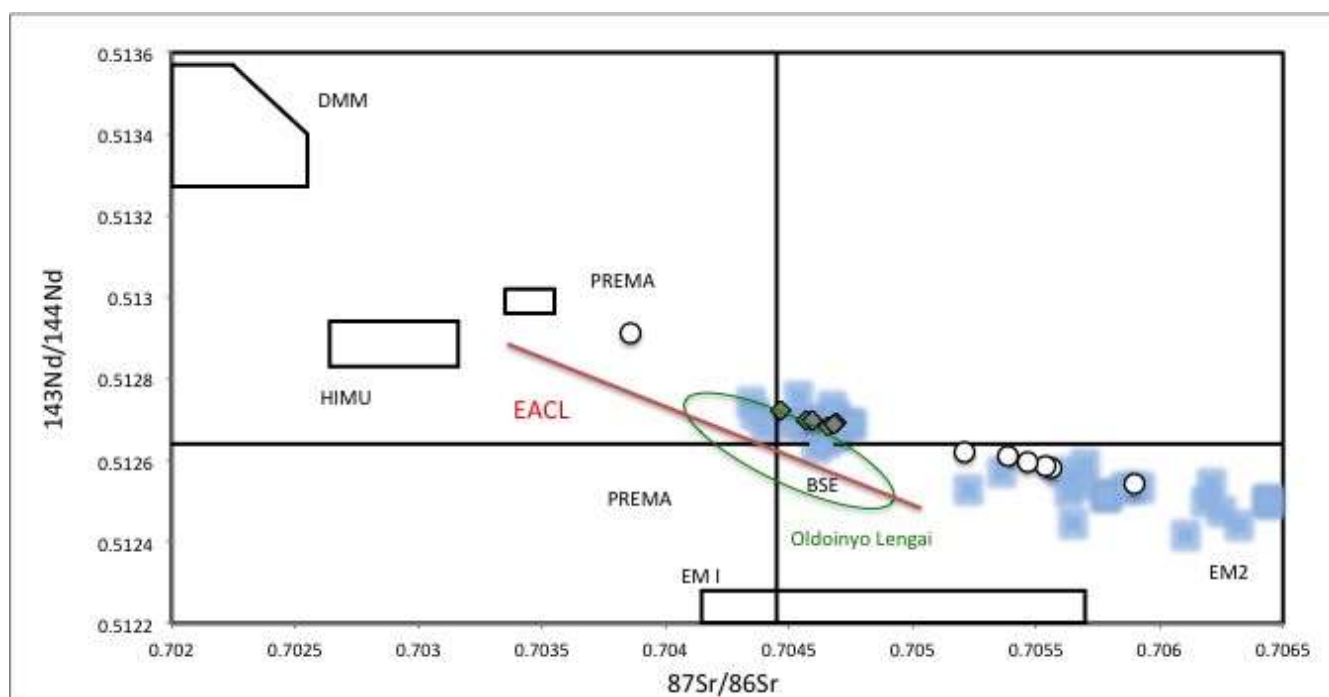


Fig 6.11 Isotopic variation diagram: Nyiragongo (grey diamonds) Nyamuragira (circles), Virunga values from Barette et al., 2016 (blu squares)

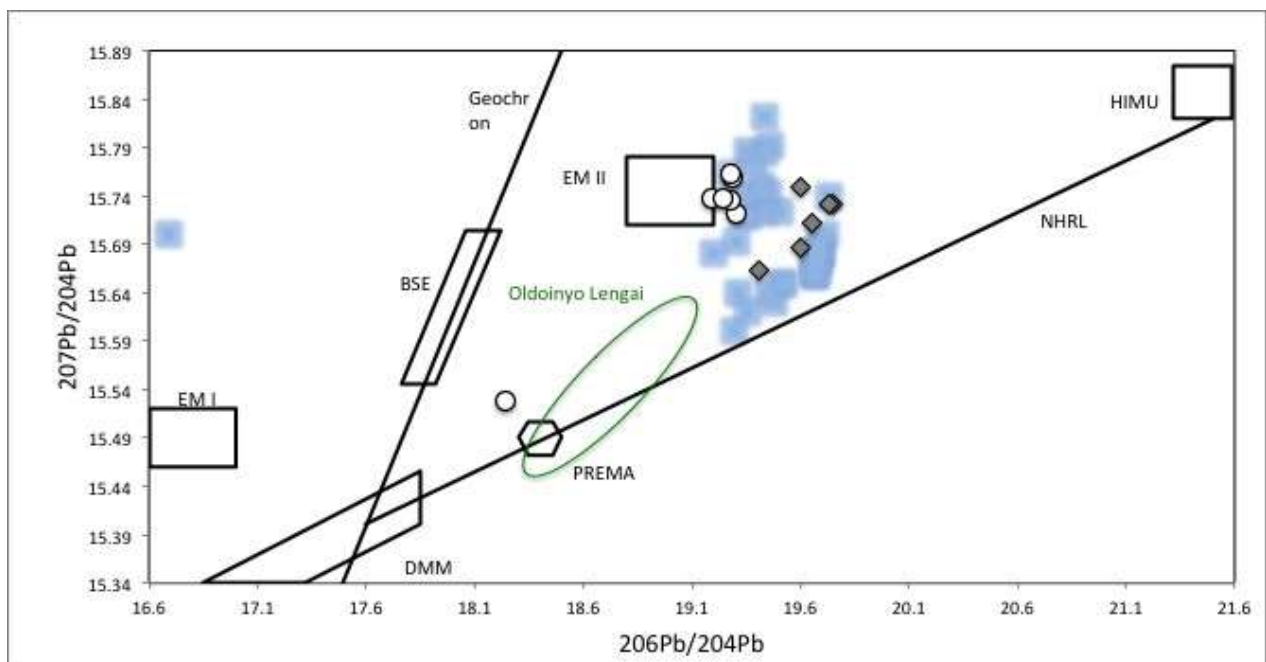
Nd-isotopic compositions of the Nyiragongo volcanics do not vary appreciably and cluster around bulk earth values (fig 6.11) whereas the Nyamuragira lavas show more enriched compositions, in the enriched quadrant of the conventional isotope diagram, with the majority of the Virunga samples. The enrichment perhaps suggests the involvement of old components during petrogenesis (Rogers et al., 1992).

All Nyiragongo lavas have lower Sr and higher Nd isotope ratios than any of the other Virunga lavas, consistent with a younger source age.

According to Chackrabarti (2009) most of the geochemical data of 2002 Nyiragongo lava and the 1972 crater-lake sample (Vollmer and Norry, 1983) overlap with the same values. Thus, on a first order of approximation, the Nyiragongo crater lava has remained uniform isotopically, and chemically, over the last 30 years.

The Nyamuragira samples, as mentioned, overlap with other Virunga volcanics from Muhavura, Gahinga (Rogers et al., 1998) and Karisimbi (Rogers et al., 1992). The silica-saturated Sabinyo volcanics (Vollmer and Norry, 1983a; Rogers et al., 1998), also from Virunga, show the most radiogenic Sr isotopic compositions among the Virunga lavas (Fig. 6.11) and have been interpreted as derivatives of mantle-derived melts mixing with a lower crustal component (Rogers et al., 1998). However, no crustal component has been envisaged in the genesis of any of the other Virunga volcanics based on combined trace element and isotopic characteristics (Rogers et al., 1998). As discussed earlier, the Nyamuragira and Nyiragongo lavas also do not show any sign of continental crustal contamination in their major and trace element characteristics, hence, their Sr–Nd–Pb isotope compositions broadly reflect those of their mantle source regions.

It is possible to argue that the position of the Nyamuragira and other Virunga volcanics in the so-called enriched field in the Nd–Sr isotopic space, in the lower right hand quadrant of Fig. 6.11, indicates contributions from an enriched mantle, such as an EM II-like (Zindler and Hart, 1986; Workman et al., 2004) source.



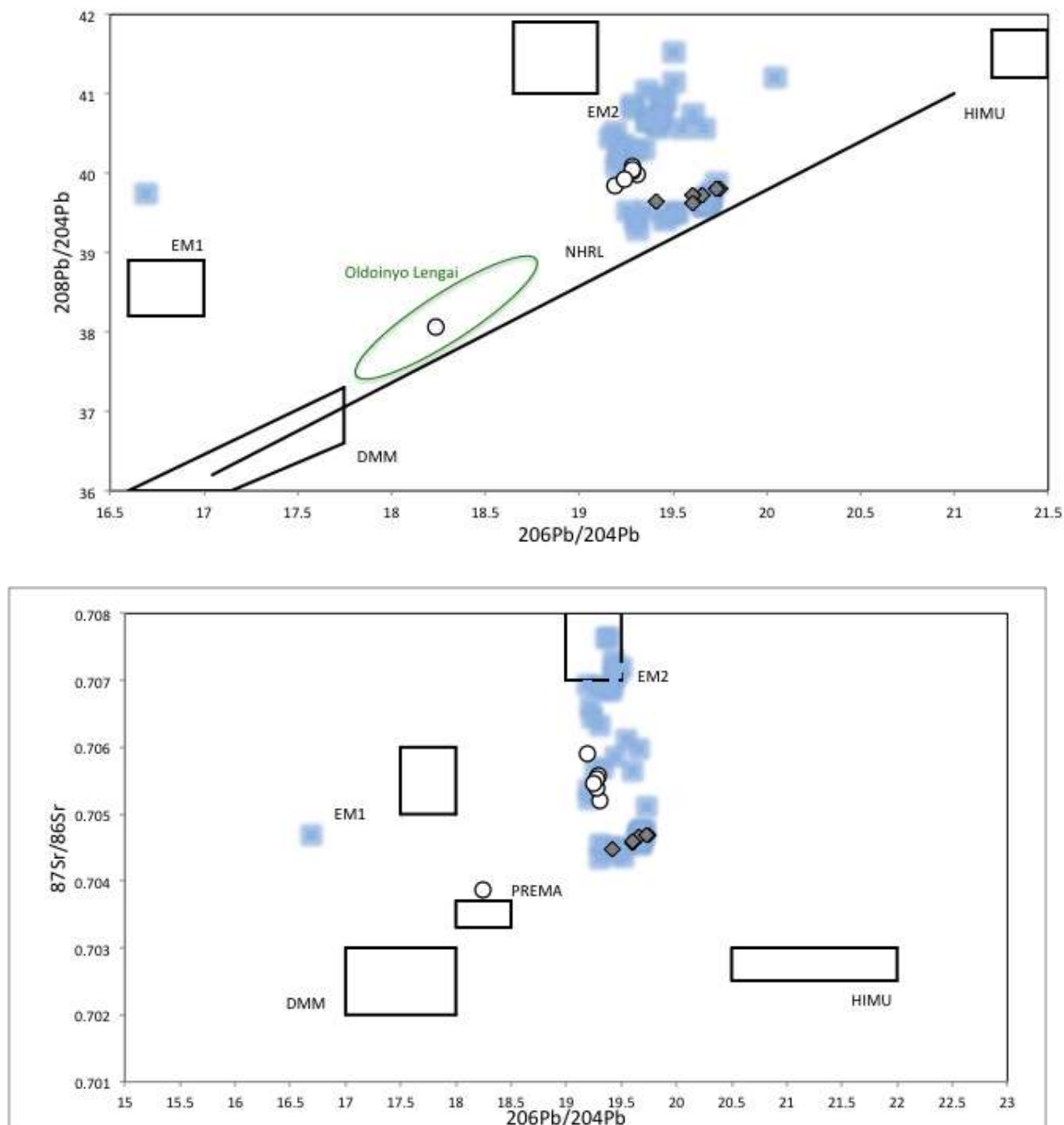


Fig 6.12-6.14 Isotopic variation diagrams: Nyiragongo (grey diamonds) Nyamuragira (circles).

The Pb-isotopic compositions of the Nyiragongo volcanics overlap with those of ocean island basalts (OIB) and can be interpreted by mixtures of several mantle reservoir sources including EM II, DMM, HIMU (Zindler and Hart, 1986). However, like the other Virunga volcanics mentioned above, the 2002 Nyiragongo lava plots in a narrow but discernible vertical trend in $^{207}\text{Pb}/^{204}\text{Pb}$ ratios when plotted against $^{206}\text{Pb}/^{204}\text{Pb}$ (Fig. 6.12), and is almost identical with the Nyiragongo 1972 Crater Lake lava data (Vollmer and Norry, 1983b).

They noticed also the similarity of some Nyiragongo lava data with part of the Group I kimberlite field (Collerson et al., 2010), fig 6.15.

The Nyamuragira volcanics have distinctly higher $^{207}\text{Pb}/^{204}\text{Pb}$ and $^{208}\text{Pb}/^{204}\text{Pb}$ but lower $^{206}\text{Pb}/^{204}\text{Pb}$ ratios compared to Nyiragongo and overlap with the compositions of other Virunga volcanics (e.g. Rogers et al., 1992, 1998) (Fig.6.12-6.14). The Nyamuragira volcanics also show higher $^{208}\text{Pb}/^{206}\text{Pb}$ and $^{207}\text{Pb}/^{206}\text{Pb}$ compared to the Nyiragongo volcanics (Chackrabarti et al., 2009).

Rogers et al. (1992) noticed also the similarity with kimberlites (fig. 6.16) they argue that basanites of Karisimbi volcano (similar of Nyamuragira ones) derived from an isotopic end member that could be represented by nephelinites of Nyiragongo and interpretation of the Pb-Pb array was that it resulted from recent mixing between the host magma and old lithospheric mantle. This implies that the latter is isotopically similar to the source regions of group II kimberlites and some lamproites, having high $^{208}\text{Pb}/^{206}\text{Pb}$ and unradiogenic $^{207}\text{Pb}/^{206}\text{Pb}$ ratios (Fraser et al., 1985; Nelson et al., 1986).

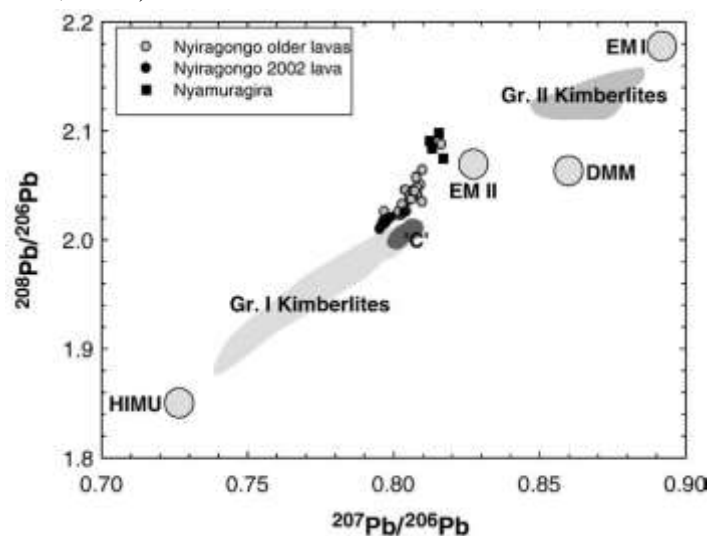


Fig 6.15

According to Furman et al., 1999 it was observed not only an affinity with kimberlites but also an affinity with carbonatites and the East African Carbonatite Line EACL.

EACL was defined by Bell and Blenkinsop (1987) on the basis of Sr–Nd isotopic variations for young carbonatite lavas and it has been interpreted as a mixture between two mantle sources Bell and Blenkinsop (1987), with compositions similar to some ocean island basalt sources Nelson et al., (1988). notably the HIMU high $^{207}\text{Pb}/^{206}\text{Pb}$ and EM I enriched mantle type 1. components as described by Zindler and Hart, (1986).

Mafic lavas from the eastern and western rift branches define an elongate Sr–Nd isotope array that, to a first approximation, lies parallel to the EACL source. The western Virunga vents of Nyiragongo, Goma and Bushwaga also have isotopic compositions that lie within the Kivu array, whereas mafic lavas from the eastern Virunga volcanoes Karisimbi, Visoke and Muhavura are the most highly enriched lavas.

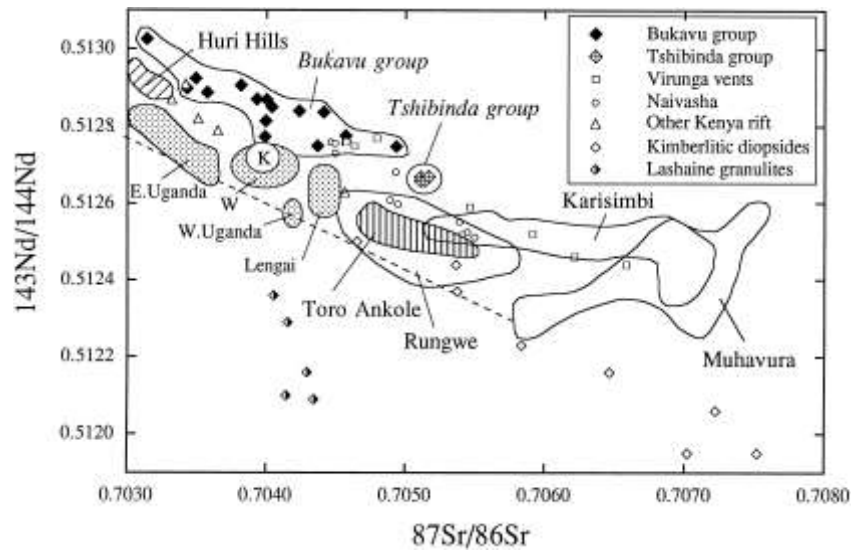


Fig 6.16

Also Bell and Simonetti (1996), taking into account the Oldoinyo Lengai carbonatites, argue that the Nd and Sr isotope data points do not cluster into groups but form a continuum /a linear array Relative to the EACL. Also Pb isotope data from Oldoinyo Lengai are closer to the isotopic composition of EMI rather than HIMU like mentioned before.

According to Collerson et al., (2010) the region of formation of the HIMU-EM complementary reservoirs is interpreted to be near the base of the lower mantle.

The HIMU component is a solid relatively refractory residue that can have a long residence time in the mantle and evolve to extreme isotopic compositions. In contrast, the EM component is a liquid melt that can react with ambient mantle and thus not evolve to extreme isotopic compositions.

Their argument is that OIBs, carbonatites and kimberlites all sampled mantle reservoirs that preserved the effect of the same process of parent–daughter (P/D) ratio fractionation in their genesis.

Final considerations about geochemistry and isotopes

The status of the age determined from Pb isotopes for the source of the Nyiragongo lavas is also unclear nevertheless Vollmer et al. (1985) cited extreme Pb isotope ratios from Nyiragongo that define an ~500 Ma age, which they interpreted as the age of enrichment. Although this age is younger than that of the basanite source, it is consistent with the $^{143}\text{Nd}/^{144}\text{Nd}$ and lower $^{87}\text{Sr}/^{86}\text{Sr}$ ratios that characterize the Nyiragongo lavas. Hence, they infer that the Nyiragongo source is distinct from the basanite source but is also located within the mantle lithosphere.

In fact according to Vollmer (1985) it is possible that ca. 500 Myr ago, beneath Nyiragongo, both silicate and carbonatite magma fractions evolved. There is some evidence from abundant groundmass carbonate in melilite nephelinites (Sahama T D1978) that unmixing was incomplete. Within the Goma nephelinite, however, there is very little carbonate and, if originally present, it must have been evolved as CO_2 , forming the observed vesicular texture or have been destroyed during the high level Fe metasomatism event.

In conclusion, their evidence suggests that carbonatite-related minerals were incorporated into the nephelinite magma and remained stable possibly until broken down during the late high-level Fe metasomatism event. Carbonatite itself or a carbonatite precursor can reasonably be regarded as a result of mantle metasomatism.

Ancient cratons such as the African shield may preserve several generations of metasomatic input and thus several re-enrichment events, in a discrete zone up to tens of kilometers thick (i.e., the mechanical boundary layer; McKenzie et al., 1989) that contributes incompatible trace elements and radiogenic isotopes to later melts rising from greater depths (Furman et al., 1995).

We envisage the genesis of the variously enriched primitive compositions in the volcanism of Virunga/Western branch is linked to a sequence of processes: (1) low-degree melting of a garnet-carbonate lherzolite (up to 4 GPa pressure) at the base of the Tanzanian lithosphere, generating volatile-rich olivine melilititic melts; (2) upwards migration of these melts (that locally were also erupted, like at Toro Ankole) and consequent trace element and isotopic enrichment of the Tanzanian lithosphere; (3) melting of this variably enriched mantle at various pressures, giving rise to the observed compositions.

It is possible to suppose that the enriching component is formed by pure *within-plate* enrichment processes similar to those observed in the African sodic alkaline volcanic rocks of Cenozoic-Recent age, from the Atlas region to the Kenya Rift and, more northwards, to the central European volcanic rocks. This is a geodynamic framework analogue to that developed by Foley (2008). As shown from the geochemical characteristics of the rocks these processes cannot be obviously related to melting sources having recycled crustal materials, and may be caused by concentration of LILE, REE, HFSE and $\text{CO}_2\text{-H}_2\text{O-F}$ -rich fluids in mantle volumes where carbonate and other volatile-rich phases are stable, with mechanisms still not well known (e.g., Rabinowicz et al., 2002).

6.5 U-Th disequilibrium

Measured $^{238}\text{U}/^{232}\text{Th}$ activity ratios on Nyiragongo whole rocks of 2 selected samples range from 1.32 to 1.29 while the $^{230}\text{U}/^{232}\text{Th}$ is similar for both samples (1.23 - 1.24), suggesting that the analyzed samples have not been affected by secondary alteration. U–Th disequilibria for whole rocks is shown in the binary diagram $^{238}\text{U}/^{232}\text{Th}$ vs. $^{230}\text{U}/^{232}\text{Th}$. The Nyiragongo have U/Th activity ratios characterized, compared to secular equilibrium, by an excess (^{238}U) relative to (^{230}Th). The 2002 event has same features (Chakrabarti et al., 2009b) as well as other Virunga samples (Condomines et al., 2015, fig.6.17) thus confirming that from 1977 since today no new features were found.

Samples	U (ppm)	Th (ppm)	Th/U	$(^{238}\text{U}/^{232}\text{Th})$	$(^{230}\text{Th}/^{232}\text{Th})$	$(^{230}\text{Th}/^{238}\text{U})$	(^{226}Ra) dpm/g	$(^{226}\text{Ra}/^{230}\text{Th})$	(^{210}Pb) dpm/g	$(^{210}\text{Pb}/^{226}\text{Ra})$
NY 1977-3	9,52 ± 0,20	21,95 ± 0,09	2,3	1,32	1,24	0,94	6,79 ± 0,03	1,023 ± 0,019	6,86 ± 0,10	1,009 ± 0,012
NY 2016	9,39 ± 0,25	22,18 ± 0,10	2,36	1,29	1,23	0,96	6,89 ± 0,03	1,038 ± 0,025	6,11 ± 0,14	0,887 ± 0,018

NY-5-02	9.63	22.41	2.33	1.30	1.26	0.97	7.29	1.06		
NY-23-02	9.60	20.71	2.16	1.41	1.26	0.90	7.17	1.12		
2003 lava lake	9.20	21.42	2.33	1.30	1.25	0.96	6.98	1.07	6.38 ± 0.22	0.90

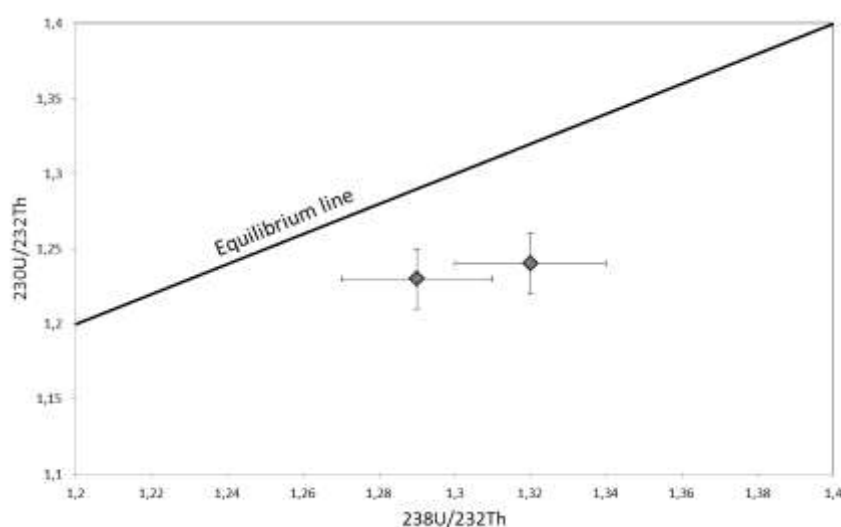


Fig 6.17 Isotopic variation diagram

Several previous studies have demonstrated the heterogeneity of the mantle sources beneath the VVF (e.g. Chakrabarti et al. 2009), most probably due to multiple metasomatic events involving silicate and carbonate melts (Rogers et al., 1992a; Williams and Gill, 1992). Available U-series data for the two active volcanoes of the VVF confirm this heterogeneity. Most U-series data come from Nyiragongo historical or recent differentiated lavas (Chakrabarti et al., 2009b).

Conclusions

Goals of this research project were the full characterization of the geochemistry, petrography, mineralogy, petrology and isotopic geochemistry of the two active volcanoes Nyiragongo and Nyamuragira within the Virunga Volcanic Province (African Rift) to better understand their petrogenesis and to constrain possible correlation in terms of mantle sources and isotopic signatures and to better understand their petrogenesis, in particular to comprehend the occurrence of such unusual and rare rocks in Central Africa such as the melilitites of Nyiragongo.

The two neighbouring volcanoes Nyamuragira and Nyiragongo are the youngest and most westerly volcanoes in the VVP. The magmas of both volcanoes are under-saturated with a strongly alkaline character. However, despite being only 15 km apart they have different mantle sources and degrees of partial melting. The rock types of Nyiragongo's lavas range from nephelinites to melilitites (Platz et al., 2004), whilst the Nyamuragira lavas range from basanites to tephritic phonolites (Aoki et al., 1985). Major and trace element analysis suggests very different melting histories at sub-lithospheric depths, with the source depth for the Nyamuragira magma being shallower than that for Nyiragongo (Chakrabarti et al., 2009). Some of the lavas from vents most distal to the Nyamuragira caldera (e.g., 1904, 1912) and Nyiragongo top crater (e.g., Lac Vert vent) are the most petrologically primitive lavas found on the volcano (Denaeyer, 1972; Aoki et al., 1985). This suggests that some of the magmas feeding these vents had pathways that avoided shallow fractionation within a crustal magma reservoir.

The collected samples were used for an integrated analytical program using multiple methodologies such as: optical microscopy (OM) on thin sections, X-ray fluorescence (XRF), scanning electron microscopy analysis (SEM), energy-dispersion X-ray spectroscopy (EDS) and Inductively Coupled Plasma mass spectrometry (ICP-MS), Thermal ionization Mass Spectrometry (TIMS) and Laser ablation analysis.

The rocks sampled in the volcanic districts of Nyiragongo and Nyamuragira are olivin melilitites, nephelinites, basanites and transitional basalts.

From a petrographic point of view, melilite rocks are characterized by paragenesis almost monotonic characterized by phenocrysts of olivine, clinopyroxene, melilite, feldspathoids, and spinel. The groundmass is composed by the same phases plus apatite and kirschsteinite for few samples.

On the contrary basanites are made of olivine and clinopyroxene plus nepheline, spinel and sparse apatite.

The texture of the rocks, the huge number of mineral phases that made the rock paragenesis, geothermal and geobarometric data, clearly indicate that the studied lavas have been generated in a relatively superficial environment in a wide temperature range.

Geochemical data regarding major and trace elements concentration and their distribution allow to hypothesize that olivine melilitites of Lac Vert of Nyiragongo are representative of

primitive melts, as well as basanite from old lavas of Nyamuragira. All of the other rocks of this thesis work show low evolved features.

The patterns of the REE normalized to the values of the chondrites of all the rocks of Nyiragongo and Nyamuragira show strong enrichment in LREE and strong depletion of the HREE and no negative trough at Eu.

This leads to think that there is a presence of garnet in the source of the magma of Virunga rocks. Indeed, the HREEs are strong compatible with this mineral respect to LREE. A magma originated for partial melting of a garnet mantle source will be enriched in LREE and depleted in HREE. The difference is clear among the rocks patterns compared to those of a typical NMorb, obtained from melting of a spinel source. Since garnet is a stable mineral for pressures above 20-30kbar, the depth of the source can be between 80 and 100km, probably within lithospheric mantle.

Moreover, the low content in SiO₂ (< 42 wt.%) and the presence of normative larnite exclude the orthopyroxene in the source (Dunworth e Wilson, 1998) but the relatively high Mg content (at least for some samples, MgO > 8 wt.%) and the high Ca content (>12 wt.%) and Sr (>2000 ppm) it is clear that in the mantle source of these rocks there is a carbonate phase stable (Dalton and Wood, 1993).

The patterns of the incompatible elements in the Wood diagrams of all lithologies of Virunga analysed rocks show strong enrichment both in LILE and HFSE, typically, anorogenic.

The difference between these types of rocks, belonging to different geodynamic environments, it depends on the degree of partial melting of the source.

In fact, for the melilite rocks low degrees of partial melting (1-2%) are suggested. In particular they appear more enriched in incompatible elements because of the degree of melting lower than the basanitic magmas and less enriched in less incompatible elements due to the higher concentrations of garnet of the source of melilite magma. Furthermore the melilite rocks show negative peaks of K and Pb related to the intrinsic features of the mantle source.

It is also evident that the strongly alkaline rocks of Nyiragongo and Nyamuragira districts derive from mantle sources with different isotopic signatures although they are located between enriched mantle sources. Thus the isotopic signature is presumably attributed to an enriched lithospheric intracontinental source.

Finally Nyamuragira have not only a different source region for its magmas from Nyiragongo, but the eruptive behaviour of the two volcanoes is also quite different. Nyiragongo has a lava lake that has been active for much of the last century, at least since about 1928 (Tazieff, 1979). Unlike the frequent flank eruptions of Nyamuragira, there have only been two recorded flank eruptions at Nyiragongo in the last hundred years; in 1977 (Tazieff, 1977, 2002; Komorowski et al., 2003; Tedesco et al., 2007). In both cases, the lava lake was drained by fissures associated with rift faulting.

Flank eruptions of Nyamuragira also occurred around the same times. So although the magma supply dynamics to the two volcanoes are quite distinct, the stress fields of the volcanoes are both susceptible to modification by crustal level tectonic forces linked to the exstetional setting that charcterised the Western Branch of the African Rift (Wautier et al., 2013).

According to this thesis work and Hertogen () a petrogenetic model is proposed as explanations of the strongly undersaturated character of the Nyiragongo rocks:

The majority of the magmas derive from a primary melilite-nephelinitic or nepheline-melilititic parental magma formed by minor partial melting of mantle peridotite enriched in H₂O and CO₂, (e.g. Brey and Green 1975, 1977). The occurrence of less undersaturated olivine-nephelinites and olivine-leucitites, and the differences between the Nyiragongo and Nyamuragira magmas in general could then be interpreted in terms of different degrees of melting or variable amounts of H₂O and CO₂ in the respective source regions (e.g., Frey et al. 1978).

Perspectives: Isotopic new data, Kd calculation new data to use for other igneous modeling works with same mineral phases; e.g. absolute new data for melilite.

Data tables

Major and trace elements (XRF) of Nyiragongo samples

Sample Name	1977-1	1977-2	1977-3	1977-4	1977-5	M2002-1	M2002-10	M2002-11	M2002-12	M2002-2	M2002-3
SiO ₂	41.70	41.85	41.31	41.27	41.60	41.24	42.38	41.83	41.35	41.31	41.56
TiO ₂	2.84	2.76	2.83	2.79	2.79	2.70	2.72	2.71	2.67	2.82	2.68
Al ₂ O ₃	12.49	12.84	13.10	13.21	13.09	13.31	12.17	13.00	13.36	12.10	12.86
Fe ₂ O ₃	13.14	12.83	13.12	12.88	12.85	12.46	12.69	12.49	12.35	13.18	12.37
MnO	0.28	0.28	0.28	0.28	0.28	0.28	0.28	0.27	0.28	0.29	0.27
MgO	5.36	5.20	5.18	5.07	5.10	5.16	5.42	5.23	4.92	5.49	5.43
CaO	12.17	12.26	12.19	12.10	12.13	12.26	12.50	12.25	12.19	12.65	12.35
Na ₂ O	5.15	5.05	5.25	5.57	5.37	5.61	4.84	5.27	5.82	5.26	5.56
K ₂ O	5.16	5.16	5.01	5.08	5.07	5.08	5.29	5.15	5.21	5.17	5.08
P ₂ O ₅	1.08	1.15	1.09	1.14	1.10	1.26	1.11	1.18	1.23	1.08	1.22
L.O.I.											
Tot.	99.37	99.38	99.36	99.39	99.38	99.36	99.40	99.38	99.38	99.35	99.38
Rb	136	135	138	132	131	146	125	132	144	140	131
Sr	2415	2399	2512	2423	2425	2495	2373	2451	2557	2581	2419
Y	39	39	39	39	39	39	38	38	38	40	38
Zr	268	263	269	267	266	264	258	256	263	273	252
Nb	207	205	212	208	207	211	202	203	213	219	199
Ba	2230	2248	2218	2214	2208	2274	2193	2229	2270	2237	2217
Cr	8	2	7	16	9	<LLD	8	9	<LLD	12	<LLD
Ni	35	30	37	30	31	44	26	29	33	27	27
Sc	10	11	10	12	9	8	8	12	9	9	12
V	302	330	316	270	289	329	345	311	311	325	331
La	177	174	181	164	170	180	172	168	175	178	171
Ce	329	338	329	336	336	340	334	333	327	357	331

Sample Name	M2002-4	M2002-5	M2002-6	M2002-7	M2002-8	M2002-9	M2002-GL	M2002-ST	NYIRA 2002	NYIRA Summit	SHAHERU Down
SiO ₂	41.73	41.61	42.16	41.90	41.60	42.32	41.43	41.57	41.67	41.18	41.90
TiO ₂	2.59	2.73	2.66	2.69	2.70	2.57	2.80	2.74	2.53	2.51	2.20
Al ₂ O ₃	13.27	12.63	12.86	12.66	12.89	13.18	11.94	13.22	14.27	14.51	15.99
Fe ₂ O ₃	12.02	12.76	12.23	12.50	12.59	11.92	13.20	12.89	12.19	11.84	10.57
MnO	0.26	0.28	0.27	0.27	0.28	0.26	0.29	0.28	0.29	0.28	0.25
MgO	4.99	5.27	5.11	5.29	5.09	5.08	5.52	4.86	4.74	4.93	4.35
CaO	12.36	12.31	12.34	12.33	12.33	12.28	12.69	12.16	10.81	11.49	10.15
Na ₂ O	5.54	5.43	5.24	5.35	5.43	5.21	5.01	5.17	5.83	6.04	6.32
K ₂ O	5.34	5.21	5.30	5.23	5.28	5.27	5.40	5.20	6.10	5.63	6.77
P ₂ O ₅	1.28	1.13	1.22	1.16	1.20	1.28	1.07	1.28	0.91	0.95	0.89
L.O.I.									-0.48	-0.34	0.02
Tot.	99.38	99.36	99.39	99.38	99.39	99.37	99.35	99.37	99.34	99.36	99.39
Rb	136	134	131	129	137	136	141	151	149	143	173
Sr	2476	2484	2417	2412	2500	2428	2573	2381	2487	2587	2461
Y	38	38	37	37	38	38	40	40	40	41	37
Zr	252	262	250	255	260	262	268	278	306	305	277
Nb	203	210	198	202	208	206	216	222	219	214	200
Ba	2325	2241	2228	2193	2239	2261	2250	2341	2444	2259	2169
Cr	<LLD	4	2	11	6	7	<LLD	<LLD	57	5	53
Ni	30	29	26	28	29	28	27	34	42	29	45
Sc	10	14	11	9	8	11	12	11	6	11	9
V	328	380	320	297	291	379	338	380	284	315	267
La	167	178	170	169	177	173	182	177	176	173	148
Ce	334	347	337	325	332	335	342	333	346	325	300

Sample Name	SHAHERU Up	KITOKO (helicopter)	2ND Pause	NYRA-2	NYRA-1	LV1	LV2	LV3	LV4	MG002	MONT Goma Sand
SiO ₂	42.46	41.75	42.59	38.75	37.66	39.89	40.17	40.54	41.68	40.38	40.60
TiO ₂	1.86	2.26	2.52	1.95	2.51	3.05	3.14	2.79	2.80	3.27	3.31
Al ₂ O ₃	17.89	15.48	16.98	11.05	11.21	10.62	10.52	13.40	12.83	12.28	12.30
Fe ₂ O ₃	8.99	10.87	9.41	12.05	12.09	12.23	12.65	12.13	13.44	14.39	14.35
MnO	0.20	0.25	0.22	0.27	0.27	0.22	0.22	0.26	0.29	0.30	0.29
MgO	3.98	4.57	4.11	4.91	4.90	9.07	8.71	5.41	6.02	5.96	5.91
CaO	8.73	10.52	9.28	11.03	11.22	16.24	16.30	12.85	13.25	13.30	12.96
Na ₂ O	7.03	6.36	6.72	4.89	4.55	5.53	3.94	5.49	4.49	3.36	3.65
K ₂ O	7.59	6.46	7.39	5.56	5.43	1.30	2.62	5.09	3.56	4.96	4.80
P ₂ O ₅	0.74	0.86	0.81	1.82	1.83	1.43	1.28	1.47	1.00	1.19	1.24
L.O.I.	0.09	-0.04	0.03			1.21	0.95	-0.34	0.36	3.09	1.41
Tot.	99.47	99.38	99.46	92.85	91.66	99.58	99.55	99.43	99.36	99.39	99.41
Rb	171	144	153	128	137	20	78	117	97	130	118
Sr	2155	2439	2198	2590	2651	1643	1544	2145	2722	2306	2189
Y	30	37	32	34	38	29	30	37	43	42	42
Zr	227	273	237	292	320	267	268	285	275	363	351
Nb	159	193	167	237	236	127	126	176	231	185	182
Ba	1782	2173	2016	2526	2633	814	1029	2051	1988	1922	1871
Cr	1	<LLD	17	5	7	380	395	10	50	27	10
Ni	23	24	23			169	155	37	55	45	32
Sc	6	8	11	5	7	24	27	12	13	14	16
V	198	293	239	279	287	426	466	395	470	428	412
La	128	154	127			105	115	160	187	159	152
Ce	247	313	261			220	210	315	355	325	322

Major and trace elements (XRF) of Nyamuragira samples

Sample Name	NYIRA Summit b	MUJA	NYAM 2010 Summit	NYAM 2011-2012 Rumungebo	NYAM A	NYAM B	NYAM C	M1508-2	M1508-1	NM1548	NM1548-2	NYAM E 2011-2012
SiO ₂	49.39	45.10	45.24	45.99	45.60	45.11	45.13	47.01	46.03	45.98	46.50	48.01
TiO ₂	3.28	2.49	3.54	3.20	2.58	2.64	3.42	3.33	3.68	3.55	3.51	1.84
Al ₂ O ₃	16.37	9.24	15.40	14.82	10.17	9.56	15.49	15.22	14.02	14.82	14.94	10.82
Fe ₂ O ₃	11.96	11.76	13.07	12.26	11.52	12.04	12.40	11.98	13.57	13.02	12.71	13.34
MnO	0.18	0.17	0.18	0.18	0.17	0.18	0.19	0.18	0.20	0.20	0.19	0.18
MgO	4.55	13.56	5.50	5.76	12.02	12.51	5.23	5.01	5.72	5.39	4.96	15.13
CaO	6.89	14.03	9.45	10.74	13.55	13.93	9.38	9.34	9.60	9.61	9.52	8.51
Na ₂ O	4.11	1.63	3.51	3.02	2.07	1.82	3.51	3.67	3.00	3.33	3.35	1.70
K ₂ O	3.66	1.49	3.29	2.85	1.78	1.86	3.43	3.42	3.45	3.34	3.50	0.29
P ₂ O ₅	0.54	0.22	0.50	0.42	0.28	0.25	0.51	0.54	0.43	0.45	0.47	0.14
L.O.I.	-0.01	-0.31	0.30	-0.57	-0.41	-0.57	0.47					-0.43
Tot.	99.65	99.99	99.89	99.71	99.72	99.70	99.89					99.76
Rb	107	42	100	66	38	44	88	88	96	99	96	1
Sr	1019	491	941	761	467	523	922	921	969	979	992	216
Y	31	15	29	29	20	22	29	29	32	32	31	19
Zr	309	171	288	296	180	179	285	280	311	305	304	106
Nb	102	45	94	73	45	49	92	89	100	100	100	8
Ba	1170	494	1070	895	544	544	1094	1096	1088	1092	1122	78
Cr	26	326	53	36	790	613	40	39	47	31	27	989
Ni	41	309	45	26	246	267	39	33	35	40	27	750
Sc	16	51	20	22	46	50	19	15	19	19	15	24
V	339	362	415	432	309	367	354	382	310	324	322	233
La	75	43	71	62	40	35	65	68	73	71	70	11
Ce	161	72	154	134	62	62	157	160	160	158	162	20

Next two pages: major and trace elements (ICP-MS) and Sr Nd Pb isotopes (TIMS)

Sample name	1977-1	1977-3	M2002-2	NYIRA 2002	SHAHERU Up	NYRA-2	NYIRA 2016	LV1	LV3
	Nyiragongo	Nyiragongo	Nyiragongo	Nyiragongo	Nyiragongo	Nyiragongo	Nyiragongo	Nyiragongo	Nyiragongo
SiO ₂	40.10	39.00	40.17	40.77	40.90	41.74	39.12	38.52	39.91
TiO ₂	14.90	14.94	14.72	16.13	20.28	11.90	14.87	10.87	14.15
Al ₂ O ₃	13.50	13.82	13.22	12.92	9.63	12.98	13.41	12.90	12.85
Fe ₂ O ₃	0.29	0.30	0.29	0.30	0.22	0.29	0.29	0.23	0.28
MnO	4.16	4.14	4.19	3.39	2.68	5.29	4.02	10.39	4.68
MgO	11.90	12.34	12.21	11.00	8.73	11.87	12.01	16.39	12.82
CaO	5.64	5.10	5.80	5.76	6.63	5.26	5.62	4.32	4.98
Na ₂ O	5.63	5.24	5.55	6.29	7.92	5.99	5.64	1.26	5.24
K ₂ O	2.88	2.92	2.74	2.54	1.91	2.71	2.81	3.19	2.89
P ₂ O ₅	1.48	1.54	1.47	1.27	0.94	1.96	1.59	1.52	1.67
L.O.I.	-1.01	-0.94	-1.63	-0.59	0.07		0.39	0.71	-0.32
Tot.	99.47	98.38	98.74	99.90	99.90	100.00	99.77	100.30	99.14
MgO ppm	25086	24966	25267	20443	16161	31901	24242	62655	28222
TiO ₂ ppm	17272	17499	16438	15203	11468	16246	16858	19142	17344
K ₂ O ppm	46740	43502	46076	52220	65752	49729	46823	10461	43502
P ₂ O ₅ ppm	6459	6721	6415	5542	4102	8553	6939	6633	7288
Sc	5	5	5	3	2		4	21	6
Be	4.00	4.00	4.00	4.00	3.00		4	2.00	3.00
V	290	293	285	241	187	234.5	287	408	334
Cr	< 20	30	< 20	< 20	< 20	5		390	< 20
Co	42	44	40	36	28	39.0	45	52	43
Ni	20	< 20	< 20	< 20	< 20	39.2	50	170	20
Cu	200	190	180	160	130	166.6	180	110	160
Zn	130	140	130	140	100	147.7	120	100	120
Ga	20.0	22.0	20.0	21.0	19.0	18.2	20	18.0	21.0
Ge	1.0	2.0	1.0	1.0	1.0	1.1	1	2.0	2.0
As	< 5	< 5	< 5	< 5	< 5			< 5	< 5
Rb	141	143	140	162	178	137.6	138	21	129
Sr	3133	2820	3474	2751	2312	2950.0	2693	1836	2653
Y	37.0	35.0	37.0	37.0	27.0	37.8	34	27.0	35.0
Zr	268	335	273	306	259	292	313	267	285
Nb	223	241	227	236	183	237	239	130	200
Mo	7.00	4.00	6.00	6.00	3.00		7	< 2	4.00
Cd									
In	< 0.2	< 0.2	< 0.2	< 0.2	< 0.2			< 0.2	< 0.2
Sn	3.00	2.00	2.00	2.00	2.00	4.77	27	1.00	2.00
Sb	< 0.5	0.70	0.50	0.50	0.60			< 0.5	< 0.5
Cs	1.50	1.60	1.50	1.60	1.50	1.84	1.5	1.30	1.30
Ba	2422	2324	2389	2593	1830	2140	2278	789	2160
La	194.00	193.00	197.00	195.00	140.00	183.15	201	131.00	180.00
Ce	357.00	355.00	365.00	364.00	263.00	332.54	373	254.00	341.00
Pr	37.30	35.60	37.70	38.20	27.50	34.86	38.8	28.10	36.50
Nd	125.00	124.00	125.00	128.00	91.70	119.61	129	100.00	124.00
Sm	18.20	18.10	18.30	18.90	13.50	17.72	18.9	15.40	18.70
Eu	5.15	5.31	5.14	5.33	3.92	5.06	5.25	4.46	5.24
Gd	12.40	12.90	12.60	12.90	9.30	11.93	12.5	10.80	13.00
Tb	1.50	1.70	1.60	1.70	1.20	1.57	1.7	1.40	1.60
Dy	7.80	8.50	8.10	8.40	6.10	7.73	8.4	6.40	7.80
Ho	1.40	1.40	1.50	1.40	1.10	1.35	1.5	1.10	1.40
Er	3.80	4.00	3.90	4.20	2.90	3.56	4	3.00	3.90
Tm	0.49	0.51	0.50	0.56	0.40	0.47	0.53	0.37	0.51
Yb	2.90	3.00	2.90	3.10	2.20	2.84	3.1	2.10	2.90
Lu	0.41	0.41	0.41	0.46	0.30	0.40	0.45	0.28	0.39
Hf	1.30	3.20	1.80	1.40	2.90	4.47	4.3	1.20	2.00
Ta	12.80	16.00	13.00	13.70	10.10	14.79	16.3	8.00	11.80
W	7.00	3.00	3.00	2.00	2.00	2.07	2	< 1	3.00
Pb	6.00	7.00	6.00	7.00	< 5		7	< 5	6.00
Bi	< 0.4	< 0.4	< 0.4	< 0.4	< 0.4			< 0.4	< 0.4
Th	20.80	22.00	21.00	20.70	14.80	20.09	22.3	12.20	17.50
U	9.10	9.80	9.00	8.40	5.60	8.65	9.9	5.00	5.80
Zr/Sm	14.73	18.51	14.92	16.19	19.19	16.47	16.60	17.34	15.24
Zr/Nb	1.20	1.39	1.20	1.30	1.42	1.23	1.30	2.05	1.43
Ba/Nb	10.86	9.64	10.52	10.99	10.00	9.02	9.50	6.07	10.80
La/Nb	0.87	0.80	0.87	0.83	0.77	0.77	0.84	1.01	0.90
Nb/U	24.51	24.59	25.22	28.10	32.68	27.42	24.00	26.00	34.48
Zr/Y	7.24	9.57	7.38	8.27	9.59	7.72	9.20	9.89	8.14
Nb/Yb	76.90	80.33	78.28	76.13	83.18	83.52	77.10	61.90	68.97
Sm/Nd	0.15	0.15	0.15	0.15	0.15	0.15	0.15	0.15	0.15
Rb/Sr	0.05	0.05	0.04	0.06	0.08	0.05	0.05	0.01	0.05
Zr/Hf	206.15	104.69	151.67	218.57	89.31	65.28	73.00	222.50	142.50
Nb/Ta	17.42	15.06	17.46	17.23	18.12	16.04	14.70	16.25	16.95
Th/U	2.29	2.24	2.33	2.46	2.64	2.32	2.30	2.44	3.02
Nb/Y	6.03	6.89	6.14	6.38	6.78	6.28	7.03	4.81	5.71
La/Nd	1.55	1.56	1.58	1.52	1.53	1.53	1.56	1.31	1.45
La/Sm	10.66	10.66	10.77	10.32	10.37	10.34	10.63	8.51	9.63
Th/Yb	7.17	7.33	7.24	6.68	6.73	7.07	7.19	5.81	6.03

Sample name	1977-1	1977-3	M2002-2	NYIRA 2002	SHAHERU Up	NYRA-2	NYIRA 2016	LV1	LV3
87Sr/86Sr	0.70		0.70	0.70	0.70		0.70		0.70
143Nd/144Nd	0.51		0.51	0.51	0.51		0.51		0.51
206Pb/204Pb	19.65		19.75	19.61	19.60		19.73		19.41
			19.75		19.61		19.73		
207Pb/204Pb	15.71		15.73	15.75	15.68		15.73		15.66
			15.73		15.69		15.74		
208Pb/204Pb	39.73		39.80	39.72	39.61		39.80		39.64
			39.81		39.65		39.83		

Sample name	LV4	MG002	MUJA	NYAM 2010 Summit	NYAM 2011-2012 Rumangabo	NYAM A	NM1938-1	NM1948	NYAM B 2011-2012
	Nyiragongo	Nyiragongo	Nyamulagira	Nyamulagira	Nyamulagira	Nyamulagira	Nyamulagira	Nyamulagira	Nyamulagira
SiO ₂	34.99	39.51	44.88	44.50	45.00	44.53	45.52	45.25	48.03
TiO ₂	13.72	14.69	9.25	16.12	15.76	10.31	16.42	16.52	9.93
Al ₂ O ₃	11.57	12.41	10.97	13.32	13.12	11.47	13.29	12.88	12.96
Fe ₂ O ₃	0.25	0.26	0.16	0.19	0.20	0.17	0.20	0.20	0.18
MnO	4.33	4.22	14.52	4.79	5.34	14.03	4.68	4.65	18.24
MgO	11.42	12.04	14.68	9.79	11.11	14.13	9.44	9.77	8.01
CaO	4.36	4.51	1.61	3.36	2.96	1.73	3.42	3.36	1.52
Na ₂ O	3.27	5.01	1.45	3.28	2.85	1.60	3.58	3.46	0.27
K ₂ O	2.44	2.97	2.49	3.80	3.54	2.68	3.73	3.71	1.67
P ₂ O ₅	1.32	1.61	0.28	0.65	0.57	0.31	0.67	0.65	0.18
L.O.I.	12.14	2.73	-0.22	0.53	-0.44	-0.79	-0.61	-0.66	-0.43
Tot.	99.80	99.97	100.10	100.30	100.00	100.20	100.30	99.79	100.60
MgO ppm	26111	25448	87561	28885	32202	84606	28222	28041	109994
TiO ₂ ppm	14598	17799	14946	22805	21222	16085	22361	22247	10024
K ₂ O ppm	27148	41593	12038	27231	23661	13283	29721	28725	2242
P ₂ O ₅ ppm	5760	7026	1222	2837	2487	1353	2924	2837	786
Sc	7	6	50	16	24	47	15	18	25
Be	3.00	3.00	1.00	2.00	2.00	1.00	2.00	2.00	< 1
V	322	302	322	349	381	325	326	333	225
Cr	< 20	< 20	880	40	20	810	30	20	970
Co	36	39	58	38	40	57	39	38	71
Ni	20	< 20	290	20	< 20	260	20	< 20	830
Cu	70	260	90	40	20	80	60	50	70
Zn	110	120	70	110	100	70	140	110	100
Ga	19.0	20.0	14.0	22.0	22.0	15.0	22.0	22.0	14.0
Ge	1.0	1.0	2.0	2.0	2.0	2.0	2.0	2.0	2.0
As	< 5	< 5	< 5	< 5	< 5	< 5	< 5	< 5	< 5
Rb	84	116	40	105	79	43	98	94	5
Sr	2537	2467	507	1035	916	565	1078	1067	230
Y	32.0	36.0	16.0	25.0	28.0	17.0	27.0	27.0	16.0
Zr	265	363	157	310	290	181	321	310	96
Nb	214	167	39	92	80	47	97	93	9
Mo	3.00	5.00	2.00	4.00	6.00	2.00	4.00	4.00	< 2
Cd									
In	< 0.2	< 0.2	< 0.2	< 0.2	< 0.2	< 0.2	< 0.2	< 0.2	< 0.2
Sn	1.00	5.00	2.00	2.00	2.00	2.00	3.00	3.00	1.00
Sb	0.60	0.50	< 0.5	< 0.5	< 0.5	< 0.5	< 0.5	< 0.5	< 0.5
Cs	1.10	1.10	< 0.5	1.00	0.90	< 0.5	1.00	1.00	< 0.5
Ba	1784	1917	472	1116	961	526	1162	1138	63
La	171.00	161.00	36.50	79.80	71.60	40.50	86.70	83.40	7.20
Ce	314.00	310.00	74.90	156.00	143.00	82.60	169.00	162.00	18.00
Pr	32.60	33.70	9.01	17.60	16.30	9.73	18.90	17.90	2.72
Nd	108.00	117.00	34.60	63.60	60.40	37.70	67.40	65.40	12.80
Sm	16.10	17.90	6.60	10.50	10.50	6.90	11.20	11.00	3.70
Eu	4.44	5.14	1.82	3.07	2.91	2.03	3.12	3.06	1.30
Gd	10.60	12.30	5.00	8.00	8.00	5.40	8.40	8.20	4.00
Tb	1.40	1.60	0.70	1.10	1.10	0.80	1.10	1.10	0.60
Dy	7.10	7.70	3.70	5.60	6.00	3.90	6.00	5.70	3.60
Ho	1.30	1.40	0.70	1.00	1.10	0.70	1.10	1.10	0.70
Er	3.50	3.70	1.80	2.80	2.90	2.00	3.00	3.00	1.80
Tm	0.45	0.50	0.23	0.39	0.41	0.25	0.42	0.41	0.24
Yb	2.70	2.80	1.40	2.50	2.60	1.50	2.50	2.50	1.40
Lu	0.38	0.40	0.21	0.35	0.40	0.23	0.37	0.37	0.20
Hf	3.10	1.10	3.30	5.50	6.00	3.80	5.90	5.50	2.00
Ta	11.20	9.90	2.50	5.80	4.80	2.90	5.90	5.60	0.50
W	2.00	2.00	1.00	3.00	2.00	2.00	9.00	3.00	1.00
Pb	7.00	6.00	< 5	8.00	7.00	< 5	8.00	8.00	< 5
Bi	< 0.4	< 0.4	< 0.4	< 0.4	< 0.4	< 0.4	< 0.4	< 0.4	< 0.4
Th	20.60	15.70	4.60	11.20	10.00	5.00	11.80	11.60	0.50
U	9.60	5.60	1.00	2.20	2.00	1.10	2.50	2.40	0.20
Zr/Sm	16.46	20.28	23.79	29.52	27.6	26.2	28.7	28.2	25.9
Zr/Nb	1.24	2.17	4.03	3.37	3.6	3.9	3.3	3.3	10.7
Ba/Nb	8.34	11.48	12.10	12.13	12.0	11.2	12.0	12.2	7.0
La/Nb	0.80	0.96	0.94	0.87	0.90	0.86	0.89	0.90	0.80
Nb/U	22.29	29.82	39.00	41.82	40	43	39	39	45
Zr/Y	8.28	10.08	9.81	12.40	10.4	10.6	11.9	11.5	6.0
Nb/Yb	79.26	59.64	27.86	36.80	30.8	31.3	38.8	37.2	6.4
Sm/Nd	0.15	0.15	0.19	0.17	0.17	0.18	0.17	0.17	0.29
Rb/Sr	0.03	0.05	0.08	0.10	0.09	0.08	0.09	0.09	0.02
Zr/Hf	85.48	330.00	47.58	56.36	48	48	54	56	48
Nb/Ta	19.11	16.87	15.60	15.86	16.7	16.2	16.4	16.6	18.0
Th/U	2.15	2.80	4.60	5.09	5.0	4.5	4.7	4.8	2.5
Nb/Y	6.69	4.64	2.44	3.68	2.86	2.76	3.59	3.44	0.56
La/Nd	1.58	1.38	1.05	1.25	1.19	1.07	1.29	1.28	0.56
La/Sm	10.62	8.99	5.53	7.60	6.82	5.87	7.74	7.58	1.95
Th/Yb	7.63	5.61	3.29	4.48	3.85	3.33	4.72	4.64	0.36
Sample name	LV4	MG002	MUJA	NYAM 2010 Summit	NYAM 2011-2012 Rumangabo	Nyam B	NM1938-1	NM1948	NYAM B 2011-2012
87Sr/86Sr				0.71	0.71	0.71	0.71	0.71	0.70
143Nd/144Nd			0.51	0.51	0.51	0.51	0.51	0.51	0.51
206Pb/204Pb			19.31	19.24	19.20	19.28	19.28	19.28	18.24
207Pb/204Pb			15.72	15.74	15.74	15.74	15.76	15.75	15.53
208Pb/204Pb			39.99	39.92	39.85	40.03	40.04	40.06	38.06
					39.82			40.11	

Major elements and CIPW norms of Nyiragongo samples.

Sample name	1977-1	1977-2	1977-3	1977-4	1977-5	M2002-1	M2002-10	M2002-11	M2002-12	M2002-2	M2002-3
	Nyiragongo	Nyiragongo	Nyiragongo	Nyiragongo	Nyiragongo	Nyiragongo	Nyiragongo	Nyiragongo	Nyiragongo	Nyiragongo	Nyiragongo
SiO ₂	41.70	41.85	41.31	41.27	41.60	41.24	42.38	41.83	41.35	41.31	41.56
TiO ₂	2.84	2.76	2.83	2.79	2.79	2.70	2.72	2.71	2.67	2.82	2.68
Al ₂ O ₃	12.49	12.84	13.10	13.21	13.09	13.31	12.17	13.00	13.36	12.10	12.86
Fe ₂ O ₃	13.14	12.83	13.12	12.88	12.85	12.46	12.69	12.49	12.35	13.18	12.37
MnO	0.28	0.28	0.28	0.28	0.28	0.28	0.28	0.27	0.28	0.29	0.27
MgO	5.36	5.20	5.18	5.07	5.10	5.16	5.42	5.23	4.92	5.49	5.43
CaO	12.17	12.26	12.19	12.10	12.13	12.26	12.50	12.25	12.19	12.65	12.35
Na ₂ O	5.15	5.05	5.25	5.57	5.37	5.61	4.84	5.27	5.82	5.26	5.56
K ₂ O	5.16	5.16	5.01	5.08	5.07	5.08	5.29	5.15	5.21	5.17	5.08
P ₂ O ₅	1.08	1.15	1.09	1.14	1.10	1.26	1.11	1.18	1.23	1.08	1.22
LOI											
TOT	99.4	99.4	99.4	99.4	99.4	99.4	99.4	99.4	99.4	99.4	99.4
Alk	10.3	10.2	10.3	10.7	10.4	10.7	10.1	10.4	11.0	10.4	10.6
Na/K	1.00	0.98	1.05	1.10	1.06	1.10	0.91	1.02	1.12	1.02	1.09
Mg#	48	48	47	47	47	48	49	48	47	48	50
Rb	136	135	138	132	131	146	125	132	144	140	131
Sr	2415	2399	2512	2423	2425	2495	2373	2451	2557	2581	2419
Y	39	39	39	39	39	39	38	38	38	40	38
Zr	268	263	269	267	266	264	258	256	263	273	252
Nb	207	205	212	208	207	211	202	203	213	219	199
Ba	2230	2248	2218	2214	2208	2274	2193	2229	2270	2237	2217
Cr	8	2	7	16	9		8	9		12	
Ni	35	30	37	30	31	44	26	29	33	27	27
Sc	10	11	10	12	9	8	8	12	9	9	12
V	302	330	316	270	289	329	345	311	311	325	331
La	177	174	181	164	170	180	172	168	175	178	171
Ce	329	338	329	336	336	340	334	333	327	357	331
qz	0.00	0.00	0.00	0.00	0.00	0.00	0.00	0.00	0.00	0.00	0.00
cor	0.00	0.00	0.00	0.00	0.00	0.00	0.00	0.00	0.00	0.00	0.00
or	0.00	0.00	0.00	0.00	0.00	0.00	0.00	0.00	0.00	0.00	0.00
ab	0.00	0.00	0.00	0.00	0.00	0.00	0.00	0.00	0.00	0.00	0.00
an	0.00	0.00	0.00	0.00	0.00	0.00	0.00	0.00	0.00	0.00	0.00
ne	19.24	20.22	21.39	21.49	21.18	21.77	17.96	20.69	21.51	18.12	20.51
lc	23.91	23.91	23.21	23.54	23.49	23.54	24.51	23.86	24.14	23.96	23.54
-wo	8.16	9.49	8.61	6.80	7.96	6.75	9.89	8.41	6.49	6.86	7.52
-en	3.89	4.55	4.10	3.19	3.76	3.24	4.81	4.06	3.06	3.30	3.71
-fs	4.15	4.80	4.39	3.53	4.11	3.41	4.92	4.22	3.35	3.46	3.67
di	16.20	18.84	17.10	13.52	15.83	13.40	19.61	16.69	12.91	13.62	14.90
wo	0.00	0.00	0.00	0.00	0.00	0.00	0.00	0.00	0.00	0.00	0.00
-en	0.00	0.00	0.00	0.00	0.00	0.00	0.00	0.00	0.00	0.00	0.00
-fs	0.00	0.00	0.00	0.00	0.00	0.00	0.00	0.00	0.00	0.00	0.00
hy	0.00	0.00	0.00	0.00	0.00	0.00	0.00	0.00	0.00	0.00	0.00
-fo	6.63	5.89	6.17	6.61	6.27	6.73	6.09	6.28	6.44	7.27	6.88
-fa	7.79	6.85	7.27	8.05	7.55	7.80	6.86	7.19	7.77	8.40	7.51
ol	14.41	12.74	13.44	14.66	13.82	14.54	12.95	13.47	14.21	15.68	14.39
cs	10.46	9.47	10.13	11.24	10.50	11.28	9.62	10.19	11.42	12.16	10.93
mt	0.00	0.45	0.72	0.00	0.05	0.00	0.00	0.00	0.00	0.00	0.00
il	5.39	5.24	5.37	5.30	5.30	5.13	5.17	5.15	5.07	5.36	5.09
ap	2.56	2.72	2.58	2.70	2.61	2.98	2.63	2.80	2.91	2.56	2.89
ac	5.80	4.77	4.35	5.68	5.58	5.50	5.60	5.51	5.45	5.82	5.46
ns	0.34	0.00	0.00	0.24	0.00	0.24	0.34	0.03	0.78	1.04	0.69
kp	0.00	0.00	0.00	0.00	0.00	0.00	0.00	0.00	0.00	0.00	0.00
ks	0.00	0.00	0.00	0.00	0.00	0.00	0.00	0.00	0.00	0.00	0.00
hl	0.00	0.00	0.00	0.00	0.00	0.00	0.00	0.00	0.00	0.00	0.00
th	0.00	0.00	0.00	0.00	0.00	0.00	0.00	0.00	0.00	0.00	0.00
hm	0.00	0.00	0.00	0.00	0.00	0.00	0.00	0.00	0.00	0.00	0.00
tn	0.00	0.00	0.00	0.00	0.00	0.00	0.00	0.00	0.00	0.00	0.00
pf	0.00	0.00	0.00	0.00	0.00	0.00	0.00	0.00	0.00	0.00	0.00
ru	0.00	0.00	0.00	0.00	0.00	0.00	0.00	0.00	0.00	0.00	0.00
fr	0.00	0.00	0.00	0.00	0.00	0.00	0.00	0.00	0.00	0.00	0.00
cc	0.00	0.00	0.00	0.00	0.00	0.00	0.00	0.00	0.00	0.00	0.00
aq	0.00	0.00	0.00	0.00	0.00	0.00	0.00	0.00	0.00	0.00	0.00
Tot	98.32	98.36	98.31	98.36	98.35	98.37	98.39	98.39	98.40	98.29	98.40
R1	-657	-602	-683	-809	-713	-812	-518	-670	-906	-725	-770
R2	1813	1822	1818	1805	1808	1829	1845	1825	1810	1863	1843
CaO/Al ₂ O ₃	0.97	0.95	0.93	0.92	0.93	0.92	1.03	0.94	0.91	1.05	0.96
SiO ₂ /Al ₂ O ₃	3.34	3.26	3.15	3.12	3.18	3.10	3.48	3.22	3.10	3.41	3.23
MgO/CaO	0.44	0.42	0.42	0.42	0.42	0.42	0.43	0.43	0.40	0.43	0.44
CaO+Na ₂ O+K ₂ O	22.48	22.47	22.45	22.75	22.57	22.95	22.63	22.67	23.22	23.08	22.99
SiO ₂ +Al ₂ O ₃	54.19	54.69	54.41	54.48	54.69	54.55	54.55	54.83	54.71	53.41	54.42

Sample name	M2002-4 Nyiragongo	M2002-5 Nyiragongo	M2002-6 Nyiragongo	M2002-7 Nyiragongo	M2002-8 Nyiragongo	M2002-9 Nyiragongo	M2002-GL Nyiragongo	M2002-ST Nyiragongo	NYIRA 2002 Nyiragongo	NYIRA Summit Nyiragongo	SHAHERU Down Nyiragongo
SiO ₂	41.73	41.61	42.16	41.90	41.60	42.32	41.43	41.57	41.95	41.45	42.16
TiO ₂	2.59	2.73	2.66	2.69	2.70	2.57	2.80	2.74	2.55	2.53	2.21
Al ₂ O ₃	13.27	12.63	12.86	12.66	12.89	13.18	11.94	13.22	14.36	14.60	16.09
Fe ₂ O ₃	12.02	12.76	12.23	12.50	12.59	11.92	13.20	12.89	12.27	11.92	10.63
MnO	0.26	0.28	0.27	0.27	0.28	0.26	0.29	0.28	0.29	0.28	0.25
MgO	4.99	5.27	5.11	5.29	5.09	5.08	5.52	4.86	4.77	4.96	4.38
CaO	12.36	12.31	12.34	12.33	12.33	12.28	12.69	12.16	10.88	11.56	10.21
Na ₂ O	5.54	5.43	5.24	5.35	5.43	5.21	5.01	5.17	5.87	6.08	6.36
K ₂ O	5.34	5.21	5.30	5.23	5.28	5.27	5.40	5.20	6.14	5.67	6.81
P ₂ O ₅	1.28	1.13	1.22	1.16	1.20	1.28	1.07	1.28	0.92	0.96	0.90
LOI									-0.48	-0.34	0.02
TOT	99.4	99.4	99.4	99.4	99.4	99.4	99.4	99.4	100.0	100.0	100.0
Alk	10.9	10.6	10.5	10.6	10.7	10.5	10.4	10.4	12.0	11.7	13.2
Na/K	1.04	1.04	0.99	1.02	1.03	0.99	0.93	0.99	0.96	1.07	0.93
Mg#	48	48	48	49	48	49	48	46	47	48	48
Rb	136	134	131	129	137	136	141	151	149	143	173
Sr	2476	2484	2417	2412	2500	2428	2573	2381	2487	2587	2461
Y	38	38	37	37	38	38	40	40	40	41	37
Zr	252	262	250	255	260	262	268	278	306	305	277
Nb	203	210	198	202	208	206	216	222	219	214	200
Ba	2325	2241	2228	2193	2239	2261	2250	2341	2444	2259	2169
Cr		4	2	11	6	7			57	5	53
Ni	30	29	26	28	29	28	27	34	42	29	45
Sc	10	14	11	9	8	11	12	11	6	11	9
V	328	380	320	297	291	379	338	380	284	315	267
La	167	178	170	169	177	173	182	177	176	173	148
Ce	334	347	337	325	332	335	342	333	346	325	300
qz	0.00	0.00	0.00	0.00	0.00	0.00	0.00	0.00	0.00	0.00	0.00
cor	0.00	0.00	0.00	0.00	0.00	0.00	0.00	0.00	0.00	0.00	0.00
or	0.00	0.00	0.00	0.00	0.00	0.00	0.00	0.00	0.00	0.00	0.00
ab	0.00	0.00	0.00	0.00	0.00	0.00	0.00	0.00	0.00	0.00	0.00
an	0.00	0.00	0.00	0.00	0.00	0.00	0.00	0.00	0.00	0.00	0.00
ne	20.87	19.48	19.85	19.50	19.99	20.83	16.98	21.15	21.51	23.60	24.28
lc	24.74	24.14	24.56	24.23	24.47	24.42	25.02	24.09	28.45	26.25	31.56
-wo	7.44	7.45	9.06	8.27	7.35	9.86	6.76	9.42	4.09	3.61	1.71
-en	3.57	3.57	4.37	4.01	3.49	4.80	3.25	4.39	1.89	1.73	0.81
-fs	3.75	3.77	4.54	4.13	3.77	4.88	3.41	4.93	2.15	1.83	0.87
di	14.76	14.79	17.97	16.40	14.60	19.54	13.42	18.74	8.13	7.16	3.39
wo	0.00	0.00	0.00	0.00	0.00	0.00	0.00	0.00	0.00	0.00	0.00
-en	0.00	0.00	0.00	0.00	0.00	0.00	0.00	0.00	0.00	0.00	0.00
-fs	0.00	0.00	0.00	0.00	0.00	0.00	0.00	0.00	0.00	0.00	0.00
hy	0.00	0.00	0.00	0.00	0.00	0.00	0.00	0.00	0.00	0.00	0.00
-fo	6.20	6.70	5.86	6.42	6.44	5.50	7.36	5.41	7.00	7.45	7.07
-fa	7.17	7.81	6.71	7.29	7.67	6.15	8.49	6.70	8.78	8.66	8.37
ol	13.38	14.51	12.57	13.72	14.11	11.65	15.85	12.10	15.78	16.11	15.44
cs	10.88	11.10	9.77	10.46	11.06	8.97	12.31	9.10	11.83	13.15	12.61
mt	0.00	0.00	0.00	0.00	0.00	0.15	0.00	0.78	0.00	0.00	0.00
il	4.92	5.18	5.05	5.11	5.13	4.88	5.32	5.20	4.84	4.80	4.20
ap	3.03	2.68	2.89	2.75	2.84	3.03	2.53	3.03	2.17	2.26	2.12
ac	5.30	5.63	5.40	5.52	5.56	4.96	5.83	4.14	5.42	5.26	4.69
ns	0.54	0.84	0.37	0.70	0.64	0.00	1.03	0.00	0.89	0.44	0.85
kp	0.00	0.00	0.00	0.00	0.00	0.00	0.00	0.00	0.00	0.00	0.00
ks	0.00	0.00	0.00	0.00	0.00	0.00	0.00	0.00	0.00	0.00	0.00
hl	0.00	0.00	0.00	0.00	0.00	0.00	0.00	0.00	0.00	0.00	0.00
th	0.00	0.00	0.00	0.00	0.00	0.00	0.00	0.00	0.00	0.00	0.00
hm	0.00	0.00	0.00	0.00	0.00	0.00	0.00	0.00	0.00	0.00	0.00
tn	0.00	0.00	0.00	0.00	0.00	0.00	0.00	0.00	0.00	0.00	0.00
pf	0.00	0.00	0.00	0.00	0.00	0.00	0.00	0.00	0.00	0.00	0.00
ru	0.00	0.00	0.00	0.00	0.00	0.00	0.00	0.00	0.00	0.00	0.00
fr	0.00	0.00	0.00	0.00	0.00	0.00	0.00	0.00	0.00	0.00	0.00
cc	0.00	0.00	0.00	0.00	0.00	0.00	0.00	0.00	0.00	0.00	0.00
aq	0.00	0.00	0.00	0.00	0.00	0.00	0.00	0.00	0.00	0.00	0.00
Tot	98.43	98.34	98.42	98.39	98.39	98.43	98.29	98.35	99.01	99.04	99.15
R1	-802	-762	-664	-712	-774	-626	-682	-674	-1096	-1084	-1363
R2	1830	1826	1826	1830	1825	1824	1866	1801	1683	1770	1625
CaO/Al ₂ O ₃	0.93	0.97	0.96	0.97	0.96	0.93	1.06	0.92	0.76	0.79	0.63
SiO ₂ /Al ₂ O ₃	3.14	3.29	3.28	3.31	3.23	3.21	3.47	3.14	2.92	2.84	2.62
MgO/CaO	0.40	0.43	0.41	0.43	0.41	0.41	0.43	0.40	0.44	0.43	0.43
CaO+Na ₂ O+K ₂ O	23.24	22.95	22.88	22.91	23.04	22.76	23.10	22.53	22.89	23.31	23.38
SiO ₂ +Al ₂ O ₃	55.00	54.24	55.02	54.56	54.49	55.50	53.37	54.79	56.31	56.05	58.25

Sample name	SHAHERU Up Nyiragongo	KITOKO (helicopter) Nyiragongo	2ND Pause Nyiragongo	NYRA-2 Nyiragongo	NYRA 2016 Nyiragongo	LV1 Nyiragongo	LV2 Nyiragongo	LV3 Nyiragongo	LV4 Nyiragongo	MG002 Nyiragongo	MONT Goma Sand Nyiragongo
SiO ₂	42.69	42.01	42.82	41.74	39.36	40.06	40.35	40.77	41.95	40.63	40.84
TiO ₂	1.87	2.27	1.96	2.71	2.83	3.06	3.15	2.81	2.82	3.29	3.33
Al ₂ O ₃	17.99	15.58	17.07	11.90	14.96	10.66	10.57	13.48	12.91	12.36	12.37
Fe ₂ O ₃	9.04	10.94	9.46	12.98	13.49	12.28	12.71	12.20	13.53	14.48	14.44
MnO	0.20	0.25	0.22	0.29	0.29	0.22	0.22	0.26	0.29	0.30	0.29
MgO	4.00	4.60	4.13	5.29	4.05	9.11	8.75	5.44	6.06	6.00	5.95
CaO	8.78	10.59	9.33	11.87	12.08	16.31	16.37	12.92	13.34	13.38	13.04
Na ₂ O	7.07	6.40	6.76	5.26	5.66	5.55	3.96	5.52	4.52	3.38	3.67
K ₂ O	7.63	6.50	7.43	5.99	5.68	1.31	2.63	5.12	3.58	4.99	4.83
P ₂ O ₅	0.74	0.87	0.81	1.96	1.60	1.44	1.29	1.48	1.01	1.20	1.25
LOI	0.09	-0.04	0.03		0.39	1.21	0.95	-0.34	0.36	3.09	1.41
TOT	100.0	100.0	100.0	100.00	100.01	100.0	100.0	100.0	100.0	100.0	100.0
Alk	14.7	12.9	14.2	11.3	11.3	6.9	6.6	10.6	8.1	8.4	8.5
Na/K	0.93	0.98	0.91			4.25	1.50	1.08	1.26	0.68	0.76
Mg#	50	49	50			63	61	50	50	48	48
Rb	171	144	153	138	138	20	78	117	97	130	118
Sr	2155	2439	2198	2950	2693	1643	1544	2145	2722	2306	2189
Y	30	37	32	38	34	29	30	37	43	42	42
Zr	227	273	237	292	313	267	268	285	275	363	351
Nb	159	193	167	237	239	127	126	176	231	185	182
Ba	1782	2173	2016	2140	2278	814	1029	2051	1988	1922	1871
Cr	1		17	5		380	395	10	50	27	10
Ni	23	24	23	39	50	169	155	37	55	45	32
Sc	6	8	11			24	27	12	13	14	16
V	198	293	239	235		426	466	395	470	428	412
La	128	154	127	183	201	105	115	160	187	159	152
Ce	247	313	261	333	373	220	210	315	355	325	322
qz	0.00	0.00	0.00	0.00	0.00	0.00	0.00	0.00	0.00	0.00	0.00
cor	0.00	0.00	0.00	0.00	0.00	0.00	0.00	0.00	0.00	0.00	0.00
or	0.00	0.00	0.00	0.00	0.00	0.00	0.00	0.00	0.00	0.00	0.00
ab	0.00	0.00	0.00	0.00	0.00	0.00	0.00	0.00	0.00	0.00	0.00
an	0.00	0.00	0.00	0.00	0.00	0.32	3.30	0.00	4.37	3.80	3.02
ne	27.10	23.80	25.16	15.11	24.42	25.45	18.14	22.11	20.71	15.50	16.83
lc	34.12	30.12	34.43	27.74	26.13	6.05	12.19	23.72	16.60	23.12	22.37
-wo	0.00	2.09	0.95	7.92	3.11	17.09	15.31	5.39	16.81	12.04	13.21
-en	0.00	1.00	0.46	3.67	1.27	10.79	9.46	2.70	8.74	6.15	6.75
-fs	0.00	1.05	0.47	4.17	1.87	5.24	4.95	2.57	7.60	5.59	6.13
di	0.00	4.15	1.88	15.76	6.24	33.12	29.72	10.66	33.15	23.78	26.09
wo	0.00	0.00	0.00	0.00	0.00	0.00	0.00	0.00	0.00	0.00	0.00
-en	0.00	0.00	0.00	0.00	0.00	0.00	0.00	0.00	0.00	0.00	0.00
-fs	0.00	0.00	0.00	0.00	0.00	0.00	0.00	0.00	0.00	0.00	0.00
hy	0.00	0.00	0.00	0.00	0.00	0.00	0.00	0.00	0.00	0.00	0.00
-fo	6.98	7.32	6.89	6.66	6.13	8.33	8.64	7.60	4.45	6.16	5.64
-fa	7.68	8.48	7.69	8.33	9.94	4.46	4.98	7.97	4.27	6.17	5.65
ol	14.66	15.80	14.58	14.99	16.06	12.79	13.62	15.57	8.72	12.33	11.29
cs	11.97	12.96	11.98	8.40	12.93	9.37	10.18	12.86	4.63	8.03	6.77
mt	0.00	0.00	0.00	0.00	1.22	2.72	2.81	0.09	2.99	3.20	3.19
il	3.55	4.32	3.72	5.15	5.34	5.82	5.99	5.33	5.35	6.25	6.32
ap	1.76	2.05	1.93	4.65	3.77	3.40	3.05	3.50	2.38	2.84	2.95
ac	3.99	4.83	4.18	4.47	2.17	0.00	0.00	5.20	0.00	0.00	0.00
ns	1.22	1.10	1.39	2.70	0.00	0.00	0.00	0.00	0.00	0.00	0.00
kp	0.90	0.00	0.00	0.00	0.00	0.00	0.00	0.00	0.00	0.00	0.00
ks	0.00	0.00	0.00	0.00	0.00	0.00	0.00	0.00	0.00	0.00	0.00
hl	0.00	0.00	0.00	0.00	0.00	0.00	0.00	0.00	0.00	0.00	0.00
th	0.00	0.00	0.00	0.00	0.00	0.00	0.00	0.00	0.00	0.00	0.00
hm	0.00	0.00	0.00	0.00	0.00	0.00	0.00	0.00	0.00	0.00	0.00
tn	0.00	0.00	0.00	0.00	0.00	0.00	0.00	0.00	0.00	0.00	0.00
pf	0.00	0.00	0.00	0.00	0.00	0.00	0.00	0.00	0.00	0.00	0.00
ru	0.00	0.00	0.00	0.00	0.00	0.00	0.00	0.00	0.00	0.00	0.00
fr	0.00	0.00	0.00	0.00	0.00	0.00	0.00	0.00	0.00	0.00	0.00
cc	0.00	0.00	0.00	0.00	0.00	0.00	0.00	0.00	0.00	0.00	0.00
aq	0.00	0.00	0.00	0.00	0.39	0.00	0.00	0.00	0.00	0.00	0.00
Tot	99.28	99.12	99.24	98.96	98.68	98.00	98.99	99.05	98.91	98.84	98.85
R1	-1722	-1324	-1569	-882	-1114	6	269	-817	-58	-106	-157
R2	1490	1666	1538	1766	1776	2406	2393	1917	1981	1972	1933
CaO/Al ₂ O ₃	0.49	0.68	0.55			1.53	1.55	0.96	1.03	1.08	1.05
SiO ₂ /Al ₂ O ₃	2.37	2.70	2.51			3.76	3.82	3.03	3.25	3.29	3.30
MgO/CaO	0.46	0.43	0.44			0.56	0.53	0.42	0.45	0.45	0.46
CaO+Na ₂ O+K ₂ O	23.47	23.49	23.52			23.17	22.96	23.56	21.44	21.75	21.54
SiO ₂ +Al ₂ O ₃	60.67	57.59	59.89			50.72	50.92	54.25	54.86	52.98	53.21

Next page major elements and CIPW norms of Nyamuragira samples

Sample name	NYIRA Summit B	MUJA	NYAM 2010 Summit	NYAM 2011-2012 Rumangabo	NYAM A	NYAM B
	Nyamulagira	Nyamulagira	Nyamulagira	Nyamulagira	Nyamulagira	Nyamulagira
SiO2	46.55	45.24	45.38	46.80	45.73	45.25
TiO2	3.29	2.50	3.55	3.21	2.57	2.65
Al2O3	16.43	9.27	15.45	14.66	10.20	9.59
Fe2O3	12.02	11.80	13.11	12.30	11.55	12.08
MnO	0.18	0.17	0.18	0.18	0.17	0.18
MgO	4.57	13.60	5.52	5.78	12.05	12.55
CaO	8.72	14.07	9.49	10.77	13.59	13.97
Na2O	4.12	1.64	3.52	3.03	2.08	1.83
K2O	3.57	1.49	3.30	2.86	1.78	1.66
P2O5	0.54	0.22	0.50	0.42	0.28	0.25
LOI	-0.01	-0.31	0.30	-0.57	-0.41	-0.57
TOT	100.00	100.00	100.00	100.00	100.00	100.00
Alk	7.70	3.13	6.82	5.89	3.86	3.49
Na/K	1.15	1.09	1.07	1.06	1.16	1.10
Mg#	46.06	72.16	48.61	51.37	70.11	70.02
Rb	107	42	100	68	38	44
Sr	1019	481	941	761	487	523
Y	31	19	29	29	20	22
Zr	309	171	288	256	180	179
Nb	102	45	94	73	45	49
Ba	1170	494	1070	895	544	544
Cr	26	926	53	36	790	813
Ni	41	309	45	28	245	267
Sc	16	51	20	22	46	50
V	339	362	415	432	309	367
La	75	43	71	62	40	35
Ce	161	72	154	134	82	92
qz	0.00	0.00	0.00	0.00	0.00	0.00
cor	0.00	0.00	0.00	0.00	0.00	0.00
or	21.11	8.83	19.50	16.89	10.55	9.84
ab	10.01	0.10	7.17	10.66	1.66	0.15
an	15.76	13.54	16.60	17.97	13.24	13.05
ne	13.48	7.44	12.25	8.11	8.62	8.29
lc	0.00	0.00	0.00	0.00	0.00	0.00
-wo	10.01	22.90	11.36	13.66	21.85	22.81
-en	5.13	15.80	6.06	7.54	14.83	15.44
-fs	4.62	5.24	4.93	5.61	5.33	5.61
di	19.76	43.94	22.35	26.81	42.01	43.86
wo	0.00	0.00	0.00	0.00	0.00	0.00
-en	0.00	0.00	0.00	0.00	0.00	0.00
-fs	0.00	0.00	0.00	0.00	0.00	0.00
hy	0.00	0.00	0.00	0.00	0.00	0.00
-fo	4.37	12.66	5.38	4.80	10.65	11.08
-fa	4.33	4.63	4.83	3.94	4.22	4.44
ol	8.70	17.29	10.21	8.74	14.87	15.51
cs	0.00	0.00	0.00	0.00	0.00	0.00
mt	2.66	2.61	2.90	2.72	2.56	2.67
il	6.25	4.74	6.74	6.10	4.88	5.03
ap	1.28	0.52	1.19	1.00	0.67	0.59
ac	0.00	0.00	0.00	0.00	0.00	0.00
ns	0.00	0.00	0.00	0.00	0.00	0.00
kp	0.00	0.00	0.00	0.00	0.00	0.00
ks	0.00	0.00	0.00	0.00	0.00	0.00
hl	0.00	0.00	0.00	0.00	0.00	0.00
th	0.00	0.00	0.00	0.00	0.00	0.00
hm	0.00	0.00	0.00	0.00	0.00	0.00
tn	0.00	0.00	0.00	0.00	0.00	0.00
pf	0.00	0.00	0.00	0.00	0.00	0.00
ru	0.00	0.00	0.00	0.00	0.00	0.00
fr	0.00	0.00	0.00	0.00	0.00	0.00
cc	0.00	0.00	0.00	0.00	0.00	0.00
aq	0.00	0.00	0.00	0.00	0.00	0.00
Tot	99.01	99.01	98.92	98.98	99.04	98.99
R1	417	1724	583	984	1537	1606
R2	1482	2362	1592	1727	2252	2306
CaO/Al ₂ O ₃	0.53	1.52	0.61	0.73	1.33	1.46
SiO ₂ /Al ₂ O ₃	2.83	4.88	2.94	3.19	4.48	4.72
MgO/CaO	0.52	0.97	0.58	0.54	0.89	0.90
CaO+Na ₂ O+K ₂ O	16.42	17.20	16.31	16.66	17.45	17.46
SiO ₂ +Al ₂ O ₃	62.98	54.51	60.83	61.46	55.93	54.83

Sample name	NYAM C	M1938-2	NM1938-1	NM1948	NM1948-2	NYAM B 2011-2012
	Nyamulagira	Nyamulagira	Nyamulagira	Nyamulagira	Nyamulagira	Nyamulagira
SiO2	46.27	47.01	46.03	45.98	46.50	48.13
TiO2	3.43	3.33	3.66	3.55	3.51	1.64
Al2O3	15.54	15.22	14.02	14.82	14.94	10.85
Fe2O3	12.44	11.96	13.57	13.02	12.71	13.37
MnO	0.19	0.18	0.20	0.20	0.19	0.18
MgO	5.25	5.01	5.72	5.39	4.98	15.17
CaO	9.41	9.34	9.60	9.61	9.52	8.53
Na2O	3.52	3.67	3.00	3.33	3.35	1.70
K2O	3.44	3.42	3.46	3.34	3.50	0.29
P2O5	0.51	0.54	0.43	0.45	0.47	0.14
LOI	0.47					-0.43
TOT	100.00	99.68	99.69	99.69	99.67	100.00
Alk	6.96	7.09	6.46	6.67	6.85	1.99
Na/K	1.02	1.07	0.87	1.00	0.96	5.86
Mg#	48.67	48.50	48.66	48.21	46.83	71.83
Rb	88	86	96	99	98	1
Sr	922	921	968	979	982	216
Y	29	29	32	32	31	19
Zr	286	280	311	306	304	106
Nb	92	89	100	100	100	8
Ba	1094	1096	1086	1092	1122	78
Cr	40	39	47	31	27	969
Ni	39	33	35	40	27	750
Sc	19	15	19	19	15	24
V	354	382	310	324	322	233
La	65	68	73	71	70	11
Ce	157	160	160	158	162	20
qz	0.00	0.00	0.00	0.00	0.00	0.00
cor	0.00	0.00	0.00	0.00	0.00	0.00
or	20.33	20.21	20.45	19.74	20.68	1.72
ab	9.07	11.56	8.67	8.77	9.79	14.42
an	16.43	14.95	14.57	15.63	15.39	21.09
ne	11.22	10.56	9.05	10.51	10.05	0.00
lc	0.00	0.00	0.00	0.00	0.00	0.00
-wo	11.23	11.63	12.63	12.15	12.01	8.48
-en	6.02	6.23	6.73	6.45	6.25	5.66
-fs	4.85	5.03	5.49	5.33	5.42	2.20
di	22.10	22.88	24.86	23.93	23.69	16.34
wo	0.00	0.00	0.00	0.00	0.00	0.00
-en	0.00	0.00	0.00	0.00	0.00	17.47
-fs	0.00	0.00	0.00	0.00	0.00	6.78
hy	0.00	0.00	0.00	0.00	0.00	24.25
-fo	4.94	4.38	5.26	4.89	4.31	10.26
-fa	4.39	3.90	4.73	4.46	4.12	4.39
ol	9.33	8.28	10.00	9.35	8.43	14.65
cs	0.00	0.00	0.00	0.00	0.00	0.00
mt	2.75	2.65	3.00	2.88	2.81	2.96
il	6.52	6.32	6.95	6.74	6.67	3.12
ap	1.21	1.28	1.02	1.07	1.11	0.33
ac	0.00	0.00	0.00	0.00	0.00	0.00
ns	0.00	0.00	0.00	0.00	0.00	0.00
kp	0.00	0.00	0.00	0.00	0.00	0.00
ks	0.00	0.00	0.00	0.00	0.00	0.00
hl	0.00	0.00	0.00	0.00	0.00	0.00
th	0.00	0.00	0.00	0.00	0.00	0.00
hm	0.00	0.00	0.00	0.00	0.00	0.00
tn	0.00	0.00	0.00	0.00	0.00	0.00
pf	0.00	0.00	0.00	0.00	0.00	0.00
ru	0.00	0.00	0.00	0.00	0.00	0.00
fr	0.00	0.00	0.00	0.00	0.00	0.00
cc	0.00	0.00	0.00	0.00	0.00	0.00
aq	0.00	0.00	0.00	0.00	0.00	0.00
Tot	98.98	98.70	98.57	98.61	98.62	98.88
R1	630	645	760	684	683	2155
R2	1572	1546	1586	1586	1559	1878
CaO/Al ₂ O ₃	0.61	0.61	0.68	0.65	0.64	0.79
SiO ₂ /Al ₂ O ₃	2.98	3.09	3.28	3.10	3.11	4.44
MgO/CaO	0.56	0.54	0.60	0.56	0.52	1.78
CaO+Na ₂ O+K ₂ O	16.37	16.43	16.06	16.28	16.37	10.53
SiO ₂ +Al ₂ O ₃	61.81	62.23	60.05	60.80	61.44	58.97

Olivine of Nyiragongo samples

Sample rock	SHD ol	SHD ol	SHD kir	SHD ol	LV1 ol	LV1 ol	LV1 ol	LV1 ol	LV1 ol	LV1 ol	LV1 ol	SHD ol	SHU ol	SHU krc	SHU krc
SiO ₂	36.83	34.21	33.04	32.60	39.79	40.36	39.88	39.87	38.55	40.54	38.99	35.24	37.78	33.44	32.75
Fe ₂ O ₃	26.26	37.80	32.19	47.01	10.97	13.76	13.88	10.86	14.77	10.80	17.52	27.91	25.50	39.94	32.88
MnO	1.26	2.23	1.97	2.93	0.39	0.14	0.17	0.19	0.10	0.34	0.51	1.13	0.93	1.82	2.22
MgO	32.62	22.08	3.78	13.52	47.29	43.98	44.74	46.09	43.45	47.76	41.97	31.16	35.57	7.58	4.18
CaO	1.85	2.21	27.90	3.31	0.43	0.51	0.98	0.34	0.76	0.38	0.93	1.42	1.50	16.60	27.34
NiO					0.00	0.00	0.33	0.36	0.42	0.07	0.43				
Tot.	98.81	98.53	98.88	99.37	98.87	98.75	99.99	97.70	98.04	99.89	100.34	96.86	101.29	99.38	99.37
Si	1.00	1.00	1.02	1.00	0.99	1.02	1.00	1.01	0.99	1.00	0.99	0.99	0.99	1.02	1.00
Fe	0.60	0.92	0.83	1.20	0.23	0.29	0.29	0.23	0.32	0.22	0.37	0.65	0.56	1.02	0.84
Mn	0.03	0.06	0.05	0.08	0.01	0.00	0.00	0.00	0.00	0.01	0.01	0.03	0.02	0.05	0.06
Mg	1.32	0.96	0.17	0.62	1.76	1.66	1.67	1.74	1.67	1.59	1.30	1.39	0.35	0.19	
Ca	0.05	0.07	0.92	0.11	0.01	0.01	0.03	0.01	0.02	0.01	0.03	0.04	0.04	0.54	0.90
Ni	0.00	0.00	0.00	0.00	0.00	0.00	0.01	0.01	0.01	0.00	0.01	0.00	0.00	0.00	0.00
Tot.	3.00	3.00	2.98	3.00	3.01	2.98	3.00	2.99	3.01	3.00	3.01	3.01	3.01	2.98	3.00
Iarnite	2.69	3.45	46.63	5.41	0.58	0.70	1.33	0.46	1.04	0.50	1.26	2.10	2.09	27.77	45.14
fayalite	31.28	48.70	44.59	63.82	11.81	14.95	14.79	11.80	15.95	11.52	19.18	33.63	28.82	54.57	45.26
forsterite	66.04	47.85	8.78	30.76	87.61	84.35	83.89	87.74	83.01	87.98	79.56	64.27	69.09	17.66	9.60
tephroite	2.07	5.08	4.49	9.49	0.46	0.17	0.21	0.23	0.13	0.40	0.68	1.96	1.43	5.03	5.03
Mg#	67.86	49.56	16.45	32.52	88.12	84.94	85.02	88.15	83.88	88.42	80.57	65.65	70.57	24.44	17.50

Sample rock	SHU krc	SHU krc	SHU ol	SHU krc	SHU krc	SHU ol	SHU krc	2002GL ol	2002GL ol	2002GL ol	2002GL ol	2002GL ol	2002GL ol	2002GL ol	2002GL ol
SiO ₂	32.74	33.29	37.20	31.07	32.77	32.24	32.06	37.59	37.52	37.32	38.32	37.10	37.86	37.92	37.35
Fe ₂ O ₃	33.17	41.09	27.27	34.24	32.78	49.07	35.20	22.56	22.29	21.00	21.84	22.57	21.43	23.64	22.52
MnO	2.04	2.75	1.32	2.24	2.66	3.07	1.85	0.53	0.96	0.51	0.66	0.82	0.54	0.76	0.81
MgO	2.43	7.21	33.58	4.76	3.28	10.62	2.53	36.86	35.96	36.88	37.97	36.26	37.48	36.97	36.43
CaO	27.94	12.89	1.48	24.78	27.40	3.63	27.45	1.53	1.38	1.49	1.53	1.40	1.48	1.60	1.48
NiO								0.00	0.00	0.00	0.52	0.18	0.47	0.00	0.17
Tot.	98.33	97.23	100.85	97.09	98.89	98.63	99.10	99.07	98.11	97.20	100.84	98.32	99.26	100.89	98.76
Si	1.02	1.04	0.99	0.98	1.01	1.01	1.00	1.00	1.00	1.00	0.99	0.99	1.00	0.99	0.99
Fe	0.86	1.08	0.61	0.91	0.85	1.28	0.92	0.50	0.50	0.47	0.47	0.51	0.47	0.52	0.50
Mn	0.05	0.07	0.03	0.06	0.07	0.08	0.05	0.01	0.02	0.01	0.01	0.02	0.01	0.02	0.02
Mg	0.11	0.34	1.34	0.22	0.15	0.50	0.12	1.45	1.43	1.47	1.47	1.45	1.47	1.44	1.45
Ca	0.93	0.43	0.04	0.84	0.91	0.12	0.92	0.04	0.04	0.04	0.04	0.04	0.04	0.04	0.04
Ni	0.00	0.00	0.00	0.00	0.00	0.00	0.00	0.00	0.00	0.00	0.01	0.00	0.01	0.00	0.00
Tot.	2.98	2.96	3.01	3.02	2.99	2.99	3.00	3.00	3.00	3.00	3.01	3.01	3.00	3.01	3.01
Iarnite	47.49	22.55	2.10	41.38	45.93	6.13	45.82	2.16	1.98	2.14	2.13	2.00	2.09	2.22	2.10
fayalite	46.76	59.90	31.66	47.57	46.41	68.89	48.30	25.45	26.10	24.14	24.43	26.05	24.24	26.43	25.89
forsterite	5.74	17.55	66.24	11.05	7.66	24.98	5.88	72.38	71.91	73.72	73.44	71.95	73.68	71.35	72.01
tephroite	4.91	8.68	2.12	5.34	6.18	11.67	4.50	0.79	1.45	0.76	0.95	1.23	0.78	1.12	1.21
Mg#	10.94	22.65	67.66	18.85	14.16	26.61	10.86	73.99	73.37	75.33	75.04	73.41	75.25	72.97	73.55

Sample rock	1977 2 ol	1977 2 ol	1977 2 ol	1977 2 ol	1977 2 ol	1977 2 ol	1977 2 ol	1977 2 ol	1977 2 ol	1977 2 ol	1977 5 ol	1977 5 ol	1977 5 ol	2ndPause ol	2ndPause ol
SiO ₂	40.06	39.73	33.29	32.56	34.42	35.93	32.96	35.87	32.92	33.99	37.32	37.52	37.08	36.29	34.07
Fe ₂ O ₃	13.94	15.54	43.30	46.62	43.64	26.98	45.67	30.32	47.84	46.29	24.68	26.95	27.68	30.49	38.24
MnO	0.31	0.54	1.88	2.78	2.01	0.86	2.78	0.86	2.46	2.72	0.99	0.78	0.97	1.45	2.00
MgO	46.35	42.04	18.00	14.68	19.51	31.84	15.30	29.78	13.86	14.52	34.31	34.62	32.22	29.22	22.57
CaO	0.56	1.50	2.11	2.40	1.91	1.72	2.03	1.69	3.06	2.57	2.30	1.73	1.84	1.62	1.84
NiO	0.18	0.00	0.25	0.00	0.29	0.00	0.00	0.00	0.00	0.32	0.26	0.40	0.47	0.00	0.00
Tot.	101.40	99.35	98.83	99.03	101.78	97.34	98.75	98.52	100.13	100.41	99.86	102.01	100.25	99.07	98.72
Si	0.99	1.01	1.00	0.99	0.99	0.99	1.00	1.00	1.00	1.02	1.00	0.99	1.00	1.00	0.99
Fe	0.29	0.33	1.08	1.19	1.05	0.62	1.16	0.70	1.21	1.16	0.55	0.59	0.62	0.71	0.93
Mn	0.01	0.01	0.05	0.07	0.05	0.02	0.07	0.02	0.06	0.07	0.02	0.02	0.02	0.03	0.05
Mg	1.71	1.59	0.80	0.67	0.84	1.31	0.69	1.23	0.63	0.65	1.36	1.36	1.29	1.21	0.98
Ca	0.01	0.04	0.07	0.08	0.06	0.05	0.07	0.05	0.10	0.08	0.07	0.05	0.05	0.05	0.06
Ni	0.00	0.00	0.01	0.00	0.01	0.00	0.00	0.00	0.00	0.01	0.01	0.01	0.01	0.00	0.00
Tot.	3.01	2.99	3.00	3.01	3.01	3.01	3.00	3.00	3.00	2.98	3.00	3.01	3.00	3.00	3.01
Iarnite	0.74	2.07	3.38	3.91	2.95	2.54	3.33	2.51	4.97	4.21	3.28	2.42	2.66	2.41	2.85
fayalite	14.60	17.32	56.52	62.84	55.10	32.09	61.87	36.08	63.75	62.70	28.60	30.26	32.41	37.11	48.60
forsterite	84.65	80.61	40.10	33.25	41.95	65.37	34.80	61.41	31.28	33.09	68.12	67.32	64.93	60.48	48.55
tephroite	0.38	0.71	5.15	8.78	5.14	1.46	8.61	1.56	8.00	8.53	1.54	1.21	1.60	2.64	4.53
Mg#	85.29	82.32	41.51	34.61	43.23	67.08	36.00	62.99	32.92	34.55	70.43	68.99	66.71	61.98	49.98

Sample rock	2002-6 ol	2002-6 ol	2002-6 ol	2002-6 ol	2002-6 ol	2002-6 ol	2002-2 ol	2016 ol	2016 ol	2016 ol	2016 ol	LV4 ol	LV4 ol	LV4 ol
SiO ₂	38.74	37.61	38.56	37.92	39.15	38.35	38.05	38.60	38.22	38.13	38.41	38.89	38.85	38.49
Fe ₂ O ₃	22.39	22.23	22.33	24.36	22.41	24.80	23.47	21.05	20.59	23.20	21.45	17.96	17.50	14.98
MnO	0.91	0.64	0.88	1.04	0.73	1.29	0.62	0.53	0.66	0.92	0.69	0.47	0.79	0.84
MgO	37.74	36.72	37.10	35.96	37.57	35.80	36.98	38.93	38.77	36.76	38.41	41.70	41.59	42.30
CaO	1.55	1.72	1.38	1.65	1.28	1.41	1.54	1.43	1.57	1.59	1.38	1.20	1.08	1.66
NiO	0.16	0.09	0.00	0.00	0.18	0.00	0.00	0.36	0.13	0.04	0.00	0.00	0.00	0.00
Tot.	101.50	99.01	100.25	100.93	101.33	101.64	100.66	100.89	99.94	100.63	100.34	100.21	99.81	98.27
Si	1.00	1.00	1.01	0.99	1.01	1.00	0.99	1.00	0.99	1.00	1.00	0.99	1.00	0.99
Fe	0.48	0.49	0.49	0.53	0.48	0.54	0.51	0.45	0.45	0.51	0.47	0.38	0.37	0.32
Mn	0.02	0.01	0.02	0.02	0.02	0.03	0.01	0.01	0.01	0.02	0.02	0.01	0.02	0.02
Mg	1.45	1.45	1.44	1.41	1.44	1.39	1.44	1.50	1.50	1.43	1.49	1.59	1.59	1.63
Ca	0.04	0.05	0.04	0.05	0.04	0.04	0.04	0.04	0.04	0.04	0.04	0.03	0.03	0.05
Ni	0.00	0.00	0.00	0.00	0.00	0.00	0.00	0.01	0.00	0.00	0.00	0.00	0.00	0.00
Tot.	3.00	3.00	2.99	3.01	2.99	3.00	3.01	3.00	3.01	3.00	3.00	3.01	3.00	3.01
larnite	2.15	2.43	1.95	2.31	1.79	1.97	2.14	1.97	2.17	2.22	1.91	1.63	1.47	2.28
fayalite	25.19	25.27	25.48	27.74	25.23	28.46	26.20	23.26	23.01	26.32	23.98	19.55	19.51	16.96
forsterite	72.67	72.29	72.57	69.95	72.97	69.57	71.66	74.77	74.81	71.46	74.11	78.83	79.02	80.76
tephroite	1.31	0.95	1.29	1.56	1.07	1.95	0.92	0.74	0.93	1.36	0.98	0.62	1.04	1.08
Mg#	74.26	74.10	74.01	71.61	74.31	70.97	73.23	76.28	76.47	73.08	75.56	80.13	80.20	82.65

Olivine Nyamura

Sample rock	Muja ol core	Muja ol rim	Muja ol core	Muja ol rim	Muja ol	Muja ol	Muja ol core	Muja ol rim	Muja ol core	Muja ol rim	Muja ol	Muja ol gm	Muja ol gm	Muja ol	Muja ol core
SiO ₂	38.62	38.64	40.17	38.75	40.34	38.61	39.58	37.54	38.77	37.94	39.89	37.23	36.52	39.89	39.57
Fe ₂ O ₃	18.65	14.74	17.53	18.76	10.85	18.43	15.67	27.45	18.91	20.10	10.64	28.29	28.02	12.29	13.73
MnO	0.46	0.32	0.26	0.38	0.34	0.32	0.48	0.70	0.64	0.73	0.21	0.73	0.50	0.17	0.36
MgO	41.57	43.06	41.77	41.28	46.94	41.30	44.41	34.06	41.72	39.59	46.90	32.74	32.85	45.58	44.48
CaO	0.43	0.67	0.22	0.58	0.71	0.41	0.61	0.73	0.30	0.39	0.31	0.57	0.56	0.51	0.34
NiO	0.19	0.26	0.22	0.39	0.05	0.25	0.04	0.05	0.29	0.00	0.54	0.00	0.13	0.25	0.36
total	99.93	97.68	100.17	100.13	99.22	99.31	100.80	100.53	100.63	98.75	98.49	99.57	98.58	98.69	98.84
Si	0.99	1.00	1.02	0.99	1.00	1.00	0.99	1.00	0.99	1.00	1.01	1.00	1.00	1.00	1.00
Fe	0.40	0.32	0.37	0.40	0.23	0.40	0.33	0.61	0.40	0.44	0.22	0.64	0.64	0.26	0.29
Mn	0.01	0.01	0.01	0.01	0.01	0.01	0.01	0.02	0.01	0.02	0.00	0.02	0.01	0.00	0.01
Mg	1.59	1.66	1.58	1.58	1.74	1.59	1.66	1.35	1.59	1.55	1.75	1.32	1.34	1.71	1.68
Ca	0.01	0.02	0.01	0.02	0.02	0.01	0.02	0.02	0.01	0.01	0.01	0.02	0.02	0.01	0.01
Ni	0.00	0.01	0.00	0.01	0.00	0.01	0.00	0.00	0.01	0.00	0.01	0.00	0.00	0.01	0.01
total	3.01	3.00	2.98	3.01	3.00	3.01	3.01	3.00	3.01	3.01	3.00	2.99	3.00	3.00	3.00
larnite	0.59	0.92	0.31	0.79	0.95	0.57	0.82	1.05	0.41	0.55	0.42	0.83	0.82	0.69	0.47
fayalite	20.39	16.25	19.23	20.48	11.69	20.19	16.82	31.35	20.74	22.67	11.44	32.95	32.49	13.21	15.02
forsterite	79.02	82.83	80.46	78.73	87.36	79.24	82.37	67.60	78.86	76.78	88.13	66.22	66.69	86.10	84.51
tephroite	0.62	0.41	0.36	0.51	0.40	0.43	0.60	1.13	0.86	1.03	0.25	1.24	0.84	0.21	0.45
Mg#	79.49	83.60	80.71	79.35	88.20	79.70	83.05	68.32	79.18	77.20	88.51	66.78	67.24	86.70	84.91

Sample rock	Muja ol	Muja ol	Muja ol core	Muja ol rim	Nyam Sum ol core	10Nyam Sum ol core	10Nyam Sum ol	10Nyam Sum ol core	10Nyam Sum ol rim	10Nyam Sum ol core	10Nyam Sum ol	10Nyam Sum ol rim	10Nyam Sum ol core	10Nyam Sum ol rim	10Nyam Sum ol core
SiO ₂	36.72	37.14	39.63	39.82	37.46	35.37	37.31	34.75	38.36	37.76	37.17	38.40	36.81	32.62	37.45
Fe ₂ O ₃	27.88	26.97	17.36	16.63	26.23	35.32	26.42	36.87	24.03	26.62	23.65	25.34	26.23	46.32	26.64
MnO	0.92	0.35	0.25	0.60	0.38	1.01	0.34	1.41	0.22	0.39	0.47	0.38	0.34	1.56	0.96
MgO	32.09	35.41	41.86	44.10	34.05	26.64	34.28	23.15	37.35	35.06	35.96	36.07	34.52	16.57	35.20
CaO	0.57	0.66	0.40	0.60	0.37	0.57	0.51	1.44	0.43	0.34	0.62	0.40	0.58	0.39	0.58
NiO	0.39	0.05	0.23	0.05	0.32	0.07	0.11	0.00	0.23	0.09	0.00	0.22	0.00	0.10	0.00
total	98.58	100.58	99.73	101.80	98.81	98.97	98.98	97.62	100.62	100.26	97.88	100.81	98.49	97.56	100.82
Si	1.00	0.99	1.01	0.99	1.01	1.00	1.00	1.01	1.00	1.00	1.01	1.00	1.00	1.00	0.99
Fe	0.64	0.60	0.37	0.35	0.59	0.83	0.59	0.90	0.52	0.59	0.53	0.56	0.59	1.19	0.59
Mn	0.02	0.01	0.01	0.01	0.01	0.02	0.01	0.03	0.00	0.01	0.01	0.01	0.01	0.04	0.02
Mg	1.31	1.40	1.59	1.64	1.37	1.12	1.37	1.00	1.45	1.39	1.44	1.41	1.39	0.76	1.39
Ca	0.02	0.02	0.01	0.02	0.01	0.02	0.01	0.04	0.01	0.01	0.02	0.01	0.02	0.01	0.02
Ni	0.01	0.00	0.00	0.00	0.01	0.00	0.00	0.00	0.00	0.00	0.00	0.00	0.00	0.00	0.00
total	3.00	3.01	2.99	3.01	2.99	3.00	3.00	2.99	3.00	3.00	3.00	2.99	3.00	3.00	3.01
larnite	0.84	0.93	0.55	0.80	0.54	0.86	0.74	2.27	0.61	0.48	0.90	0.56	0.84	0.65	0.81
fayalite	33.22	29.94	18.99	17.84	30.32	42.98	30.24	47.05	26.54	30.04	27.10	28.42	29.91	61.45	30.31
forsterite	65.94	69.14	80.46	81.36	69.14	56.16	69.03	50.68	72.85	69.48	72.00	71.02	69.25	37.90	68.88
tephroite	1.58	0.55	0.33	0.77	0.62	2.07	0.56	3.21	0.33	0.63	0.73	0.60	0.56	4.98	1.51
Mg#	66.50	69.78	80.90	82.01	69.52	56.64	69.54	51.86	73.30	69.82	72.65	71.42	69.84	38.15	69.44

Sample rock	Nyam Sum 10	Nyam Sum 10	Nyam Sum 10	Nyam Sum 10	Nyam Sum 10	Nyam Sum 10	Nyam Sum 10	Nyam Sum 10	Nyam Sum 10	Nyam Sum 10	Nyam Sum 10	Nyam B 11-12	Nyam B 11-12	Nyam B 11-12	Nyam B 11-12
	ol rim	ol core	ol rim	ol core	ol rim	ol	ol	ol	ol	ol?	ol?	ol	ol	ol	ol
SiO ₂	37.49	37.18	37.11	37.08	34.77	36.17	34.54	33.47	37.77	34.53	37.54	40.27	40.13	40.46	38.66
Fe ₂ O ₃	32.35	24.41	27.10	26.41	37.82	33.70	41.73	50.02	26.06	41.95	29.36	11.09	14.20	11.04	19.91
MnO	0.32	0.62	0.64	0.45	0.98	0.62	0.82	1.72	0.26	1.35	0.76	0.05	0.00	0.15	0.08
MgO	31.45	34.67	32.79	34.33	25.66	27.89	20.51	14.21	36.00	20.47	31.72	47.12	45.55	48.11	40.20
CaO	0.62	0.66	0.61	0.72	0.64	0.54	0.24	0.34	0.38	0.30	0.80	0.32	0.36	0.27	0.17
NiO	0.00	0.00	0.00	0.00	0.25	0.62	0.00	0.00	0.15	0.00	0.00	0.61	0.28	0.22	0.86
total	102.22	97.53	98.25	99.00	100.12	99.55	97.84	99.76	100.61	98.60	100.19	99.47	100.52	100.27	99.86
Si	1.00	1.01	1.01	1.00	0.99	1.01	1.02	1.01	0.99	1.01	1.01	1.00	1.00	1.00	1.00
Fe	0.72	0.55	0.62	0.59	0.90	0.78	1.03	1.27	0.57	1.03	0.66	0.23	0.30	0.23	0.43
Mn	0.01	0.01	0.01	0.01	0.02	0.01	0.02	0.04	0.01	0.03	0.02	0.00	0.00	0.00	0.00
Mg	1.25	1.40	1.33	1.38	1.08	1.16	0.90	0.64	1.41	0.90	1.27	1.75	1.69	1.77	1.55
Ca	0.02	0.02	0.02	0.02	0.02	0.02	0.01	0.01	0.01	0.01	0.02	0.01	0.01	0.01	0.00
Ni	0.00	0.00	0.00	0.00	0.01	0.01	0.00	0.00	0.00	0.00	0.00	0.01	0.01	0.00	0.02
total	3.00	2.99	2.99	3.00	3.01	2.99	2.98	2.99	3.01	2.99	2.99	3.00	3.00	3.00	3.00
larnite	0.88	0.97	0.90	1.04	0.96	0.82	0.38	0.57	0.53	0.48	1.17	0.42	0.49	0.36	0.23
fayalite	36.50	28.55	31.90	30.20	45.46	40.51	53.58	66.76	28.93	54.02	34.36	11.67	14.82	11.50	21.76
forsterite	62.62	70.48	67.20	68.76	53.58	58.67	46.03	32.68	70.54	45.50	64.47	87.90	84.70	88.14	78.01
tephroite	0.57	0.99	1.08	0.73	2.07	1.22	2.20	6.34	0.40	3.57	1.32	0.07	0.00	0.17	0.11
Mg#	63.18	71.17	67.81	69.49	54.10	59.15	46.21	32.86	70.91	45.72	65.23	88.28	85.11	88.45	78.19

Sample rock	Nyam B 11-12	Nyam B 11-12	Nyam B 11-12	Nyam B 11-12	Nyam B 11-12	Nyam B 11-12	Nyam C	Nyam C	Nyam C	Nyam C	Nyam C	Nyam C	Nyam C	Nyam C	Nyam C
	ol	ol	ol	ol	ol	ol	ol	ol	ol	ol	ol	ol	ol	ol	ol
SiO ₂	40.01	40.03	40.41	40.49	39.01	37.96	37.81	40.58	36.48	38.04	36.96	36.64	36.34	37.00	36.14
Fe ₂ O ₃	14.43	13.47	14.29	14.29	30.79	30.03	27.91	30.26	26.24	24.55	22.26	23.31	28.60	26.13	26.45
MnO	0.18	0.13	0.44	0.13	0.63	0.31	0.47	0.36	0.86	0.28	0.64	0.23	0.54	0.63	0.33
MgO	46.01	45.89	45.26	46.08	26.03	33.12	34.15	37.32	34.93	37.72	36.44	35.43	31.77	34.11	32.77
CaO	0.32	0.21	0.23	0.42	0.85	0.52	0.61	0.69	0.67	0.37	0.68	0.54	0.43	0.40	0.57
NiO	0.30	0.00	0.26	0.34	0.00	0.18	0.00	0.00	0.05	0.16	0.00	0.00	0.00	0.26	0.00
total	101.25	99.75	100.89	101.74	97.32	102.11	100.94	109.21	99.24	101.11	96.99	96.16	97.68	98.53	96.26
Si	0.99	1.00	1.00	1.00	1.08	1.00	1.00	0.99	0.98	0.99	1.00	1.00	1.00	1.00	1.00
Fe	0.30	0.28	0.30	0.29	0.72	0.66	0.62	0.62	0.59	0.53	0.50	0.53	0.66	0.59	0.61
Mn	0.00	0.00	0.01	0.00	0.01	0.01	0.01	0.01	0.02	0.01	0.01	0.01	0.01	0.01	0.01
Mg	1.70	1.71	1.68	1.69	1.08	1.30	1.35	1.36	1.40	1.46	1.47	1.44	1.31	1.38	1.36
Ca	0.01	0.01	0.01	0.01	0.03	0.01	0.02	0.02	0.02	0.01	0.02	0.02	0.01	0.01	0.02
Ni	0.01	0.00	0.01	0.01	0.00	0.00	0.00	0.00	0.00	0.00	0.00	0.00	0.00	0.01	0.00
total	3.01	3.00	3.00	3.00	2.92	3.00	3.00	3.01	3.02	3.01	3.00	3.00	3.00	3.00	3.00
larnite	0.42	0.29	0.31	0.55	1.38	0.74	0.87	0.90	0.95	0.51	0.98	0.79	0.63	0.58	0.85
fayalite	15.06	14.22	15.39	14.85	39.83	33.69	31.52	31.25	30.05	26.84	25.82	26.94	33.77	30.39	31.16
forsterite	84.52	85.49	84.30	84.60	58.79	65.57	67.61	67.85	69.00	72.66	73.20	72.26	65.59	69.03	67.98
tephroite	0.22	0.16	0.54	0.16	1.33	0.52	0.76	0.54	1.37	0.42	0.98	0.37	0.95	1.02	0.56
Mg#	84.87	85.74	84.56	85.07	59.62	66.06	68.20	68.47	69.66	73.03	73.93	72.84	66.01	69.43	68.57

Sample rock	Nyam C	Nyam C	Nyam C	Nyam C	Nyam salt10	Nyam salt10	Nyam salt10	Nyam salt10	NM1938	NM1938	NM1938	NM1938	NM1938	NM1938	NM1938
	ol	ol	ol	ol	ol	ol	ol	ol	ol	ol	ol	ol	ol	ol	ol
SiO ₂	37.44	38.08	34.28	31.88	37.64	36.42	36.44	37.84	37.17	38.18	37.68	38.02	37.94	38.63	38.31
Fe ₂ O ₃	25.47	24.61	41.80	49.06	26.51	27.36	30.05	27.44	27.77	26.01	25.74	25.09	24.59	24.56	24.09
MnO	0.56	0.51	1.05	0.97	0.70	0.61	0.59	0.69	0.54	0.18	0.63	0.76	0.68	0.26	0.58
MgO	35.68	37.18	19.85	14.97	34.41	32.79	32.15	34.57	33.98	35.05	36.71	37.06	37.47	37.60	38.47
CaO	0.44	0.40	0.34	0.89	0.88	0.64	0.67	0.73	0.48	0.73	0.43	0.43	0.43	0.48	0.47
NiO	0.06	0.00	0.00	0.19	0.15	0.00	0.00	0.00	0.00	0.29	0.06	0.19	0.00	0.05	0.20
total	99.65	100.78	97.31	97.95	100.29	97.82	99.90	101.27	99.94	100.45	101.25	101.55	101.12	101.58	102.13
Si	1.00	1.00	1.02	0.99	1.00	1.00	0.99	1.00	1.00	1.01	0.99	0.99	0.99	1.00	0.99
Fe	0.57	0.54	1.04	1.27	0.59	0.63	0.68	0.61	0.62	0.57	0.56	0.55	0.54	0.53	0.52
Mn	0.01	0.01	0.03	0.03	0.02	0.01	0.01	0.02	0.01	0.00	0.01	0.02	0.02	0.01	0.01
Mg	1.41	1.45	0.88	0.69	1.36	1.34	1.30	1.36	1.36	1.38	1.43	1.44	1.46	1.45	1.48
Ca	0.01	0.01	0.01	0.03	0.03	0.02	0.02	0.02	0.01	0.02	0.01	0.01	0.01	0.01	0.01
Ni	0.00	0.00	0.00	0.00	0.00	0.00	0.00	0.00	0.00	0.01	0.00	0.00	0.00	0.00	0.00
total	3.00	3.00	2.98	3.01	3.00	3.00	3.01	3.00	3.00	2.99	3.01	3.01	3.01	3.00	3.01
larnite	0.62	0.56	0.55	1.46	1.25	0.94	0.96	1.03	0.68	1.05	0.59	0.60	0.60	0.66	0.64
fayalite	28.87	27.34	54.48	64.28	30.35	32.06	34.51	31.03	31.64	29.23	28.56	27.97	27.30	26.85	26.30
forsterite	70.51	72.11	44.97	34.26	68.39	66.99	64.53	67.94	67.67	69.72	70.85	71.43	72.10	72.49	73.06
tephroite	0.88	0.77	2.87	3.39	1.12	1.04	1.02	1.11	0.88	0.29	0.96	1.15	1.02	0.38	0.84
Mg#	70.95	72.51	45.22	34.77	69.26	67.63	65.16	68.65	68.14	70.46	71.27	71.86	72.54	72.97	73.53

Sample rock	NM1938 ol	Nsum B ol core	Nsum B ol rim	Nsum B ol	Nsum B ol	Nsum B ol	Nsum B ol	Nsum B ol	Nsum B ol	NM1938-2 ol core	NM1938-2 ol rim	NM1938-2 ol	NM1938-2 ol core	NM1938-2 ol rim	NM1938-2 ol core
SiO ₂	36.91	38.41	36.14	34.82	38.15	36.42	37.07	35.57	35.25	37.42	35.71	34.16	38.61	37.86	38.34
Fe ₂ O ₃	28.30	28.22	28.24	38.62	27.30	27.52	27.49	32.51	27.33	23.08	31.39	43.53	24.14	23.15	24.78
MnO	0.77	0.25	0.66	0.74	0.30	0.40	0.71	0.38	0.59	0.21	0.89	1.79	0.59	0.55	0.66
MgO	34.57	35.57	33.22	24.21	34.92	33.53	34.41	28.86	31.83	38.72	29.53	20.24	37.94	38.44	36.78
CaO	0.68	0.40	0.64	0.63	0.31	0.44	0.32	0.61	0.51	0.44	0.51	0.44	0.46	0.52	0.46
NiO	0.19	0.00	0.17	0.00	0.20	0.40	0.16	0.00	0.00	0.00	0.00	0.00	0.16	0.53	0.00
total	101.42	102.85	99.06	99.02	101.17	98.70	100.16	97.93	95.51	99.86	98.03	100.17	101.89	101.05	101.02
Si	0.98	1.00	0.98	1.00	1.00	0.99	0.99	1.00	0.99	0.98	1.00	1.00	1.00	0.98	1.00
Fe	0.63	0.61	0.64	0.93	0.60	0.63	0.62	0.76	0.64	0.51	0.73	1.06	0.52	0.50	0.54
Mn	0.02	0.01	0.02	0.02	0.01	0.01	0.02	0.01	0.01	0.00	0.02	0.04	0.01	0.01	0.01
Mg	1.37	1.38	1.35	1.04	1.37	1.36	1.37	1.21	1.34	1.51	1.23	0.88	1.46	1.49	1.43
Ca	0.02	0.01	0.02	0.02	0.01	0.01	0.01	0.02	0.02	0.01	0.02	0.01	0.01	0.01	0.01
Ni	0.00	0.00	0.00	0.00	0.00	0.01	0.00	0.00	0.00	0.00	0.00	0.00	0.00	0.01	0.00
total	3.02	3.00	3.02	3.00	3.00	3.01	3.01	3.00	3.01	3.02	3.00	3.00	3.00	3.02	3.00
larnite	0.96	0.55	0.92	0.97	0.44	0.64	0.46	0.92	0.76	0.60	0.76	0.69	0.63	0.72	0.64
fayalite	31.75	30.83	32.50	47.25	30.59	31.64	31.36	38.64	32.74	25.08	37.74	55.31	26.61	25.52	27.79
forsterite	67.29	68.62	66.58	51.79	68.97	67.72	68.19	60.44	66.49	74.32	61.50	44.00	72.75	73.76	71.57
tephroite	1.23	0.40	1.09	1.68	0.48	0.66	1.15	0.72	1.04	0.30	1.67	4.73	0.87	0.80	1.01
Mg#	67.94	69.00	67.19	52.29	69.28	68.16	68.50	61.00	67.00	74.77	61.97	44.31	73.22	74.29	72.03

Sample rock	NM1938-2 ol rim	NM1938-2 ol core	NM1938-2 ol rim	NM1938-2 ol	NM1938-2 ol	NM1938-2 ol	NM1948 ol	NM1948 ol	NM1948 ol	NM1948 ol	NM1948-1 ol core	NM1948-1 ol rim	NM1948-1 ol	NM1948-1 ol
SiO ₂	36.89	39.58	36.80	36.47	36.52	37.78	37.20	36.31	36.62	34.25	41.34	37.54	36.47	37.66
Fe ₂ O ₃	29.27	15.00	30.10	30.40	31.05	23.49	28.76	26.82	27.71	40.48	13.69	29.11	34.45	26.84
MnO	0.34	0.00	0.78	0.83	0.71	0.48	0.60	0.58	0.44	0.71	0.35	0.79	0.80	0.37
MgO	32.27	44.96	31.42	30.44	30.56	38.48	33.29	31.06	32.25	21.75	46.69	34.89	30.40	34.54
CaO	0.55	0.38	0.27	0.56	0.53	0.47	0.29	0.58	0.54	0.62	0.31	0.54	0.55	0.34
NiO	0.36	0.00	0.21	0.00	0.39	0.00	0.00	0.00	0.00	0.00	0.05	0.34	0.00	0.00
total	99.68	99.92	99.58	98.70	99.77	100.70	100.15	95.35	97.55	97.80	102.44	103.20	102.67	99.75
Si	1.00	0.99	1.00	1.01	1.00	0.98	1.00	1.02	1.01	1.01	1.01	0.98	0.98	1.00
Fe	0.66	0.32	0.69	0.70	0.71	0.51	0.65	0.63	0.64	1.00	0.28	0.64	0.78	0.60
Mn	0.01	0.00	0.02	0.02	0.02	0.01	0.01	0.01	0.01	0.02	0.01	0.02	0.02	0.01
Mg	1.30	1.68	1.28	1.25	1.25	1.49	1.33	1.30	1.32	0.95	1.69	1.36	1.22	1.37
Ca	0.02	0.01	0.01	0.02	0.02	0.01	0.01	0.02	0.02	0.02	0.01	0.02	0.02	0.01
Ni	0.01	0.00	0.00	0.00	0.01	0.00	0.00	0.00	0.00	0.00	0.00	0.01	0.00	0.00
total	3.00	3.01	3.00	2.99	3.00	3.02	3.00	2.98	2.99	2.99	2.99	3.02	3.02	3.00
larnite	0.80	0.51	0.40	0.83	0.78	0.65	0.42	0.89	0.80	0.99	0.40	0.75	0.79	0.49
fayalite	33.72	15.68	35.40	36.24	36.55	25.73	32.97	32.82	32.62	51.01	14.38	32.23	39.11	30.49
forsterite	65.48	83.81	64.20	62.93	62.66	73.62	66.61	66.29	66.59	48.00	85.21	67.03	60.10	69.01
tephroite	0.59	0.00	1.37	1.51	1.28	0.70	1.01	1.03	0.76	1.77	0.43	1.24	1.45	0.59
Mg#	66.01	84.24	64.46	63.46	63.16	74.10	66.89	66.89	67.12	48.48	85.56	67.53	60.58	69.35

Sample rock	Nyam Rum ol core	Nyam Rum ol rim	Nyam Rum ol core	Nyam Rum ol gm	Nyam Rum ol gm	Nyam Rum ol gm	Nyam Rum ol core	Nyam Rum ol rim	Nyam Rum ol core	Nyam Rum ol rim	Nyam Rum ol core	Nyam Rum ol rim	Nyam Rum ol rim
SiO ₂	39.44	38.01	39.38	37.30	37.75	37.04	38.58	35.89	38.79	35.85	37.05	34.51	32.84
Fe ₂ O ₃	20.09	26.62	19.68	29.04	28.24	27.77	20.17	37.99	20.02	32.13	29.95	44.18	47.56
MnO	0.33	0.38	0.40	0.49	0.44	0.41	0.34	0.69	0.27	0.61	0.49	0.92	1.00
MgO	40.59	36.65	41.25	34.57	34.74	33.28	41.67	25.71	41.33	29.44	33.83	20.62	16.61
CaO	0.59	0.44	0.43	0.54	0.54	0.34	0.47	0.70	0.37	0.48	0.53	0.58	1.49
NiO	0.09	0.07	0.18	0.14	0.02	0.12	0.13	0.02	0.16	0.00	0.07	0.00	0.00
total	101.14	102.17	101.32	102.09	101.74	98.96	101.36	101.01	100.95	98.51	101.93	100.80	99.51
Si	1.00	0.99	1.00	0.98	0.99	1.00	0.98	1.00	0.99	1.00	0.98	1.00	0.99
Fe	0.43	0.58	0.42	0.64	0.62	0.63	0.43	0.89	0.43	0.75	0.67	1.07	1.20
Mn	0.01	0.01	0.01	0.01	0.01	0.01	0.01	0.02	0.01	0.01	0.01	0.02	0.03
Mg	1.54	1.42	1.56	1.36	1.36	1.34	1.58	1.07	1.57	1.22	1.34	0.89	0.75
Ca	0.02	0.01	0.01	0.02	0.02	0.01	0.01	0.02	0.01	0.01	0.02	0.02	0.05
Ni	0.00	0.00	0.00	0.00	0.00	0.00	0.00	0.00	0.00	0.00	0.00	0.00	0.00
total	3.00	3.01	3.00	3.02	3.01	3.00	3.02	3.00	3.01	3.00	3.02	3.00	3.01
larnite	0.81	0.61	0.59	0.75	0.76	0.50	0.63	1.05	0.51	0.71	0.74	0.89	2.38
fayalite	21.84	29.06	21.34	32.15	31.42	32.05	21.51	45.29	21.49	38.15	33.30	54.61	60.65
forsterite	77.35	70.33	78.08	67.09	67.82	67.46	77.86	53.65	78.00	61.14	65.96	44.49	36.97
tephroite	0.46	0.58	0.54	0.79	0.71	0.69	0.46	1.47	0.37	1.15	0.81	2.42	3.12
Mg#	77.98	70.76	78.54	67.60	68.34	67.79	78.35	54.23	78.40	61.58	66.45	44.90	37.87

Clinopyroxenes of Nyiragongo samples:

Sample rock	SHD cpx	SHD cpx	SHD cpx	SHD cpx	SHD cpx	SHD cpx	SHD cpx	SHD cpx	SHD cpx	SHD cpx	SHD cpx	SHD cpx	SHD cpx
SiO ₂	45.21	44.30	52.85	44.48	47.04	51.67	44.99	50.35	42.04	44.75	49.73	42.53	46.36
TiO ₂	3.15	3.03	0.46	3.98	2.74	1.75	3.28	1.37	3.22	3.23	2.23	3.98	3.15
Al ₂ O ₃	4.47	4.08	0.57	5.98	4.57	1.63	2.22	1.83	7.54	7.51	5.91	8.21	6.60
FeO	9.80	14.76	11.37	7.86	8.12	8.70	14.79	9.73	7.04	7.59	6.39	7.34	6.96
MnO	0.29	0.59	0.31	0.24	0.26	0.53	0.29	0.20	0.08	0.23	0.20	0.16	0.38
MgO	10.25	7.17	11.73	11.51	12.09	13.10	7.03	12.27	10.73	11.48	13.67	11.16	12.13
CaO	22.96	22.35	23.30	23.13	23.12	22.95	21.78	22.34	24.94	23.78	22.91	22.68	23.95
Na ₂ O	0.50	0.59	0.58	0.83	0.48	0.63	0.81	0.72	0.38	0.52	0.56	0.41	0.35
V ₂ O ₅	0.00	0.06	0.00	0.00	0.00	0.00	0.13	0.00	0.28	0.00	0.31	0.35	0.00
Cr ₂ O ₃	0.18	0.00	0.00	0.25	0.13	0.00	0.07	0.00	0.00	0.00	0.00	0.00	0.00
Tot.	96.81	96.93	101.17	98.26	98.55	100.96	95.39	98.82	96.26	99.10	101.92	96.83	99.87
Si	1.78	1.79	1.98	1.72	1.80	1.92	1.85	1.92	1.66	1.71	1.81	1.66	1.75
Ti	0.09	0.09	0.01	0.12	0.06	0.05	0.10	0.04	0.10	0.09	0.06	0.12	0.09
Al 4*	0.22	0.21	0.02	0.28	0.20	0.08	0.15	0.08	0.34	0.29	0.19	0.34	0.25
Al 6*	-0.01	-0.02	0.00	-0.01	0.01	-0.01	-0.05	0.00	0.02	0.04	0.07	0.04	0.03
Fe 3*	0.07	0.09	0.03	0.12	0.07	0.03	0.06	0.05	0.16	0.10	0.04	0.10	0.06
Fe 2*	0.25	0.41	0.32	0.14	0.19	0.24	0.45	0.26	0.08	0.14	0.16	0.14	0.15
Mn	0.01	0.02	0.01	0.01	0.01	0.02	0.01	0.01	0.00	0.01	0.01	0.01	0.01
Mg	0.60	0.43	0.65	0.66	0.69	0.73	0.43	0.70	0.63	0.65	0.74	0.65	0.68
Ca	0.97	0.97	0.94	0.96	0.95	0.91	0.96	0.91	1.06	0.97	0.90	0.95	0.97
Na	0.04	0.05	0.04	0.06	0.04	0.05	0.06	0.05	0.03	0.04	0.04	0.03	0.02
V	0.00	0.00	0.00	0.00	0.00	0.00	0.00	0.00	0.01	0.00	0.01	0.01	0.00
Cr	0.01	0.00	0.00	0.01	0.00	0.00	0.00	0.00	0.00	0.00	0.00	0.00	0.00
Tot.	4.57	4.74	4.40	4.58	4.50	4.36	4.64	4.42	4.66	4.63	4.46	4.66	4.40
Mg#	65.09	46.40	64.76	72.28	72.64	72.86	45.87	69.21	73.08	72.95	79.23	73.04	75.66
Wollastonite (Ca)	50.91	50.44	47.80	50.88	49.73	47.42	50.25	47.37	54.90	51.85	48.67	51.47	51.44
Enstatite (Mg)	31.62	22.50	33.47	35.21	36.19	37.68	22.57	36.19	32.85	34.84	40.40	35.23	36.25
Ferrosilite (Fe)	17.47	27.06	18.72	13.92	14.08	14.90	27.18	16.44	12.24	13.31	10.93	13.30	12.31
Tot.	100.00	100.00	100.00	100.00	100.00	100.00	100.00	100.00	100.00	100.00	100.00	100.00	100.00

Sample rock	LV1SHD 2 cpx	LV1SHD 2 cpx	LV1SHD 2 cpx	LV1SHD 2 cpx	LV1SHD 2 cpx	LV1SHD 2 cpx	LV1SHD 2 cpx	SHD cpx	SHD cpx	SHD cpx	SHAHERU UP cpx	SHAHERU UP cpx	SHAHERU UP cpx	SHAHERU UP cpx
SiO ₂	45.67	46.73	40.74	44.03	46.41	42.64	46.41	48.58	49.92	49.42	51.13	50.48	51.33	50.75
TiO ₂	2.94	3.50	6.19	3.66	2.55	4.10	3.36	3.10	2.51	2.75	1.30	1.28	0.84	2.07
Al ₂ O ₃	6.59	6.04	10.11	5.30	6.30	8.70	5.63	3.07	2.91	3.39	1.25	0.98	0.92	2.00
FeO	6.02	6.35	7.12	10.82	5.71	6.50	6.27	10.26	9.69	9.95	10.97	7.78	8.62	9.60
MnO	0.45	0.08	0.20	0.11	0.20	0.00	0.16	0.51	0.15	0.10	0.66	0.26	0.55	0.57
MgO	12.38	13.00	10.04	11.67	13.11	11.06	13.12	11.27	11.47	11.47	11.38	13.29	12.58	12.49
CaO	23.55	23.94	23.05	21.90	24.35	23.83	24.15	22.70	24.12	23.48	23.47	23.42	23.42	22.83
Na ₂ O	0.00	0.00	0.13	0.13	0.00	0.16	0.05	0.36	0.38	0.33	0.27	0.16	0.03	0.05
V ₂ O ₅	0.00	0.10	0.00	0.12	0.07	0.03	0.06	0.00	0.00	0.18	0.00	0.05	0.07	0.00
Cr ₂ O ₃								0.12	0.00	0.12				
Tot.	97.58	99.73	97.59	97.74	98.69	97.03	99.20	99.97	101.14	101.20	100.43	98.02	98.36	100.35
Si	1.75	1.75	1.58	1.72	1.76	1.66	1.75	1.85	1.87	1.85	1.93	1.93	1.96	1.91
Ti	0.08	0.10	0.18	0.11	0.07	0.12	0.10	0.09	0.07	0.08	0.04	0.04	0.02	0.06
Al 4*	0.25	0.25	0.42	0.28	0.24	0.34	0.25	0.15	0.13	0.15	0.07	0.07	0.04	0.09
Al 6*	0.05	0.02	0.04	-0.03	0.04	0.05	0.00	-0.02	0.00	0.00	-0.01	-0.02	0.00	-0.01
Fe 3*	0.03	0.03	0.02	0.10	0.06	0.06	0.05	0.02	0.02	0.02	0.02	0.03	-0.01	-0.01
Fe 2*	0.16	0.17	0.21	0.25	0.12	0.15	0.14	0.31	0.28	0.30	0.22	0.28	0.28	0.31
Mn	0.01	0.00	0.01	0.00	0.01	0.00	0.00	0.02	0.00	0.00	0.02	0.01	0.02	0.02
Mg	0.71	0.73	0.58	0.68	0.74	0.64	0.74	0.64	0.64	0.64	0.64	0.76	0.72	0.70
Ca	0.97	0.96	0.96	0.92	0.99	0.99	0.98	0.92	0.97	0.94	0.95	0.97	0.96	0.92
Na	0.00	0.00	0.01	0.01	0.00	0.01	0.00	0.03	0.03	0.02	0.01	0.00	0.00	0.00
V	0.00	0.00	0.00	0.00	0.00	0.00	0.00	0.00	0.00	0.00	0.00	0.00	0.00	0.00
Cr	0.00	0.00	0.00	0.00	0.00	0.00	0.00	0.00	0.00	0.00	0.00	0.00	0.00	0.00
Tot.	4.51	4.48	4.71	4.65	4.49	4.64	4.48	4.47	4.44	4.47	4.41	4.31	4.31	4.38
Mg#	78.58	78.50	71.55	65.80	80.36	75.22	78.87	66.19	67.84	67.27	64.89	75.27	72.22	69.89
Wollastonite (Ca)	51.39	50.90	53.94	46.93	51.57	53.80	50.93	48.52	50.51	49.66	48.51	48.92	48.71	47.41
Enstatite (Mg)	37.59	38.44	32.70	34.79	38.65	34.75	38.49	33.51	33.41	33.76	32.71	38.13	36.39	36.10
Ferrosilite (Fe)	11.02	10.66	13.37	18.27	9.78	11.45	10.57	17.97	16.09	16.59	18.78	12.95	14.90	16.49
Tot.	100.00	100.00	100.00	100.00	100.00	100.00	100.00	100.00	100.00	100.00	100.00	100.00	100.00	100.00

Sample rock	SHAHERU UP cpx	SHAHERU UP cpx	SHAHERU UP cpx	NYIRA SUM cpx	NYIRA SUM cpx	1977 2 cpx	1977 2 cpx	1977 2 cpx?	1977 2 cpx	1977 2 cpx	1977 2 cpx	1977-5 cpx	1977-5 cpx	1977-5 cpx
SiO ₂	48.96	48.12	49.93	48.50	49.61	46.94	48.98	46.78	48.99	48.53	48.03	46.09	40.41	47.48
TiO ₂	2.77	2.18	3.02	3.08	1.44	3.18	2.94	1.60	2.83	1.69	3.24	2.93	5.34	2.11
Al ₂ O ₃	3.43	0.79	1.17	4.23	1.68	3.42	1.88	3.47	2.09	1.12	4.54	10.95	6.98	6.98
FeO	9.31	15.79	13.50	9.28	12.56	12.31	12.95	15.27	11.73	14.41	10.74	6.68	8.16	5.12
MnO	0.44	0.45	0.20	0.43	0.51	0.61	0.61	0.00	0.70	0.65	0.45	0.06	0.15	0.22
MgO	11.86	7.35	9.17	11.85	9.69	9.05	9.16	9.00	10.20	8.33	10.25	12.74	9.83	13.96
CaO	22.48	19.94	21.71	22.89	21.67	21.61	21.24	21.54	22.61	22.60	22.78	24.35	22.84	23.90
Na ₂ O	0.22	1.19	1.12	0.48	0.73	0.83	0.98	0.57	0.34	1.07	0.55	0.00	0.00	0.13
V ₂ O ₅	0.00	0.42	0.00	0.00	0.26	0.24	0.24	1.05	0.05	0.17	0.00	0.00	0.40	0.35
Cr ₂ O ₃				0.12	0.00	0.00	0.00	0.46	0.00	0.00	0.00	0.09	0.00	0.30
Tot.	99.45	96.23	99.81	100.84	98.14	98.20	98.99	99.74	99.54	98.56	100.59	100.49	98.08	100.57
Si	1.86	1.95	1.92	1.82	1.93	1.84	1.90	1.83	1.88	1.92	1.82	1.72	1.57	1.76
Ti	0.08	0.07	0.09	0.09	0.04	0.09	0.09	0.05	0.08	0.05	0.08	0.08	0.16	0.06
Al 4*	0.14	0.05	0.08	0.18	0.07	0.16	0.10	0.17	0.12	0.08	0.18	0.28	0.43	0.24
Al 6*	0.01	-0.02	-0.03	0.01	0.01	0.00	-0.01							

Sample rock	1977-5 cpx	1977-5 cpx	1977-5 cpx	2nd Pause cpx	2nd Pause cpx	2nd Pause cpx	2nd Pause cpx	KH cpx	KH cpx	KH cpx	KH cpx	KH cpx	KH cpx	M2002-6 cpx
SiO ₂	45.81	46.34	46.85	46.71	42.44	47.71	46.81	44.24	47.28	47.77	46.35	47.89	47.02	40.59
TiO ₂	2.75	2.97	3.52	3.87	4.87	2.72	4.22	4.12	2.37	3.29	2.23	2.32	3.17	7.42
Al ₂ O ₃	6.76	5.37	3.84	3.56	7.82	4.43	4.94	8.53	5.73	5.17	5.82	6.21	5.57	8.93
FeO	6.91	7.24	13.13	10.41	8.89	9.25	9.63	7.84	6.48	7.93	6.77	6.03	6.77	9.48
MnO	0.00	0.00	0.54	0.42	0.47	0.26	0.18	0.31	0.65	0.09	0.37	0.41	0.41	0.35
MgO	13.03	12.62	7.98	9.96	10.75	11.72	11.24	10.95	12.82	12.59	11.85	12.00	12.80	9.77
CaO	23.15	23.76	21.99	21.98	22.30	23.09	22.62	23.48	23.78	22.71	23.53	22.95	23.22	22.88
Na ₂ O	0.04	0.07	0.77	0.39	0.24	0.44	0.43	0.00	0.00	0.12	0.00	0.00	0.00	0.06
V ₂ O ₅	0.41	0.00	0.39	0.00	0.44	0.03	0.09	0.00	0.15	0.35	0.26	0.62	0.00	0.40
Cr ₂ O ₃	0.26	0.00	0.00	0.18	0.00	0.00	0.00	0.00	0.00	0.00	0.00	0.71	0.00	0.08
Tot.	99.12	98.39	99.00	97.49	98.22	99.65	100.16	99.47	99.25	100.01	97.19	99.15	98.96	99.95
Si	1.73	1.77	1.83	1.82	1.65	1.81	1.77	1.68	1.78	1.79	1.79	1.80	1.78	1.56
Ti	0.08	0.09	0.10	0.11	0.14	0.08	0.12	0.12	0.07	0.09	0.06	0.07	0.09	0.21
Al 4 ⁺	0.27	0.23	0.17	0.18	0.35	0.19	0.23	0.32	0.22	0.21	0.21	0.20	0.22	0.44
Al 6 ⁺	0.04	0.01	0.00	-0.01	0.01	0.01	-0.01	0.06	0.04	0.02	0.05	0.08	0.03	-0.03
Fe 3 ⁺	0.07	0.05	0.02	-0.02	0.08	0.05	0.02	0.02	0.04	0.01	0.03	-0.03	0.01	0.04
Fe 2 ⁺	0.15	0.18	0.41	0.36	0.21	0.24	0.28	0.22	0.16	0.24	0.19	0.22	0.20	0.26
Mn	0.00	0.00	0.02	0.01	0.02	0.01	0.01	0.01	0.02	0.00	0.01	0.01	0.01	0.01
Mg	0.74	0.72	0.46	0.58	0.62	0.66	0.63	0.62	0.72	0.70	0.68	0.67	0.72	0.56
Ca	0.94	0.97	0.92	0.92	0.93	0.94	0.92	0.96	0.96	0.91	0.97	0.92	0.94	0.94
Na	0.00	0.01	0.06	0.03	0.02	0.03	0.03	0.00	0.00	0.01	0.00	0.00	0.00	0.00
V	0.01	0.00	0.01	0.00	0.01	0.00	0.00	0.00	0.00	0.01	0.01	0.02	0.00	0.01
Cr	0.01	0.00	0.00	0.01	0.00	0.00	0.00	0.00	0.00	0.00	0.00	0.02	0.00	0.00
Tot.	4.55	4.50	4.61	4.50	4.68	4.52	4.54	4.64	4.48	4.48	4.49	4.44	4.47	4.73
Mg#	77.07	75.65	52.01	63.05	68.31	69.32	67.53	71.36	77.91	73.89	75.73	78.02	77.10	64.75
Wollastonite (Ca)	49.61	50.58	50.25	49.62	50.04	49.32	49.26	52.08	50.40	48.86	51.60	51.37	49.80	51.84
Enstatite (Mg)	38.84	37.39	25.36	31.29	33.56	34.83	34.06	33.80	37.79	37.67	36.16	37.38	38.17	30.78
Ferrosillite (Fe)	11.56	12.03	24.39	19.09	16.40	15.85	16.69	14.12	11.81	13.47	12.24	11.25	12.03	17.38
Tot.	100.00	100.00	100.00	100.00	100.00	100.00	100.00	100.00	100.00	100.00	100.00	100.00	100.00	100.00

Sample rock	M2002-6 cpx	M2002-2 cpx	M2002-2 cpx	Nyira 2016 cpx	Nyira 2016 cpx	Nyira 2016 cpx	Nyira 2016 cpx	Nyira 2016 cpx	Nyira 2016 cpx	LV4 cpx	LV4 cpx	NYIRA SUM cpx	NYIRA SUM cpx
SiO ₂	48.87	41.23	36.96	47.91	48.59	50.72	42.97	45.15	46.54	43.56	48.50	49.61	
TiO ₂	1.86	6.67	8.27	2.09	1.63	1.16	5.47	4.26	2.04	3.74	3.08	1.44	
Al ₂ O ₃	2.41	10.57	11.50	4.00	3.72	1.25	8.82	6.80	5.61	7.48	4.23	1.68	
FeO	10.41	8.74	10.17	6.74	6.51	7.87	8.44	8.48	5.80	6.71	9.28	12.56	
MnO	0.40	0.03	0.25	0.16	0.06	0.25	0.16	0.21	0.19	0.20	0.43	0.51	
MgO	11.32	9.77	8.76	12.93	13.41	13.43	10.26	11.60	12.99	12.12	11.85	9.69	
CaO	22.83	23.58	22.80	23.38	24.27	23.41	22.96	23.43	23.81	23.50	22.89	21.67	
Na ₂ O	0.17	0.14	0.09	0.18	0.09	0.28	0.35	0.00	0.00	0.11	0.48	0.73	
V ₂ O ₅	0.13	0.14	0.10	0.00	0.03	0.00	0.00	0.07	0.00	0.00	0.00	0.26	
Cr ₂ O ₃	0.00	0.00	0.00	0.00	0.07	0.07	0.29	0.06	0.00	0.08	0.12	0.00	
Tot.	98.39	100.86	98.89	97.39	98.38	98.43	99.72	100.06	96.99	97.50	100.84	98.14	
Si	1.89	1.56	1.45	1.84	1.85	1.93	1.64	1.71	1.79	1.68	1.82	1.93	
Ti	0.05	0.19	0.24	0.06	0.05	0.03	0.16	0.12	0.06	0.11	0.09	0.04	
Al 4 ⁺	0.11	0.44	0.55	0.16	0.15	0.07	0.36	0.29	0.21	0.32	0.18	0.07	
Al 6 ⁺	0.00	0.03	-0.02	0.02	0.01	-0.01	0.03	0.01	0.04	0.02	0.01	0.01	
Fe 3 ⁺	0.02	0.04	0.09	0.03	0.05	0.04	0.03	0.04	0.05	0.08	0.03	0.03	
Fe 2 ⁺	0.31	0.24	0.24	0.18	0.15	0.21	0.23	0.23	0.14	0.14	0.26	0.38	
Mn	0.01	0.00	0.01	0.01	0.00	0.01	0.01	0.01	0.01	0.01	0.01	0.02	
Mg	0.65	0.55	0.51	0.74	0.76	0.76	0.58	0.65	0.74	0.70	0.66	0.56	
Ca	0.94	0.96	0.96	0.96	0.99	0.95	0.94	0.95	0.98	0.97	0.92	0.91	
Na	0.01	0.01	0.01	0.01	0.01	0.02	0.03	0.00	0.00	0.01	0.03	0.06	
V	0.00	0.00	0.00	0.00	0.00	0.00	0.00	0.00	0.00	0.00	0.00	0.01	
Cr	0.00	0.00	0.00	0.00	0.00	0.00	0.01	0.00	0.00	0.00	0.00	0.00	
Tot.	4.46	4.77	4.91	4.41	4.40	4.32	4.68	4.59	4.46	4.60	4.49	4.50	
Mg#	65.98	66.57	60.56	77.39	78.60	75.26	68.42	70.92	79.95	76.31	69.48	57.90	
Wollastonite (Ca)	48.55	53.57	52.87	50.00	50.50	48.33	52.24	50.55	51.15	51.36	48.75	47.78	
Enstatite (Mg)	33.50	30.87	28.26	38.49	38.83	38.57	32.48	34.82	38.81	36.86	35.11	29.72	
Ferrosillite (Fe)	17.95	15.56	18.87	11.51	10.67	13.09	15.28	14.63	10.05	11.78	16.14	22.50	
Tot.	100.00	100.00	100.00	100.00	100.00	100.00	100.00	100.00	100.00	100.00	100.00	100.00	

Next pages Clinopyroxenes and orthopyroxenes of Nyamuragira samples

Sample rock	NM1948 1 cpx	NM1948 1 cpx core	NM1948 1 cpx rim	NM1948 1 cpx	Nyam b 2011-2012 cpx	Nyam b 2011-2012 cpx	Nyam b 2011-2012 cpx	Nyam b 2011-2012 cpx?	Nyam b 2011-2012 cpx pig	Nyam b 2011-2012 cpx pig	Nyam b 2011-2012 cpx
SiO ₂	49.43	47.28	43.73	47.54	44.30	51.75	52.46	48.28	52.89	52.12	48.53
TiO ₂	2.98	3.30	4.71	3.23	2.58	1.16	0.66	1.50	0.81	1.15	3.10
Al ₂ O ₃	4.84	6.46	9.71	5.84	12.26	1.99	2.09	2.41	1.78	1.77	12.90
FeO	8.59	7.81	7.93	8.68	8.80	12.68	10.24	16.46	16.22	15.82	9.87
MnO	0.24	0.30	0.21	0.33	0.04	0.51	0.20	0.67	0.41	0.31	0.08
MgO	13.18	12.25	11.39	13.44	8.35	18.45	18.70	12.52	20.11	20.46	6.37
CaO	21.83	22.92	22.78	22.26	22.05	14.71	14.33	16.52	8.15	8.01	18.86
Na ₂ O	0.11	0.11	0.13	0.02	0.35	0.00	0.00	0.10	0.00	0.00	0.64
K ₂ O	0.00	0.19	0.08	0.15	0.00	0.00	0.00	0.33	0.07	0.08	0.03
Cr ₂ O ₃	0.03	0.00	0.00	0.07	0.09	0.00	0.60	0.00	0.11	0.23	0.17
Tot.	101.22	100.63	100.67	101.56	98.83	101.25	99.27	98.78	100.54	99.95	100.56
Si	1.83	1.76	1.64	1.76	1.68	1.90	1.94	1.88	1.95	1.93	1.78
Ti	0.08	0.09	0.13	0.09	0.07	0.03	0.02	0.04	0.02	0.03	0.09
Al 4*	0.17	0.24	0.36	0.24	0.32	0.10	0.06	0.12	0.05	0.07	0.22
Al 6*	0.04	0.05	0.07	0.02	0.23	-0.01	0.03	-0.01	0.02	0.01	0.34
Fe 3*	-0.02	0.01	0.04	0.04	-0.04	0.04	-0.02	0.05	-0.02	-0.01	-0.25
Fe 2*	0.29	0.23	0.21	0.23	0.31	0.35	0.34	0.48	0.52	0.50	0.56
Mn	0.01	0.01	0.01	0.01	0.00	0.02	0.01	0.02	0.01	0.01	0.00
Mg	0.73	0.68	0.64	0.74	0.47	1.01	1.03	0.73	1.10	1.13	0.35
Ca	0.86	0.92	0.91	0.88	0.90	0.58	0.57	0.69	0.32	0.32	0.74
Na	0.01	0.01	0.01	0.00	0.03	0.00	0.00	0.01	0.00	0.00	0.05
V	0.00	0.00	0.00	0.00	0.00	0.00	0.00	0.01	0.00	0.00	0.00
Cr	0.00	0.00	0.00	0.00	0.00	0.00	0.02	0.00	0.00	0.01	0.01
Tot.	4.47	4.53	4.70	4.54	4.81	4.50	4.40	4.67	4.57	4.56	4.74
Mg#	73.21	73.66	71.91	73.39	62.85	72.17	76.50	57.55	68.85	69.74	53.48
Wollastonite (Ca)	46.38	49.51	50.63	46.39	54.35	29.02	29.55	34.91	16.60	16.33	53.14
Enstatite (Mg)	38.96	36.82	35.24	38.96	28.63	50.66	53.65	36.81	56.98	56.01	24.96
Ferrosilite (Fe)	14.66	13.67	14.13	14.66	17.01	20.32	16.81	28.28	26.43	25.66	21.90
Tot.	100.00	100.00	100.00	100.00	100.00	100.00	100.00	100.00	100.00	100.00	100.00

Sample rock	Nyam b 2011-2012 cpx pig	Nyam b 2011-2012 cpx	Nyam b 2011-2012 cpx	Nyam b 2011-2012 cpx	Nyam b 2011-2012 cpx pig	Nyam b 2011-2012 cpx pig	Nyam b 2011-2012 cpx	Nyam b 2011-2012 cpx	Nyam b 2011-2012 cpx pig	Nyam b 2011-2012 cpx	Nyam b 2011-2012 cpx
SiO ₂	52.45	52.33	48.47	48.05	51.97	52.98	49.42	51.13	53.18	50.17	50.17
TiO ₂	0.59	0.55	1.66	1.51	0.73	0.48	1.69	0.93	0.09	1.69	1.69
Al ₂ O ₃	1.38	2.33	2.09	2.25	2.04	2.50	2.25	3.06	1.35	2.65	2.65
FeO	16.99	8.98	14.66	15.10	16.59	10.83	13.92	8.85	12.42	14.52	14.52
MnO	0.13	0.29	0.37	0.00	0.28	0.26	0.00	0.39	0.07	0.06	0.06
MgO	21.92	20.66	13.93	12.92	20.41	25.23	13.54	17.94	25.26	17.27	17.27
CaO	5.75	13.44	15.48	17.51	7.94	7.41	17.37	16.73	4.76	13.26	13.26
Na ₂ O	0.00	0.00	0.00	0.00	0.00	0.00	0.00	0.00	0.00	0.00	0.00
K ₂ O	0.18	0.21	0.34	0.24	0.26	0.25	0.00	0.04	0.10	0.19	0.19
Cr ₂ O ₃	0.12	1.06	0.00	0.00	0.06	0.61	0.09	0.07	0.46	0.15	0.15
Tot.	99.52	99.84	97.01	97.59	100.28	100.55	98.27	99.16	97.69	99.95	99.95
Si	1.95	1.91	1.90	1.88	1.92	1.90	1.90	1.90	1.96	1.88	1.88
Ti	0.02	0.02	0.05	0.04	0.02	0.01	0.05	0.03	0.00	0.05	0.05
Al 4*	0.05	0.09	0.10	0.12	0.08	0.10	0.10	0.10	0.04	0.12	0.12
Al 6*	0.01	0.01	-0.01	-0.01	0.01	0.01	0.00	0.02	0.02	0.00	0.00
Fe 3*	0.01	0.01	0.01	0.04	0.02	0.04	-0.01	0.03	0.00	0.02	0.02
Fe 2*	0.52	0.26	0.46	0.45	0.49	0.28	0.45	0.26	0.38	0.43	0.43
Mn	0.00	0.01	0.01	0.00	0.01	0.01	0.00	0.01	0.00	0.00	0.00
Mg	1.21	1.13	0.81	0.75	1.13	1.35	0.78	0.99	1.39	0.97	0.97
Ca	0.23	0.53	0.65	0.73	0.32	0.29	0.72	0.67	0.19	0.53	0.53
Na	0.00	0.00	0.00	0.00	0.00	0.00	0.00	0.00	0.00	0.00	0.00
V	0.00	0.01	0.01	0.01	0.01	0.01	0.00	0.00	0.00	0.00	0.00
Cr	0.00	0.03	0.00	0.00	0.00	0.02	0.00	0.00	0.01	0.00	0.00
Tot.	4.59	4.38	4.58	4.62	4.61	4.45	4.55	4.42	4.44	4.58	4.58
Mg#	69.70	80.40	62.89	60.39	68.69	80.60	63.41	78.32	78.38	67.95	67.95
Wollastonite (Ca)	11.58	27.19	33.22	37.04	16.04	14.48	36.90	34.21	9.58	27.24	27.24
Enstatite (Mg)	61.49	58.16	41.60	38.02	57.37	68.60	40.01	51.03	70.79	49.37	49.37
Ferrosilite (Fe)	26.93	14.65	25.18	24.94	26.59	16.92	23.09	14.76	19.63	23.38	23.38
Tot.	100.00	100.00	100.00	100.00	100.00	100.00	100.00	100.00	100.00	100.00	100.00

Leucites of Nyiragongo samples

Sample rock	SHD lc	SHD lc	SHD lc	SHD lc	SHD lc	SHD lc	SHD lc	SHD lc	LV1SHD 2 lc	M2002GL lc	M2002GL lc	M2002GL lc	M2002GL lc
SiO ₂	52.91	54.40	53.55	53.76	52.89	53.55	54.39	53.05	53.44	53.23	52.68	54.25	53.57
Al ₂ O ₃	22.93	23.65	23.41	23.21	23.30	22.92	22.86	23.26	23.36	23.29	23.04	23.24	22.82
FeO	0.28	0.42	0.70	0.47	0.63	0.43	0.40	0.66	0.50	0.46	0.31	0.75	0.67
CaO	0.00	0.08	0.13	0.12	0.41	0.21	0.09	0.30	0.26	0.12	0.05	0.36	0.13
Na ₂ O	0.25	0.07	0.29	0.13	0.32	0.16	0.25	0.53	0.29	0.67	0.21	0.56	0.03
K ₂ O	21.55	21.22	20.95	21.76	19.47	21.58	21.46	21.15	20.31	21.33	21.56	20.84	21.76
BaO	0.00	0.00	0.00	0.00	0.00	0.00	0.00	0.00	0.71	0.47	0.14	0.59	0.15
SrO	0.62	0.00	0.00	0.47	0.10	0.35	0.00	0.00	0.00	0.27	0.00	0.00	0.00
Tot.	98.54	99.84	99.04	99.92	97.12	99.18	99.44	98.95	98.88	99.84	97.99	100.59	99.15
Si	1.97	1.98	1.97	1.97	1.97	1.98	2.00	1.96	1.97	1.96	1.97	1.98	1.98
Al	1.01	1.02	1.02	1.00	1.03	1.00	0.99	1.01	1.02	1.01	1.02	1.00	1.00
Fe	0.01	0.01	0.02	0.01	0.02	0.01	0.01	0.02	0.02	0.01	0.01	0.02	0.02
Ca	0.00	0.00	0.01	0.00	0.02	0.01	0.00	0.01	0.01	0.00	0.00	0.01	0.01
Na	0.02	0.00	0.02	0.01	0.02	0.01	0.02	0.04	0.02	0.05	0.02	0.04	0.00
K	1.03	0.99	0.98	1.02	0.93	1.02	1.00	1.00	0.96	1.00	1.03	0.97	1.03
Ba	0.00	0.00	0.00	0.00	0.00	0.00	0.00	0.00	0.01	0.01	0.00	0.01	0.00
Sr	0.01	0.00	0.00	0.01	0.00	0.01	0.00	0.00	0.00	0.01	0.00	0.00	0.00
Tot.	4.05	4.01	4.02	4.04	3.99	4.04	4.02	4.05	4.01	4.06	4.04	4.03	4.04

Sample rock	M2002GL	M2002GL	M2002GL	M2002GL	M2002GL	SHD	SHD	SHAHERU UP	NYIRA SUM	NYIRA SUM	NYIRA SUM	NYIRA SUM	NYIRA SUM
	lc	lc	lc	lc	lc	lc	lc	lc	leu	leu	leu	leu	leu
SiO ₂	54.81	52.12	51.89	54.38	53.55	54.33	54.41	55.92	53.40	53.61	52.78	54.81	53.44
Al ₂ O ₃	22.95	23.83	21.96	23.49	22.98	23.59	22.93	23.22	22.97	23.10	22.69	23.76	23.74
FeO	0.44	0.44	0.10	0.44	0.60	0.34	0.09	0.72	0.60	0.03	0.60	0.00	0.82
CaO	0.00	0.00	0.00	0.00	0.17	0.25	0.00	0.14	0.09	0.00	0.44	0.25	0.16
Na ₂ O	0.12	0.57	0.42	0.27	0.17	0.00	0.00	0.00	0.00	0.00	0.11	0.00	0.00
K ₂ O	21.12	20.84	21.07	21.93	21.22	22.06	22.41	22.42	21.15	21.14	21.13	22.34	21.23
BaO	0.00	1.03	0.00	0.33	0.00	0.70	0.57	0.00	0.28	0.00	0.00	0.21	0.34
SrO	0.00	0.00	0.00	0.00	0.00	0.00	0.00	0.00	0.65	0.26	1.02	0.38	1.16
Tot.	99.44	98.82	95.43	100.83	98.68	101.26	100.42	102.41	99.14	98.14	98.78	101.75	100.89
Si	2.00	1.94	1.99	1.98	1.98	1.97	1.99	2.00	1.98	1.99	1.97	1.98	1.95
Al	0.99	1.05	0.99	1.01	1.00	1.01	0.99	0.98	1.00	1.01	1.00	1.01	1.02
Fe	0.01	0.01	0.00	0.01	0.02	0.01	0.00	0.02	0.02	0.00	0.02	0.00	0.03
Ca	0.00	0.00	0.00	0.00	0.01	0.01	0.00	0.01	0.00	0.00	0.02	0.01	0.01
Na	0.01	0.04	0.03	0.02	0.01	0.00	0.00	0.00	0.00	0.00	0.01	0.00	0.00
K	0.98	0.99	1.03	1.02	1.00	1.02	1.05	1.02	1.00	1.00	1.01	1.03	0.99
Ba	0.00	0.01	0.00	0.00	0.00	0.01	0.01	0.00	0.00	0.00	0.00	0.00	0.00
Sr	0.00	0.00	0.00	0.00	0.00	0.00	0.00	0.00	0.01	0.01	0.02	0.01	0.02
Tot.	4.00	4.05	4.05	4.04	4.02	4.03	4.04	4.02	4.02	4.01	4.04	4.03	4.03

Sample rock	1977 2	1977 2	1977 2	1977 2	1977-5	1977-5	1977-5	2nd Pause	2nd Pause	2nd Pause	KH	KH	KH
	leu	leu	leu	leu	leu	leu	leu	leu	leu	leu	leu	leu	leu
SiO ₂	53.03	53.69	53.13	54.03	53.92	54.88	55.13	54.13	54.53	52.98	55.04	54.30	55.09
Al ₂ O ₃	23.73	23.08	22.97	23.90	23.89	23.30	23.80	23.57	23.20	22.57	23.84	23.53	23.13
FeO	0.75	0.58	0.90	0.48	0.57	0.34	0.81	0.39	0.43	0.82	0.42	0.95	0.46
CaO	0.27	0.00	0.23	0.12	0.06	0.05	0.22	0.07	0.05	0.57	0.10	0.08	0.00
Na ₂ O	0.00	0.00	0.00	0.00	0.12	0.05	0.11	0.00	0.00	0.00	0.00	0.00	0.00
K ₂ O	21.67	22.09	21.77	21.36	22.18	21.38	21.76	22.22	21.55	20.51	22.07	20.94	22.06
BaO	0.47	0.00	0.00	0.00	0.00	0.00	0.00	0.34	0.00	0.61	0.46	0.54	1.14
SrO	0.27	0.17	0.04	0.71	1.19	0.27	0.41	0.78	0.42	0.76	0.85	0.47	0.32
Tot.	100.18	99.60	99.05	100.59	101.92	100.26	102.24	101.50	100.19	98.82	102.78	100.81	102.20
Si	1.95	1.98	1.97	1.97	1.95	1.99	1.97	1.97	1.99	1.98	1.97	1.98	1.99
Al	1.03	1.00	1.00	1.02	1.02	1.00	1.00	1.01	1.00	0.99	1.01	1.01	0.98
Fe	0.02	0.02	0.03	0.01	0.02	0.01	0.02	0.01	0.01	0.03	0.01	0.03	0.01
Ca	0.01	0.00	0.01	0.00	0.00	0.00	0.01	0.00	0.00	0.02	0.00	0.00	0.00
Na	0.00	0.00	0.00	0.00	0.01	0.00	0.01	0.00	0.00	0.00	0.00	0.00	0.00
K	1.02	1.04	1.03	0.99	1.03	0.99	0.99	1.03	1.00	0.98	1.01	0.97	1.02
Ba	0.01	0.00	0.00	0.00	0.00	0.00	0.00	0.00	0.00	0.01	0.01	0.01	0.02
Sr	0.01	0.00	0.00	0.02	0.03	0.01	0.01	0.02	0.01	0.02	0.02	0.01	0.01
Tot.	4.04	4.04	4.04	4.02	4.05	4.00	4.02	4.04	4.01	4.02	4.03	4.01	4.03

Sample rock	KH	KH	KH	M2002-6	M2002-6	M2002-6	Nyira 2016	Nyira 2016	Nyira 2016	Nyira 2016	Nyira 2016
	leu	leu	leu	leu	leu	leu	leu	leu	leu	leu	leu
SiO ₂	54.56	53.76	53.90	55.03	54.31	53.83	53.90	54.05	52.54	55.29	54.19
Al ₂ O ₃	22.94	23.09	23.19	23.72	23.81	23.58	23.53	23.43	23.46	22.76	23.24
FeO	0.00	0.50	0.00	0.31	0.58	0.72	0.79	0.77	0.64	0.71	0.57
CaO	0.15	0.00	0.25	0.00	0.17	0.02	0.20	0.00	0.27	0.27	0.03
Na ₂ O	0.00	0.00	0.00	0.00	0.00	0.00	0.00	0.18	1.01	0.19	0.22
K ₂ O	21.76	20.97	21.92	21.80	22.20	20.74	21.89	21.52	19.48	20.51	21.55
BaO	0.25	0.00	0.68	0.00	0.26	0.00	0.19	0.39	0.38	0.00	0.00
SrO	0.53	0.00	0.14	0.68	0.51	1.20	0.21	0.14	0.35	0.00	0.00
Tot.	100.19	98.33	100.07	101.54	101.84	100.10	100.71	100.48	98.13	99.74	99.80
Si	1.99	1.99	1.98	1.98	1.96	1.97	1.97	1.97	1.96	2.01	1.98
Al	0.99	1.01	1.00	1.01	1.01	1.02	1.01	1.01	1.03	0.98	1.00
Fe	0.00	0.02	0.00	0.01	0.02	0.02	0.02	0.02	0.02	0.02	0.02
Ca	0.01	0.00	0.01	0.00	0.01	0.00	0.01	0.00	0.01	0.01	0.00
Na	0.00	0.00	0.00	0.00	0.00	0.00	0.00	0.01	0.07	0.01	0.02
K	1.02	0.99	1.03	1.00	1.02	0.97	1.02	1.00	0.93	0.95	1.01
Ba	0.00	0.00	0.01	0.00	0.00	0.00	0.00	0.01	0.01	0.00	0.00
Sr	0.01	0.00	0.00	0.01	0.01	0.03	0.00	0.00	0.01	0.00	0.00
Tot.	4.02	4.00	4.03	4.02	4.04	4.01	4.04	4.03	4.03	3.98	4.03

Leucites of Nyamuragira samples

Sample rock	Nyam C lc	Nyam C lc	N5UM b lc	NM1948 1 lc
SiO ₂	55.26	54.95	55.57	55.18
Al ₂ O ₃	22.82	23.16	22.58	22.78
FeO	0.51	0.36	1.10	0.36
CaO	0.23	0.18	0.57	0.17
Na ₂ O	0.00	0.00	0.80	0.72
K ₂ O	21.47	21.21	19.48	20.07
BaO	0.42	0.27	0.00	0.18
SrO	0.22	0.00	0.32	0.00
Tot.	100.91	100.13	100.42	99.46
Si	2.00	2.00	2.01	2.01
Al	0.98	0.99	0.96	0.98
Fe	0.02	0.01	0.03	0.01
Ca	0.01	0.01	0.02	0.01
Na	0.00	0.00	0.06	0.05
K	0.99	0.98	0.90	0.93
Ba	0.01	0.00	0.00	0.00
Sr	0.00	0.00	0.01	0.00
Tot.	4.01	4.00	3.99	3.99

Nephelines of Nyiragongo samples

Sample rock	SHD neph	SHD neph	SHD neph	SHD neph	SHD neph	SHD neph	SHD neph	SHD neph	SHD neph	SHD neph	SHD neph	SHD neph	SHD neph	LV1SHD 2 neph	LV1SHD 2 neph
SiO ₂	41.23	40.35	42.00	40.83	40.87	42.99	41.02	40.86	42.11	40.90	41.12	40.57	44.79	43.30	
Al ₂ O ₃	33.34	33.15	34.23	33.60	33.28	33.39	33.81	33.82	32.78	33.13	33.72	33.55	31.54	31.50	
FeO	0.26	0.67	0.61	0.57	0.61	0.97	0.71	0.49	1.05	0.33	0.67	0.80	1.70	0.95	
CaO	0.78	1.00	1.12	0.85	0.73	0.30	0.53	0.57	0.13	1.00	0.78	0.58	0.36	1.70	
Na ₂ O	12.10	11.94	14.41	12.31	13.45	16.03	14.71	14.92	15.13	11.29	12.75	12.84	14.96	14.85	
K ₂ O	12.00	12.50	9.64	11.41	9.81	8.73	8.80	8.93	9.55	12.83	11.51	11.80	6.82	7.16	
SrO	0.51	0.00	0.00	0.00	0.64	0.17	0.00	0.00	0.00	0.00	0.28	0.06	0.21	0.21	
Tot.	100.22	99.60	102.01	99.56	99.39	102.58	99.58	99.60	100.76	99.49	100.83	100.20	100.39	99.68	
Si	1.02	1.01	1.02	1.02	1.02	1.03	1.01	1.01	1.03	1.02	1.01	1.01	1.08	1.07	
Al	0.49	0.49	0.49	0.49	0.49	0.47	0.49	0.49	0.47	0.49	0.49	0.49	0.45	0.46	
Fe	0.01	0.01	0.01	0.01	0.01	0.02	0.01	0.01	0.02	0.01	0.01	0.01	0.02	0.02	
Ca	0.00	0.00	0.00	0.00	0.00	0.00	0.00	0.00	0.00	0.00	0.00	0.00	0.00	0.00	
Na	0.29	0.29	0.34	0.30	0.32	0.37	0.35	0.36	0.36	0.27	0.30	0.31	0.35	0.36	
K	0.19	0.20	0.15	0.18	0.16	0.13	0.14	0.14	0.15	0.20	0.18	0.19	0.10	0.11	
Sr	0.01	0.00	0.00	0.00	0.01	0.00	0.00	0.00	0.00	0.00	0.00	0.00	0.00	0.00	
Tot.	2.00	2.01	2.01	2.00	2.01	2.03	2.01	2.01	2.03	2.00	2.01	2.01	2.02	2.02	
Neph	9.47	9.97	7.42	9.06	7.76	6.57	6.90	7.00	7.33	10.25	9.02	9.29	5.19	5.59	
Kals	0.37	0.00	0.00	0.00	0.46	0.12	0.00	0.00	0.00	0.00	0.20	0.05	0.15	0.15	

Sample rock	LV1SHD 2 neph	M2002GL neph	M2002GL neph	M2002GL neph	M2002GL neph	M2002GL neph	M2002GL neph	M2002GL neph	SHD neph	SHD neph	SHD neph	SHD neph	SHAHERU UP ne-c	SHAHERU UP ne-r
SiO ₂	43.08	42.29	41.54	41.43	41.80	41.58	42.10	42.09	41.16	41.08	41.88	41.87	40.59	42.35
Al ₂ O ₃	31.95	33.02	32.27	32.68	33.24	31.77	33.60	33.67	33.13	33.96	33.93	32.33	33.34	34.49
FeO	0.76	0.98	0.76	0.95	0.77	1.03	0.54	1.26	0.73	0.74	0.69	1.28	0.73	0.50
CaO	0.67	1.57	1.30	1.32	1.21	1.72	1.30	1.27	1.13	0.91	0.59	0.36	0.70	0.68
Na ₂ O	15.04	13.36	12.66	13.03	12.38	12.54	13.45	15.21	13.44	12.92	13.52	13.29	11.04	13.53
K ₂ O	6.66	8.59	9.88	9.31	9.98	9.38	7.49	6.38	9.51	10.68	9.76	9.19	12.46	10.37
SrO	0.69	0.46	0.00	0.00	0.08	0.11	0.72	0.57	0.32	0.31	0.79	0.00	0.82	0.07
Tot.	98.85	100.26	98.40	98.72	99.46	98.14	99.20	100.45	99.42	100.60	101.16	98.32	99.68	101.98
Si	1.06	1.04	1.04	1.04	1.04	1.05	1.04	1.03	1.02	1.01	1.02	1.04	1.02	1.02
Al	0.46	0.48	0.48	0.48	0.49	0.47	0.49	0.48	0.49	0.49	0.49	0.47	0.49	0.49
Fe	0.02	0.02	0.02	0.02	0.02	0.02	0.01	0.03	0.02	0.02	0.01	0.03	0.02	0.01
Ca	0.00	0.00	0.00	0.00	0.00	0.00	0.00	0.00	0.00	0.00	0.00	0.00	0.00	0.00
Na	0.36	0.32	0.31	0.32	0.30	0.31	0.32	0.36	0.32	0.31	0.32	0.32	0.27	0.32
K	0.10	0.13	0.16	0.15	0.16	0.15	0.12	0.10	0.15	0.17	0.15	0.15	0.20	0.16
Sr	0.01	0.01	0.00	0.00	0.00	0.01	0.01	0.01	0.00	0.00	0.01	0.00	0.01	0.00
Tot.	2.01	2.00	2.00	2.00	1.99	2.00	1.99	2.00	2.00	2.00	2.00	2.01	2.00	2.00
Neph	5.19	6.74	7.90	7.42	7.91	7.54	5.93	4.96	7.52	8.38	7.57	7.26	9.94	7.98
Kals	0.49	0.33	0.00	0.00	0.06	0.08	0.52	0.40	0.23	0.22	0.56	0.00	0.59	0.05

Sample rock	SHAHERU UP ne	SHAHERU UP neph	SHAHERU UP ne	SHAHERU UP ne	SHAHERU UP ne	NYIRA SUM nef	NYIRA SUM nef	NYIRA SUM nef	NYIRA SUM nef	NYIRA SUM nef	NYIRA SUM nef	NYIRA SUM nef	NYIRA SUM nef	NYIRA SUM nef
SiO ₂	43.69	41.28	41.12	41.13	42.39	41.58	42.61	40.80	40.36	42.09	41.67	40.77	40.76	41.43
Al ₂ O ₃	34.20	33.50	33.75	33.35	32.06	33.26	34.17	32.56	32.97	33.21	32.99	32.34	33.18	33.64
FeO	0.78	1.07	0.74	0.84	1.10	0.59	0.69	0.73	0.91	0.34	1.30	1.17	0.41	0.57
CaO	0.18	0.05	0.87	0.10	0.25	0.93	0.82	0.70	0.77	0.71	0.84	0.86	0.90	0.75
Na ₂ O	13.89	14.07	14.05	14.41	13.81	11.30	12.51	10.50	10.28	11.30	13.35	13.34	13.93	14.27
K ₂ O	9.38	9.41	8.34	8.68	8.83	12.35	11.13	13.60	13.23	12.49	9.26	8.68	8.08	8.27
SrO	0.18	0.62	0.92	0.40	0.19	0.13	0.00	0.00	0.53	0.00	0.09	0.81	0.00	0.66
Tot.	102.30	100.00	99.78	98.91	98.63	100.14	101.91	98.89	99.04	100.14	99.50	97.96	97.26	99.60
Si	1.04	1.01	1.02	1.02	1.05	1.03	1.03	1.03	1.02	1.04	1.03	1.03	1.02	1.02
Al	0.48	0.49	0.49	0.49	0.47	0.49	0.49	0.48	0.49	0.48	0.48	0.48	0.49	0.49
Fe	0.02	0.02	0.02	0.02	0.02	0.01	0.01	0.02	0.02	0.01	0.03	0.02	0.01	0.01
Ca	0.00	0.00	0.00	0.00	0.00	0.00	0.00	0.00	0.00	0.00	0.00	0.00	0.00	0.00
Na	0.32	0.34	0.34	0.35	0.33	0.27	0.29	0.26	0.25	0.27	0.32	0.33	0.34	0.34
K	0.14	0.15	0.13	0.14	0.14	0.20	0.17	0.22	0.21	0.20	0.15	0.14	0.13	0.13
Sr	0.00	0.01	0.01	0.01	0.00	0.00	0.00	0.00	0.01	0.00	0.00	0.01	0.00	0.01
Tot.	2.00	2.01	2.00	2.01	2.01	2.00	2.00	2.00	2.00	2.00	2.01	2.01	1.99	2.00
Neph	7.12	7.33	6.56	6.81	6.93	9.77	8.60	10.92	10.65	9.85	7.28	6.94	6.50	6.49
Kals	0.13	0.44	0.66	0.29	0.13	0.09	0.00	0.00	0.39	0.00	0.06	0.59	0.00	0.47

Sample rock	1977 2 nef	1977 2 nef	1977 2 nef	1977 2 nef	1977 2 nef	1977-5 nef	1977-5 nef	1977-5 nef	1977-5 nef	1977-5 nef	2nd Pause nef	2nd Pause nef	2nd Pause nef	2nd Pause nef
SiO ₂	42.21	40.91	41.61	40.53	44.00	41.77	42.96	42.01	43.02	42.10	41.57	41.52	41.34	43.37
Al ₂ O ₃	32.68	34.04	34.03	34.03	32.53	34.37	34.01	33.15	33.84	33.98	34.03	33.87	34.06	32.89
FeO	1.08	0.68	0.70	0.71	1.04	0.61	0.84	1.18	0.47	0.65	1.09	1.06	0.45	1.47
CaO	0.69	0.99	0.89	0.92	0.23	1.51	1.04	1.30	1.20	1.30	1.15	0.96	1.10	0.56
Na ₂ O	14.11	13.02	13.52	12.62	15.08	14.81	15.41	14.18	15.40	15.02	14.29	13.51	13.58	14.17
K ₂ O	7.52	9.99	9.11	10.21	7.94	6.82	6.60	6.99	7.09	6.28	7.25	8.47	9.19	7.86
SrO	0.00	0.31	0.00	0.42	0.00	0.55	0.07	0.36	0.06	0.30	0.36	0.27	0.00	0.00
Tot.	98.29	99.95	99.86	99.45	100.82	100.43	100.93	99.17	101.08	99.62	99.74	99.65	99.71	100.32
Si	1.04	1.01	1.02	1.01	1.06	1.02	1.04	1.04	1.04	1.03	1.02	1.02	1.02	1.05
Al	0.48	0.50	0.49	0.50	0.46	0.49	0.48	0.48	0.48	0.49	0.49	0.49	0.49	0.47
Fe	0.02	0.01	0.01	0.01	0.02	0.01	0.02	0.02	0.01	0.01	0.02	0.02	0.01	0.03
Ca	0.00	0.00	0.00	0.00	0.00	0.00	0.00	0.00	0.00	0.00	0.00	0.00	0.00	0.00
Na	0.34	0.31	0.32	0.30	0.35	0.35	0.36	0.34	0.36	0.36	0.34	0.32	0.32	0.33
K	0.12	0.16	0.14	0.16	0.12	0.11	0.10	0.11	0.11	0.10	0.11	0.13	0.14	0.12
Sr	0.00	0.00	0.00	0.01	0.00	0.01	0.00	0.01	0.00	0.00	0.01	0.00	0.00	0.00
Tot.	2.00	2.00	1.99	1.99	2.02	1.99	2.00	2.00	2.00	1.99	1.99	1.99	1.99	2.01
Neph	5.93	7.89	7.16	8.12	6.05	5.33	5.08	5.51	5.46	4.92	5.69	6.66	7.25	6.06
Kals	0.00	0.22	0.00	0.31	0.00	0.39	0.05	0.26	0.05	0.21	0.26	0.19	0.00	0.00

Sample rock	2nd Pause nef	KH nef	KH nef	KH nef	KH nef	KH nef	KH nef	M2002-6 nef	M2002-6 nef	M2002-6 nef	M2002-2 nef	M2002-2 nef	Nyiragongo 2016 nef	Nyiragongo 2016 nef
SiO ₂	41.07	41.83	41.63	41.33	42.72	41.79	40.63	42.66	40.36	44.45	42.22	41.63	41.32	40.85
Al ₂ O ₃	32.29	33.42	34.02	34.22	31.78	32.91	32.62	34.14	35.74	32.79	33.49	32.16	33.37	33.29
FeO	1.15	0.67	0.30	0.59	0.83	1.21	0.47	0.90	0.82	0.59	0.79	0.76	0.84	0.72
CaO	0.95	0.79	0.86	0.73	0.69	0.75	0.78	1.33	1.68	0.33	1.20	0.91	0.99	1.18
Na ₂ O	13.59	10.75	12.34	12.05	13.55	13.84	10.10	14.34	13.01	14.77	11.41	12.43	13.00	11.96
K ₂ O	7.42	12.28	10.31	11.07	8.40	8.41	13.06	7.33	6.74	7.69	11.24	9.21	9.50	10.94
SrO	0.23	0.65	0.65	0.31	0.00	0.15	0.11	0.38	0.21	0.17	0.49	0.00	0.00	0.00
Tot.	96.72	100.38	100.12	100.31	97.98	99.08	97.76	101.09	98.56	100.79	100.84	97.09	99.02	98.95
Si	1.04	1.03	1.02	1.02	1.06	1.03	1.03	1.03	1.00	1.07	1.04	1.05	1.03	1.02
Al	0.48	0.49	0.49	0.50	0.47	0.48	0.49	0.49	0.52	0.46	0.48	0.48	0.49	0.49
Fe	0.02	0.01	0.01	0.01	0.02	0.03	0.01	0.02	0.02	0.01	0.02	0.02	0.02	0.02
Ca	0.00	0.00	0.00	0.00	0.00	0.00	0.00	0.00	0.00	0.00	0.00	0.00	0.00	0.00
Na	0.33	0.26	0.29	0.29	0.33	0.33	0.25	0.34	0.31	0.34	0.27	0.30	0.31	0.29
K	0.12	0.19	0.16	0.17	0.13	0.13	0.21	0.11	0.11	0.12	0.18	0.15	0.15	0.17
Sr	0.00	0.01	0.01	0.00	0.00	0.00	0.00	0.01	0.00	0.00	0.01	0.00	0.00	0.00
Tot.	2.00	1.99	1.99	1.99	2.01	2.01	1.99	1.99	1.96	2.01	1.99	2.00	2.00	1.99
Neph	5.98	9.70	8.14	8.73	6.65	6.62	10.62	5.68	5.43	5.87	8.84	7.42	7.54	8.76
Kals	0.17	0.47	0.47	0.22	0.00	0.11	0.08	0.27	0.16	0.12	0.35	0.00	0.00	0.00

Sample rock	Nyiragongo 2016 nef	Nyiragongo 2016 nef	Nyiragongo 2016 nef	NYIRA SUM nef	NYIRA SUM nef	NYIRA SUM nef	NYIRA SUM nef	NYIRA SUM nef	NYIRA SUM nef	NYIRA SUM nef	NYIRA SUM nef	NYIRA SUM nef	NYAM SUM 10 nef	NYAM SUM 10 nef
SiO ₂	41.04	41.86	41.29	41.58	42.61	40.80	40.36	42.09	41.67	40.77	40.76	41.43	55.53	53.51
Al ₂ O ₃	32.80	32.77	33.95	33.26	34.17	32.56	32.97	33.21	32.99	32.34	33.18	33.64	26.97	27.94
FeO	0.92	1.11	0.92	0.59	0.69	0.73	0.91	0.34	1.30	1.17	0.41	0.57	0.59	0.93
CaO	1.39	1.03	1.05	0.93	0.82	0.70	0.77	0.71	0.84	0.86	0.90	0.75	0.54	0.70
Na ₂ O	11.38	11.70	11.10	11.30	12.51	10.50	10.28	11.30	13.35	13.34	13.93	14.27	14.23	16.10
K ₂ O	11.70	11.07	12.33	12.35	11.13	13.60	13.23	12.49	9.26	8.68	8.08	8.27	1.54	1.44
SrO	0.14	0.35	0.00	0.13	0.00	0.00	0.53	0.00	0.09	0.81	0.00	0.66	0.35	0.00
Tot.	99.36	99.90	100.64	100.14	101.91	98.89	99.04	100.14	99.50	97.96	97.26	99.60	99.76	100.62
Si	1.03	1.04	1.02	1.03	1.03	1.03	1.02	1.04	1.03	1.03	1.02	1.02	1.27	1.23
Al	0.49	0.48	0.49	0.49	0.49	0.48	0.49	0.48	0.48	0.48	0.49	0.49	0.36	0.38
Fe	0.02	0.02	0.02	0.01	0.01	0.02	0.02	0.01	0.03	0.02	0.01	0.01	0.01	0.02
Ca	0.00	0.00	0.00	0.00	0.00	0.00	0.00	0.00	0.00	0.00	0.00	0.00	0.00	0.00
Na	0.28	0.28	0.27	0.27	0.29	0.26	0.25	0.27	0.32	0.33	0.34	0.34	0.32	0.36
K	0.19	0.18	0.19	0.20	0.17	0.22	0.21	0.20	0.15	0.14	0.13	0.13	0.02	0.02
Sr	0.00	0.01	0.00	0.00	0.00	0.00	0.01	0.00	0.00	0.01	0.00	0.01	0.00	0.00
Tot.	2.00	2.00	1.99	2.00	2.00	2.00	2.00	2.00	2.01	2.01	1.99	2.00	2.00	2.01
Neph	9.36	8.75	9.74	9.77	8.60	10.92	10.65	9.85	7.28	6.94	6.50	6.49	1.13	1.05
Kals	0.10	0.25	0.00	0.09	0.00	0.00	0.39	0.00	0.06	0.59	0.00	0.47	0.23	0.00

Sample rock	NYAM SUM 10 nef	NYAM SUM 1 nef	NYAM SUM 10 nef	NM1938-2 nef?	NM1938-2 nef	NM1938-2 nef
SiO ₂	53.44	53.19	54.76	54.23	51.79	53.92
Al ₂ O ₃	26.63	26.53	27.98	27.04	26.57	26.91
FeO	0.95	0.73	0.52	1.41	1.56	1.08
CaO	0.73	0.69	0.23	0.74	1.27	0.16
Na ₂ O	13.26	13.38	15.24	13.94	14.99	13.23
K ₂ O	2.40	1.43	1.90	0.66	1.47	1.04
SrO	0.00	0.27	0.68	0.00	0.25	0.00
Tot.	97.41	96.22	101.31	98.02	97.91	96.34
Si	1.26	1.27	1.25	1.27	1.24	1.27
Al	0.37	0.37	0.38	0.37	0.37	0.37
Fe	0.02	0.01	0.01	0.03	0.03	0.02
Ca	0.00	0.00	0.00	0.00	0.00	0.00
Na	0.30	0.31	0.34	0.32	0.35	0.30
K	0.04	0.02	0.03	0.01	0.02	0.02
Sr	0.00	0.00	0.01	0.00	0.00	0.00
Tot.	1.99	1.99	2.00	1.99	2.02	1.98
Neph	1.81	1.09	1.38	0.50	1.11	0.79
Kals	0.00	0.19	0.45	0.00	0.17	0.00

Nephelines of Nyamuragira samples:

Apatites of Nyiragongo
samples:

Sample rock	SHD ap	SHD ap	SHD ap	SHD ap	SHD ap	LV1SHD 2 ap	LV1SHD 2 ap	M2002GL ap	M2002GL ap	M2002GL ap	M2002GL ap	M2002GL ap
P₂O₅	40.26	40.04	41.15	40.24	40.44	38.28	40.10	38.52	39.60	37.09	36.71	38.71
CaO	53.20	53.59	53.77	52.58	53.58	51.79	54.24	52.98	53.29	53.71	51.50	52.86
SrO	0.82	0.58	0.92	1.28	0.79	0.17	0.73	0.82	1.01	0.63	0.55	1.39
F	4.34	2.34	2.98	2.05	2.78	1.42	1.67	1.09	2.12	2.09	2.04	2.04
Cl	0.10	0.06	0.05	0.04	0.02	0.09	0.19	0.02	0.09	0.16	0.16	0.24
Tot.	98.72	96.61	98.87	96.18	97.60	91.76	96.95	93.42	96.12	93.69	90.97	95.24
SiO₂	0.46	0.36	0.40	0.62	0.51	1.58	0.78	1.60	1.08	1.92	2.29	1.79
Al₂O₃	0.06	0.17	0.12	0.09	0.20	0.42	0.06	0.28	0.00	0.23	0.47	0.00
FeO	0.60	0.10	0.00	0.14	0.00	0.69	0.00	0.71	0.29	0.47	0.85	1.05
CaO	53.20	53.59	53.77	52.58	53.58	51.79	54.24	52.98	53.29	53.71	51.50	52.86
Na₂O	0.00	0.17	0.00	0.00	0.00	0.04	0.00	0.20	0.00	0.24	0.13	0.08
P₂O₅	40.26	40.04	41.15	40.24	40.44	38.28	40.10	38.52	39.60	37.09	36.71	38.71
SrO	0.82	0.58	0.92	1.28	0.79	0.17	0.73	0.82	1.01	0.63	0.55	1.39
Y₂O₃	0.00	0.00	0.00	0.00	0.00	0.00	0.00	0.00	0.00	0.00	0.00	0.00
La₂O₃	0.00	0.00	0.52	0.25	0.74	0.55	0.00	0.27	0.83	0.00	0.44	0.28
Ce₂O₃	0.36	0.00	0.94	0.33	1.08	0.47	0.00	0.00	1.09	0.44	1.26	0.61
Nd₂O₃	0.00	0.70	0.00	0.00	0.13	0.37	0.13	0.84	0.46	0.00	0.17	0.67
ThO₂	0.00	0.07	0.16	0.21	0.19	0.28	0.09	0.00	0.00	0.00	0.00	0.26
UO₂	0.00	0.27	0.00	0.25	0.00	0.00	0.00	0.40	0.10	0.00	0.00	0.00
F	4.34	2.34	2.98	2.05	2.78	1.42	1.67	1.09	2.12	2.09	2.04	2.04
Cl	0.10	0.06	0.05	0.04	0.02	0.09	0.19	0.02	0.09	0.16	0.16	0.24
SO₃	0.25	0.25	0.00	0.12	0.08	0.00	0.00	0.27	0.00	0.11	0.00	0.00
Tot.	100.44	98.69	101.01	98.19	100.53	96.15	98.01	97.98	99.97	97.09	96.57	99.97
O=F,Cl	4.44	2.40	3.02	2.08	2.80	1.51	1.87	1.10	2.21	2.26	2.21	2.29
Tot.	96.00	96.29	97.99	96.11	97.73	94.64	96.15	96.88	97.76	94.83	94.36	97.68
Al	0.01	0.04	0.02	0.02	0.04	0.09	0.01	0.06	0.00	0.05	0.10	0.00
Fe	0.08	0.01	0.00	0.02	0.00	0.10	0.00	0.10	0.04	0.07	0.13	0.15
Ca	9.33	9.80	9.56	9.70	9.63	9.84	10.02	9.97	9.76	10.07	9.75	9.71
Na	0.00	0.06	0.00	0.00	0.00	0.01	0.00	0.07	0.00	0.08	0.04	0.03
Sr	0.08	0.06	0.09	0.13	0.08	0.02	0.07	0.08	0.10	0.06	0.06	0.14
Y	0.00	0.00	0.00	0.00	0.00	0.00	0.00	0.00	0.00	0.00	0.00	0.00
La	0.00	0.00	0.03	0.02	0.05	0.04	0.00	0.02	0.05	0.00	0.03	0.02
Ce	0.02	0.00	0.06	0.02	0.07	0.03	0.00	0.00	0.07	0.03	0.08	0.04
Nd	0.00	0.04	0.00	0.00	0.01	0.02	0.01	0.05	0.03	0.00	0.01	0.04
Th	0.00	0.00	0.01	0.01	0.01	0.01	0.00	0.00	0.00	0.00	0.00	0.01
U	0.00	0.01	0.00	0.01	0.00	0.00	0.00	0.02	0.00	0.00	0.00	0.00
Tot.	9.52	10.02	9.77	9.92	9.88	10.16	10.12	10.37	10.06	10.35	10.19	10.13
Si	4.34	2.34	2.98	2.05	2.78	1.42	1.67	1.09	2.12	2.09	2.04	2.04
P	96.00	96.29	97.99	96.11	97.73	94.64	96.15	96.88	97.76	94.83	94.36	97.68
S	0.00	0.04	0.00	0.00	0.01	0.02	0.01	0.05	0.03	0.00	0.01	0.04
Tot.	100.35	98.68	100.97	98.16	100.51	96.09	97.83	98.02	99.91	96.93	96.42	99.77
F	2.25	1.26	1.56	1.11	1.47	0.80	0.91	0.60	1.15	1.16	1.14	1.11
Cl	0.03	0.02	0.01	0.01	0.01	0.03	0.06	0.01	0.03	0.05	0.05	0.07
OH	-0.28	0.72	0.42	0.88	0.52	1.18	1.03	1.39	0.83	0.79	0.81	0.82
Tot.	2.00	2.00	2.00	2.00	2.00	2.00	2.00	2.00	2.00	2.00	2.00	2.00
Si*100/(Si+P)	1.32	1.04	1.15	1.78	1.45	4.66	2.25	4.66	3.11	5.75	6.86	5.17

Sample rock	KH ap	KH ap	Nyira 2016 ap	Nyira 2016 ap incl	Nyira 2016 ap incl	Nyira 2016 ap	Nyira 2016 ap	NYIRA SUM ap	NYIRA SUM ap	NYIRA SUM ap
P₂O₅	41.09	41.80	43.14	39.43	40.72	40.74	40.86	40.31	38.57	38.59
CaO	54.41	54.78	55.72	53.70	54.01	53.96	54.73	53.27	52.66	52.10
SrO	2.41	2.44	2.25	1.88	1.92	1.88	2.09	0.89	0.92	0.76
F	4.13	4.71	1.80	2.61	3.08	2.74	4.91	2.60	0.41	2.20
Cl	0.25	0.04	0.16	0.19	0.15	0.20	0.16	0.00	0.08	0.15
Tot.			103.07	97.80	99.88	99.53	102.75	97.06	92.63	93.79
SiO₂	0.39	0.39	0.42	0.88	0.63	0.79	0.76	0.68	1.88	0.78
Al₂O₃	0.00	0.00	0.00	0.07	0.00	0.03	0.18	0.02	0.48	0.24
FeO	0.30	0.30	0.00	1.33	0.52	0.77	0.23	0.31	0.78	0.00
CaO	53.96	53.96	55.47	53.62	53.86	53.86	54.60	53.27	52.66	52.10
Na₂O	0.00	0.00	0.19	0.00	0.13	0.00	0.00	0.07	0.02	0.13
P₂O₅	40.54	40.54	42.48	38.75	40.17	40.15	40.31	40.31	38.57	38.59
SrO	0.79	0.79	1.01	0.71	0.86	0.84	0.86	0.89	0.92	0.76
Y₂O₃	0.00	0.00	0.00	0.00	0.00	0.00	0.00	0.00	0.00	0.00
La₂O₃	0.19	0.19	0.80	0.00	0.00	0.34	0.00	0.27	0.57	0.00
Ce₂O₃	0.08	0.08	0.22	0.12	0.35	0.16	0.99	0.67	0.37	0.00
Nd₂O₃	0.32	0.32	0.30	0.00	0.07	0.00	0.00	0.00	0.00	0.23
ThO₂	0.00	0.00	0.00	0.18	0.00	0.18	0.25	0.09	0.08	0.47
UO₂	0.00	0.00	0.23	0.00	0.12	0.00	0.30	0.00	0.24	0.00
F	2.18	2.18	1.13	1.13	2.33	2.22	3.99	2.60	0.41	2.20
Cl	0.20	0.20	0.16	0.19	0.15	0.21	0.16	0.00	0.08	0.15
SO₃	0.17	0.17	0.00	0.00	0.00	0.00	0.14	0.00	0.00	0.21
Tot.	99.11	99.11	102.42	96.97	99.19	99.54	102.78	99.17	97.06	95.85
O=F,Cl	2.38	2.38	1.29	1.32	2.48	2.42	4.16	2.60	0.49	2.34
Tot.	96.73	96.73	101.13	95.65	96.71	97.12	98.62	96.58	96.57	93.51
Al	0.00	0.00	0.00	0.01	0.00	0.01	0.03	0.00	0.10	0.05
Fe	0.04	0.04	0.00	0.20	0.07	0.11	0.03	0.04	0.12	0.00
Ca	9.82	9.82	9.93	10.17	9.81	9.80	9.49	9.67	10.05	9.80
Na	0.00	0.00	0.06	0.00	0.04	0.00	0.00	0.02	0.01	0.04
Sr	0.08	0.08	0.10	0.07	0.09	0.08	0.08	0.09	0.10	0.08
Y	0.00	0.00	0.00	0.00	0.00	0.00	0.00	0.00	0.00	0.00
La	0.01	0.01	0.05	0.00	0.00	0.02	0.00	0.02	0.04	0.00
Ce	0.01	0.01	0.01	0.01	0.02	0.01	0.06	0.04	0.02	0.00
Nd	0.02	0.02	0.02	0.00	0.00	0.00	0.00	0.00	0.00	0.01
Th	0.00	0.00	0.00	0.01	0.00	0.01	0.01	0.00	0.00	0.02
U	0.00	0.00	0.01	0.00	0.00	0.00	0.01	0.00	0.01	0.00
Tot.	9.98	9.98	10.18	10.47	10.04	10.03	9.71	9.89	10.45	10.01
Si	2.18	2.18	1.13	1.13	2.33	2.22	3.99	2.60	0.41	2.20
P	96.73	96.73	101.13	95.65	96.71	97.12	98.62	96.58	96.57	93.51
S	0.02	0.02	0.02	0.00	0.00	0.00	0.00	0.00	0.00	0.01
Tot.	98.93	98.93	102.27	96.78	99.04	99.33	102.62	99.17	96.98	95.72
F	1.17	1.17	0.60	0.63	1.25	1.19	2.05	1.39	0.23	1.22
Cl	0.06	0.06	0.05	0.06	0.04	0.06	0.04	0.00	0.02	0.04
OH	0.77	0.77	1.36	1.31	0.70	0.75	-0.09	0.61	1.75	0.74
Tot.	2.00	2.00	2.00	2.00	2.00	2.00	2.00	2.00	2.00	2.00
Si*100/(Si+P)	1.11	1.11	1.16	2.62	1.81	2.28	2.18	1.96	5.45	2.34

Opagues of Nyiragongo samples:

Sample rock	SHD mgt	SHD mgt	SHD mgt	LV1SHD 2 chr	LV1SHD 2 chr	LV1SHD 2 chr	LV1SHD 2 chr	LV1SHD 2 chr	LV1SHD 2 mgt	LV1SHD 2 chr	LV1SHD 2 mgt	LV1SHD 2 mgt	M2002GL mgt
SiO ₂	0.23	0.33	0.13	0.43	0.41	0.65	0.11	0.20	0.30	0.29	0.23	0.18	0.18
TiO ₂	22.30	21.61	17.40	2.60	2.82	7.28	2.96	19.22	2.56	20.59	16.82	19.17	19.17
Al ₂ O ₃	1.51	1.47	4.51	16.73	16.33	15.83	15.68	6.71	16.05	5.89	6.83	4.90	4.90
FeO(t)	67.46	68.41	61.68	25.51	26.28	47.79	25.37	59.47	25.39	61.11	64.28	63.26	63.26
MnO	1.94	1.76	0.79	0.27	0.30	0.68	0.64	1.00	0.00	0.77	0.82	0.83	0.83
MgO	1.24	0.64	5.63	14.47	13.27	10.90	14.03	5.03	13.64	3.79	8.27	6.35	6.35
Na ₂ O	0.00	0.00	0.00	0.00	0.00	0.00	0.00	0.00	0.00	0.00	0.00	0.00	0.00
V ₂ O ₅	0.68	0.59	0.78	0.00	0.17	0.00	0.30	0.78	0.00	1.16	0.50	0.69	0.69
Cr ₂ O ₃	0.00	0.00	0.00	40.52	40.39	11.41	39.69	4.77	39.44	0.05	0.00	0.00	0.00
NiO	0.00	0.00	0.00	0.22	0.08	0.52	0.00	0.00	0.00	0.44	0.00	0.00	0.00
Tot.	95.35	94.81	90.92	100.53	99.97	94.54	98.79	97.17	97.39	93.66	97.75	95.39	95.39
Si	0.01	0.01	0.00	0.01	0.01	0.02	0.00	0.01	0.01	0.01	0.01	0.01	0.01
Ti	0.63	0.62	0.49	0.06	0.07	0.18	0.07	0.51	0.06	0.57	0.43	0.51	0.51
Al	0.07	0.07	0.20	0.61	0.60	0.62	0.58	0.28	0.60	0.25	0.27	0.21	0.21
Fe ²⁺	1.51	1.54	1.15	0.40	0.45	0.64	0.40	1.22	0.42	1.34	0.99	1.15	1.15
Fe ³⁺	0.62	0.65	0.78	0.26	0.24	0.68	0.27	0.53	0.26	0.54	0.83	0.73	0.73
Mn	0.06	0.06	0.02	0.01	0.01	0.02	0.02	0.03	0.00	0.02	0.02	0.03	0.03
Mg	0.07	0.04	0.31	0.66	0.62	0.54	0.66	0.26	0.65	0.21	0.42	0.34	0.34
V	0.02	0.01	0.02	0.00	0.00	0.00	0.01	0.02	0.00	0.03	0.01	0.02	0.02
Cr	0.00	0.00	0.00	0.99	1.00	0.30	0.99	0.13	1.00	0.00	0.00	0.00	0.00
Ni	0.00	0.00	0.00	0.01	0.00	0.01	0.00	0.00	0.00	0.01	0.00	0.00	0.00
Tot.	2.99	2.99	2.99	3.00	3.00	3.00	3.00	2.99	3.00	2.98	2.99	2.99	2.99

Sample rock	M2002GL mgt	M2002GL mgt	M2002GL mgt	SHD mgt	SHAHERU UP mgt	SHAHERU UP mgt	SHAHERU UP mgt	SHAHERU UP mgt	NYIRA SUM mgt	NYIRA SUM mgt	1977 2 mag	1977-5 mag
SiO ₂	0.33	0.42	0.14	0.39	0.49	0.10	0.27	0.39	0.12	0.11	0.11	0.43
TiO ₂	18.48	18.53	20.00	18.85	24.31	25.37	21.43	22.08	17.48	19.04	16.91	25.64
Al ₂ O ₃	4.70	5.14	4.71	5.17	2.50	0.88	4.04	2.06	5.43	4.47	5.90	2.49
FeO(t)	63.99	61.94	63.74	66.66	62.85	62.30	62.10	67.55	65.10	66.15	65.99	63.89
MnO	1.18	0.83	1.16	0.81	1.96	2.23	0.54	1.62	1.16	1.16	1.08	1.60
MgO	6.50	6.87	6.04	5.84	0.62	0.91	5.18	0.73	4.71	3.54	3.87	1.95
Na ₂ O	0.00	0.00	0.00	0.00	0.00	0.00	0.00	0.00	0.00	0.00	0.00	0.00
V ₂ O ₅	0.96	0.54	0.50	0.55	0.87	0.35	0.88	0.28	0.98	0.24	0.49	0.70
Cr ₂ O ₃	0.00	0.24	0.06	0.00	0.06	0.06	0.00	0.00	0.00	0.26	0.00	0.15
NiO	0.00	0.00	0.00	0.00	0.00	0.22	0.00	0.00	0.00	0.00	0.00	0.00
Tot.	96.14	94.51	96.34	98.27	93.65	92.20	94.44	94.72	94.98	94.97	94.34	96.84
Si	0.01	0.01	0.01	0.01	0.02	0.00	0.01	0.02	0.00	0.00	0.00	0.02
Ti	0.49	0.50	0.53	0.49	0.70	0.75	0.59	0.63	0.47	0.53	0.46	0.71
Al	0.20	0.22	0.20	0.21	0.11	0.04	0.17	0.09	0.23	0.19	0.25	0.11
Fe ²⁺	1.12	1.12	1.18	1.18	1.62	1.62	1.29	1.55	1.18	1.30	1.22	1.57
Fe ³⁺	0.77	0.73	0.71	0.76	0.41	0.43	0.60	0.60	0.78	0.73	0.79	0.41
Mn	0.04	0.03	0.03	0.02	0.06	0.07	0.02	0.05	0.04	0.04	0.03	0.05
Mg	0.34	0.37	0.32	0.30	0.04	0.05	0.28	0.04	0.25	0.19	0.21	0.11
V	0.02	0.01	0.01	0.01	0.02	0.01	0.02	0.01	0.02	0.01	0.01	0.02
Cr	0.00	0.01	0.00	0.00	0.00	0.00	0.00	0.00	0.00	0.01	0.00	0.00
Ni	0.00	0.00	0.00	0.00	0.00	0.01	0.00	0.00	0.00	0.00	0.00	0.00
Tot.	2.98	2.99	2.99	2.99	2.98	2.98	2.98	2.99	2.98	3.00	2.99	2.99

Sample rock	1977-5 mag	1977-6 mag	2nd Pass mag	KH mgf	KH ox	KH mgf	M2002-1 mgf	M2002-6 ox	M2002-2 mgf	Nyira 2016 mag	Nyira 2016 mag	Nyira 2016 mag
SiO ₂	0.12	0.24	0.11	0.40	0.28	0.13	0.50	0.44	0.28	0.28	0.28	0.28
TiO ₂	18.80	10.89	17.95	20.80	18.49	18.04	20.29	19.30	19.64	17.89	19.05	17.70
Al ₂ O ₃	0.03	0.34	0.02	3.30	4.54	0.25	4.44	5.93	0.43	0.08	0.89	0.87
FeO(H)	64.08	72.00	65.28	65.34	65.78	65.60	63.33	65.13	63.23	65.85	63.48	65.54
MnO	0.75	0.80	1.00	1.07	1.07	0.94	0.85	0.97	0.81	0.78	0.84	0.88
MgO	0.05	7.28	0.04	2.78	3.91	0.44	0.94	0.91	0.01	0.99	7.07	7.08
Na ₂ O	0.00	0.00	0.00	0.00	0.00	0.00	0.00	0.00	0.00	0.00	0.00	0.00
VO ₂	0.94	0.29	0.07	0.38	0.48	0.41	0.44	0.79	0.64	0.96	0.48	0.79
Cr ₂ O ₃	0.12	0.10	0.00	0.30	0.34	0.15	0.41	0.00	0.35	0.00	0.00	0.00
NiO	0.00	0.45	0.00	0.00	0.00	0.00	0.29	0.00	0.18	0.42	0.00	0.35
Tot.	96.88	98.05	96.08	92.93	95.54	96.88	96.01	97.47	95.96	98.10	96.88	98.00
Si	0.00	0.01	0.00	0.02	0.01	0.00	0.02	0.02	0.01	0.01	0.01	0.00
Ti	0.44	0.28	0.47	0.59	0.50	0.48	0.54	0.48	0.48	0.45	0.48	0.45
Al	0.27	0.25	0.23	0.15	0.19	0.22	0.19	0.24	0.23	0.23	0.24	0.27
Fe ²⁺	1.10	0.89	1.13	1.40	1.27	1.11	1.21	1.15	1.13	1.07	1.09	1.07
Fe ³⁺	0.80	1.15	0.79	0.01	0.79	0.81	0.07	0.74	0.74	0.81	0.77	0.79
Mn	0.02	0.02	0.03	0.05	0.03	0.03	0.03	0.03	0.02	0.02	0.02	0.02
Mg	0.30	0.37	0.32	0.18	0.21	0.34	0.31	0.31	0.35	0.36	0.37	0.36
V	0.02	0.01	0.02	0.01	0.01	0.01	0.01	0.02	0.01	0.02	0.01	0.02
Cr	0.00	0.00	0.00	0.01	0.00	0.00	0.01	0.00	0.01	0.00	0.00	0.00
Ni	0.00	0.01	0.00	0.00	0.00	0.00	0.01	0.00	0.01	0.01	0.00	0.01
Tot.	2.98	3.00	2.98	2.98	2.99	2.99	2.99	2.99	2.99	2.99	2.99	2.99

Sample rock	Nyira 2016 mag	Nyira 2016 mag	Nyira 2016 mag	LV4 ox	LV4 mgf	MUJA spinello	MUJA spinello	MUJA mgf	MUJA mgf	MUJA mgf	NYAM SUM 10 ox ilm	NYAM SUM 10 mgf
SiO ₂	0.31	0.29	0.36	0.33	0.30	0.64	0.11	0.37	0.30	0.30	0.79	0.21
TiO ₂	18.28	17.04	17.38	12.11	12.81	20.33	21.39	21.31	20.89	18.73	44.14	18.57
Al ₂ O ₃	0.02	7.37	0.80	5.90	8.04	7.93	8.41	8.05	8.05	10.24	0.41	1.08
FeO(H)	64.08	63.77	62.00	61.13	60.02	55.69	54.09	62.06	63.21	65.41	48.74	73.83
MnO	0.77	0.73	0.82	0.98	0.87	0.38	0.81	0.32	0.30	0.48	1.44	1.08
MgO	0.98	0.98	7.25	4.94	7.89	8.20	8.64	3.28	3.04	7.42	2.20	1.19
Na ₂ O	0.00	0.00	0.00	0.00	0.00	0.00	0.00	0.00	0.00	0.00	0.00	0.00
VO ₂	0.00	0.02	0.04	0.40	0.23	0.81	0.98	0.89	0.55	0.71	0.70	0.34
Cr ₂ O ₃	0.00	0.04	0.19	0.00	0.89	0.89	1.15	0.47	0.00	3.32	0.00	0.03
NiO	0.19	0.36	0.14	0.10	0.29	0.00	0.00	0.23	0.25	0.00	0.48	0.00
Tot.	97.01	96.88	94.74	85.41	95.38	96.07	96.39	94.30	89.17	95.03	98.41	94.30
Si	0.01	0.01	0.01	0.01	0.01	0.03	0.00	0.01	0.01	0.01	0.03	0.01
Ti	0.48	0.44	0.49	0.26	0.33	0.52	0.55	0.59	0.56	0.48	1.16	0.47
Al	0.27	0.30	0.24	0.28	0.33	0.32	0.34	0.22	0.22	0.41	0.02	0.05
Fe ²⁺	1.10	1.07	1.07	1.09	0.90	1.07	1.04	1.40	1.37	1.10	1.41	1.38
Fe ³⁺	0.75	0.77	0.78	0.96	0.96	0.82	0.80	0.52	0.60	0.49	0.00	0.07
Mn	0.02	0.02	0.02	0.02	0.02	0.01	0.02	0.01	0.03	0.01	0.04	0.03
Mg	0.35	0.38	0.38	0.29	0.40	0.47	0.49	0.18	0.17	0.38	0.11	0.07
V	0.00	0.01	0.01	0.01	0.01	0.02	0.02	0.02	0.01	0.02	0.02	0.01
Cr	0.00	0.00	0.01	0.00	0.02	0.02	0.03	0.01	0.00	0.09	0.00	0.00
Ni	0.01	0.01	0.00	0.00	0.01	0.00	0.00	0.01	0.01	0.00	0.01	0.00
Tot.	3.00	2.99	2.99	2.99	3.00	2.99	2.98	2.98	2.99	2.99	2.79	2.99

Sample rock	1977-5 mag	1977-5 mag	2nd Pass mag	KH mgf	KH ox	KH mgf	M2002-6 mgf	M2002-6 ox	M2002-2 mgf	Nyira 2016 mag	Nyira 2016 mag	Nyira 2016 mag
SiO ₂	0.12	0.24	0.11	0.42	0.28	0.13	0.50	0.44	0.28	0.28	0.28	0.28
TiO ₂	18.00	10.00	17.95	20.00	18.40	16.04	20.00	18.30	18.64	17.89	18.05	17.70
Al ₂ O ₃	0.02	0.24	0.02	0.32	4.54	0.25	4.44	0.93	0.43	0.08	0.89	0.87
FeO(t)	64.08	72.00	65.28	63.34	66.76	65.00	65.33	65.13	63.23	65.65	63.40	65.54
MnO	0.75	0.80	1.00	1.57	1.07	0.94	0.85	0.97	0.81	0.79	0.84	0.88
MgO	0.05	7.28	0.04	2.78	3.91	0.44	5.94	0.91	0.01	0.90	7.07	7.08
Na ₂ O	0.00	0.00	0.00	0.00	0.00	0.00	0.00	0.00	0.00	0.00	0.00	0.00
V ₂ O ₅	0.94	0.29	0.07	0.38	0.45	0.41	0.44	0.79	0.84	0.90	0.45	0.79
Cr ₂ O ₃	0.12	0.10	0.00	0.33	0.04	0.15	0.41	0.00	0.35	0.00	0.00	0.00
NiO	0.00	0.45	0.00	0.08	0.00	0.00	0.20	0.00	0.18	0.42	0.00	0.35
Tot.	96.88	98.05	96.68	92.93	95.54	96.88	98.01	97.47	96.96	98.10	96.88	98.00

Sample rock	Nyira 2016 mag	Nyira 2016 mag	Nyira 2016 mag	LV4 ox	LV4 mgf	MUJA spinello	MUJA spinello	MUJA mgf	MUJA mgf	MUJA mgf	NYAM SUM 10 ox ilm	NYAM SUM 10 mgf
SiO ₂	0.51	0.29	0.36	0.33	0.30	0.84	0.11	0.37	0.30	0.30	0.79	0.21
TiO ₂	18.25	17.94	17.38	12.11	12.81	20.33	21.39	21.31	20.09	18.70	44.14	16.57
Al ₂ O ₃	0.02	7.37	0.80	5.93	8.94	7.93	8.41	5.05	5.05	10.24	0.41	1.05
FeO(t)	64.08	63.77	62.00	61.13	60.02	55.69	54.06	62.06	63.21	66.41	48.74	73.85
MnO	0.77	0.73	0.82	0.88	0.87	0.38	0.81	0.93	0.48	0.48	1.44	1.08
MgO	0.98	0.98	7.25	4.94	7.08	8.20	8.64	3.28	3.04	7.42	3.20	1.78
Na ₂ O	0.00	0.00	0.00	0.00	0.00	0.00	0.00	0.00	0.00	0.00	0.00	0.00
V ₂ O ₅	0.00	0.02	0.04	0.40	0.23	0.81	0.96	0.89	0.55	0.71	0.70	0.34
Cr ₂ O ₃	0.00	0.04	0.19	0.00	0.00	0.88	1.15	0.47	0.00	3.32	0.00	0.03
NiO	0.19	0.36	0.14	0.10	0.20	0.00	0.00	0.23	0.25	0.00	0.48	0.00
Tot.	97.01	98.88	94.74	85.41	96.38	95.07	96.39	94.36	93.17	96.03	98.41	94.30

Sample rock	NYAM SUM 10 mgf	NYAM SUM 10 ilm	NYAM SUM 10 mgf	NYAM SUM 10 ox	NYIRA SUM mgf	NYIRA SUM mgf	NYAM SUM 10 mag	Nyam b 2011-2012 cr	Nyam b 2011-2012 cr	Nyam b 2011-2012 cr	Nyam b 2011-2012 mgf	Nyam b 2011-2012 mgf
SiO ₂	0.25	0.70	0.37	0.24	0.12	0.11	0.19	0.12	0.33	0.31	1.32	0.24
TiO ₂	11.11	48.02	18.50	21.61	17.48	19.04	15.78	1.38	1.26	0.94	13.47	44.33
Al ₂ O ₃	6.82	0.21	1.01	5.07	5.43	4.47	3.20	13.07	11.99	12.24	2.73	0.39
FeO(t)	73.74	43.84	70.03	62.09	65.10	66.15	70.74	20.73	21.54	21.75	72.89	43.18
MnO	0.39	1.43	1.21	0.72	1.16	1.16	1.00	0.05	0.05	0.57	0.43	0.41
MgO	2.67	1.96	1.28	2.68	4.71	3.54	0.87	12.93	12.65	10.82	1.63	4.87
Na ₂ O	0.00	0.00	0.00	0.00	0.00	0.00	0.00	0.00	0.00	0.00	0.00	0.00
V ₂ O ₅	1.18	0.39	0.70	1.36	0.98	0.24	0.73	0.31	0.00	0.30	0.45	1.79
Cr ₂ O ₃	0.36	0.00	0.00	0.79	0.00	0.26	0.29	51.18	52.77	51.76	0.00	0.08
NiO	0.41	0.13	0.55	0.00	0.00	0.00	0.00	0.39	0.47	0.82	0.00	0.22
Tot.	96.52	96.55	93.10	94.56	94.98	94.97	92.80	99.78	100.58	98.69	92.93	95.30

Si	0.01	0.02	0.01	0.01	0.00	0.00	0.01	0.00	0.01	0.01	0.05	0.01
Ti	0.30	1.25	0.53	0.60	0.47	0.53	0.45	0.03	0.03	0.02	0.38	1.16
Al	0.29	0.01	0.05	0.22	0.23	0.19	0.14	0.49	0.45	0.47	0.12	0.02
Fe ²⁺	1.14	1.27	1.43	1.43	1.18	1.30	1.37	0.42	0.44	0.48	1.33	1.26
Fe ³⁺	1.05	0.00	0.82	0.49	0.78	0.73	0.89	0.13	0.14	0.11	0.99	0.00
Mn	0.01	0.04	0.02	0.04	0.04	0.04	0.03	0.00	0.00	0.02	0.01	0.01
Mg	0.14	0.10	0.07	0.15	0.25	0.19	0.05	0.61	0.60	0.53	0.09	0.25
V	0.03	0.01	0.02	0.03	0.02	0.01	0.02	0.01	0.00	0.01	0.01	0.04
Cr	0.01	0.00	0.00	0.02	0.00	0.01	0.01	1.29	1.33	1.33	0.00	0.00
Ni	0.01	0.00	0.02	0.00	0.00	0.00	0.00	0.01	0.01	0.02	0.00	0.01
Tot.	2.98	2.71	2.99	2.98	2.98	2.98	2.98	3.00	3.00	3.00	2.99	2.76

Olivine trace elements (LA-ICPMS)

Sample name	Nyira 2016	Nyira 2016	Nyira 2016	Nyira 2016	M2002 GL	M2002 GL	Nyira 2016	Nyira 2016
	03NY16C1OL1A ol	04NY16C1OL1B ol	03NY16C2OL2A ol	04NY16C2OL2B ol	18NY02C1OL2A ol	19NY02C1OL3A ol	03NY16OL1A ol	04NY16OL2A ol
Li	3.98	4.87	7.40	7.14	6.11	14.72	12.76	13.83
B	27.39	31.36	12.80	13.30	41.15	0.00	0.00	74.70
Mg	32.81	32.94	40.24	32.69	34.63	33.08	32.79	34.81
Si	38.60	38.22	38.13	38.13	38.22	38.22	38.22	38.60
Ca	1.89	1.74	1.68	2.35	2.28	2.48	1.78	1.95
Sc	4.57	4.48	3.95	3.16	2.52		4.64	
Ti	0.12	0.07	0.05	0.11	0.23	0.16	0.16	0.05
V	17.84	8.91	6.97	16.08	33.84	16.36	21.88	
Cr		5.39	12.68	10.46	11.75			114.30
Co	221.01	220.04	209.49	206.59	211.21	193.49	212.66	215.34
Ni	382.97	384.01	373.51	340.79	301.58	286.81	412.50	306.93
Zn	235.59	229.39	188.11	160.53	234.29	205.94	186.01	272.45
Rb		0.41	0.21	3.42	0.38	5.72	0.74	1.50
Sr	38.03	35.29	27.61	121.82	53.23	152.74	40.53	40.61
Y	2.58	2.09	1.69	5.15			1.48	2.29
Zr	1.05	1.54	0.53	9.99	5.44	15.07	3.11	2.39
Nb	0.37	0.85	0.31	5.87	1.53	11.52	1.86	
Cs				0.04	0.31			0.97
Ba	1.81	5.98	1.80	54.46	5.25	104.52	14.09	3.76
La	10.07	9.53	8.08	28.87	18.50	22.29	7.02	6.30
Ce	16.77	16.42	13.22	51.03	30.65	40.30	13.63	18.00
Pr	1.67	1.76	1.48	5.32	2.41	4.30	1.40	1.77
Nd	6.60	6.54	5.63	19.99	9.63	13.41	4.43	6.99
Sm	0.96	0.85	0.78	2.21	1.56	2.18	1.51	1.73
Eu	0.29			0.90	0.52	0.51		
Gd	0.77			1.48	0.74	1.56	1.30	
Tb	0.11	0.11	0.08	0.21				
Dy	0.60	0.62	0.45	1.22	0.49		0.79	
Ho	0.10	0.10	0.09	0.16				
Er		0.20	0.15	0.40				
Tm		0.03	0.02	0.06				
Yb	0.28	0.25		0.30				
Lu	0.10	0.10	0.06	0.14				
Hf	0.21			0.13				
Ta	0.01	0.10		0.31		0.83		
Pb	0.11	0.20		0.17		0.40		
Th	0.53	0.48	0.21	1.93	0.94	2.26		1.39
U	0.03	0.07	0.03	0.55	0.19		0.30	0.32

Melilites and clinopyroxenes trace elements (LA-ICPMS):

Sample name	M2002 GL	M2002 GL	M2002 GL	M2002 GL	M2002 GL	M2002 GL	M2002 GL	M2002 GL	M2002 GL	M2002 GL	Nyira 2016
	11NY02C2MEL1A	<NY02C2MAL1>	17NY02C2AP2A	09NY02C2MEL2A	10NY02C2MEL2B	11NY02C2MEL2C	12NY02C2MEL2D	14NY02C1MEL3A	15NY02C1MEL4A	34NY02C3MEL5A	11NY16C1MEL1A
	mel	mel	mel	mel	mel	mel	mel	mel	mel	mel	mel
Li	1.22		1.53	3.35	0.85	2.39	1.13	0.49	5.90	1.10	2.23
B	15.22		18.44	21.32	7.35	19.80	26.26	29.62	15.67	26.74	25.81
Mg	6.83	6.42	7.20	7.28	7.30	7.43	7.26	6.70	6.93	7.01	7.15
Si	40.56	40.36	44.29	41.32	40.73	45.18	42.39	38.08	38.48	40.38	42.73
Ca	33.99	35.10	33.99	35.41	35.41	35.41	35.41	34.98	34.98	34.37	35.90
Sc	1.33		0.85	2.16	1.23	1.38	1.54	2.31	1.75	0.76	1.89
Ti	0.08	0.08	0.07	0.14	0.17	0.38	0.10	0.07	0.06	0.10	0.11
V	10.45	22.55	7.86	14.96	27.02	40.00	10.81	16.81	12.44	11.44	11.48
Cr	3.83				5.54			5.43	5.78		
Co	37.52	41.84	39.60	41.76	41.84	44.57	41.97	35.04	37.32	38.40	41.90
Ni	9.51	12.84	4.34	8.37	6.28	12.17	8.87	10.32	5.19	6.78	13.11
Zn	322.77	203.17	228.54	310.20	352.64	341.93	355.22	270.44	255.09	209.76	389.40
Rb	1.04	2.02	3.12	3.93	0.87	15.04	2.59	0.70	0.16	1.61	6.01
Sr	4704.57	4788.71	4692.58	5181.71	5088.11	5196.03	5035.21	4928.18	5003.74	4674.95	5094.51
Y	8.17	18.54	6.24	8.13	9.61	8.87	10.51	15.87	8.69	7.00	8.07
Zr	1.65	3.88	3.32	11.54	1.32	31.70	6.27	3.02	1.52	3.47	8.92
Nb	0.74	2.05	1.29	8.98	1.25	25.96	5.31	0.84	0.44	3.06	8.29
Cs					0.07	0.30		0.16			
Ba	100.08	128.92	113.13	183.27	109.15	342.06	140.52	110.46	100.82	115.90	148.19
La	88.05	170.43	66.67	77.50	89.69	86.61	94.67	146.67	90.81	83.82	86.55
Ce	178.80	320.36	124.28	158.13	169.36	174.07	187.63	287.52	179.66	158.42	160.88
Pr	18.49	34.14	13.14	15.92	19.00	18.75	18.97	30.85	19.04	16.84	17.31
Nd	67.20	123.26	54.82	60.02	66.37	67.30	71.44	115.95	68.36	62.65	63.10
Sm	7.02	12.85	7.79	6.26	7.17	9.31	13.80	9.62	5.62	8.27	9.48
Eu	2.80	5.36	2.12	2.59	1.85	3.12	1.94	5.00	3.39	2.49	3.09
Gd	4.79	13.21	2.57	3.88	4.92	4.86	5.59	6.13	4.42	4.06	4.74
Tb	0.52	1.17	0.30	0.50	0.60	0.73	0.59	1.64	0.69	0.46	0.49
Dy	2.23	5.79	1.60	1.88	3.29	2.93	2.42	2.98	2.50	2.05	2.07
Ho	0.25	1.01	0.26	0.52	0.39	0.38	0.15	0.56	0.51	0.31	0.35
Er	0.51	1.55		0.35	0.69	0.89	0.52	0.81	1.01	0.55	0.83
Tm		0.24	0.09			0.16	0.07	0.10	0.03	0.07	0.09
Yb	0.55			0.97				0.84			
Lu				0.14			0.05	0.10	0.11	0.04	0.10
Hf	0.06		0.30	0.20			0.21				
Ta		0.27	0.09	0.44		1.59	0.36	0.07		0.11	0.44
Pb	0.76	2.01	1.41	1.64	0.60	1.05	0.44	0.23	1.19	0.85	1.56
Th	1.65	4.59	0.34	1.67	1.29	2.37	0.91	4.47	1.05	1.32	0.80
U	0.14	1.35		0.46	0.16	1.15	0.34	0.66	0.18	0.23	0.35

Sample name	Nyira 2016	Nyira 2016	Nyira 2016	Nyira 2016	Nyira 2016	Nyira 2016	Nyira 2016	Nyira 2016	Nyira 2016	Nyira 2016
	12NY16C1MEL1B	13NY16C1MEL1C	15NY16C1MEL2A	10NY16C2MEL3A	11NY16C2MEL3B	12NY16C2MEL4A	16NY16C3MEL5A	06NY16MEL2A	18NY16C5CPX1A	19NY16C5CPX1B
	mel	mel	mel	mel	mel	mel	mel	mel	cpx	cpx
Li	4.94	1.69	0.70	1.53	0.57	1.91	4.21	1.31	0.45	0.43
B	31.16	36.97	42.18		21.37	25.59	6.86		14.86	4.99
Mg	7.25	7.52	7.18	7.71	7.77	7.45	7.30	7.44	11.48	11.28
Si	44.66	46.60	46.66	42.12	44.46	42.54	44.53	41.99	48.60	45.83
Ca	35.90	35.90	34.84	35.91	35.91	34.59	34.62	34.84	23.41	23.41
Sc		3.42	2.78	1.37	2.51	1.46	1.92	<0.80	24.00	22.65
Ti	0.21		0.24	0.97	0.26	0.30	0.29	0.06	1.64	1.92
V	31.70	70.25	30.86	153.06	32.47	49.48	33.65	9.84	199.58	219.86
Cr		9.48	3.55	5.54				7.02		6.45
Co	47.83	50.14	42.39	56.69	43.66	45.40	42.51	46.50	40.46	35.99
Ni	15.01	14.95	12.43	35.29	19.73	17.33	12.66	10.72	27.79	39.51
Zn	396.47	342.51	313.03	314.08	299.18	272.94	283.79	321.65	42.53	40.54
Rb	1.55	17.88	1.08	1.09	1.09	5.15	12.22	0.18	0.48	1.20
Sr	5093.95	5215.28	5007.42	4938.97	5054.81	4782.91	5019.48	4916.27	1212.97	841.59
Y	8.61	13.06	11.10	8.30	6.89	7.69	10.91	7.04	25.30	28.63
Zr	4.19	24.69	6.40	2.38	3.97	3.97	27.12	0.15	336.15	348.54
Nb	3.07		9.02	3.44	0.95	2.43	21.77	0.18	6.65	6.85
Cs							0.08			
Ba	118.05		194.14	113.56	103.28	112.80	278.77	96.52	11.65	28.96
La	93.04	113.15	99.35	90.37	79.53	85.41	106.82	77.32	60.10	86.69
Ce	169.96	199.89	176.58	176.71	146.66	158.19	192.11	147.81	139.41	182.12
Pr	17.33	20.82	19.26	20.13	17.01	16.67	20.90	15.98	17.47	21.76
Nd	66.04	76.25	73.88	69.46	64.15	62.25	81.21	56.10	73.48	91.93
Sm	7.67	8.42	7.85	11.49	10.96	8.52	9.64	7.03	11.77	16.38
Eu	3.24	3.59	3.15	2.75	1.88	2.85	2.81	1.76	3.78	4.81
Gd	4.87	5.58	5.77	6.64	4.72	4.62	5.67	3.89	8.04	12.91
Tb	0.50	0.64	0.58	0.37	0.38	0.53	0.49	0.45	1.25	1.47
Dy	2.00	4.17	3.42	1.73	1.69	1.51	2.63	1.98	5.50	6.96
Ho	0.35	0.63	0.58	0.32	0.26	0.28	0.47	0.33	1.08	1.38
Er	0.70	1.12	1.12			0.75	0.68	2.35	2.70	2.70
Tm	0.08	0.00				0.10		0.07	0.32	0.40
Yb		1.37	1.22	0.81		0.66			2.00	2.52
Lu	0.12								0.30	0.37
Hf	0.28		0.42	0.18			0.28		6.50	7.56
Ta	0.20		0.57	0.30	0.07	0.19	1.03		1.16	1.40
Pb	1.15	1.50	1.47	0.29	0.45	0.40	1.11	1.17		0.93
Th	1.19		1.87	1.22	0.58	1.08	2.95	0.17	1.18	2.45
U	0.34		0.20	0.74	0.30	0.26	0.78		0.30	0.73

Leucites and nephelines trace elements (LA-ICPMS):

Sample name	M2002 GL 07NY02C2LEU1A lc	M2002 GL 08NY02C2LEU1B lc	M2002 GL 09NY02C2LEU1C lc	Nyira 2016 <NY16C1LEU1> lc	M2002 GL 16NY02C1LEU2A lc	M2002 GL 17NY02C1LEU2B lc	M2002 GL 20NY02C1LEU3A lc	M2002 GL 21NY02C1LEU3B lc	M2002 GL 04NY02C2NEF1A ne	M2002 GL 05NY02C2NEF2A ne	M2002 GL 06NY02C2NEF1B ne
Li				0.69							0.37
B		7.04	15.36	64.14	3.36			1.26	38.16	12.87	35.89
Mg	0.01	0.06	0.03	0.08	46.60	21.55	54.47	10.28	0.19	0.15	0.19
Si	53.69	53.69	53.69	54.05	0.02	0.02	0.02	0.01	37.20	41.76	41.76
Ca		0.17	0.19	0.26	53.69	53.69	53.57	53.57	1.13	1.23	1.26
Sc	1.1	1.23	1.74	1.64	0.11	0.06			4.78	0.79	2.18
Ti	0.223	0.258	0.190	0.298	4.33		1.49	1.70	0.09	0.09	0.09
V	1.18	13.23	1.57	18.82	0.17	0.18	0.19	0.17	1.74	1.18	1.85
Cr				5.74	3.02	3.38	2.36	1.13	20.88	4.24	
Co		1.38	0.15	1.95		5.70		3.91	0.56	1.5	1.61
Ni		1.55	0.57	3.38				0.55			
Zn		19.29	2.28	8.935		0.86		1.66	28.15	23.48	17.41
Rb	1408.16	1208.17	1301.47	1584.04		8.43	8.45		88.6	95.77	101.27
Sr	48.28	49.84	41.98	74.15	1258.6	1173.70	1324.99	1204.66	705.95	801.64	828.63
Y	0.31	0.149	0.412	0.54	45.4	36.3	38.4	36.1	0.095	0.04	0.416
Zr	1.01	2.17	1.07	2.115	0.49	0.19	0.18	0.38		0.4	
Nb	0.29	0.156	0.302	1.0655	1.18	1.85	0.77	1.60	0.26	0.314	0.134
Cs	26.04	24.3	24.25	37.325	0.71	1.76	0.12	0.11	0.3	0.058	0.309
Ba	3535.93	3077.16	2692.09	2398.465	22.9	23.1	27.4	20.5	242.79	260.73	291.0
La	0.17	0.29	2.87	3.495	1918.40	1905.84	2717.11	2593.04		0.214	
Ce		0.26	2.75	7.195	0.29	1.21		0.08		0.64	
Pr	0.23		0.34	0.97	0.92	2.27	0.07	0.40		0.05	
Nd			1.85	3.56		0.11	0.07	0.04			
Sm		0.21	0.61	0.68		0.72					
Eu		0.06	0.06	0.35				0.63			0.143
Gd		0.18	0.37	0.23		0.17					
Tb				0.03		0.32		0.62			
Dy		0.47	0.09	0.21							
Ho			0.03	0.03							
Er				0.09							
Tm	0.07				0.33	0.23					
Yb	0.42										
Lu											
Hf		0.17			0.07	0.04					
Ta	0.20	0.43	0.13	0.43	0.79					0.07	0.08
Pb	1.29	0.32	0.07	0.12	0.40	0.33		0.22	0.38		0.17
Th		0.04	0.13	0.27							0.12
U	0.11		0.38	0.07		0.05	0.74	0.17		0.06	

Sample name	M2002 GL 06NY02C2NEF2C ne	M2002 GL 07NY02C2NEF3A ne	M2002 GL 22NY02C1NEF4A ne	M2002 GL 23NY02C1NEF4B ne	M2002 GL 24NY02C1NEF5B ne	M2002 GL 25NY02C1NEF6A ne	M2002 GL 33NY02C3NEF7A ne	Nyira 2016 17NY16C3NEF1A ne	Nyira 2016 20NY16C4NEF2A ne	Nyira 2016 21NY16C4NEF2B ne
Li			2.13	0.58	2.3		1.68	1.38	2.31	1.91
B	0.56	36			16.97	39.45		14.18	25.99	24.37
Mg	42.05	0.04	0.17	0.18	0.01	0.18	0.33	0.12	0.11	0.12
Si	0.03	40.98	41.43	41.43	53.69	42.10	40.98	41.04	41.29	41.29
Ca	40.98	0.23	1.01	1.30	0.10	0.95	1.34	1.08	1.09	1.06
Sc	0.08	2.45	2.83	3.45	3.42	1.76		1.21	1.16	1.045
Ti	1.63	0.15	0.09	0.09	0.21	0.07	0.08	0.03	0.05	0.05
V	0.13	3.41	1.91	2.09	1.77	1.49	1.19	0.82	1.17	0.59
Cr	1.33					5.86		2.85	2.66	
Co		0.12	0.84	1.84	0.18	1.05	0.61	0.90	0.60	0.81
Ni	0.40	0.33					1.05	2.41	0.53	
Zn		13.05		6.33	4.68	9.95	22.87	5.5	2.93	2.75
Rb		988.61	116.28	100.35	1367.34	102.85	95.22	139.17	149.38	142.73
Sr	926.04	114.24	829.19	720.31	46.17	711.47	599.97	787.05	773.78	751.52
Y	30.0	0.54		0.075	0.09	0.26	0.067	0.112		
Zr		2.47	1.36	0.25		0.15	2.27	2.19	0.14	
Nb	1.14	0.49	0.27	0.41	0.246		0.356	1.149	0.03	0.02
Cs	0.20	21.4	0.128	0.277	26.08	0.277	0.19	0.18	0.33	0.42
Ba	14.6	2212.46	273.77	265.49	3136.84	246.48	240.12	282.66	304.89	295.75
La	2098.93	5.31	1.65	2.08	0.72	2.38	0.979	0.27		
Ce	0.13	20.98	1.77	2.54	1.12	1.48	14.67	0.73		
Pr	0.39	1.02	0.31	0.7	0.05	0.372	0.131	0.06		
Nd	0.08	1.17	0.83	0.5	0.28	2.45	0.2	0.23		
Sm		1.56	0.94	0.33	0.83		0.26	0.09		
Eu		0.17		0.34	0.32			0.11		
Gd				0.93			0.212	0.08		
Tb	0.23			0.121						
Dy		0.2				0.26	0.281			
Ho		0.05			0.04		0.059			
Er				0.52						
Tm	0.32		0.083							
Yb					0.34		0.49			
Lu										
Hf		0.17		0.53			0.31			0.03
Ta	0.28	0.142		0.18	0.35	0.07	0.08	0.08		0.02
Pb	0.16	0.12		0.30	0.36			0.08		0.16
Th	0.46	0.56		0.23	0.12		0.14	0.17	0.01	0.02
U	0.13	0.20				0.06				

Apatites and magnetites trace elements (LA-ICPMS):

Sample name	M2002 GL	Nyira 2016	M2002 GL	M2002 GL	Nyira 2016	Nyira 2016	Nyira 2016	Nyira 2016
	32NY02C3AP3C	08NY16C1AP1A	35NY02C3MAG2A	36NY02C3MAG3A	05NY16C2MAG2A	06NY16C2MAG2B	07NY16C2MAG2C	14NY16C3MAG3A
	ap	ap	mag	mag	mag	mag	mag	mag
Li			1.68	2.83	1.65	1.08	0.85	2.37
B		16.6	8.82	14.76	13.47	16.41	8.39	9.14
Mg	0.14	0.21	5.87	5.93	7.40	7.37	7.43	6.85
Si	1.79	0.89	0.41	1.47	0.25	0.33	0.28	0.24
Ca	53.29	55.72	0.15	0.29	0.07	0.18	0.08	0.06
Sc			7.10	8.49	8.70	9.03	8.63	7.13
Ti	0.00	0.13	15.38	15.38	18.25	18.25	18.25	17.04
V	156.92	192.91	2077.04	2058.19	3389.12	3428.08	3358.40	3182.63
Cr		4.80	44.60	45.73	365.67	385.31	353.62	398.21
Co		2.39	279.59	277.50	350.61	357.77	353.80	333.82
Ni	4.47	4.24	320.33	326.29	689.14	717.69	687.19	650.86
Zn	21.58	20.58	476.88	582.68	688.65	688.61	714.30	654.93
Rb		0.277	0.31	0.98		0.06	0.031	
Sr	4963.33	5967.69	18.96	18.96	0.33	14.24	1.81	0.17
Y	132.10	164.21	0.23	0.59	0.20	0.61	0.24	0.23
Zr	11.06	14.83	87.54	96.31	81.99	83.35	81.02	71.92
Nb	0.31	1.19	42.89	45.61	51.82	51.87	50.61	47.99
Cs				0.07				
Ba	97.38	126.06	71.33	106.00	0.03	2.94	0.10	0.05
La	1046.58	1304.25	1.47	1.31	0.01	2.57	0.40	0.04
Ce	2000.03	2373.54	2.17	2.33	0.15	5.25	0.89	0.15
Pr	199.19	259.97	0.28	0.22	0.01	0.61	0.09	0.02
Nd	804.78	986.68	0.41	1.13	0.06	2.60	0.19	
Sm	114.81	135.89	0.10			0.53	0.21	0.08
Eu	28.53	35.58	0.07		0.01		0.05	
Gd	78.11	86.93			0.07	0.46	0.09	
Tb	6.59	9.39	0.01		0.01	0.06	0.02	0.02
Dy	30.00	37.07		0.14	0.05	0.15	0.08	0.13
Ho	4.38	6.30	0.01	0.06	0.01	0.02	0.01	0.02
Er	9.92	12.85				0.22		
Tm	1.02	1.28			0.01	0.03	0.01	0.01
Yb	5.09	6.92	0.46					
Lu	0.65	0.74	0.03	0.06	0.01			
Hf	0.51	0.07	0.96	1.13	1.73	1.93	1.35	1.65
Ta		0.11	4.04	3.57	4.64	4.76	4.79	4.56
Pb	1.53	0.23	0.24	1.38	0.11	0.66		
Th	29.07	40.99	0.26	0.12	0.01	0.18		
U	6.77	7.87	0.07	0.19		0.05	0.03	0.00

Next page: glasses trace elements (LAICPMS) of 2002 and 2016 Nyiragongo samples.

Sample Rock	M2002 GL 12NY02C2GL1A	M2002 GL 13NY02C2GL1B	M2002 GL 16NY02C2GL1C	M2002 GL 08NY02C2GL2	M2002 GL 27NY02C1GL3A	M2002 GL 37NY02C3GL4A	Nyira 2016 05NY16C1GL1A	Nyira 2016 06NY16C1GL2A	Nyira 2016 09NY16C1GL2B	Nyira 2016 10NY16C1GL3A	Nyira 2016 18NY16C1QL4A	Nyira 2016 08NY16C2QL5A	Nyira 2016 09NY16C2QL5B	Nyira 2016 15NY16C3GL	Nyira 2016 22NY16C4GL7A	Nyira 2016 23NY16C5GL8A	M2002 GL 38NY02C3GL5A	Nyira 2016 05NY16C6GL1A	Nyira 2016 07NY16C6GL3A	average
Li	16.42	16.92	16.78	12.31	18.61	13.74	12.92	13.26	12.41	14.02	13.55	13.71	14.00	13.04	13.41	16.06	16.83	10.00	13.41	14.33
B	18.33	16.09	12.43	34.06	27.41	18.11	61.90	55.24	55.16	54.75	49.96	21.87	27.75	24.03	26.91	23.88	31.08	10.18	30.39	31.67
MgO	3.38	3.10	3.33	3.03	3.35	3.07	3.34	3.56	3.43	3.43	3.43	3.59	3.56	3.50	3.70	3.65	3.08	3.29	3.32	3.37
SiO ₂	40.99	36.33	40.96	34.79	38.18	36.47	37.78	39.70	37.95	38.39	38.39	38.66	38.64	38.34	40.72	40.12	35.11	36.00	36.00	38.26
CaO	11.16	10.71	11.20	10.62	11.26	10.71	11.25	11.82	11.18	11.25	11.12	11.22	11.48	11.17	12.53	10.81	10.71	10.81	10.18	11.46
Sc	6.51	6.06	6.04	6.54	6.11	5.73	6.51	6.83	6.41	6.74	5.94	5.81	5.36	5.73	5.73	5.81	6.12	5.86	5.22	5.86
TiO ₂	2.70	2.49	2.58	2.45	2.61	2.49	2.51	2.63	2.47	2.65	2.42	2.57	2.55	2.46	2.54	2.53	2.33	2.29	2.35	2.51
V	231.02	213.18	223.22	212.74	236.25	207.39	239.79	251.73	242.81	238.13	238.13	268.69	258.62	236.66	248.74	237.20	204.77	221.51	222.43	234.61
Cr	3.73	<1.28	1.38	5.59	2.20	1.62	5.33	3.18	3.62	1.93	5.30	7.47	5.15	2.90	3.16	5.32	3.57	41.73	36.39	3.84
Co	37.69	35.21	36.93	35.50	38.74	36.53	40.49	47.15	38.92	47.56	39.35	42.25	42.54	38.75	41.05	41.20	33.95	41.73	38.53	39.53
Ni	9.61	8.79	7.90	10.02	7.22	10.30	14.56	14.66	16.25	15.45	13.59	22.25	19.89	15.15	16.33	16.33	6.59	13.50	16.74	13.19
Zn	222.36	180.08	171.89	190.97	160.99	146.51	209.75	225.04	211.25	231.98	162.44	155.83	150.59	147.57	148.90	155.62	152.56	207.45	158.37	179.54
Rb	112.39	104.46	118.12	110.05	115.79	97.59	147.57	153.56	143.62	151.63	138.99	139.26	139.61	138.99	144.58	145.86	104.84	136.83	136.81	130.55
Sr	2920.69	2723.28	2807.58	2776.40	2928.72	2636.08	2721.10	2890.20	2731.68	2758.19	2609.89	2629.36	2696.94	2605.04	2831.46	2652.69	2633.94	2598.84	2484.40	2730.67
Y	43.06	42.66	42.28	42.45	43.92	40.33	38.14	39.93	37.15	42.40	36.52	36.88	36.75	37.15	40.12	37.78	41.01	36.25	34.29	39.71
Zr	414.04	385.31	403.95	396.37	413.95	367.60	346.09	369.08	344.52	360.72	325.30	325.09	333.28	330.35	335.53	333.32	377.33	316.85	326.12	359.93
Nb	322.35	297.40	308.90	288.66	318.67	294.73	282.61	286.45	286.13	288.54	247.35	250.18	251.38	245.41	257.97	253.00	281.05	242.93	243.64	274.88
Cs	0.97	0.84	0.93	0.78	0.96	0.95	1.66	1.54	1.40	1.71	1.48	1.56	1.48	1.49	1.60	1.58	0.79	1.91	1.34	1.31
Ba	2890.89	2664.70	2791.19	2687.34	2828.56	2580.23	2451.03	2607.50	2459.56	2571.97	2298.15	2360.52	2394.32	2337.21	2403.33	2363.80	2516.17	2287.82	2308.02	2523.41
La	233.01	225.99	219.68	225.40	222.88	208.41	219.30	210.54	211.42	199.07	197.06	197.06	203.03	196.83	226.56	199.78	223.21	194.39	192.29	213.69
Ce	402.84	394.11	386.25	400.33	394.88	400.64	384.01	385.95	362.24	345.45	357.01	350.43	357.80	350.43	408.31	355.15	390.41	382.00	336.79	377.29
Pr	38.95	40.00	37.47	40.87	39.39	37.34	36.48	39.06	35.75	36.37	35.03	34.88	36.00	34.88	40.35	34.99	39.72	33.96	31.94	37.27
Nd	137.44	141.27	135.81	135.91	145.30	134.92	125.85	137.89	131.46	130.01	122.19	121.93	128.29	125.61	146.58	121.45	136.18	121.88	113.83	132.22
Sm	21.18	21.39	19.85	21.71	21.10	19.24	17.31	17.90	18.45	19.31	18.15	17.13	17.67	17.66	21.54	18.79	21.84	16.55	18.07	19.28
Eu	6.03	5.97	6.16	6.10	6.15	4.92	5.34	5.65	5.19	4.83	4.94	4.87	5.46	4.87	5.89	4.79	5.86	4.95	4.29	5.49
Gd	15.84	14.87	14.25	14.63	13.26	10.70	11.89	14.27	12.23	13.49	11.50	10.96	12.46	12.46	13.37	12.97	11.78	11.86	11.00	12.90
Tb	1.60	1.74	1.97	1.75	1.77	1.60	1.68	1.61	1.78	1.61	1.63	1.57	1.58	1.64	1.81	1.54	1.55	1.50	1.66	1.66
Dy	9.67	8.65	7.85	9.94	10.08	8.63	8.12	9.37	8.61	9.45	7.99	7.42	7.87	7.63	9.64	8.35	9.99	9.63	8.00	8.88
Ho	1.52	1.79	1.60	1.52	1.85	1.55	1.62	1.65	1.62	1.61	1.56	1.60	1.45	1.39	1.73	1.45	1.73	1.30	1.40	1.59
Er	3.30	3.66	4.20	3.70	4.10	3.66	4.00	3.90	3.83	3.80	4.15	4.29	3.87	3.30	3.89	3.84	3.61	3.60	3.61	3.84
Tm	0.58	0.62	0.65	0.51	0.58	0.58	0.47	0.49	0.53	0.50	0.51	0.42	0.44	0.47	0.63	0.44	0.57	0.58	0.53	0.53
Yb	3.20	3.60	2.83	3.35	3.55	3.93	3.31	2.94	3.36	3.30	3.31	3.18	2.85	3.11	3.65	3.42	3.73	3.70	3.14	3.35
Lu	0.48	0.49	0.36	0.56	0.49	0.49	0.45	0.41	0.36	0.40	0.42	0.40	0.46	0.50	0.54	0.39	0.54	0.52	0.50	0.46
Hf	5.22	4.68	5.88	5.41	5.40	5.46	5.32	4.96	4.73	4.15	4.51	4.05	4.53	4.73	4.93	4.63	5.40	3.94	3.42	4.86
Ta	16.70	16.09	16.90	15.22	17.53	16.02	13.46	14.37	12.90	14.19	12.74	12.84	13.33	12.91	13.86	12.98	15.82	12.53	13.02	14.47
Pb	6.52	5.80	6.84	6.02	6.00	6.66	4.74	5.88	5.52	5.95	4.54	4.86	4.96	4.66	5.18	5.16	6.05	4.02	3.50	5.54
Th	28.45	27.85	26.88	26.88	24.11	23.38	22.82	24.11	23.38	23.62	23.09	24.29	23.36	23.82	25.23	23.50	25.93	23.63	24.52	24.84
U	13.32	12.54	12.97	12.77	12.33	12.35	9.25	10.17	9.86	9.97	10.02	10.02	9.69	9.60	10.57	10.10	11.59	7.77	8.91	10.82

References

- Andersen T., Eldburg M., Erambert M. (2012). Petrology of combeite- and gotzenite-bearing nephelinite at Nyiragongo, Virunga Volcanic Province in the East African Rift. *Lithos* 152, 105-121.
- Andersen T., Eldburg M., Erambert M. (2014). Extreme peralkalinity in delhayelite- and adremeyerite-bearing nephelinite from Nyiragongo volcano, East African Rift. *Lithos* 206-207, 164-178.
- Aoki, K.-I., Yoshida, T. (1983). Petrological and geochemical studies on the 1981– 1982 lava from Nyamuragira volcano. In: Hamaguchi, H. (Ed.), *Volcanoes Nyiragongo and Nyamuragira: Geophysical Aspects*. The Faculty of Science, Tôhoku University, Sendai, Japan, 91–96.
- Avanzinelli R., Boari E., Conticelli S., Francalanci L., Guarnieri L., Perini G., Petrone C.M., Tommasini S., Ulivi M. (2005). High precision Sr, Nd, and Pb isotopic analyses using the new generation Thermal Ionisation Mass Spectrometer ThermoFinnigan Triton-Ti®. *Periodico di Mineralogia* 75, 147-166.
- Barette F., Poppe S., Smets B., Benbakkar M., Kervyn M. (2016). Spatial variation of volcanic rock geochemistry in the Virunga Volcanic Province: Statistical analysis of an integrated database. *Journal of African Earth Sciences* 30, 1-16.
- Barker DS, Nixon PH* (1989) High-Ca, low-alkali carbonatite volcanism at Fort Portal, Uganda. *Contrib Mineral Petrol* 103: 166–177
- Baxter P., Allard P., Halbwachs M., Komorowski C. J., Woods A., Ancia A. (2002). Human health and vulnerability in the Nyiragongo volcano eruption and humanitarian crisis at goma, democratic republic of Congo. Human health and vulnerability in the Nyiragongo Volcano eruption. *Acta Vulcanologica*, 14, 109-114.
- Bell K. and Blenkinsop J. (1987) Nd and Sr isotopic compositions of East African carbonatites: implications for mantle heterogeneity. *Geology* 15, 99–102.
- Bell K. and Simonetti A.(1996). Carbonatite magmatism and plume activity: implications from the Nd, Pb and Sr isotope systematics of Oldoinyo Lengai. *J. Petrol.* 37, 1321–1339.
- Bultitude R.J. & Green D.H. (1968) Experimental study at high pressures on the origin of olivine nephelinite and olivine melilite nephelinite magmas. *Earth and Planet Sci Lett.* 3-325-337

- Bell K & Powell J. L (1969) Strontium Isotopic Studies of alkalic rocks:the potassium rich lavas of the Birunga and Toro-Ankole Regions, East and central Equatorial Africa *Journal of Petrology*, 10, 3, 536–572
- Brey G., Green D.H. (1975) The role of CO₂ in the genesis of olivine melilitite *Contrib.Mineral Petrol* 49. 93-103
- Brey G, Green D.H.(1977) Systematic study of liquidus phase relations in olivine melilitite +H₂O+CO₂ at high pressures and petrogenesis of an olivine melilitite magma. *Contrib. Mineral. Petrol*, 61. 141-162
- Brey G. Origin of olivine melilitites—chemical and experimental constraints, *Journal of Volcanology and Geothermal Research* 1978, vol. 3 (pg. 61-88)
- Bultitude, R. J. & Green, D. H., 1968. Experimental study at high pressures on the origin of olivine nephelinite and olivine melilitite nephelinite magmas. *Earth and Planetary Science Letters* 3, 325-337.
- Burton, M. R., G. M. Sawyer, and D. Granieri (2013), Deep carbon emissions from volcanoes, *Rev. Mineral. Geochem.*, **75**, 323–354.
- Callebaut, K., Elsen, J., Van Balen, K., & Viaene, W. (2001). Nineteenth century hydraulic restoration mortars in the Saint Michael's Church (Leuven, Belgium): Natural hydraulic lime or cement?. *Cement and Concrete Research*, 31(3), 397-403.
- Campion R., (2014) . New lava lake at Nyamuragira volcano revealed by combined ASTER and OMI SO₂ measurements. *Geophys. Res. Lett.*, 41 (2014), pp. 7485-7492.
- Capaccioni B., Vaselli O., Santo A P., Yalire M.M. (2002). Monogenic and polygenic volcanoes in the area between the Nyiragongo summit crater and the lake Kivu shoreline. *Acta Vulcanologica*, 14, 129-136.
- Capaccioni B., Vaselli O., Santo A. P. and Yalire M. M. (2003). Monogenic and polygenic volcanoes in the area between the Nyiragongo summit crater and the Kivu shoreline. *Acta Vulcanol.*, 1-2, 129-136.
- Carn S. A. (2003). Eruptive and passive degassing of sulphur dioxide at nyiragongo volcano (d. r. congo): the 17 january 2002 eruption and its aftermath. *Acta Vulcanologica*, 14, 75-86.
- Chakrabarti, R., Basu, A.R., Santo, A.P., Tedesco, D., Vaselli, O., 2009a. Isotopic and geochemical evidence for a heterogeneous mantle plume origin of the Virunga volcanics, Western rift, East African Rift system. *Chem. Geol.* 259, 273-289.

- Chakrabarti, R., Sims, K.W.W., Basu, A.R., Reagan, M., Durieux, J., 2009b. Timescales of magmatic processes and eruption ages of the Nyiragongo volcanics from ^{238}U - ^{230}Th - ^{226}Ra - ^{210}Pb disequilibria. *Earth Planet. Sci. Lett.* 288, 149-157.
- Chu D. Gordon R.G., 199. Evidence for motion between Nubia and Somolia along the Southwest Indian Ridge, *Nature*, 398, 64-67.
- Condomines M, Tanguy JC, Kieffer G, Allègre CJ (1982) Magmatic evolution of a volcano studied by ^{230}Th - ^{238}U -disequilibrium and trace elements systematics: the Etna case. *Geochim Cosmochim Acta* 46:1397-1416
- Condomines M, Tanguy JC, Michaud V (1995) Magma dynamics at Mt Etna: constraints from U-Th-Ra-Pb radioactive disequilibria and Sr isotopes in historical lavas. *Earth Planet Sci Lett* 132:25-41
- Condomines M., Carpentier M., Ongendangen T (2015). Extreme radium deficit in the 1957 A.D. Mugogo lava (Virunga volcanic field, Africa): its bearing on olivine-melilitite genesis. *Contrib Mineral Petrol.* 169:29, 2-19.
- Corti G., Bonini M., Innocenti F., Manetti P., Mulugeta G., Sokoutis D., Cloetingh S. (2003). Rift-parallel magma migration and localisation of magmatic activity in transfer zones. *Acta Vulcanologica*, 14, 17-26.
- Chorowicz J. (2005). The East African rift system. *Journal of African Earth Sciences* 43, 379-410
- Clague D.A. & Frey F.A. (1982). Petrology and trace element geochemistry of the Honolulu volcanics, Oahu: implications for the oceanic mantle below Hawaii. *Journal of Petrology*, v. 23, 3, p. 447-504, 1982.
- Collerson K.D., Williams, A.E., Ewart, D.T., Murphy Origin of HIMU and EM-1 domains sampled by ocean island basalts, kimberlites and carbonatites: the role of CO_2 -fluxed lower mantle melting in thermochemical upwellings. *Physics of the Earth and Planetary Interiors*, 181 (1) (2010), pp. 112-131
- Corti G., Bonini M., Innocenti F., Manetti P., Mulugeta G., Sokoutis D., Cloetingh S. (2002). Rift-parallel magma migration and localisation of magmatic activity in transfer zones. *Acta Vulcanologica*, 14, 1-9.
- Cox, K.G., 1980. A model for flood basalt vulcanism. *Journal of Petrology* 21, 629-650.

- Dalton, J. A., & Wood, B. J. (1993). The compositions of primary carbonate melts and their evolution through wallrock reaction in the mantle. *Earth and Planetary Science Letters*, 119(4), 511-525.
- Dawson, J., Smith, J., 1988. Metasomatised and veined upper-mantle xenoliths from Pello Hill, Tanzania: evidence for anomalously-light mantle beneath the Tanzanian sector of the East Africa Rift Valley. *Contrib. Mineral. Petrol.* 100, 510–527.
- Demant A., Lestrade P., Ruananza T.L, Kampunzu A.B., Durieux J. (1994), Volcanological and petrological evolution of Nyiragongo volcano, Virunga volcanic field, Zaire, *Bull. Volcanol.*, 56, 47– 61.
- Durieux J. (2002). Volcano nyiragongo (d. r. congo): evolution of then crater and lava lakes from the discovery to the present. *Acta Vulcanologica*, 14, 137-144.
- Ebinger, C.J. (1989). Tectonic development of the western branch of the East African rift system. *Bull. Geol. Soc. Am.* 101, 885-903.
- Ebinger C. and Furman T. (2003). Geodynamical setting of the Virunga volcanic province, East Africa. *Acta Vulcanologica*, 14, 9-16.
- Eggler, D.H., Kushiro, I. and Holloway, J.R., 1976. Stability of carbonate minerals in a hydrous mantle. *Annu. Rep. Dir. Geophys. Lab., Washington*, 75: 631---636.
- Ewart A., Chappell B.W., Menzies M.A. (1988). An overview of the geochemical and isotopic characteristics of the Eastern Australian Cainozoic volcanic provinces. *Journal of Petrology*, special Lithosphere issue 225-273.
- Foley, S.F., 2007. Volcanoes and volcanic sources in the East African rift. *Proc. Belgian Acad. Sci.* 43–55.
- Foley, S., 2008. Rejuvenation and erosion of the cratonic lithosphere. *Nat. Geosci.* 1, 503–510.
- Foley, S. F. et al. The composition of near-solidus melts of peridotite in the presence of CO₂ and H₂O at 40–60 kbar. *Lithos* 112S, 274–283 (2009).
- Foley, S. F., Link, K., Tiberindwa, J. V. & Barifaijo, E. Patterns and origin of igneous activity around the Tanzanian craton. *J. Afr. Earth Sci.* 62, 1–18 (2012).
- Foley S. F. Fischer T.P. 2017. An essential role for continental rifts and lithosphere in the deep carbon cycle. *Nature Geosc* 10, 897-902

- Franzini, M., Leoni, L., & Saitta, M. (1975). Revisione di una metodologia analitica per fluorescenza-X, basata sulla correzione completa degli effetti di matrice. *Rend. Soc. Ital. Mineral. Petrol.*, 31(2), 365-378.
- Fraser, K.J, Hawkesworth, C.J., Erlank, A.J., Mitchell, R.H. and Scott-Smith, B.H., 1986. Sr, Nd and Pb isotope and minor element geochemistry of lamproites and kimberlites. *Earth Planet. Sci. Lett.*, 76: 57-70.
- Frey, F. A., Green, D. H., & Roy, S. D. (1978). Integrated models of basalt petrogenesis: a study of quartz tholeiites to olivine melilitites from south eastern Australia utilizing geochemical and experimental petrological data. *Journal of petrology*, 19(3), 463-513.
- Furman 1995 Furman, T., 1995. Melting of metasomatized subcontinental lithosphere undersaturated mafic lavas from Rungwe, Tanzania. *Contrib. Mineral. Petrol.* 122, 97–115.
- Furman 1999 Furman, T., Graham, D., 1999. Erosion of lithospheric mantle beneath the East African Rift system: geochemical evidence from the Kivu volcanic province. *Lithos* 48, 237–262.
- Furman T. (2007). Geochemistry of East African Rift basalts: An overview. *Jour. Afric Earth Scien.* 48, 147-160.
- Green, D.H., Falloon, T.J., 1998. Pyrolite: a ringwood concept and its current expression. In: Jackson, I. (Ed.), *The Earth's Mantle*. Cambridge University Press, Cambridge, pp. 311–378.
- Green et 2015 Green D. H. (2015) Experimental petrology of peridotites, including effects of water and carbon on melting in the Earth's upper mantle. *Phys. Chem. Miner.* 42, 95–122.
- Gregoire, M., Bell, D. R. & le Roex, A. P. (2003). Garnet lherzolites from the Kaapvaal Craton (South Africa): trace element evidence for a metasomatic history. *Journal of Petrology* 44, 629–657.
- Gudfinnsson, G. H. & Presnall, D. C. Continuous gradations among primary carbonatitic, kimberlitic, melilititic, basaltic, picritic and komatiitic melts in equilibrium with garnet lherzolite at 3–8 GPa. *J. Petrol.* 46, 1645–1659 (2005).
- Herzberg C. and Asimow P. D. (2008) Petrology of some oceanic island basalts: PRIMELT2.xls software for primary magma calculation. *Geochim. Geophys. Geosyst.* 9, Q09001.

- HOLMES, A., and H. F. HARWOOD: Petrology of the volcanic fields east and southeast of Ruwenzori, Uganda. *Quart. J. Geol. Soc. London* **88**, 370–442 (1932).
- Irvine T.N. & Baragar W.R.A. (1971). A guide to the chemical classification of the common volcanic rocks. *Canadian Journal of Earth Sciences*, 8, 523, 548.
- Janse, A.J.A., Sheahan, P.A., 1995. Catalog of world wide diamond and kimberlite occurrences – a selective and annotative approach. *Journal of Geochemical Exploration* 53, 73–111.
- Kavotha S. K., Mavonga T., Durieux J., Mukambilwa K. (2003). Towards a more detailed seismic picture of the January 17th, 2002 Nyiragongo eruption. *Acta Vulcanologica*, 14, 87-100.
- Keller, J., Zaitsev, A.N., Wiedenmann, D., 2006. Primary magmas at Oldoinyo Lengai: the role of olivine melilitites. *Lithos* 91, 150–172
- Kerr et al., 1997 Kerr, A.C., Tarney, J., Marriner, G.F., Nivia, A., Saunders, A.D., 1997. The Caribbean-Colombian Cretaceous igneous province: the internal anatomy of an oceanic plateau. In: Mahoney, J.J., Coffin, M.F. (Eds.), *Large Igneous Provinces, Geophysical Monograph* 100. American Geophysical Union, Washington, pp. 123–144.
- Komorowski J-C, Tedesco D. Kasereka M., Allard P. Papale P., Vaselli O., Durieux J., Baxter P., Halbwachs M., Akumbe M., Baluku B., Briole P., Ciraba M., Dupin J-C., Etoy O., Garcin D., Hamaguchi H., Houlié N., Kavotha K. S., Lemarchand A., Lockwood J., Lukaya N., Mavonga G., de Michele M., Mpore S., Mukambilwa K., Munyololo F., Newhal C., Ruch J. Yalire M., Wafula. M. (2003). The January 2002 flank eruption of Nyiragongo volcano (Democratic Republic of Congo): chronology, evidence for a tectonic rift trigger, and impact of lava flows on the city of Goma. *Acta Vulcanologica*, 14, 27-62.
- Le Bas, M.J., 1987. Nephelinites and carbonatites. In: Fitton, J.G., Upton, B.G.J. (Eds.), *Alkaline Igneous Rocks: Geological Society of London, Special Publication.*, 30, 53-83.
- Le Bas M.J.; LeMaitre R.W.; Streckeisen A. and Zanettin B., «A chemical classification of volcanic rocks based on the total alkali-silica diagram». *Journal of Petrology*, v. 27, p. 745, 750p, 1986
- Le Maitre R.W., Bateman P., Dudek A., Keller J., Lameyre J., Le Bas M.J., Sabine P.A., Schmid R., Sorensen H., Streckeisen A., Woolley A.R., Zanettin B. (1989). *A Classification of Igneous Rocks and Glossary of Terms: Recommendations of the International Union of Geological Sciences Subcommission - Systematics of Igneous Rocks*. Blackwell, Oxford. Onuma N.
- Le Roex, A. P., D. R. Bell, and P. Davis (2003), Petrogenesis of Group 1 kimberlites from Kimberley, South Africa: Evidence from bulk-rock geochemistry, *J. Petrol.*, **44**, 2261–2286.

- Leoni, L., & Saitta, M. (1976). X-ray fluorescence analysis of 29 trace elements in rock and mineral standards. *Rend. Soc. Ital. Mineral. Petrol.*, 32(2), 497-510.
- Mallik A. and Dasgupta R. (2013) Reactive infiltration of MORB eclogite- derived carbonated silicate melt into fertile peridotite at 3 GPa and genesis of alkaline magmas. *J. Petrol.* 54, 2267–2300.
- Mallik A. and Dasgupta R. (2014) Effect of variable CO₂ on eclogite-derived andesite and lherzolite reaction at 3 GPa – implications for mantle source characteristics of alkalic ocean island basalts. *Geochem. Geophys. Geosyst.* 15, doi 1.1002/ 2014GC005251.
- McKenzie D. P. 1970 The plate tectonics of the Mediterranean region *Nature* 226-239
- Melluso L., Conticelli S. De Gennaro R. (2010) Kirschsteinite in Capo di Bove melilite leucitite lava (cecilite), Alban Hills, Italy *Miner Mag.*, 74(5), 887-902
- Melluso, L., De'Gennaro, R., Fedele, L., Franciosi, L., & Morra, V. (2012). Evidence of crystallization in residual, Cl–F-rich, agpaitic, trachyphonolitic magmas and primitive Mg-rich basalt–trachyphonolite interaction in the lava domes of the Phlegrean Fields (Italy). *Geological Magazine*, 149(3), 532-550.
- Middendorf, B., Hughes, J. J., Callebaut, K., Baronio, G., & Papayianni, I. (2005). Investigative methods for the characterisation of historic mortars—part 1: mineralogical characterisation. *Materials and Structures*, 38(8), 761-769.
- Miller, C., Zanetti, A., Thöni, M., & Konzett, J. (2007). Eclogitisation of gabbroic rocks: redistribution of trace elements and Zr in rutile thermometry in an Eo-Alpine subduction zone (Eastern Alps). *Chemical Geology*, 239(1), 96-123.
- Nelson, D.R., McCulloch, M.T. and Sun, S-S., 1986. The origins of ultrapotassic rocks as inferred from Sr, Nd and Pb isotopes. *Geochim. Cosmochim. Acta*, 50:231-245.
- Ninomiya S., Nagasawa H. (1981). Mineral/groundmass partition coefficient for nepheline, melilite, clinopyroxene and perovskite in melilite-nepheline basalt, Nyiragongo, Zaire. *Geochemic Journ.*, 15, 221-228.
- Niu Y., Waggoner D. G., Sinton J. M. and Mahoney J. J. (1996) Mantle source heterogeneity and melting processes beneath seafloor spreading centers: the East Pacific Rise, 18°–19°S. *J. Geophys. Res.* 101, 27711–27733.
- Nixon, P., 1973. Kimberlitic volcanoes in East Africa. *Oversea Geol. Mineral. Resources, Inst. Geol. Sci.* 41, 119–138.

- Onuma N., Ninomiya Sh., Nagasawa H. (1981). Mineral/groundmass partition coefficients for nepheline, melilite, clinopyroxene and perovskite in melilite–nepheline basalt, Nyiragongo, Zaire *Geochem. J.*, 15 (1981), pp. 221-228
- Pilleyre, T., Sanzelle, S., Miallier, D., Fain, J., & Courtine, F. (2006). Theoretical and experimental estimation of self-attenuation corrections in determination of ^{210}Pb by γ -spectrometry with well Ge detector. *Radiation measurements*, 41(3), 323-329.
- Platz T., Foley S.F., Andr e L. (2004). Low-pressure fractionation of the Nyiragongo volcanic rocks, Virunga province, D.R. Congo. *J. Volcanol. Geotherm Res.* 136, 269-295.
- Pouchou, J. L., & Pichoir, F. (1988). A simplified version of the “PAP” model for matrix corrections in EPMA. *Microbeam analysis*, 315-318.
- Poucllet A., Bellon H., Bram K. (2016). The Cenozoic volcanism in the Kivu rift: Assessment of the tectonic setting, geochemistry, and geochronology of the volcanic activity in the South-Kivu and Virunga regions. *J. African Earth Sc* 121, 219-246.
- Rabinowicz et 2002 Rabinowicz M., Richard Y. and Gre Algoire M. (2002) Compaction in a mantle with a very small melt concentration: implications for the generation of carbonatitic and carbonate-bearing high alkaline mafic melt impregnations. *Earth Planet. Sci. Lett.* 203, 205–220.
- Rock NMS (1991) *Lamprophyres*. Blackie, London
- Roeder PL, Emslie RF (1970) Olivine-liquidequilibrium. *Contrib Mineral Petrol* 29: 275-289
- Rogers, N. W., Hawkesworth, C. J. & Palacz, Z. A. (1992a). Phlogopite in the generation of olivine-melilitites from Namaqualand, South Africa, and its implications for element fractionation processes in the upper mantle. *Lithos* 28, 347–365.
- Rogers N.W. (1992b) Potassic magmatism as a key to trace-element enrichment processes in the upper mantle *Journal of Volcanology and Geothermal Research*, 50 (1992), pp. 85-99
- Rogers, N. W., De Mulder, M., Hawkesworth, C. J. (1992c). An enriched mantle source for potassic basanites: evidence from Karisimbi volcano, Virunga volcanic province, Rwanda. *Contributions to Mineralogy and Petrology* 111, 543–556.
- Rogers N. W., James D., Kelley S. P., and De Mulder M. (1998) The generation of potassic lavas from the eastern Virunga province, Rwanda. *J. Petrol.* 39, 1223–1247.
- Rollinson H.R. (1992). *Using Geochemical Data: Evaluation, Presentation, Interpretation*.

- Rosenthal A., Foley S.F., Pearson D.G., Nowell G.M., Tappe S. (2009) Petrogenesis of strongly alkaline primitive volcanic rocks at the propagating tip of the western branch of the East African Rift *Earth and Planetary Science Letters*, 284, 236-248
- Ruch J. and Tedesco D. (2002). One year after the nyiragongo volcano alert: evolution of the communication between goma inhabitants (populations), scientists and local authorities. *Acta Vulcanologica* 14, 101-108.
- Rudnick, R., McDonough, W., 1993. Carbonatite metasomatism in the northern Tanzanian mantle: petrographic and geochemical characteristics. *Earth Planet. Sci. Lett.* 114, 463—475.
- Sahama T.G. (1957). Complex nepheline–kalsilite phenocrysts in Kabfumu lava, Nyiragongo area, north Kivu in Belgian Congo. *Journal of Geology* 65, 515–526.
- Sahama, T.G. (1960). Kalsilite in the lavas of Mount Nyiragongo (Belgian Congo). *Journal of Petrology*, 146–171.
- Sahama, T.G. (1962). Petrology of Mt. Nyiragongo: a review. *Transactions of the Edinburgh Geological Society* 19, 1–28.
- Sahama, T.G. (1973). Evolution of the Nyiragongo magma. *Journal of Petrology* 14, 33–48.
- Sahama T.G. (1976). Compositions of clinopyroxene and melilite in the Nyiragongo rocks. *Carnegie Institution in Washington, Year Book*, 75, 585-591.
- Sahama, T.G. (1978). The Nyiragongo main cone. *Musee Royal de l’Afrique Centrale, Tervuren (Belgique). Ann. Sci. Geol.* 81, 88.
- Sambo G.K., Karume K., Mateso H.C., Bibentyo T.M., Mahinda C.K., Milungu A.K., Kaleghetso E.K., Mukengere F.M. (2016). Contribution to Geochemical study of geological formations of the Nyiragongo volcano: Case of the Lac Vert cone in Goma, North Kivu, DR Congo. *Innovative Space of Scientific Research Journals*, 15, 685-696.
- Santo A.P., Capaccioni B., Tedesco D., Vaselli O. (2003). Petrographic and geochemical features of the 2002 Nyiragongo lava flows. *Acta Vulcanologica*, 14 (1-2), 63-66.
- Sawyer G.M., Carn S.A., Tsanev V.I., Oppenheimer C., Burton M. Investigation into magma degassing at Nyiragongo volcano, Democratic Republic of the Congo *Geochemistry Geophysics Geosystems*, 9 (2008), p. Q02017,

- Schmid M., Tietze K., Halbwachs M., Lorke A., McGinnis D., Wüest A. (2002). How hazardous is the gas accumulation in lake Kivu? Arguments for a risk assessment in light of the Nyiragongo volcano eruption of 2002. *Acta Vulcanologica*, 14, 115-122.
- Shaw D.M. Trace element fractionation during anatexis *Geochim. Cosmochim. Acta*, 34 (1970), pp. 237-243
- Smets B., Wauthier C., d'Oreye N. (2010) A new map of the lava flow field of Nyamulagira (D.R. Congo) from satellite imagery. *Journal of African Earth Sciences*, 58, 778-786.
- Smets B., Kervyn M., Kervyn N., d'Oreye N. (2015). Spatio-temporal dynamics of eruptions in a youthful extensional setting: Insights from Nyamulagira Volcano (D.R. Congo), in the western branch of the East African Rift. *Earth-Science Reviews* 150, 305-328.
- Spath A., Le Roex A. P., Opiyo-Akech N. (2001). Plume-lithosphere interaction and the origin of continental rift-related alkaline volcanism – the Chyulu Hills volcanics province, Southern Kenya. *Journal of Petrology* v. 42,4 , p 765-787.
- Tappe, S. et al. Genesis of ultramafic lamprophyres and carbonatites at Aillik Bay, Labrador: a consequence of incipient lithospheric thinning beneath the North Atlantic craton. *J. Petrol.* 47, 1261–1315 (2006).
- Tazieff, H. (1977). An exceptional eruption: Mt. *Nyiragongo*, *January 10th*, 1-12.
- Tazieff, H. (1979). *Nyiragongo, the forbidden volcano*. Barron's/Woodbury.
- Tedesco D. (2004). 1995 Nyiragongo and Nyamulagira activity in the Virunga National Park: A volcanic crisis. *Acta Vulcanologica*, Istituti Editoriali e Poligrafici Internazionali, 14-15, 149-155
- Tedesco, D., Vaselli, O., Papale, P., Carn, S. A., Voltaggio, M., Sawyer, G. M., ... & Tassi, F. (2007). January 2002 volcano-tectonic eruption of Nyiragongo volcano, Democratic Republic of Congo. *Journal of Geophysical Research: Solid Earth*, 112(B9).
- Tedesco D.; Tassi F.; Vaselli O.; Poreda R.J.; Darrah T., Cuoco E., Yalire N.M. (2010) Gas isotopic signatures (He, C, and Ar) in the Lake Kivu region (western branch of the East African rift system): Geodynamic and volcanological implications. *Journal of geophysical research*, 115.

- Toscani L., Capedri S., Oddone M. (1990). New chemical and petrographic data of some undersaturated lavas from Nyiragongo and Mikeno (Virunga-Western African rift – Zaire). *Neues Jahrb. Min. Abh* 161, 287-302.
- Wadge, G., Biggs, J., Lloyd, R., Kendall, J.-M. (2016). Historical volcanism and the state of stress in the East African Rift System. *Frontiers*,
- Wauthier, C., Cayol, V., Poland, M., Kervyn, F., d'Oreye, N., Hooper, A., ... & Smets, B. (2013). Nyamulagira's magma plumbing system inferred from 15 years of InSAR. *Geological Society, London, Special Publications*, 380(1), 39-65.
- Williams et 1978 Williams, L. A. J. in *Continental and Oceanic Rifts* (ed Pålmason, G.) 193–222 (American Geophysical Union, 1978).
- Wilson, M. J.M. Rosenbaum, E.A. Dunworth Melilitites: partial melts of the thermal boundary layer? *J. Petrol.*, 32 (1995), pp. 181-196
- Wolfenden E., Ebinger C., Yirgu G., Renne P. R., Kelley S. P. (2005). Evolution of a volcanic rifted margin: Southern Red Sea, Ethiopia. *GSA Bull.* 117, 846-864.
- Woolley, A.R., Bergman, S.C., Edgar, A.D., Le Bas, M.J., Mitchell, R.H., Rock, N.M.S., Scott Smith, B.H., 1996. Classification of lamprophyres, lamproites, kimberlites, and the kalsilitic, melilitic, and leucitic rocks. *The Canadian Mineralogist* 34, 175–186.
- Workman et 2004 Workman, R.K., et al., 2004. Recycled metasomatic lithosphere as the origin of the Enriched Mantle II (EM2) end-member: evidence from the Samoan volcanic chain. *Geochemistry, Geophysics, Geosystems* 5 (4).
- Wright R. and Flynn L. P. (2003). Satellite observations of thermal emission before, during, and after the January 2002 eruption of Nyiragongo. *Acta Vulcanologica* 14, 67-74.
- Wyllie, P.J., Huang, W.L., 1976. Carbonation and melting reactions in the system CaO–MgO–SiO₂–CO₂ at mantle pressures with geophysical and petrological applications. *Contrib. Mineral. Petrol.* 54, 79–107.
- Wyllie PJ (1979) *Magmas and volatile components*. *Am Mineral* 64:469–500
- Vaselli O., Capaccioni B., Tedesco D., Tassi F., Yalire M. M., Mahinda C. K. (2002). The evil's winds' (mazukus) at nyiragongo volcano (Democratic Republic of Congo). *Acta Vulcanologica*, 14, 123-128.
- Vollmer and Norry 1983 Vollmer, R., Norry, M.J., 1983a. Possible origin of K-rich

volcanic rocks from Virunga, East Africa, by metasomatism of continental crust material: Pb, Nd and Sr isotopic evidence. *Earth Planet. Sci. Lett.* 64, 374–386.

Vollmer, R., Norry, M.J., 1983b. Unusual isotopic variations in Nyiragongo nephelinites. *Nature* 301, 141–143.

Vollmer et 1985 Vollmer, R., Nixon, P.H., Condliffe, E., 1985. Petrology and geochemistry of a U and Th enriched nephelinite from Mt. Nyiragongo, Zaire: its bearing on ancient mantle metasomatism. *Bull. Geol. Soc. Finland* 57, 37–46.

Zindler, A., Hart, S.R., 1986. Chemical geodynamics. *Ann. Rev. Earth Planet. Sci.* 14, 493–571.